Non-invasive techniques for predicting soft tissue during pressure induced ishaemia.

Knight, Sarah Louise

NON-INVASIVE TECHNIQUES FOR PREDICTING SOFT TISSUE STATUS DURING PRESSURE INDUCED ISCHAEMIA

SARAH LOUISE KNIGHT (NÉE GIGG)

BA MSC

IRC IN BIOMEDICAL MATERIALS

QUEEN MARY & WESTFIELD COLLEGE

UNIVERSITY OF LONDON

1997

QUEEN MARY
AND WESTFIELD COLLEGE
UNIVERSITY OF LONDON

This thesis is presented as part of the requirements

for the degree of Doctor of Philosophy

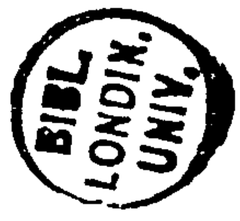

ABSTRACT

Soft tissue breakdown occurs in association with biochemical changes that can be attributed to a reduction in blood and lymph flow to a localised tissue area in response to applied pressure. The resulting ischaemia can lead to a reduction in available oxygen and accumulation of waste products. Tissue breakdown leading to the development of pressure sores afflicts patients who are already debilitated, although not all patients appear to be equally susceptible.

Measurement of sweat biochemistry and blood gas tensions may reflect the biochemical process in the underlying tissues and provide a simple and non-invasive method of investigating the status of soft tissues. The potential of specific sweat metabolites to act as markers of soft tissue status during and following loading has been investigated at a clinically relevant site in healthy volunteers, and in two clinically relevant patient groups. A range of validation procedures were undertaken and a series of parameters derived to investigate the temporal profile of sweat biochemistry, and identify various modes of gas tension response.

Investigations at the loaded sacrum of healthy individuals showed a statistically significant increase in sweat lactate, urea, urate and chloride concentrations which were dependent upon the level of externally applied pressure. Mean increases of between 10%-60% were demonstrated for sweat metabolite concentrations at the loaded site compared to the control site for applied pressures in the range 40-120 mmHg. Similar increases were demonstrated in sweat collected from highly loaded tissue areas within the stump socket of lower limb amputees.

A threshold value for pO_2 tension was identified, amounting to a 60% reduction from the unloaded value, which was associated with elevated tissue carbon dioxide levels as well as increased sweat metabolite concentrations in the loaded phase.

This finding may provide a useful predictor of soft tissue status during prolonged loading.

No pessimist ever discovered the secrets of the stars, or sailed
to an uncharted land, or opened a new heaven to the human spirit.

Helen Adams Keller (1880-1968)

ACKNOWLEDGEMENTS

I would like to take this opportunity to express my gratitude to a number of people who have given their support and encouragement throughout the duration of this thesis.

Dr Dan Bader, for his continual motivation and inspiration, and knowledge, especially throughout the last year.

Dr Richard Taylor, at the Department of Clinical Biochemistry, John Radcliffe Hospital, Headingley, Oxford for his unfailing help and advice.

Ms Liz Moore, from Department of Medical Physics & Bioengineering, King's College Hospital, London, and the staff of the King's Healthcare Rehabilitation Centre, for their co-operation and help with the clinical study on the amputee population.

Dr M Brooke, Department of Sports Medicine, Royal London Hospital, for his help and co-operation with the amputee athlete population.

Lone Rose and Maureen Cosgrave, Seating Clinic, National Spinal Injuries Centre, Stoke Mandeville Hospital for their help with the spinal cord injured study.

I would also like to thank my family for their patience and encouragement, and for inspiring me to undertake this thesis.

Most importantly, a big Thank you to all the friends (and family) who willingly(?) volunteered their bodies for the purposes of this project. Especially to Martin, who not only donated a large quantity of sweat, but also became my husband.

TABLE OF CONTENTS

LIST OF TABLES

LIST OF FIGURES

PREFACE

The most widespread and recognised example of soft tissue breakdown is the pressure sore, also known as the bed sore or decubitus ulcer. Paget [153] stated the pathological definition of pressure sores as the 'sloughing and mortification or death of a part produced by pressure'. This pressure is most commonly the result of non-compliant support surfaces such as wheelchair seats and prosthetic/orthotic devices in addition to mattresses. As such, the terms bed sore and decubitus ulcer are misleading in the implication that they occur purely as a result of prolonged bed lying.

The problem of pressure sores is by no means a recent one. Indeed there is evidence to suggest that Egyptian mummies suffered from tissue breakdown [46]. However, it was not until the late 19th century that eminent surgeons such as Paget [153] and Charcot [36] stressed the importance of the prevention and treatment of pressure sores as part of a successful patient management strategy. Charcot was also responsible for the earliest scientific research carried out to determine the causative factors in development of tissue breakdown. As a result of this work and successive work by a select number of researchers, the aetiology and pathogenesis of tissue breakdown is fairly well understood. In spite of this knowledge, pressure sores still occur in large numbers, approximately 30,000 reported per annum, and in some cases are a significant contributory cause of death in debilitated patients. The main reason for this inadequacy is thought to be ineffective allocation of resources and healthcare management rather than lack of preventative knowledge. The cost of treatment of pressure sores has been estimated at £750 million [160] per annum and in addition, successful litigation against health authorities by patients who developed pressure sores whilst hospitalised have resulted in large awards for damages. With an ever increasing aged population and advances in medicine allowing greater longevity in subject groups such as the spinal cord injured, this financial burden will undoubtedly increase. Clearly, the most effective mechanism for reducing this expenditure, in the long term, is prevention.

One of the most recent advances in prevention and treatment of tissue breakdown is the concept of tissue viability and the measurement of its parameters. The Tissue Viability Society was created in the early 1980's as a forum for professionals from various disciplines to meet and promote research in this 'unglamorous' area. Measurement of tissue viability or status can effectively be divided into three categories; pressure, blood flow and tissue biochemistry measurement.

At present the most effective method of preventing pressure sores is by the use of pressure relieving support surfaces, such as specialised mattresses and seating materials. The development of accurate interface pressure measuring devices could allow routine assessment of all patient support and handling systems. There are still few guidelines regarding the optimum pressure distribution, which would be applicable for all patient groups. Historically, the value of 32 mmHg has been used, based on the mean interstitial pressure measured in the nail-fold capillary [121]. However, this value for interface pressures is clearly inappropriate.

Due to the high cost of some pressure relieving support surfaces it is certainly not feasible to prescribe these measures to all patients. Therefore, an important feature in prevention is the identification of those patients who may be at greatest risk from developing tissue breakdown, in order that these patients can receive appropriate prophylaxis. At present the most commonly used method for determining susceptibility is the use of risk scales designed for professional nurses and therapists. However, these are not always objective and reliability is often questionable [46]. More recently advances have been made with the use of other physiological measurements of tissue viability such as blood flow and tissue biochemistry and transcutaneous gas tensions [24-25] and laser Doppler blood flux monitoring which are now slowly being introduced into the clinical setting.

Despite the present understanding of the aetiology and pathophysiology of tissue breakdown, pressure sores still occur in our hospitals. In order to reduce this distressing and avoidable condition, relevant research which has direct clinical application is required.

1. SOFT TISSUE CHARACTERISATION

1.1 INTRODUCTION

The skin and subcutaneous soft tissue performs important functions including maintaining body homeostasis, providing an effective barrier against injury and a supporting surface for the underlying body structures. Skin and soft tissues are living organs and as such require a balance between nutrient supply and waste product removal to ensure viability. A compromise to the viability of soft tissue may lead to the development of soft tissue breakdown, such as pressure sores and leg ulcers. This can lead to further complications in patients who may be already debilitated. In order to investigate the pathophysiology of tissue breakdown it is important to understand the anatomy and function of healthy skin and soft tissue. For the purposes of this thesis, soft tissue will refer to all tissues between the epithelium and the bone, including the epidermis and dermis of the skin, the subcutaneous tissue and associated muscle, as well as adnexal structures such as blood and lymph vessels and sweat glands. Figure 1-1 shows a cross section through the skin and subcutaneous tissues, illustrating adnexal structures.

1.2 ANATOMY & FUNCTION OF SKIN AND SOFT TISSUE

1.2.1 SKIN

The skin is the largest organ in the body, it covers a total area of between 1.2 - 2.2 m^2 and makes up 8% of the total body mass providing an expansive sensory surface as well as regulation of body temperature. Skin is structurally complex due to its specialised nature and the body is covered with two functionally different types of skin, hirsute and glabrous. Hirsute skin is thin and hairy, it is responsible for the general skin functions, including sensory, thermoregulatory and mechanical, over the whole body surface. Glabrous skin is thick and hairless, it provides a frictional surface for manipulation and locomotion and has higher strength than hirsute skin. It is generally

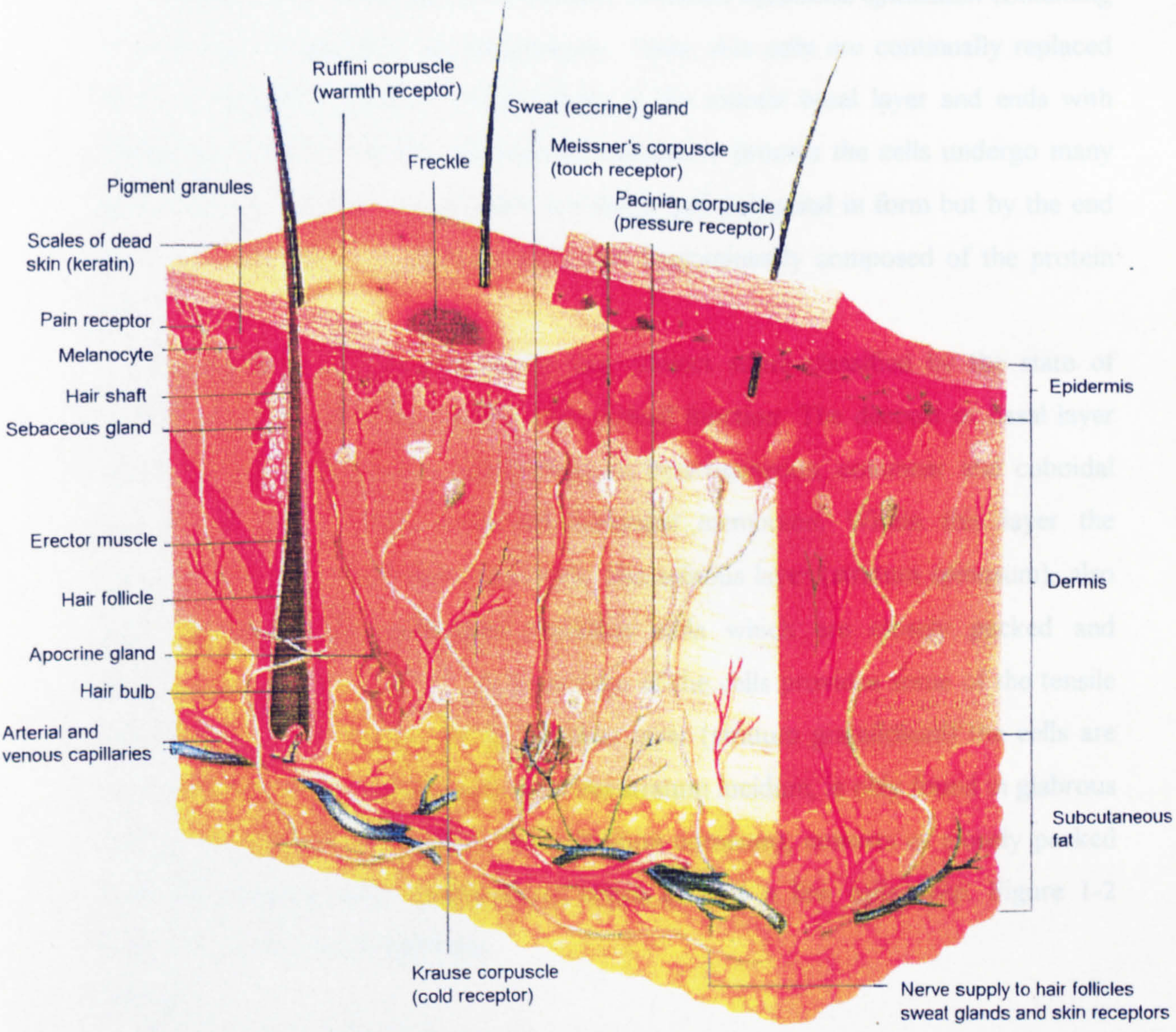

Figure 1-1 Cross section through the skin and subcutaneous tissues.

found on the soles of the feet and the palms of the hands and has a higher density of sweat glands and nerve endings than hirsute skin. Both hirsute and glabrous skin are formed by the intimate association between two distinct layers, the epidermis and the dermis.

EPIDERMIS

The epidermis is composed of keratinised, stratified squamous epithelium containing keratinocytes, phagocytes and melanocytes. These skin cells are continually replaced during a maturation process, which begins at the mitotic basal layer and ends with shedding at the skin surface. During this maturation process the cells undergo many morphological changes. Initially they are viable and polygonal in form but by the end of the process, they are flattened, dead and predominantly composed of the protein keratin.

The epidermis can be divided into five distinct strata classified by the state of maturation of the keratinocytes and their overall function. The deepest or basal layer (stratum basale) comprises a single layer of heterogeneous, columnar and cuboidal cells which lie in contact with the basement membrane. Within this layer the keratinocytes are formed from stem cells. The spinous layer (stratum spinosum), also known as the prickle cell layer, contains cells which are closely packed and interdigitate with one another, the anchorage of the cells provides some of the tensile properties of the epidermis. In the granular layer (stratum granulosum) the cells are more ellipsoid in form. The fourth layer, the stratum lucidum, is only found in glabrous skin and the surface or cornified layer (stratum corneum), consists of closely packed layers of flattened, dead keratinocytes which lie only a few cells deep. Figure 1-2 details the layers of the epidermis.

DERMIS

The dermis is comprised of moderately dense connective tissue which itself comprises a meshwork of fibres in a matrix of extracellular ground substance together with blood vessels, lymphatics and nerves. The dermis can be divided into two layers; the papillary layer which is immediately sub-epidermal and the reticular layer. At the interface between the papillary layer and the basement membrane of the epidermis there are many papillae which interdigitate providing mechanical anchorage and

metabolic support to the epidermis. Glabrous skin contains more papillae than hirsute skin due to the mechanical function of this type of skin. The reticular layer contains bundles of collagen and elastin fibres, which have a preferred fibre orientation along the line of greatest applied force. This can be represented by the characteristic Langers lines at the surface of the skin. Sweat ducts are contained within the deeper reticular regions comprised of loose connective and adipose tissues.

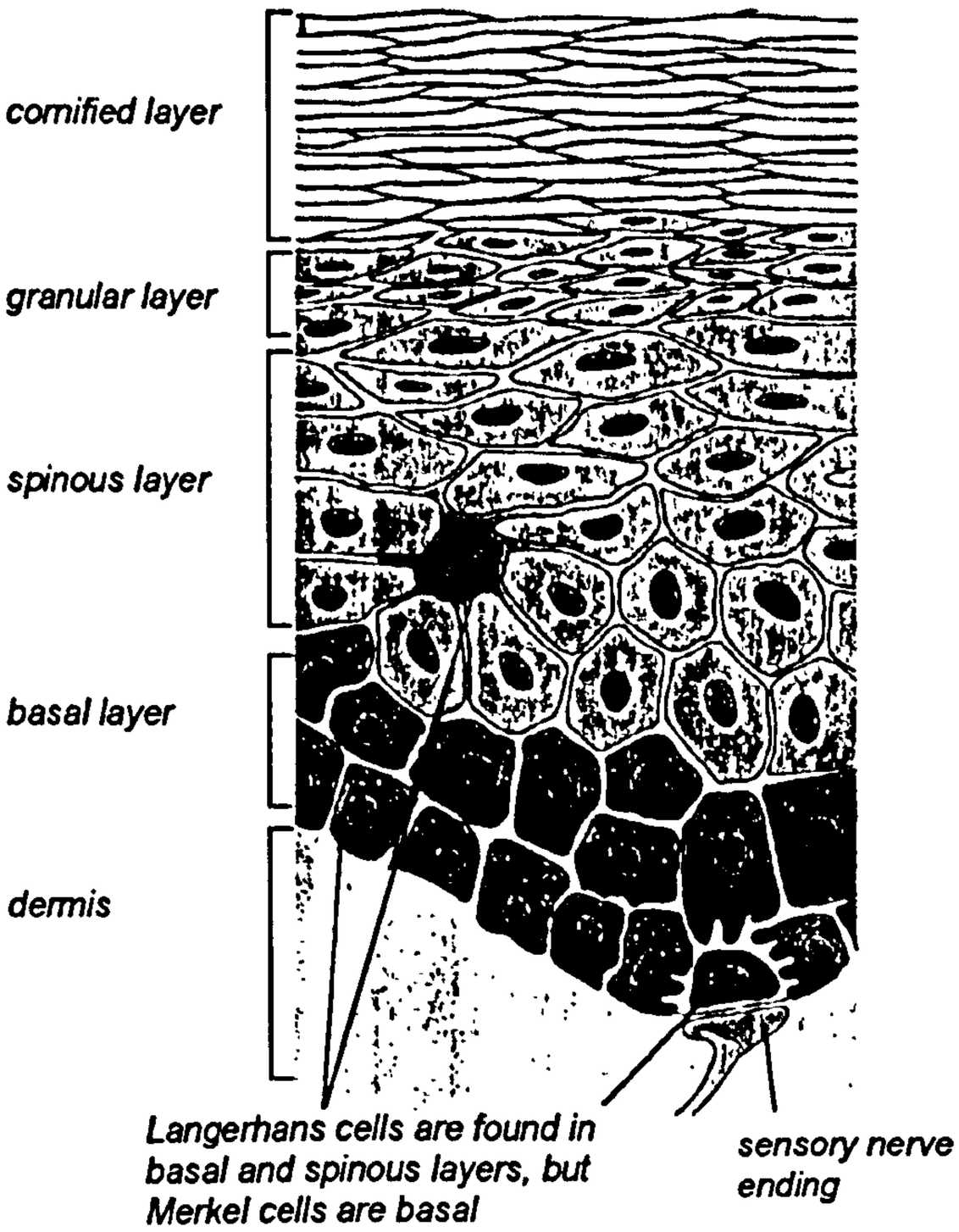

Figure 1-2 Schematic representation of the layers of the epidermis. Adapted from [82].

1.2.2 Subcutaneous Tissue

Subcutaneous tissue can be considered a multi-phase system comprising cells, collagen, elastin and hydrated proteoglycan aggregates, with a free interstitial fluid present in the microscopic channels between the components of the matrix. It comprises of compartments separated by fibrous septa, this separation prevents the rapid flow of fluid between compartments when the soft tissue layers are subjected to

compression. The interstitium of the subcutaneous tissue also contains sensory nerves for touch, pain and pressure, autonomic nerves which control arterioles and the associated blood flow rate and vessels of the vascular and lymphatic systems.

COLLAGEN

Collagen is a fibrous protein and much of its function within the body is to provide a strong yet flexible framework to contain cells and tissues. The collagen protein is composed of linear, unbranching sequences of 20 or more naturally occurring amino acids. Approximately one third of the amino acid content is made up of the small molecule glycine, with proline and hydroxyproline making up about 50% of the remainder. Thus, the amino acid sequence in the tropocollagen molecule may be represented as $[Gly\text{-}X\text{-}Y\text{-}Gly\text{-}Hydroxyproline\text{-}Proline]_n$. The basic unit of collagen is a triple helix comprising three polypeptide chains in a left hand helical configuration, which are wound around each other forming a right hand super helix. These form rods that are 30 nm long and 1.5 nm in diameter with non-helical ends and show a banded pattern under the electron microscope with a periodicity of 67 nm. The high strength and stability of collagen is attributed to the covalent crosslinks both within and between adjacent molecules; the destruction of these cross links will diminish the integrity of the collagen fibre structure. Collagen is highly specialised and exists in at least 16 genetically different types many of which have been identified in skin as detailed in Table 1-1.

Table 1-1 Structure of the collagen types found in skin. Adapted from [4]

Collagen Type	Tissue	Structure
I	Skin, tendon, bone, cartilage	Large diameter 67 nm banded fibrils
III	Skin, aorta, uterus, gut	Small diameter 67 nm banded fibrils
V	Skin, bone, placental tissue	9 nm diameter non-banded fibrils
VI	Skin, cornea, uterus, cartilage	5-10 nm diameter microfibrils, 100 nm periodicity
VII	Skin, oesophagus, amniotic membrane	Anchoring fibrils
XII	Skin, tendon, cartilage	fibril associated collagen with interrupted triple helix (FACIT), non-fibrillar
XIV	Skin, tendon, cartilage	FACIT, non-fibrillar

ELASTIN

In common with collagen, elastin is a protein which contains hydroxyproline. The protein chain also contains a high proportion of non-polar amino acids. When extracted from tissue, using biochemical methods, elastin appears as a yellow-brown sticky material with properties similar to those of highly extensible elastomers and rubbers.

PROTOEGLYCANS

Proteoglycans consist of unbranching chains of disaccharides including hyaluronic acid, heparan sulphate and dermatan sulphate. These molecules, with their sulphate groups, may be electrostatically attached to the positive groups associated with the collagen and elastin fibres in the matrix, as well as the hydrogen atoms of water molecules. Thus proteoglycans have a high affinity for water and form a polymer gel.

1.2.3 BLOOD VESSELS

The smallest vessels in the circulatory system form the crucial connection between the arterial and venous blood supply systems as they are required to exchange water, gas and solutes between blood and tissues. The micro-circulatory system is divided into a number of vessels, the diameters and functions of which are described in Table 1-2

The function of these vessels can be divided into three groups; resistance vessels which control flow, exchange vessels for respiration and reservoir vessels which store blood. The low velocity of blood flow within the capillaries allows adequate time for exchange of gases, nutrients and waste products between blood and tissues. The blood flow within the capillaries is not always constant due to the contraction of muscle fibres in arterioles and pre-capillaries. This results in an intermittent flow, known as vasomotion, which is controlled by oxygen concentration in the tissues [32].

Table 1-2 Vessels of the micro-circulatory system. Adapted from [82]

Vessel	Diameter	Form	Innervation
terminal arteries	> 50 μm	endothelium, internal elastic lamina, 2 rings of vascular smooth muscle	sympathetic & circulating vasodilators and constrictors
arterioles	20 -50 μm	as above but a single layer of smooth muscle	sympathetic & circulating vasodilators and constrictors
metarterioles	8 - 15 μm	endothelium with intermittent smooth muscle	sympathetic & circulating vasodilators and constrictors
precapillary sphincters		cuff of smooth muscle	vasoactive substances only
arterial capillaries	4 - 5 μm	endothelial cells with 10 nm holes	passive
venous capillaries	7 - 10 μm		
venules	10 - 15 μm	endothelium, connective tissue and basal lamina	not innervated or affected by vasoactive substances
muscular venules	> 50 μm	as terminal arterioles	sympathetic and vaso active substances to a lesser extent than metarterioles

The micro-circulatory anatomy of the skin is shown in Figure 1-3, the precise anatomy is dependent upon region, age and adjoining structures. Small branches of the subcutaneous arteries penetrate the deep dermis and freely anastamose in a plane horizontal to the skin. This area is known as the deep plexus and the vessels supply the sweat glands and hair follicles. Arterioles arise from this plexus and ascend obliquely through the dermis. By the subpapillary region only metarterioles are present, these vessels anastamose just under the epidermis to form the superficial plexus. The dermal papillae are supplied by small hairpin loops arising from this plexus. The basal cells of the epidermis are supplied by capillaries ascending into the papillae.

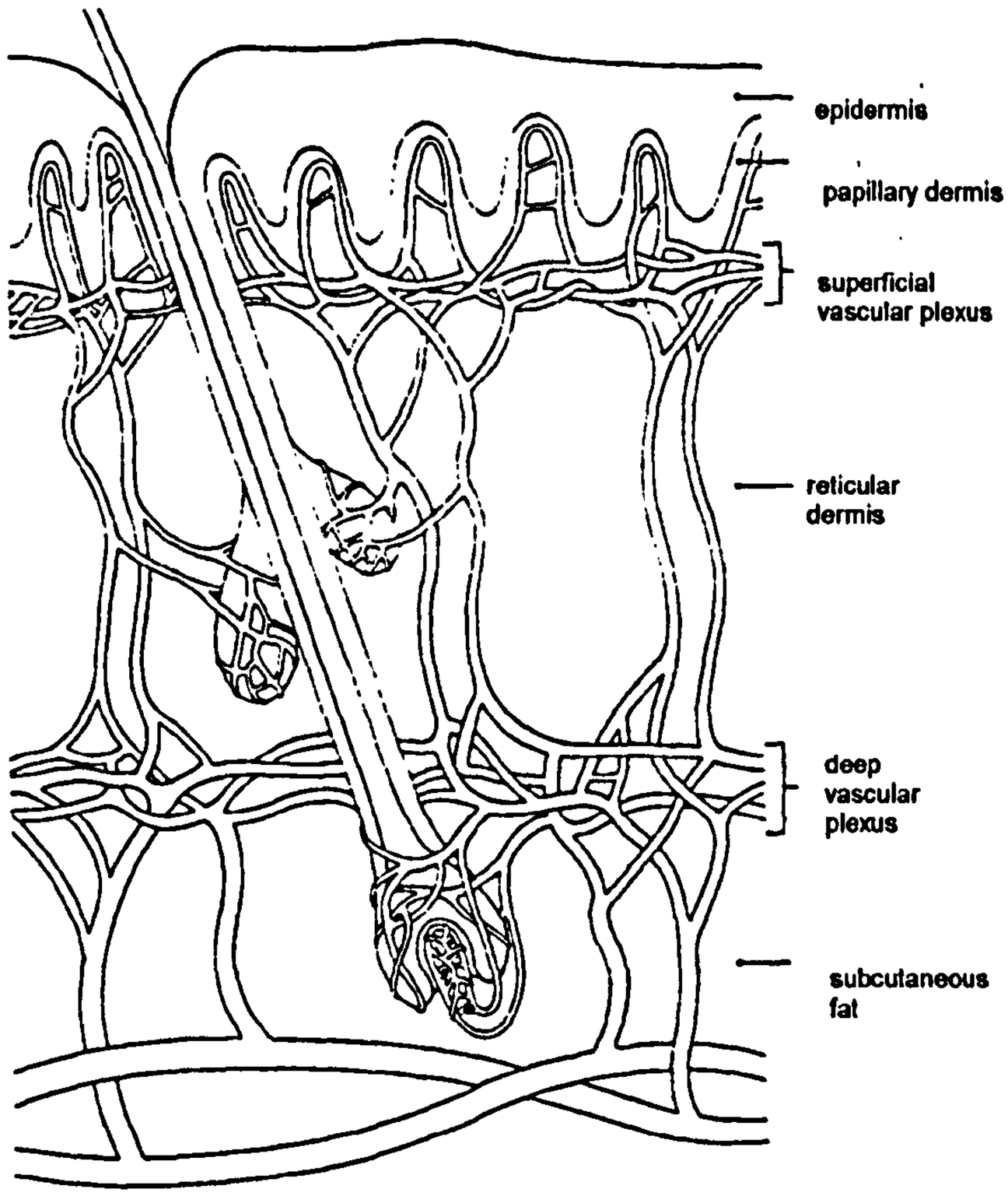

Figure 1-3 Schematic diagram of the micro-circulatory anatomy of the skin.

An important feature of the micro-circulation is the arterio-venous anastamosis (A-VA), which provides a direct connection between the arterioles and the venules in the dermis without exchange of nutrition. The density of A-VAs in the skin depends on the region of the body; smaller branches of arteries anastamose more frequently than large ones, and between the smallest vessels these anastamoses become so numerous as to constitute a close network that pervades nearly every tissue of the body [82]. A-VA's occur most abundantly at sites which are likely to suffer from both thermal and mechanical injury, for example, the fingertips and the gluteal region [173]. The nature of the arterio-venous anastamoses can alter in response to age and disease.

1.2.4 SWEAT GLANDS

The primary function of the sweat gland is thermoregulation of the body. The size of the sweat glands generally increases with body size, and is larger in males than in females. There are an average of 1.6-4.0 x10^6 sweat glands distributed over the whole body [119,187], the density of sweat glands in different regions of the body are detailed in Table 1-3.

Table 1-3 Sweat gland density in different regions of the body. Adapted from [187].

Region of the body	Density glands / cm^2
Back	64
Forearms	108
Forehead	181
Palmar and plantar regions	600-700

Sweat glands are generally divided into two groups depending upon structure and location, known as apocrine and eccrine glands.

APOCRINE GLAND

The apocrine or majores sweat glands are simple, branched tubular glands which are distributed primarily in the axilla, the pubic region and in pigmented areas such as the areola of the breast.

The secretory portion of the apocrine gland is located in the dermal or subcutaneous tissue and the excretory portion opens into the hair follicle. Apocrine sweat glands function predominantly after puberty and produce a milky, viscous secretion of sweat. In many parts of the body the apocrine glands have evolved to perform specific functions, for example, the mammary glands and the wax producing ceruminous glands in the ear.

ECCRINE GLAND

The main purpose of the eccrine sweat gland is to produce sweat in response to thermal stimulation and, as such, it is the gland of most interest in the current study.

Eccrine sweat glands are distributed throughout the skin and are found in all regions with a few exceptions which include the margins of the lips and the nail fold beds. These sweat glands are most numerous on the soles of the feet and the palms of the hands. A schematic diagram of the human eccrine sweat gland is shown in Figure 1-4.

The human eccrine glands consists of a basal coil located at the border of the dermis and subcutaneous tissue, from which a duct leads through the dermis directly into the epidermis where sweat is excreted. The coil and duct can be divided into secretory, interdermal and interepidermal segments. The secretory portion, which makes up about half of the basal coil, comprises of one distinct layer of secretory cell types, known as clear and dark cells, and non-secretory myoepithelial cells. The clear cells are generally larger than the dark cells and secrete an aqueous material containing glycogen. The dark cells or mucous cells are found along the luminal border and have no nucleus. The myoepithelial cells contain a spindle nucleus and long contractile fibres running in spirals with their axis lying obliquely to the secretory tubule. Clear cells respond to both cholinergic and adrenergic stimulation, whereas dark and myoepithelial cells respond only to cholinergic stimulation [163]. The interdermal portion has no basement membrane and consists of two layers of small, cuboidal, basophilic, epithelial cells. The interepidermal portion, or the acrosyringium, contains cells which are distinct from the surrounding epidermis, this portion follows a spiral course from the interface between the epidermis and the dermis to the skin surface. It is comprised of a single layer of inner luminal cells and two or three layers of outer cells. The straight duct contains projections at the junctions of intercellular channels which may behave as valves or as a method of increasing the surface area of the lumen [142].

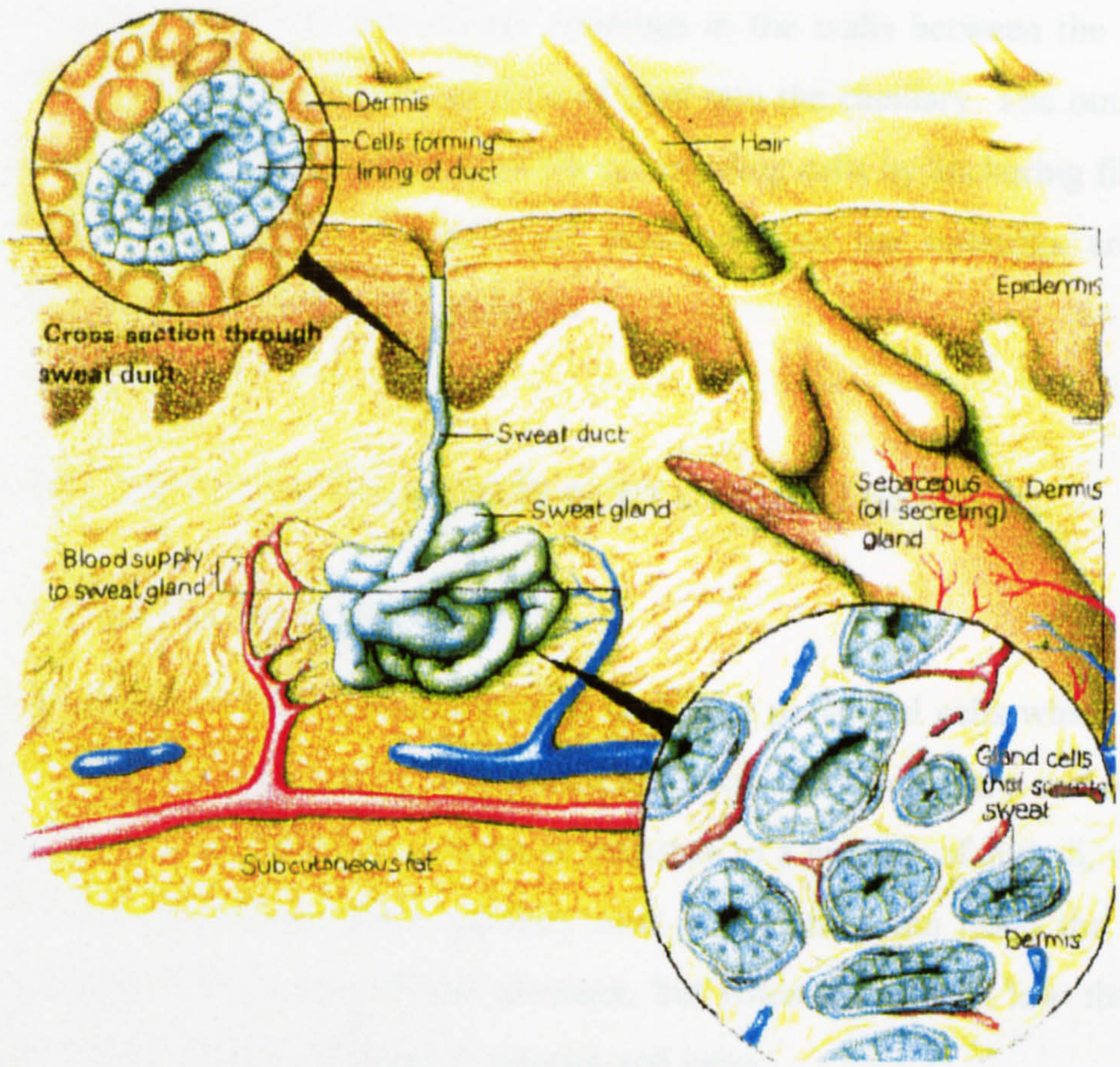

Figure 1-4 The human eccrine sweat gland

1.2.5 LYMPHATICS

The lymphatic system comprises a network of vessels which convey electrolytes, water and proteins, in the form of lymph, from tissue fluids to the blood stream. The lymphatic vessels originate as microscopic vessels in the spaces between cells where they are known as terminal lymph capillaries. These lymph capillaries occur both singly and in extensive plexi, they are very delicate with a single layer of endothelial cells and have no muscular or contractile elements. These vessels have a diameter of approximately 10-30 μm with minute openings in the walls between the endothelial cells, which facilitate unidirectional flow of fluid into the capillary. The outer surfaces of the endothelial cells are attached to the surrounding cells by anchoring filaments. In oedematous tissues, these filaments are tensioned and the openings are widened enabling extra fluid to enter the capillaries.

1.3 PHYSIOLOGY OF SKIN AND SUBCUTANEOUS TISSUES

1.3.1 MICRO-CIRCULATION

Capillaries are formed by thin flattened nucleated polygonal cells which are joined together by a cementing agent. The calibre and tone of the capillary can be changed independently of arterioles and venules in response to a number of stimuli, even in the absence of muscle fibres. When capillary tone is high they can resist the distending force of raised venous or arteriolar pressure, but when the tone is low they tend to passively follow pressure changes in arteries and veins.

The capillary tone is controlled by local physical and chemical conditions in addition to agents, known as vasoactive substances. These substances can be divided into vasodilators and vasoconstrictors, as mentioned in Table 1-2. Vasodilators include raised CO_2 tension, increase in H^+ concentration, histamine and various non-acidic dilator substances which are released during activity. During ischaemia locally acting dilator substances accumulate; the accumulation of vasodilators is responsible for the increased blood flow or hyperaemia during reperfusion [82]. The duration of occlusion

determines the degree of resulting hyperaemia which is characterised by dilation of capillaries and arterioles, leading to flushing, increased blood flow and pulsatile volume. Vasoconstrictors cause a narrowing of the blood vessels and a resulting decrease in flow, with examples of vasoconstrictors including acetylcholine, adrenaline, angiotensin and bradykinin.

1.3.2 INTERNAL RESPIRATION

The exchange of oxygen and carbon dioxide between blood and tissues is called internal respiration. Oxygenated blood enters the capillaries with an oxygen tension or partial pressure (pO_2) of 105 mmHg (14 kPa), whereas cells in tissues have an average pO_2 of 40 mmHg (5.3 kPa). This difference in tension leads to the diffusion of oxygen from the capillaries into the tissues. The partial pressure or tension of carbon dioxide (pCO_2) of cells in tissues is 45 mmHg (6.0 kPa) compared to the pCO_2 of capillary oxygenated blood of 40 mmHg (5.3 kPa). This difference leads to a diffusion of carbon dioxide from the tissue to the capillary blood. The partial pressures of O_2, CO_2, and N_2 at different stages of respiration are shown in Table 1-4.

Table 1-4 Partial pressures of gases at various stages of respiration. All values in mmHg (kPa)

	Atmospheric Air at sea level	**Alveolar Air**	**Deoxygenated Blood**	**Oxygenated Blood**	**Tissue Cells**
pO_2	160 (21.3)	105 (14.0)	40 (5.3)	105 (14.0)	40 (5.3)
pCO_2	0.3 (0.04)	40 (5.3)	45 (6.0)	40 (5.3)	45 (6.0)
pN_2	597 (79.5)	569 (75.8)	569 (75.8)	569 (75.8)	569 (75.8)

OXYGEN TRANSPORT

Oxygen does not dissolve readily in water and therefore very little oxygen is carried in the blood in its pure state. Indeed, only 3% of oxygen is carried in plasma while the remaining 97% is transported in chemical combination with haemoglobin (Hb) present in red blood cells. Oxygen and haemoglobin combine in a reversible reaction to form oxyhaemoglobin (HbO_2) as shown in Equation 1-1.

$$Hb + O_2 \Leftrightarrow HbO_2 \quad \textit{Equation 1-1}$$

When Hb is completely converted to HbO_2 the blood is fully or 100% saturated. The most important variable determining the extent to which oxygen combines and dissociates with haemoglobin is the oxygen tension (pO_2). The relationship between percentage saturation and pO_2 is referred to as the oxygen-haemoglobin dissociation curve and is illustrated in Figure 1-5. When pO_2 is high, haemoglobin binds with large amounts of oxygen and is almost completely saturated. When pO_2 is low, haemoglobin is only partially saturated and oxygen is released from oxyhaemoglobin. At these low levels of pO_2, the oxygen release is sensitive to small changes in pO_2. This is especially important in tissues which have high metabolic activity and therefore may experience reduced pO_2 levels during periods of high activity.

The amount of oxygen released from haemoglobin is also influenced by the pH of the blood. A low pH, or acid environment, encourages oxygen to dissociate more readily from haemoglobin, this phenomena is known as the Bohr Effect. Low blood pH can result from high pCO_2 levels or high levels of lactic acid produced during anaerobic muscle contraction.

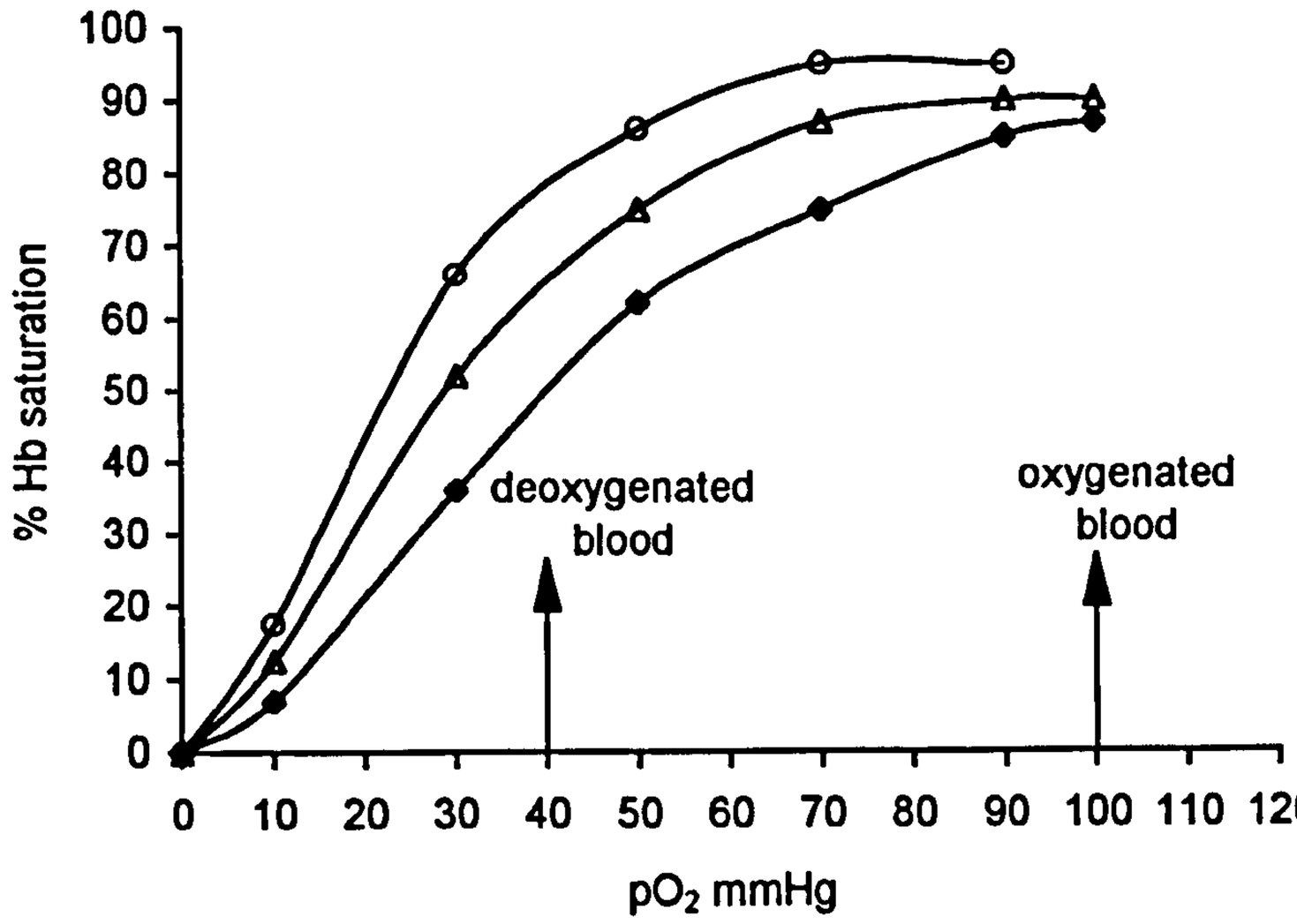

Figure 1-5 Oxygen-haemoglobin dissociation curves.
(Δ) normal blood pH, normal pCO_2. (◆) low blood pH, high pCO_2. (o) high blood pH, low pCO_2.

Temperature also affects the oxygen-haemoglobin dissociation curve, as shown in Figure 1-6. Within limits, an increase in temperature leads to a corresponding increase in the amount of oxygen released from haemoglobin. Heat energy is a by-product of the metabolism of cells and contraction of muscle fibres and, therefore, active cells and muscles will increase the local temperature thereby releasing more oxygen from haemoglobin to maintain homeostasis.

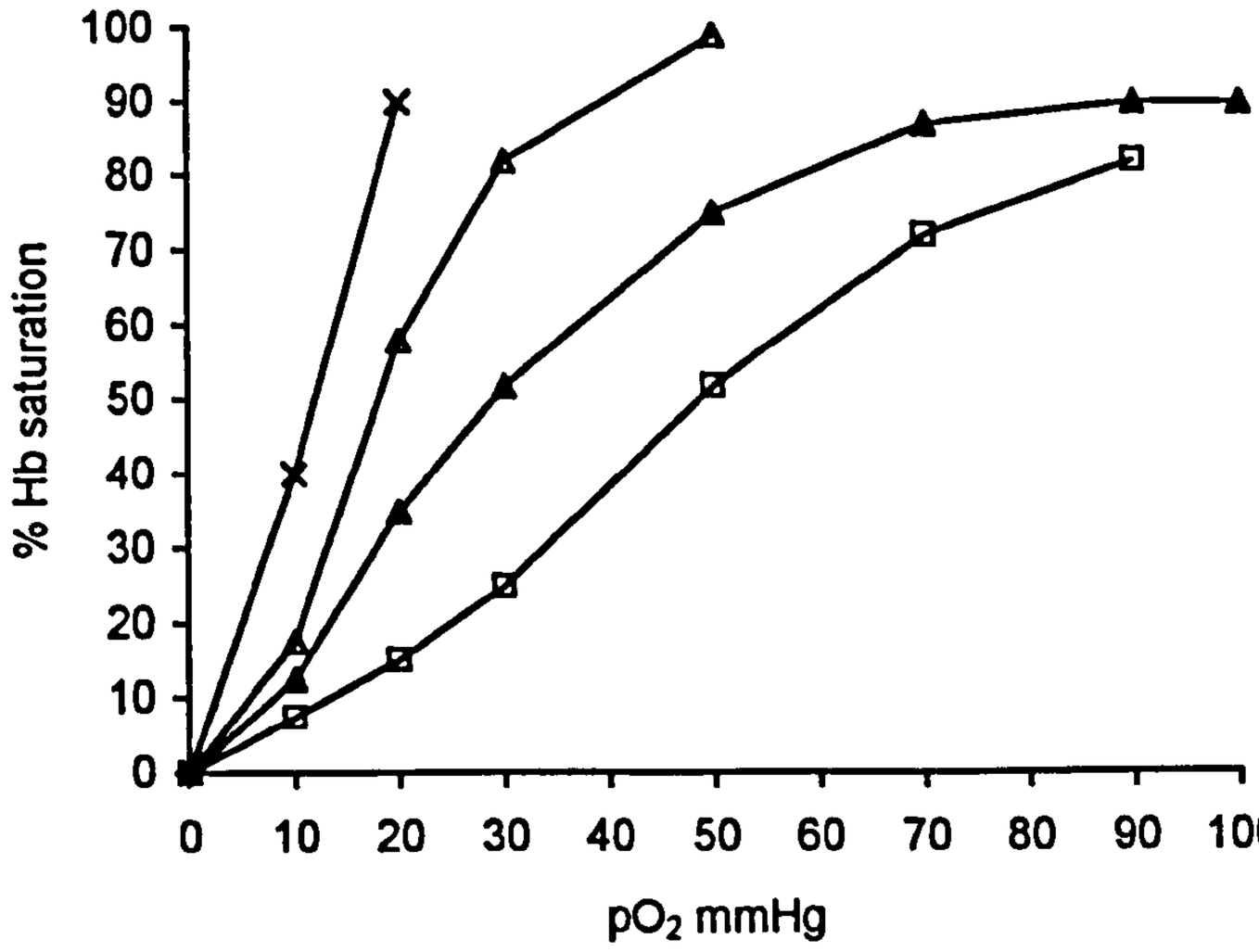

Figure 1-6 Graph showing the effect of temperature on the oxygen-haemoglobin dissociation curve. (x) 10°C, (Δ) 20°C, (▲) 38°C, and (□) 43°C.

CARBON DIOXIDE TRANSPORT

Under normal resting conditions deoxygenated blood contains 4ml per 100ml of carbon dioxide carried in several forms. The smallest proportion (7%) of this component is dissolved in the plasma. About 23% of the CO_2 combines with the globin portion of haemoglobin to form carbaminohaemoglobin. ($HbCO_2$) as shown in Equation 1-2.

$$Hb + CO_2 \Leftrightarrow HbCO_2 \quad \textit{Equation 1-2}$$

The formation of carbaminohaemoglobin is greatly influenced by pCO_2. For example, in tissue capillaries where pCO_2 is relatively high formation of

carbaminohaemoglobin is encouraged. However in the pulmonary capillaries where pCO_2 is relatively low, CO_2 readily dissociates from the globin and enters the alveoli by diffusion. The greatest proportion of CO_2, about 70%, is transported in plasma in the form of bicarbonate ions. The reactions are shown in Equation 1-3.

$$CO_2 + H_2O \Leftrightarrow H_2CO_3 \Leftrightarrow H^+ + HCO_3^- \quad \textit{Equation 1-3}$$

As CO_2 diffuses into tissue capillaries and enters the red blood cells, it reacts with water in the presence of carbonic anhydrase to form carbonic acid which dissociates into hydrogen and bicarbonate ions. The hydrogen ions combine mainly with haemoglobin, whereas the bicarbonate ions leave the red blood cell and enter the plasma, where they combine with sodium ions to form sodium bicarbonate. In exchange, chloride ions diffuse from the plasma into the red blood cells. This exchange of negative ions maintains the ionic balance between red blood cells and plasma, and is known as the chloride shift.

The binding of O_2 to haemoglobin causes the release of CO_2 from the blood known as the Haldane effect. It occurs because the combination of haemoglobin with O_2 produces a stronger acid than that formed by the combination of CO_2 with haemoglobin.

PROTEIN TRANSPORT

In addition to the transport of gases, blood also supplies cells with nutrients such as proteins; ultrafiltration of plasma across the capillary walls yields a gradient of plasma proteins and a hydrostatic pressure directed from the blood to the interstitial fluid. Capillaries have a high protein reflection coefficient and most protein is retained in the blood.

Normal capillary filtration is equal to lymph flow and can be described by Equation 1-4.

$$J_v = K_{FC}\left[\left(P_c - P_t\right) - \sigma_d\left(\pi_p - \pi_t\right)\right] \quad \textit{Equation 1-4}$$

J_v - volume flow across capillary wall, K_{FC} - capillary filtration coefficient, P_c - microvascular pressure, P_t - interstitial fluid pressure, σ_d - osmotic reflection coefficient for proteins, π_t and π_p - colloid osmotic pressures of plasma and tissue fluid.

1.3.3 Circulatory Changes due to Age and Disease

Age

Ageing is accompanied by a changes in the mechanical properties of cardiovascular vessels [82], including an increase in stiffness and decrease in distensibility. This increased stiffness can lead to an increase in blood pressure, although, hypotension or low blood pressure, can also occur in the very old or infirm. Peripheral vascular disease (PVD) causes symptoms in 2% of the late middle aged population and demonstrable blood flow impairment is present in 8%. PVD is associated with ischaemia of the terminal portion of a limb, most generally the lower limb, due to atheromatous obstruction of major vessels by plaques or thrombosis. Risk factors for the development of peripheral vascular disease include smoking, diabetes mellitus and hypertension. In addition, iron deficiency can lead to microcytic anaemia in elderly patients, and chronic venous insufficiency can lead to venous ulcers.

Spinal Cord Injury

During the initial period after spinal cord injury patients enter a phase known as spinal shock. This stage is characterised by an altered pattern of reflex activities; one consequence of this alteration is a reduction of vasomotor tone which can reduce blood flow to skin and subcutaneous tissues [85].

1.3.4 Thermoregulation

Human body temperature must be maintained between very close physiologically limits in order to sustain life. Below 37°C enzymatic activity becomes very low and above 41°C irreversible damage occurs to the central nervous system. Thermoregulation or temperature control involves many bodily functions and appears to operate on several levels. The most precise control occurs from the hypothalamus, although subordinate thermoregulatory structures are able to initiate localised and less precise control if hypothalamic control is impaired [103]. Thermoregulation employs feedback of thermal information from thermoreceptors to the controller and this

thermal information is influenced by various bodily mechanisms intended to lose or maintain heat.

Thermoreceptors are small, unencapsulated nerve endings distributed unevenly throughout the body. There are concentrations of thermoreceptors in the palms of the hands, the feet, the lips and the pelvic area. Thermoreceptors appear to be of two types, warm or cold. Warm receptors exhibit an increase in discharge frequency, with an increase in temperature, in the thermoneutral region, whereas cold receptors exhibit a decreased discharge frequency, with temperature increase, in the thermoneutral region, but a sharp increase in discharge frequency at temperatures in excess of 45°C. The graph in Figure 1-7 shows the output of warm and cold receptors.

The main thermoregulatory responses to increased temperature are vasodilation and the onset of sweating.

1.3.5 Sweat Gland Innervation

Individual sweat glands are innervated by postganglionic, non-myelinated class C fibres but, in contrast to normal sympathetic innervation, the principle neurotransmitter is acetylcholine (ACh) [187]. The level of sweat gland stimulation is dependent on the integration of sudomotor neuronal impulses from the central nervous system and the effect of the micro-environment at the gland. Factors which raise general sympathetic activity, such as hypotension and hypoglycaemia, may also increase sudomotor function.

The rate of sweating can be controlled by local heat and other stimuli but body temperature is the main stimulant. The thermoregulatory centres of the hypothalamus are influenced by core temperature as well as afferent nerve impulses from the periphery and sweat glands. An increase in the body temperature above a certain point, known as the temperature set point, results in the onset of sweating. Localised warming has also been shown to increase sweat rate and this effect is attributed to both an increase of transmitter at the neuroglandular junction [58] and an increased glandular response to the transmitter [151]. Local sweating can be stimulated and inhibited by administration of chemical mediators, such as pilocarpine and adrenaline.

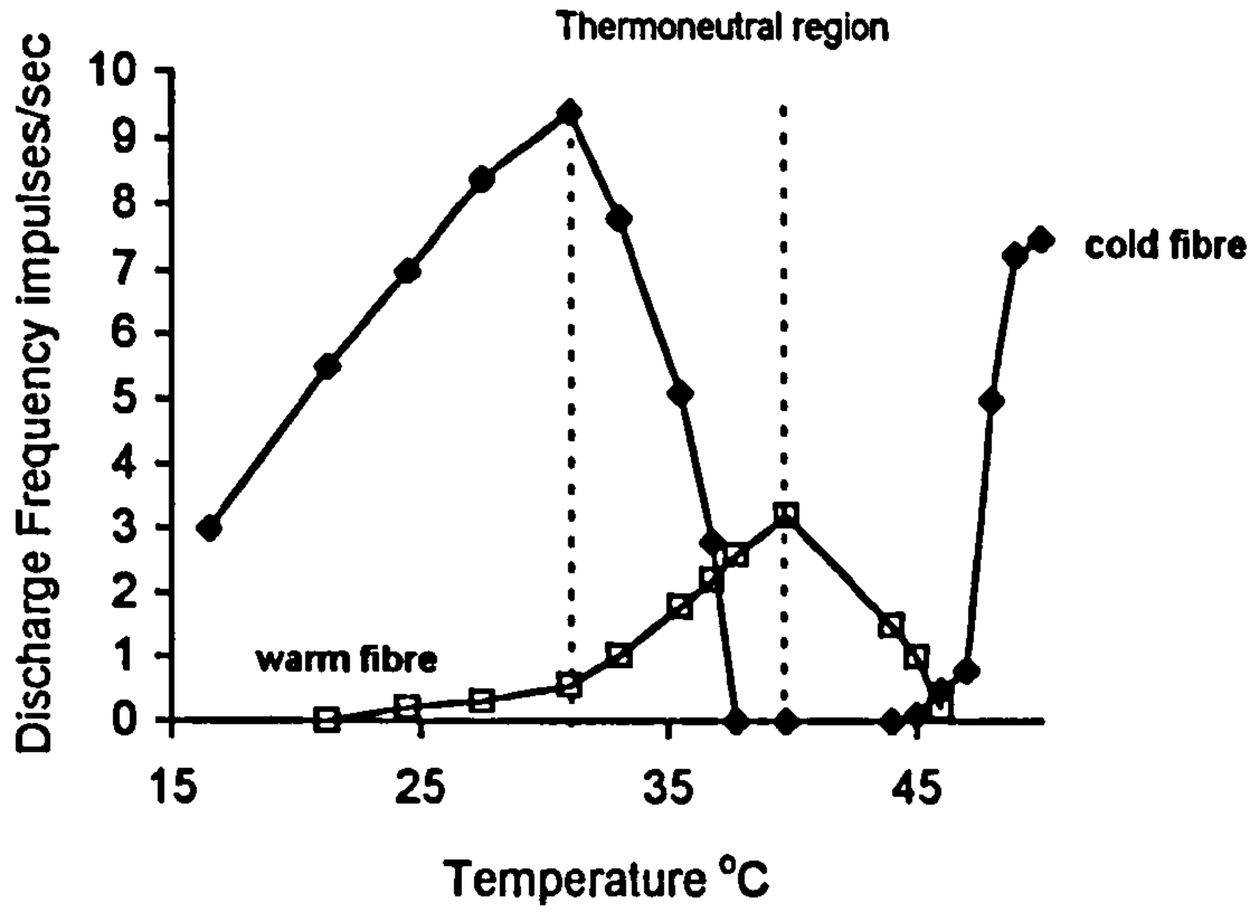

Figure 1-7 Discharge frequency of impulses to warm and cold thermoreceptors.

Different areas of the body have different preferred temperatures and therefore begin sweating at different times. As greater loss of heat is required the surface area engaged in sweating is increased as is the rate of sweating in each area. The progression of recruitment is generally from the lower extremities toward the central regions of the body and towards the head. Table 1-5 describes the order of recruitment of individual sweat glands.

Table 1-5 Table of the recruitment of sweat glands in the body. Adapted from [103]

Region of the body	General Order of Recruitment
Dorsum foot	1
Lateral calf	2
Medial calf	3
Lateral thigh	4
Medial thigh	5
Abdomen	6
Dorsum hand	7 or 8
Chest	3 or 7
Ulnar forearm	9
Radial forearm	10
Medial arm	11
Lateral arm	12

1.3.6 PRODUCTION OF SWEAT

The production of sweat takes place following stimulation by neuronal impulses, the diagram in Figure 1-8 shows the stages of sweat production in the human eccrine sweat gland. According to Cage *et al.* [31] the precursor sweat is not an ultra-filtrate like some other body fluids, but is derived from active secretion and absorption.

1.3.7 SWEAT GLAND METABOLISM

The metabolic activity of the isolated eccrine sweat glands has been studied *in vitro* by a number of researchers [183-187,219]. Wolfe *et al.* [219] showed that the removal of glucose from the incubation medium of isolated sweat glands led to a rapid exponential decrease to negligible levels, in the secretional activity of the gland within 10-15 minutes. However, the secretion ability was rapidly restored by the re-introduction of glucose into the medium.

Secreted acetylcholine (ACh) enters sweat gland
through basal lamina and intercellular channels,
where clear cells are depolarised

⇓

Na^+ ions and interstitial fluid from
dilated blood vessels flows into cell

⇓

Osmotic balance between clear cell
and intercellular channels

⇓

Na^+ pumped across luminal cytomembrane
followed by interstitial fluid and lactate
and glycolysis products

⇓

Precursor sweat expands lumen of
secretory segment and myoepithelial cells
contract to propel fluid

⇓

Isotonic precursor fluid is reabsorbed in coiled duct
by dark and myoepithelial cells

⇓

Hypotonic sweat reaches the skin surface

Figure 1-8 Flow diagram indicating the stages of sweat production.

It is generally concluded that sweat glands rely exclusively on exogenous substrates as a fuel source. Although cellular glycogen is mobilised in the eccrine sweat gland during secretion, its absolute amount is too small to sustain a continued high rate of sweat secretion [219]. These findings are also supported by the fact that acclimatised people are able to sweat more profusely, despite the limited levels of glycogen in their sweat gland cells.

Sato *et al.* [187] has shown that, although the sweat gland can utilise lactate and pyruvate from exogenous substrates, the most efficient substrate for sweat gland function is glucose. Wolfe *et al.* [219] proposed that the sweat gland produces high levels of lactate which they suggest is produced by anaerobic metabolism of glucose, however their experimental findings did not support this theory. Consequently, it is thought that glycolytic activity of the normal sweat gland is not the main energy pathway. The main route of energy production is thought to be the oxidative phosphorylation of ATP (adenosine triphosphate), utilising substrate glucose with glycolytic activity providing less than 10% of sweat gland energy [219]. However experiments have shown that alterations to sweat gland oxygen supply can radically alter the composition of secreted sweat [119,212-213,207]. The role of glycolysis in the absence of sufficient blood supply may provide a more important role in sweat gland metabolism.

1.3.8 Composition of Normal Human Eccrine Sweat

The main secretion of the human eccrine sweat gland is water although electrolytes, heavy molecules, organic compounds and macromolecules are also secreted. The concentration of these chemicals in sweat is affected by a number of factors, including sweat rate and the metabolism of the sweat gland. Table 1-6 outlines the major components of human eccrine sweat.

The primary secretion of the sweat gland is nearly always isotonic with plasma, with changes in the composition arising due to ductal moderation [81]. As ductal moderation is a function of sweat rate, it would follow that the concentration of a number of sweat components is also a function of sweat rate.

The most extensively studied sweat component is sodium concentration [Na^+]. In primary fluid, sodium is nearly isotonic with plasma irrespective of sweat rate [35]. However, sweat sodium concentration increases with sweat rate since the sweat concentration is dependent upon the ductal ability to absorb sodium. The mechanism of sodium absorption in the ductal region is not properly understood, although it is thought that aldosterone may be a regulator [221].

Table 1-6 The composition of human eccrine sweat. Adapted from [122].

Components	Concentration	Range	Notes
Inorganic			
Sodium	46.8 mmol/L <50yr 60.0 mmol/L >50yr	-	May increase with sweat rate. Acclimatisation leads to decrease. Concentration reflected by sodium concentration in diet
Chloride	29.7 mmol/L <50yr 38.9 mmol/L >50yr	-	Changes with age, following similar changes in sodium concentration. Greatly increased in cystic fibrosis.
Potassium	8.6 mmol/L	-	Concentration affected at high sweat rates, and by method of stimulation.
Organic			
Urea	19.6 mmol/L	11.8 - 33.1 mmol/L	At low sweat rates, concentration in sweat is about 4 times that in serum. At higher rates, it is closer to serum level.
Uric Acid	12.0 µmol/L	-	
Lactic Acid	25.5 mmol/L	14 - 42 mmol/L	Concentration decreases with increasing sweat rate. The concentration of sweat lactate exceeds that in serum by 4 - 40 times. Higher concentration in male sweat.
Creatinine	41 µmol/L	19 - 74 µmol/L	Concentration decreases with increasing sweat rate.
Ammonia	3.02 mmol/L	-	Concentration varies greatly due to the production of ammonia by bacteria. The amount far exceeds that found in serum.
Amino acids	-	1.2 - 3.6 mmol/L	
Histamine	121 mmol/L	85-180 mmol/L	
Protein	77.3 mg/L	60-115 mg/L	

The sweat potassium concentration [K^+] of precursor sweat is isotonic with plasma and similar to that of interstitial fluid [81]. Sweat potassium concentration is a function of potassium permeability and electrical potential of duct walls; again aldosterone is thought to play some part in the control of sweat potassium concentration [183]. The concentration of potassium has been shown to increase linearly with sweat rate above a threshold level of sweat rate.

Sweat chloride concentration [Cl^-] increases with sweat rate in proportion to sweat sodium concentration, although chloride concentration is usually 20-25 mM lower than sodium concentration in both primary and final sweat. Yates *et al.* [221] showed that the re-absorption of chloride is highly dependent on aldosterone, and therefore abnormally high levels of sweat chloride concentration are found during adrenal insufficiency.

Sweat lactate is derived mainly from the sweat gland as an endpoint of glycolysis [184]. The lactate concentration in precursor sweat is similar to the bicarbonate concentration in interstitial fluid although sweat contains no bicarbonate ions. There is an inverse relationship between lactate concentration and sweat rate, with highest lactate concentrations at lowest sweat rates [207]. Sweat lactate may be instrumental in controlling desquamation of the stratum corneum, as evidenced by the well known beneficial effects of topical lactate preparations on retention hyperkeratosis [185].

There is argument as to whether sweat urea is derived from the passive diffusion of urea from the plasma [113], or is a product of the sweat gland metabolism [187]. Urea can cross the glandular wall readily and a 'urea frost' can be seen on the skin of patients with uraemia [185].

1.3.9 Changes in Sweat Gland Function due to Age and Disease

Age

Rates of sweating show variations with age; infants demonstrate the lowest sweat rates, which increase over the next two decades, followed by a decrease towards old age [122]. Foster *et al.* [74] carried out a study on a large number of subjects to investigate the differences in sweat response between the young and the old. They found an increased threshold of core temperature required for the onset of sweating and a reduced sweat rate in the elderly group, which was particularly significant in

females. Atrophy of sweat glands is associated with ageing skin and general poor skin conditions [142].

SPINAL CORD INJURY

Sudomotor function in the spinal cord injured depends upon the level and the extent of the lesion and the time after injury. Indeed, an incomplete lesion where the spinothalamic tract is spared will not affect the sweating response. However, complete interruption of the sudomotor pathways between the hypothalamus and the sympathetic outflow will abolish the thermoregulatory function and lead to anhydrosis. In the early stages of spinal cord injury sudomotor deficiency is extensive, but with time sweating may return and can even be present in a few dermatomes below the level of the lesion. In the body section near the lesion exaggerated activity of the sweat glands may be caused by the autonomic border zone reactions, which could be related to increased pilomotor or vasomotor responses. In addition, reflex sweating may occur in some patients elicited by intrinsic or extrinsic stimuli, for example, a change in posture or infection [85].

1.4 BIOMECHANICS OF SKIN AND SUBCUTANEOUS TISSUE

1.4.1 INTRODUCTION

In vivo and *in vitro* studies on skin and soft tissue have led to a greater understanding of their mechanical properties. The relationship between the properties of tissue elements, their structure and chemical bonding, have also increased the understanding of the mechanical behaviour of tissue.

Human tissue is a complex, layered, fibre-reinforced composite, comprising of fibrous proteins, collagen and elastin, and a gel of hydrated proteoglycans. Therefore the mechanical properties of soft tissue can be described as a combination of the properties of the individual components.

Collagen forms 70% of the dry weight of skin and is present in the form of a 3D meshwork of fibres. Tensile tests on tissues with high collagen content, such as tendon,

show that collagen fibres are strong and stiff, but with low extensibility. Collagen fibres are described as having an elastic modulus of 1-2 GPa [13] and a strain to failure of 10-15% [13]. Elastin forms only 4% of the dry weight of skin, it remains elastic over very large ranges and has a modulus much lower than that of collagen, at about 0.3 MPa [13]. However, the elastin network has little inherent strength, as without the collagen fibre, the framework ruptures at strains an order of magnitude smaller than those observed in a single elastin fibre [13]. This finding reinforces the fact that it is the interaction of the various components of the tissue which are responsible for its mechanical properties, rather than the properties of the individual components.

Mechanical testing of skin and soft tissues usually takes the form of the uniaxial or biaxial tensile tests or compression tests, though some torsional tests have been performed [13]. Soft tissues are non-homogeneous in nature with a high degree of orientation, and therefore direction of testing is an important factor. *In vivo*, skin is under biaxial tension and therefore these kinds of test can more accurately represent the *in vivo* situation. However biaxial tests are notoriously complicated and difficult to perform accurately. There are a number of problems inherent in the *in vitro* study of tissue mechanical properties, including preconditioning, gripping of specimen, strain measurement, specimen dimensions, storage, moisture gradients, temperature and solute concentrations which can cause variation during *in vitro* testing.

1.4.2 Tensile Properties of Skin and Soft Tissue

Simple tensile tests on specimens of skin and soft tissue yield a characteristic non-linear stress-strain relationship. The characteristic curve shows two distinct regions, one occurring at low strain and the other at high strain. The low strain region is linear up to strains of 40% and exhibits a modulus of 5 kPa, 100 times less than that of soft rubber or elastin [49]. Within this region of the curve, the tissue exhibits elastic behaviour and the properties are thought to be influenced by elastin and proteoglycan content [49] rather than collagen. The elastin fibres act as an elastomeric material and provide a spring return mechanism for the collagen network [48]. Wijn *et al.* [215] modelled the collagen as sinusoidal crimped fibres which merely straighten during the

initial region. At high strains the collagen fibres have become fully straightened and the properties of the tissue reflect the properties of the fibres themselves, showing high modulus of elasticity and low strain to failure.

It is interesting to note that the stress-strain curves for skin are dependent upon the direction of loading, highlighting the anisotropic nature of the tissue. The graph in Figure 1-9 shows the force-strain curves for specimens loaded parallel and perpendicular to the direction of the Langer's lines. North [150] demonstrated the difference between the stress-strain curves for skin, including only epidermis and dermis, and those including both skin and subcutaneous tissue, highlighting that the attachment of the subcutaneous tissue significantly increased the ultimate tensile strength of the skin. This work showed that the properties of the skin and underlying tissue were important in enabling it to support load by absorbing energy through deformation and eventual rupture.

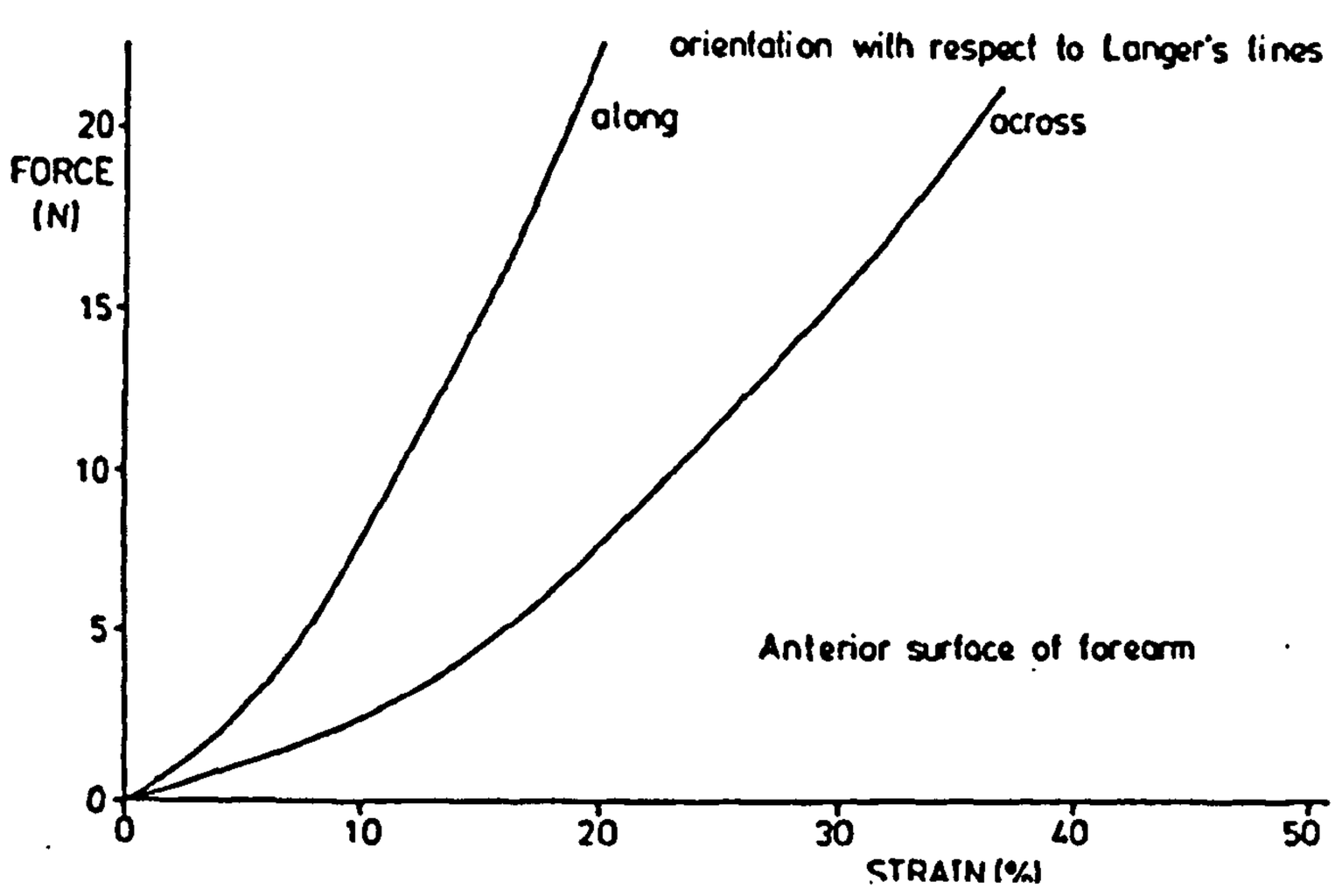

Figure 1-9 The force-strain curve for skin. Adapted from [6].

1.4.3 Compressive Properties of Skin and Soft Tissue

Skin and soft tissue are subjected to compressive loading when they come into contact with any supporting surface, such as a mattress, wheelchair or seating device

or even a prosthetic or orthotic device, such as a socket for an artificial limb. Therefore the compressive properties of skin and soft tissue have more relevance to physiological loading conditions than tensile properties.

Compressive properties of tissues have been studied *in vitro* and to a lesser extent *in vivo* [6,10,13,39,49,111,150,222]. Similar to the response in tension, stress-strain curves for tissue in compression are also non-linear and exhibit viscoelastic behaviour. Models for the compression of soft tissue have been based on the movement of fluid away from the compressed tissue. There is a continuing debate as to whether tissue is incompressible due to the large water content or whether fluid transport is one of the mechanisms of tissue deformation. A model of fluid transport is shown in the Figure 1-10.

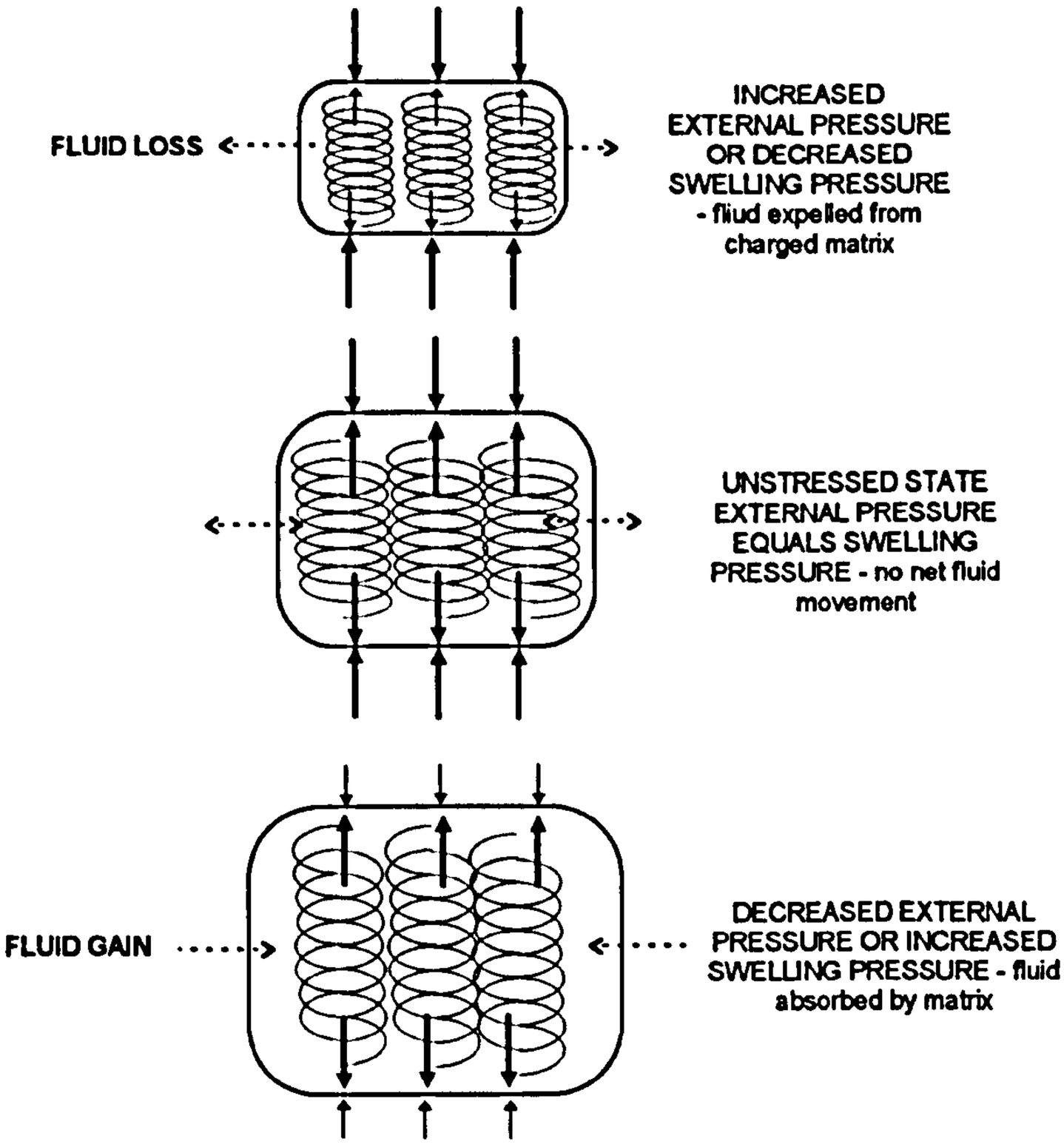

Figure 1-10 Fluid transport in to and out of tissue during compression. Adapted from [93].

Daly [49] used ultrasound to measure the thickness of skin during compression in order to investigate the properties of soft tissue. He noted very large changes in the

volume of skin which were attributed to fluid expulsion. However, the changes in acoustic velocity of the tissue during compression were not considered, which would lead to inaccuracies in this method of measurement.

1.4.4 VISCOELASTICITY

A number of different techniques have been employed to measure viscoelastic properties of soft tissue. Indenters have been used to measure uniaxial creep [223] and torsional creep [13] *in vivo*. In contrast, Pereira *et al.* [154] and Potts *et al.* [159] used wave propagation techniques to investigate the frequency response of soft tissues *in vivo*. At frequencies up to 500 Hz the viscoelastic properties were influenced mainly by the epidermis, while at higher frequencies the properties appeared to be more dependent on the proteoglycan component of the soft tissue. Manschot *et al.* [130] suggests that the elastin content of tissue is more important to its viscoelastic response after load removal, than during load application.

There are two basic models of viscoelastic response, which can be modified to describe the behaviour of a number of different materials including soft tissue. The two models are the Maxwell and Voigt models, which comprise of an arrangement of springs and dashpots. The springs represent the linear elastic components of the material, whereas the dashpots represent the viscous components. Kett & Levine [110] developed an extended model of the viscoelastic properties of tissue undergoing uniaxial tension and torsion shown in Figure 1-11. K_1 and K_2 represent the elastic behaviour, B_2 represents the viscoelastic behaviour, B_1 represents the body fluid imbibed in and expelled from the tissue by the externally applied pressure and V_1 is the fluid source.

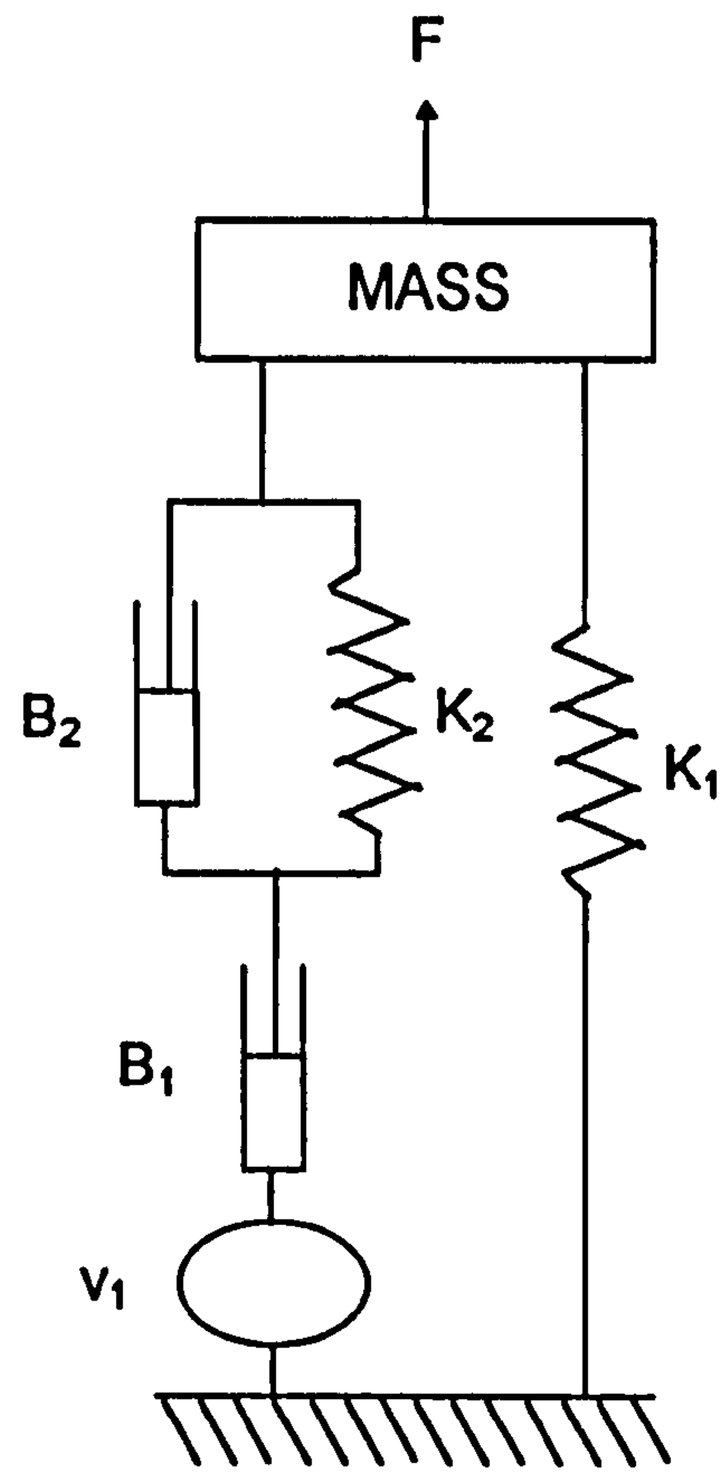

Figure 1-11 Viscoelastic model of skin. Adapted from [110].

1.4.5 Biomechanical Changes due to Ageing and Disease

The biomechanical properties of tissue can be affected by the natural process of ageing and specific disease. Normal ageing is accompanied by dermal and epidermal atrophy which leads to wrinkling, loss of elasticity, and flattening of the dermal papillary ridges which decreases the inherent resistance to shear forces. Ageing is also accompanied by a reduction in the ratio of type I to type III collagen fibres [82]. Ultraviolet radiation can cause thickening of elastin fibres and degradation of collagen fibres, which leads to a decrease in the skin extensibility and elastic recoil.

Kirk & Kvorning [111] found a number of mechanical changes in ageing skin compared to young skin, including a decrease in the elastic properties, an increased tissue stiffness, and a reduced recovery after removal of load. Hickman *et al.* [94] also reported a reduction in the instantaneous elastic compression and a delayed elastic recovery in the tissue of ageing subjects compared to young subjects. They also found

that oedematous tissue exhibited less elastic compression and more delayed compression with a slower recovery. Changes in mechanical properties are attributed to the increase in non-reducible cross-links of fibrous constituents of older soft tissues, changes in the elastic network, and an increased fluid flow away from tissues which leaves them stiffer [49].

1.5 SUMMARY

This chapter has described some of the anatomy and physiology important to the understanding of viable skin and subcutaneous tissues, whose main mechanical function is to provide supporting surfaces for the underlying body structures. The viability of the tissue is maintained by a balance between supply and removal of nutrients by the micro-circulatory system which is aided by the removal of harmful waste products and toxins by the lymph system. The eccrine sweat gland, a metabolically active unit contained within the layers of the dermis has also been described. This gland will play an important part in the rest of the thesis. Finally the concept of the mechanical function of the skin and soft tissue was described, in terms of how the skin and soft tissues respond to mechanical deformation.

2. SOFT TISSUE BREAKDOWN

2.1 INTRODUCTION

Soft tissue breakdown is a generic term which can be used to describe ulceration of the skin and underlying soft tissue. This can occur in a number of different physiological situations but most commonly at the interface between the skin and a supporting surface. Examples of soft tissue breakdown include the development of pressure sores in elderly or immobile patients who remain supine, prone or wheelchair bound for long periods of time. Similar tissue problems are experienced by lower limb amputees as a result of functional support from their prostheses.

The problem is by no means a recent one and renowned surgeons such as Charcot [36], Paget [153] and Hunter [97] all regarded the management of pressure sores as essential in surgery and medicine. Indeed in 1873, Paget [153] described the pathological definition of pressure sores as the 'sloughing and mortification or death of a part produced by pressure'. The problem of soft tissue breakdown has taken on new importance in the last few years in a society where health care litigation is becoming more commonplace and the cost of health care more accountable.

2.2 AETIOLOGY

Although there are a number of factors implicated in the aetiology of tissue breakdown, the common factor is prolonged pressure applied to the tissue. Pressure applied to the skin can take the form of compression, shear or frictional forces. These forces can occur due to the interaction between the tissues and a supporting surface such as a mattress, chair or external prosthesis.

Some tissues of the body are designed to carry high compressive loads, for example articular cartilage, which is avascular and aneural, and have developed specific mechanical properties which resist tissue breakdown under the influence of prolonged periods of cyclic loading. Problems occur however, when tissues which are not

specifically designed to withstand prolonged loading are subjected to such conditions at the patient-support surface interface.

The viability of soft tissue and skin, as living organs, is dictated by a delicate balance between nutrient supply and waste product removal. Any disruption to this equilibrium can lead to cell injury or necrosis, and potentially to complete tissue breakdown. It is clear that although tissue breakdown will not occur in the absence of pressure, pressure may not be solely responsible, as some people can tolerate high pressures without tissue damage. There appears to be many other factors which predispose tissue to compromise of its biochemical and structural integrity; these can be divided into extrinsic and intrinsic factors. Extrinsic factors are generally the result of the external environment and can therefore potentially be controlled whilst intrinsic factors are inherent to the individual and as such are much more difficult to control. Individual factors will be discussed under these two classifications.

2.2.1 Extrinsic Factors

Pressure

Pressure applied to soft tissues is undoubtedly one of the major causes of tissue breakdown. Normal cell metabolism is dependent upon the delivery and removal of nutrients and waste products via a healthy blood supply. Any factor which disrupts the transport of blood to the soft tissues will eventually disrupt the normal cell metabolism and can consequently lead to cell and tissue necrosis. Disruption of capillary flow can lead to insufficient supply of nutrients to surrounding tissue and obstruction of lymph prevents drainage of catabolic waste, extracellular proteins and excess fluids [86,87]. The major cause of blood flow disruption is externally applied pressure due to the reaction of forces at a patient-support interface.

Figure 2-1 shows the effect of varying pressure on soft tissues highlighting the distortion of the soft tissue structures.

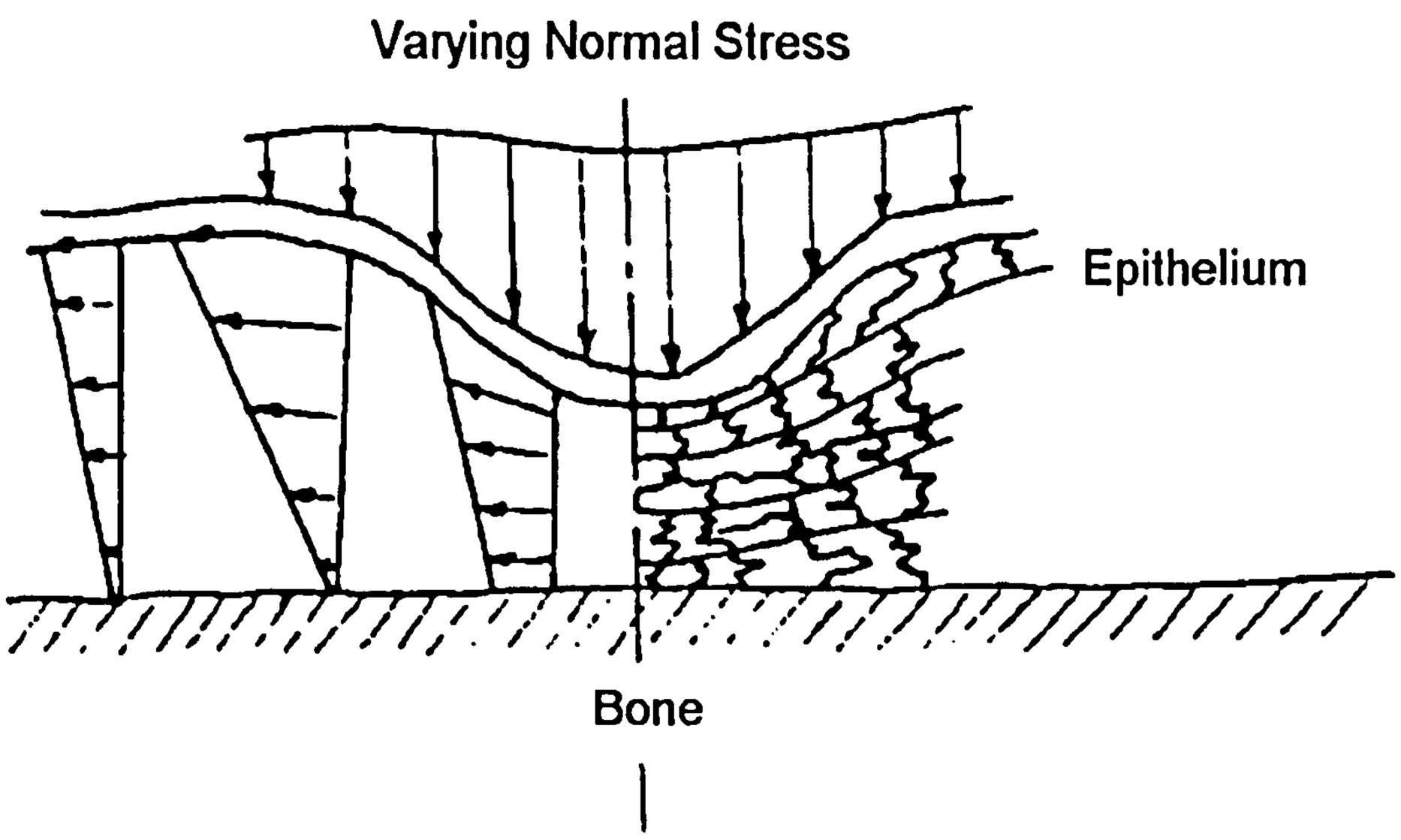

Figure 2-1 Pressure distribution in soft tissue. Adapted from [21]

Many researchers have postulated that externally applied pressures, in excess of the capillary perfusion pressure, will cause capillary closure. Landis [121] showed that pressures above 32 mmHg (4.26 kPa) were sufficient to close the capillaries of the nail bed, consequently this figure is often quoted as a safe maximum above which tissue breakdown may occur. However, due to the nature of the experimental technique and the specific site chosen to measure perfusion pressures, this figure is probably not indicative of critical pressure within soft tissues adjacent to bony prominences. It also can not be used as a safe threshold for externally applied pressures.

Excessive loading and pressures can be induced by inappropriate posture or uncompliant support surfaces. A patients own body weight has implications for excessive loading. Thus, an obese person has the problem of distributing a much larger load, whereas an emaciated patient may have a much lower body weight but may have exaggerated bony prominences and a reduction in effective area of support tissues.

SHEAR

In most loading situations, the tissues of the body are subjected to a complex distribution of stresses. Stress is a second order tensor, whereas pressure is a scalar quantity. In normal situations the term pressure is used to substitute normal stress, i.e. stress in a direction perpendicular to the surface of the skin. Shear stress is defined as a stress in the direction of the surface of the skin or surface to which load is applied. With respect to soft tissue two models of shear are shown in the Figure 2-2.

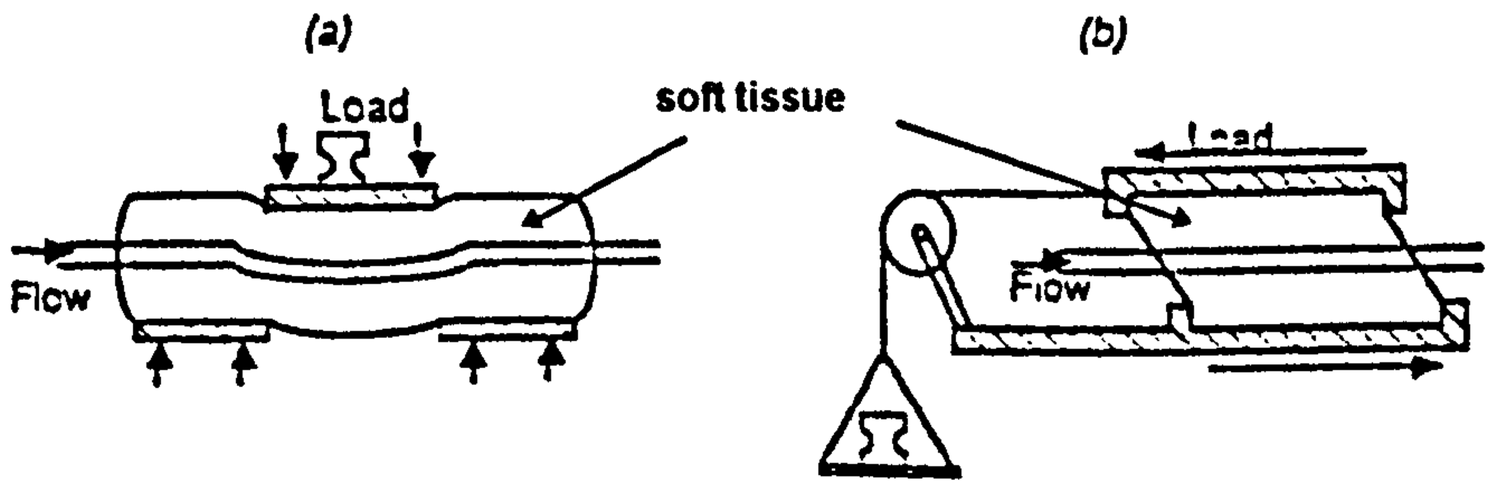

Figure 2-2 Shear models a) pinch b) horizontal. Based on [17].

The emphasis in the literature appears to be upon the effect of normal pressure on tissue breakdown, although the effect of shear has occasionally been discussed. With respect to spinal cord injury, Guttmann [85] proposed that 'one must distinguish between purely vertical pressure and shear stress, of which shear stress is much more disastrous, for it cuts off larger areas from their vascular supply'.

Horizontal shear or friction between the skin surface and underlying surface can cause the loosely attached superficial tissues to slide over the deeply anchored fascia through which the blood vessels pass, as shown in Figure 2-3. The vessels can become obliterated, kinked or ruptured leading to deep necrosis of the tissue [169]. Pinch shear (Figure 2-2b) can occur at the site of a bony prominence and can also cause the obstruction and occlusion of blood vessels leading to tissue death.

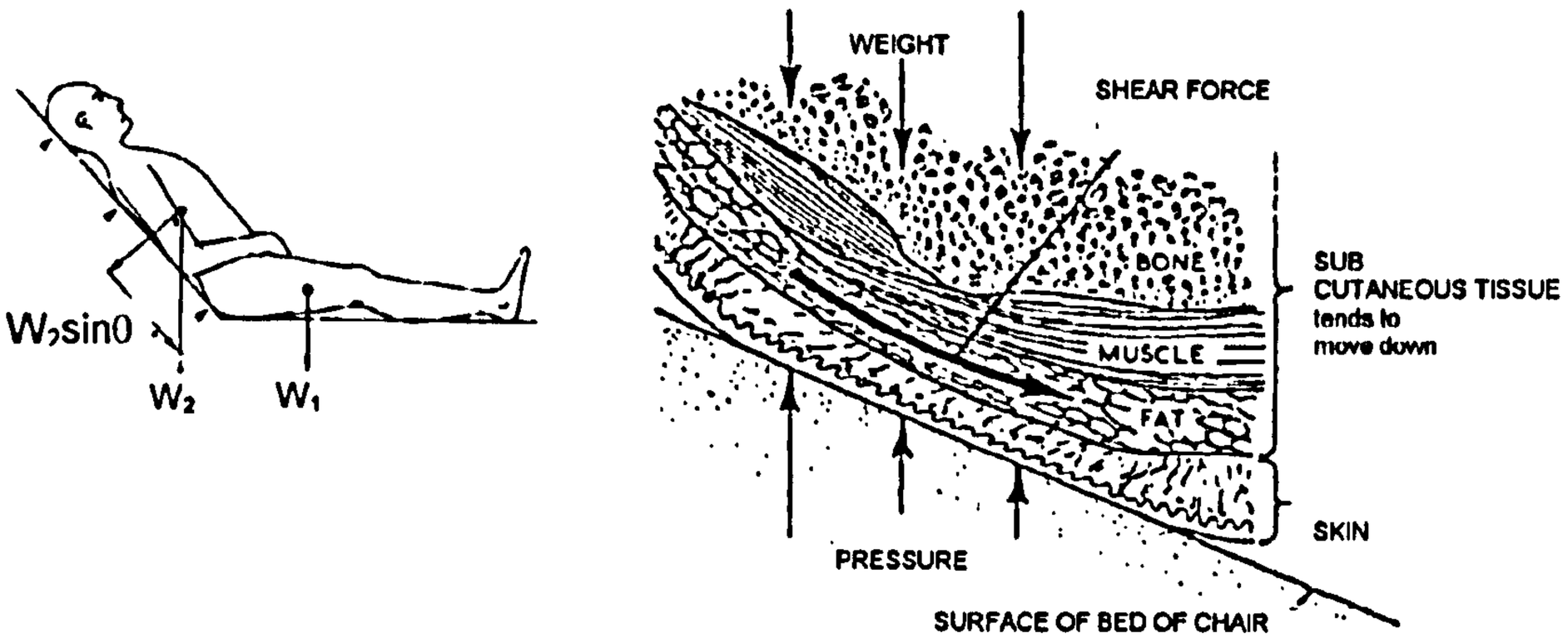

Figure 2-3 Effect of shear forces on soft tissue, resulting from body posture. Adapted from [26].

Bennett *et al.* [17] carried out experiments on blood flow and showed that the pressure required to produce occlusion of blood vessels can be reduced by 50% if accompanied by shear forces. This finding has consequences for the prevention of tissue breakdown, where shear forces become particularly important in the positioning and transferring of patients on a mattress or support surface.

TIME

Although pressure and shear have been identified as major factors in the development of tissue breakdown, time is also of great importance. Early researchers [115,116,98] showed that although very high pressures could be tolerated by soft tissues if they were applied for a very short period of time, relatively low pressures that were maintained for long periods of time could however be very damaging. This observation led to the development of pressure-time curves which show the relationship between continuous pressure, duration and the development of tissue breakdown. Examples of such curves are shown in Figure 2-4. It is clear that each model relationship exhibits a similar inverse form, although events were observed at different absolute values.

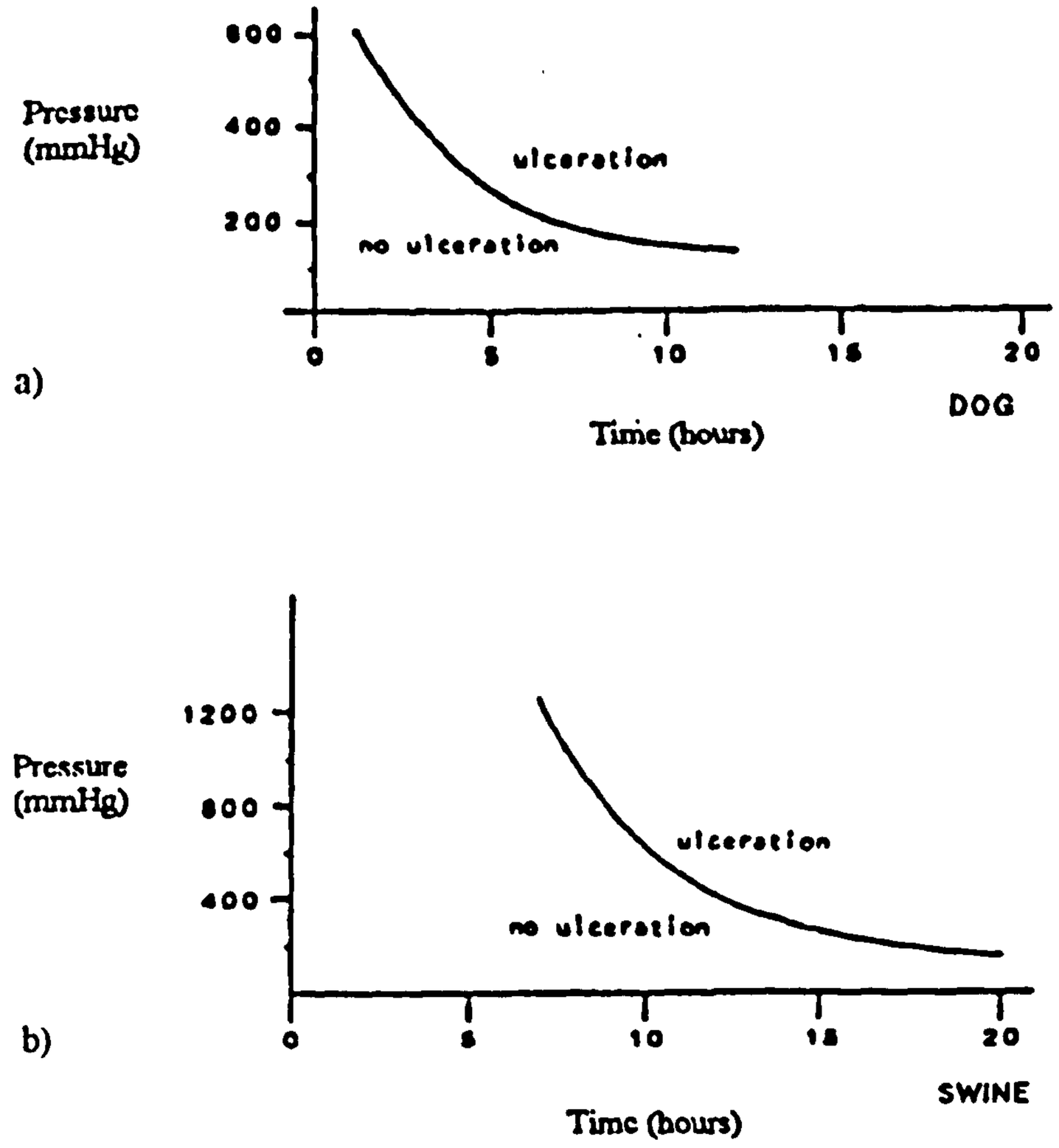

Figure 2-4 Pressure-time relationships for different model systems . a) dogs, b) swine, c) humans. Adapted from [50,115].

Sacks *et al.* [176] developed a theoretical model function using dimensional analysis based on the curves in Figure 2-4. The model is shown in Equation 2-1 and highlights the importance of pressure, time, blood flow and tissue properties.

$$P_s = f\left(\frac{\rho Q^{2/3}}{Et^{4/3}}\right) \qquad \textit{Equation 2-1}$$

P_s. allowable pressure, p - tissue density, Q - local blood flow, E - tissue elastic modulus, t - time

MOISTURE

Elevated temperatures and moisture at the interface between the soft tissues of the body and a supporting surface can increase the susceptibility to tissue breakdown. Moisture can lead to the maceration of tissues, which can decrease their ability to withstand pressure and shear forces. Excessive moisture produced by incontinence is a particular problem as it can lead to the incubation of microbial activity which can increase the severity of any tissue damage that does occur.

2.2.2 INTRINSIC FACTORS

MOBILITY

The ability of a patient to move freely, in order to redistribute the forces over a larger area of soft tissue, is of significant importance in the maintenance of tissue viability. Measurements of bodily movements during a seven hour period at night have shown that a reduction in the number of movements is directly related to the incidence of pressure sores in a group of elderly patients [65]. The ability to move is reduced in a number of patient groups including patients suffering from paralysis, locomotor disorders or fractures, patients who are drowsy or stuporose, sedated, or undergoing surgical procedures under general anaesthesia. Due to the inability to redistribute pressure, these patients are at a particularly high risk from developing tissue breakdown.

SENSATION

When the ability to perceive pain caused by excessive loading or ischaemia is impaired, the susceptibility to tissue breakdown increases. Spinal cord injured subjects who are not able to feel pain below the level of their lesion are particularly susceptible. It is interesting to note that a comparable group of subjects with poliomyelitis, who are

paralysed, but can still perceive pain, exhibit a much lower incidence of tissue breakdown compared to the spinal cord injured [65]. The normal response to pressure pain signal is shown in Figure 2-5.

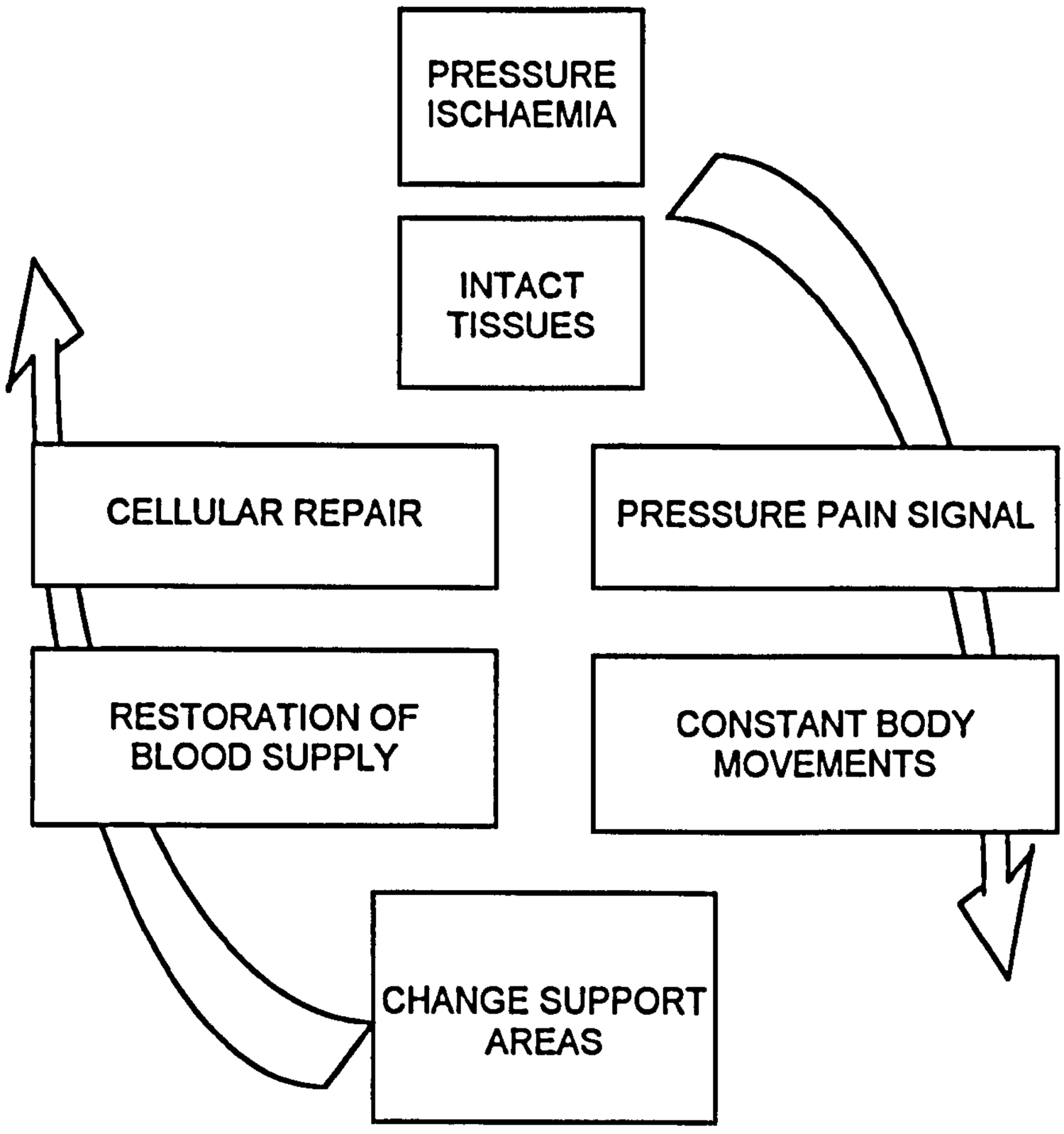

Figure 2-5 Healthy response to tissue ischaemia caused by pressure.

NUTRITION

Changes in the nutritional status of patients has been implicated in the susceptibility to tissue breakdown; protein, nitrogen, calcium and sulphur balances [143], as well as vitamin C depletion [100], have all been associated with tissue viability. A reduction in the nutritional status of patients also affects the rate of healing and can hinder the recovery of patients suffering from tissue breakdown.

BLOOD FLOW

Blood flow is crucial to the viability of tissues and cells in terms of supply of nutrients and removal of waste products. Pressure and shear can act to reduce this blood flow and, if this is combined with other factors which may already have caused a reduction in blood flow, the potential for development of tissue breakdown is enhanced. Factors which can decrease tissue micro-circulation include diabetes, anaemia, peripheral vascular disease, hypotension, spinal cord injury and oedema, during which swelling increases the normal diffusion pathways between the cells and the blood supply.

TISSUE INTEGRITY

The structural integrity of tissue can be diminished due to a number of factors which may lead to a decreased ability to withstand pressure and shear. Dehydration, oedema, atrophy, loss of tone of muscle tissue and changes in collagen biochemistry [43,44,117], can all lead to reduced ability to support load.

CONTINENCE

Urinary and faecal incontinence can lead to excessive moisture and increased microbial activity at the interface between tissues and support surfaces. For this reason proper treatment of incontinence will reduce the susceptibility to tissue breakdown caused by maceration of the tissues.

2.3 PATHOPHYSIOLOGY OF TISSUE BREAKDOWN

Tissue breakdown is the result of ischaemia developed in tissues due to the application of forces which can occlude blood flow and upset the balance between nutrient supply and waste product removal. Histological studies have shown that after pressure has been applied for a period of time, there is dilation of capillaries and venules and an associated swelling of endothelial cells, changes in osmotic pressures and fibrinolytic activity. A number of theories have been proposed to describe the consequence of this occlusion, many of which have been based on the results of

pressure applied to tissues employing animal models. The seminal studies are highlighted in Table 2-1.

Table 2-1 Key studies into the pathophysiology of tissue breakdown using animal models.

Reference	Model	Applied Pressures*	Times	Site	Comments
Husain [98]	rat	100-600 mmHg (13.3-80 kPa)	1-6 hours	tail - cuff	cord transection
	guinea pig	100-300 mmHg (13.3-40 kPa)	1-3 hours	legs	
Kosiak [115]	dog	100-550 mmHg (13.3-73.3 kPa)	1-12 hours	trochanter, IT	
Kosiak [116]	rat	35-240 mmHg (4.66-32 kPa) (alternating/constant)	1-4 hours	hamstrings	
Daniel *et al.* [50,51]	pig	100-1000 mmHg (13.3-133.3 kPa)	4-16 hours	trochanter	normal and paraplegic
Dinsdale [53]	pig	160-1100 mmHg (21-146.6 kPa) with and without friction	3 hours	iliac spine	paraplegic and normal
Sapega *et al.* [182]	dog	350 mmHg tourniquet cuff	3x1 hours 2x1.5 hours 2+1 hours 3 hours	hind limb	anaesthetised

* All pressures applied using an indenter unless stated.

Husain [98] carried out some of the earliest experiments on the effects of pressure on soft tissue and the development of tissue breakdown using both rat and guinea pig models. Pressure was applied to the tails and legs using pressure cuffs. Varying magnitudes and durations of pressure were applied and some animals were transected at the spinal cord to model paraplegia. His main conclusions were that uniformly distributed pressure was less damaging than localised or point pressure and that low pressures maintained for long periods of time produced more tissue damage than high pressures for short periods. The work suggested that pressure caused an increase in the permeability of capillaries producing oedema whereby lymphatics and venous channels become blocked. Pathological changes included loss of muscle striations, conversion of

sarcoplasm into homogeneous material, fragmentation, granularity and necrosis of muscle fibres.

Kosiak [116] carried out experiments in which the magnitude and duration of pressure applied to the legs of dogs was varied and the relationship between pressure and time correlated with degree of tissue breakdown. At pressures less than 100 mmHg (13.3 kPa) applied for less than 2 hours reported events included cellular infiltration, interstitial capillary haemorrhage and cellular degeneration. At pressures of approximately 100 mmHg (13.3 kPa) applied for 6 hours the results were of a similar nature but more severe and included extravasation and hyaline degeneration. At pressures above 100 mmHg (13.3 kPa) applied for periods up to 12 hours, muscle necrosis and venous thrombosis were reported in addition to the previous accumulated damage.

Daniel *et al.* [50] carried out similar pressure time studies but used a pig model since this is the most appropriate in terms of similarities in structure to human skin. They reported three stages of tissue breakdown; no damage, muscle damage and skin and muscle damage. They suggested that pathological changes occur first in the muscle and progress upwards towards the skin with increasing pressure and duration. This finding was in contrast to Kosiak [116], who suggested that breakdown occurred at all tissue levels at the same time. Experiments were also carried out on paraplegic pigs, with a considerable period of time between transection and experiment. These paraplegic pigs were more susceptible to tissue breakdown due to changes in tissue integrity. Daniel's findings showed that, although the paraplegic pigs demonstrated a similar inverse relationship between pressure and time, the actual magnitudes of these pressures and times were significantly less than in the normal pigs. These differences were attributed to atrophy of the soft tissue in the paraplegic pigs.

Witkowski & Parish [218] studied histological sections taken from human decubitus ulcers and showed that there was an infiltration of platelet aggregates and red blood cell engorgement in the dermis, though similar changes in the epidermis were not noted until later stages of ischaemia. This suggested that epidermal cells have a greater ability to withstand prolonged absence of oxygen than dermal cells.

Sapega *et al.* [182] were interested in the effect of a period of reperfusion during tourniquet induced ischaemia. Various indicators were monitored including high energy phosphate profile, cell pH and leakage of creatinine phosphokinase as well as ultrastructural degeneration. They found that a period of 5 minutes or more of reperfusion significantly reduced the degree of ischaemic injury. They suggested that tourniquet ischaemia could be safely administered for a period of one and a half hours but with a period of reperfusion, this could be doubled.

Krouskop [117] has suggested that ischaemia can result in the synthesis of a soluble form of collagen and Claus-Walker *et al.* [43,44] observed a breakdown in collagen in spinal cord injured patients. These effects could lead to a reduction in the mechanical properties of the tissue and a disruption of the transport of nutrients and also an inability to remove toxic substances following removal of pressure. Krouskop [117] highlighted the importance of the role of lymphatics in the drainage of toxins from tissue. Lymph propulsion is largely dependent upon lymphatic smooth muscle contractions and the motility of these vessels is very sensitive to distension, hypoxia and circulating hormones especially histamine, serotonin and prostaglandins. Lymphoedema, an accumulation of lymph, results in tissue necrosis which is very similar to the tissue breakdown seen in pressure sores [140]. A modified model of tissue breakdown is shown in Figure 2-6.

2.4 Cascade of Tissue Breakdown

Tissue breakdown can be described as 'a new or established area of skin and/or tissue discoloration or damage which persists after the removal of pressure and which is likely to be due to the effects of pressure on tissues' [160]. Examples of tissue breakdown are shown in Figure 2-7.

Tissue breakdown may develop by one of two types, designated superficial or deep. Superficial sores tend to develop in the skin surface and progress downwards into the tissue. These sores can be identified visually and with careful nursing will be generally treated quickly. By comparison, the deep sore initiates in the muscle over the site of a bony prominence and progresses upwards; it may not be detected until the skin is

finally broken revealing the full extent of the damage. This deep penetrating necrosis involves the destruction of subcutaneous tissues such as the fascia, muscle and eventually bone.

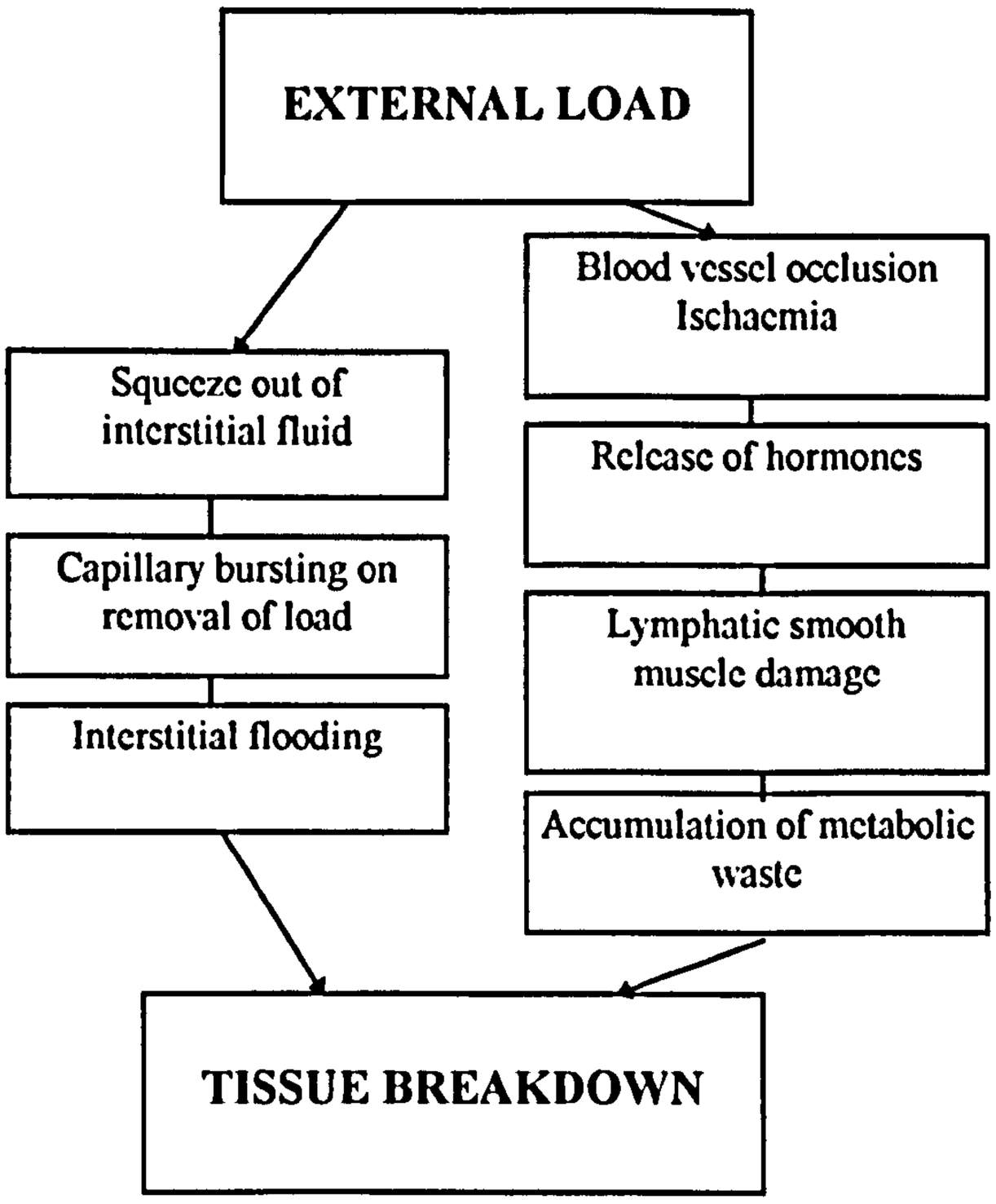

Figure 2-6 Proposed mechanism for soft tissue breakdown. Adapted from [117]

If the patient has more than one sore, it is possible that they may join forming a deep sinus which connects with large bursae. These deeper sores may require reconstructive surgery that involves excision of the underlying bone so that, once healed, the bony prominence cannot cause the same problem.

A number of categories exist to describe the degree of tissue breakdown. These categories are designed to enable an objective assessment of the degree of damage and the rate of healing of an area of tissue breakdown. Tissue breakdown may be represented in four stages;

- Stage I-Non-blanchable erythema of intact skin.
- Stage II-Partial thickness skin loss involving epidermis and/or dermis.
- Stage III-Full thickness skin loss involving injury or necrosis of subcutaneous tissue.
- Stage IV-Full thickness skin loss with extensive destruction to muscle, bone or supporting structures.

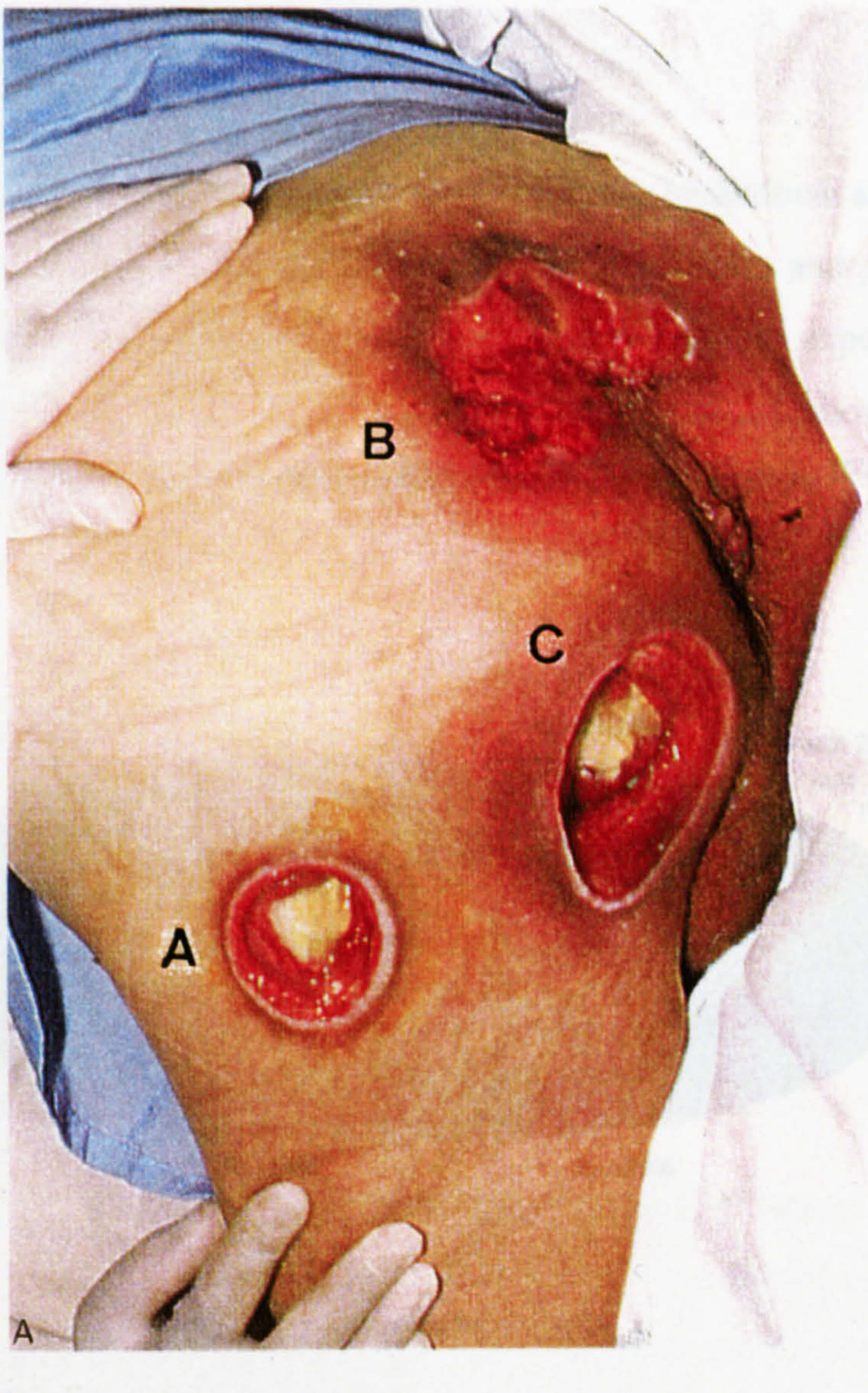

Figure 2-7 Examples of tissue breakdown adjacent to bony prominences.
(A) greater trochanter, (B) sacrum, (C) ischial tuberosities.

These stages do not always predict or account for some forms of tissue breakdown. For example, the internal sores which originate deeper within the tissues, where an area of tissue may undergo extensive subcutaneous damage without the involvement of the superficial skin layers until the later stages of injury. This would result in an abrupt transition in classification from a Stage I to a Stage IV sore.

2.5 OCCURRENCES

Areas of the body which are susceptible to tissue breakdown are often adjacent to a bony prominence including the sacrum, ischial tuberosities and greater trochanter. In typical seated or bed lying positions, tissue in these areas can experience high pressures which are exacerbated by the bony prominence. Figure 2-8 shows a summary of the areas of the body which are most affected by tissue breakdown [12,134,155].

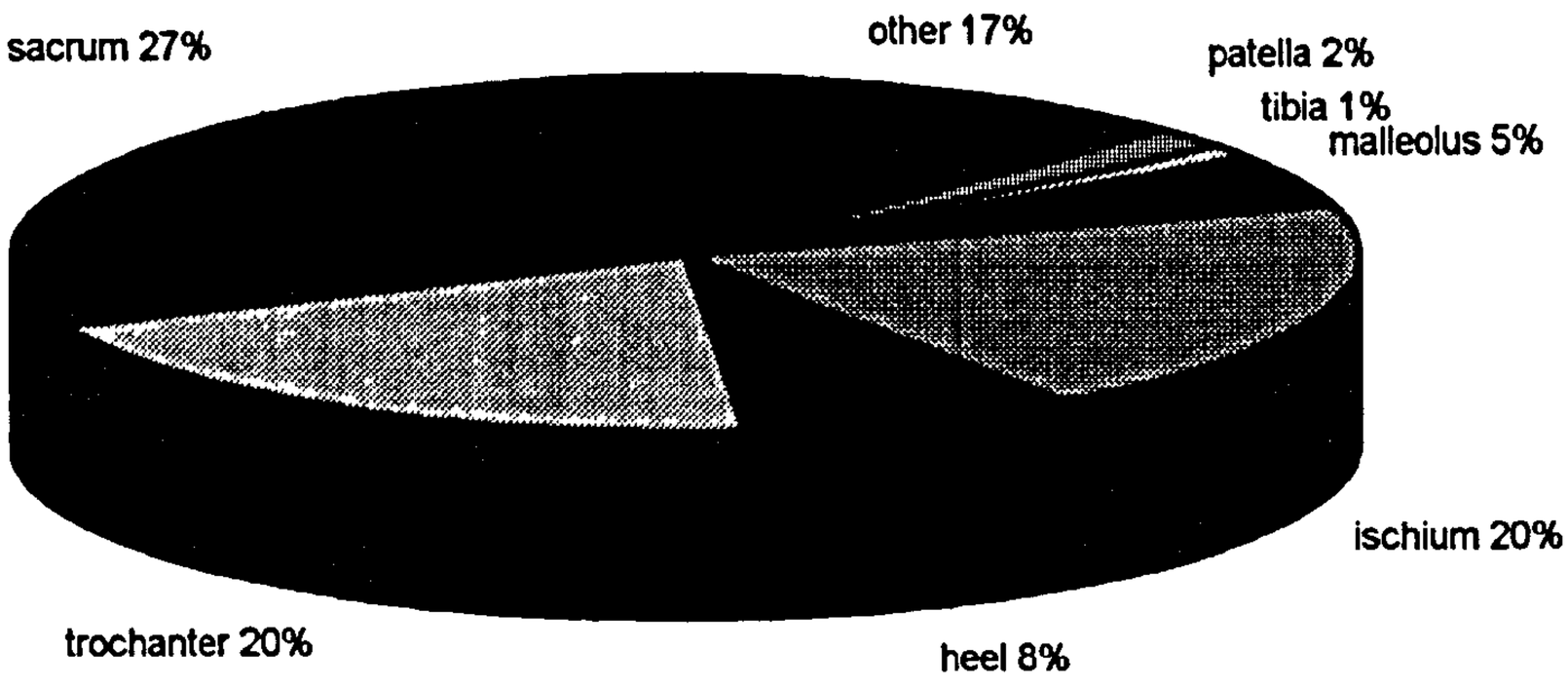

Figure 2-8 Occurrence of tissue breakdown at different sites.

Table 2-2 outlines some studies carried out to determine the incidence and prevalence of tissue breakdown in a number of clinical situations in a variety of countries.

Table 2-2 Incidence and prevalence of tissue breakdown in a number of studies.

Reference	Subject Group	Population Group	Incidence	Prevalence
Petersen & Bittmann [155]	Total patient community	517,000 patients from Denmark	3%	Prevalence of 43 patients per 100,000 (62 total sores)
Jordan & Clark [106]	Total patient community	10,751 patients from Glasgow, UK	8.8%	Prevalence rates of 86 patients per 100,000
Jordan *et al.* [105]	Total patient community	946 patients from Borders, UK	9.6%	Prevalence 95 patients per 100,000
Jensen & Juncker [101]	Patients admitted for # neck of femur revision	156 patients in Sonderburg, Denmark	30%	N/A
Versluysen [210]	Patients admitted for # neck of femur revision	100 patients at St Bart's, UK	29%	N/A
Sheppard *et al.* [192]	Patients admitted for THR	100 patients at Oswestry, UK	21%	N/A
Hackler [88]	SCI	175 patients at Richmond, USA	22%	N/A
Brandeis *et al.* [28]	Elderly nursing home residents	20,000 residents from 51 nursing homes in USA	11.3%	N/A

2.6 Susceptible Patient Groups

The nature of the intrinsic factors described in the Section 2.2.2 indicates that certain subject groups have a higher potential risk of developing soft tissue breakdown. These subgroups of the population are inherently more susceptible to tissue breakdown due to certain physical changes in their tissue, usually associated with their underlying pathology. Three such groups are discussed in the following sections.

2.6.1 ELDERLY POPULATION

A number of factors can increase the susceptibility of elderly patients to potential tissue breakdown, although ageing per se, often termed physiological ageing, does not necessarily lead to tissue breakdown. However, there are a number of pathological changes which are associated with the advancement of years, these include some of the intrinsic factors mentioned, such as diabetes, peripheral vascular disease, incontinence, malnourishment and general ill health. Table 2-2 highlights the high risk associated with traumatic orthopaedic surgery, where elderly patients undergoing surgery for fractured neck of femur are particularly vulnerable to tissue breakdown [210]. General bad health and terminal illness may impair the immune system and increase risk of tissue breakdown, in addition to the normal ageing processes which may leave tissue structurally vulnerable to compromised viability.

2.6.2 SPINAL CORD INJURED POPULATION

Spinal cord injury (SCI) can result in complete or partial paralysis, the extent of which is dependent upon the level and severity of the lesion. Following the acute stages of the injury, patients are generally mobilised in a wheelchair. The patient support interface is therefore subjected to prolonged loading, with the ischial tuberoscity being the most vulnerable site for tissue breakdown. It should be noted however that not all SCI injured subjects appear to be susceptible to tissue breakdown, indeed some subjects can remain seated for a whole life time and never suffer from this problem [25].

Guttmann [85] discussed the four intrinsic factors which predispose spinal cord injured patients to pressure sore formation. Deterioration in tissue integrity may be caused by alterations in vasomotor control mechanisms, which may result in a loss of tone, termed flaccid paralysis, in which the resulting tissues are less resistant to pressure damage. Conversely spasticity in the paralysed limbs causes spasms which can result in high shear forces being applied to the skin, continuous friction and changes in relative body anatomy can also lead to tissue breakdown. Insensitivity to pain caused by a lesion in the sensory pathways of the spinal cord means that the normal feedback

systems operational in an able bodied person, as detailed in Figure 2-5, will be inhibited or blocked. Tissue vascularity may also be compromised due to damaged neural control to the blood vessels, which may lead to changes in tissue perfusion. This is particularly important during the initial phase of spinal cord injury, termed spinal shock.

2.6.3 AMPUTEE POPULATION

Amputation of the whole or part of a lower limb can be the result of congenital deformity, systemic disease such as diabetes or cancer, or trauma. The problems of amputation affect the whole age range, with the greater proportion of young patients losing limbs due to trauma, whilst elderly amputees suffer from vascular-related disease. The nature of amputation leads to high loads being carried by residual tissues that have not been designed for this function. The integrity of the stump tissue is vital to the maintenance of the stump-socket interface and the functioning of the prosthesis [123], and the stresses and frictional forces experienced within the socket can lead to vascular occlusion, oedema and other dermatological problems. Problems can range from superficial erosion of the distal end to deep ulcers developing from poor cutaneous nutrition and circulation [123]. The rate of stump healing after amputation has been shown to be a function of tissue viability, as measured by transcutaneous oxygen tension levels at various sites on the limb prior to amputation [55,66].

2.7 COST OF PRESSURE SORES IN ENGLAND

A study commissioned by the Department of Health and carried out by a major accounting company Touche Ross [160] calculated the costs of prevention and treatment of pressure sores and tissue breakdown in English hospitals. Table 2-3 shows a summary of their findings.

Table 2-3 Financial costs associated with the treatment and prevention of tissue breakdown.

	Lowest	Highest
Cost of Treatment	£180 million	£321 million
Cost of Prevention	£180 million	£755 million

It is worthy of note that prevention costs are likely to appear higher as they are associated with a larger patient group who receive preventative measures compared to the specific group who receive treatment. Clearly, the unit cost of treatment is much greater than the cost of prevention. Treatment costs escalate due to the extended length of hospital stay, nursing time, cost of dressings and the possible requirement of surgery. Such financial considerations can not quantify the pain and psychological cost in suffering to the patient with a pressure sore. They also do not include the potential cost of litigation, which is a factor of increasing importance. The present figure for damages awarded to a patient suing a health authority for development of a pressure sore during a hospital stay stands at £200,000 [160]. The financial demands on a Health Service highlight the need for good predictive methods of identifying those patients who are at greatest risk from developing tissue breakdown. This would enable preventative action to be directed towards those most likely to suffer.

2.8 Prediction of Susceptibility

One of the most important initial steps for prevention is to recognise those patients at greatest risk from developing tissue breakdown. One of the simplest methods at present is the recording of a score using one of the available grading scales, such as the Norton Scale, which is shown in Table 2-4. Although accuracies of 98% have been reported for the Norton scale [217], many workers have found that the scales are not specific to particular patient groups. This has resulted in a number of different scoring systems being developed with the emphasis on different parameters according to the characteristics of the patient group.

Table 2-4 The Norton scale for predicting susceptibility to tissue breakdown.

Physical Condition		Mental State		Activity		Mobility		Incontinence	
Good	4	Alert	4	Ambulant	4	Full	4	Not	4
Fair	3	Apathetic	3	Walks with help	3	Slightly limited	3	Occasionally	3
Poor	2	Confused	2	Chair bound	2	Very limited	2	Urine	2
Very Bad	1	Stuperous	1	Bed Fast	1	Immobile	1	Double	1

At the present time grading scales remain the most commonly used predictors of patient susceptibility, even though lack of sensitivity and specificity have been reported [46]. There is obviously a great need for an improved objective method of assessing soft tissue status and predicting those patients who are most likely to suffer from breakdown at the tissue support interface.

2.9 Prevention

The most obvious means of preventing tissue breakdown is the reduction of pressures at the body support interface. Pressures can be relieved by regular turning of the patient by nursing staff, however, this is a very time consuming and intensive use of valuable nursing resources, which may not always be available. This necessitates the use of pressure relief systems, which can be divided into a number of categories:

- Semi-automatic turning beds - such as the Stryker frame which automatically turn the patient without the need for nursing intervention for 24 hours a day.
- Pressure redistributing beds - such as the Clinitron and the low air loss bed, which redistribute pressure by mimicking fluid suspension.
- Alternating pressure mattresses - such as the Airwave system (Pegasus Ltd, Waterlooville) and the BASE mattress (Talley Group Ltd, Romsey). These systems function by alternating pressures over the support tissue of the body over a fixed cycle time. Thus at some points of the cycle tissues are subjected to low or zero pressures and are therefore able to recover from any pressure-induced ischaemia, which may otherwise lead to tissue breakdown. There are also equivalent commercially available cushions.

Although interface pressures on a selection of different mattresses have been measured to allow comparison between different mattresses [198-200], there have been

relatively few clinical trials to investigate the efficacy of these devices in preventing tissue breakdown.

2.10 SUMMARY

The problem of soft tissue breakdown has been attributed to a number of factors, principally the application of pressure to tissue which results in cessation of blood and lymph flow. Subsequent ischaemia and accumulation of harmful waste products is thought to lead to necrosis of the tissue. Tissue breakdown is very costly to health services, in terms of treatment, prevention and possible litigation. However, what is clearly lacking are reliable objective methods of predicting those patients at greatest risk of developing tissue breakdown.

3. MEASUREMENT OF SOFT TISSUE STATUS

3.1 INTRODUCTION

In the previous chapter several parameters were highlighted which have been implicated in the development of soft tissue breakdown. The most important factor was identified as the application of forces to the soft tissues which can lead to occlusion of the blood vessels causing ischaemia, reduction in available oxygen and an accumulation of waste products.

This chapter is devoted to the identification of measurement techniques for investigating soft tissue status and monitoring the effect of factors implicated in tissue breakdown. The ideal technique for the measurement of tissue status would involve a method which is continuous, non-invasive and causes minimal discomfort to patients. This chapter includes sections on the measurement of pressure, blood flow and tissue biochemistry in the determination of tissue status and concludes with the aims and objectives of the present work.

3.2 MEASUREMENT OF PRESSURE IN SOFT TISSUES

3.2.1 INTRODUCTION

During normal daily activities the skin and soft tissues are subjected to a number of physical forces such as compression, shear and friction. These forces are normally supported by healthy tissue without compromising its integrity. However, if these forces become excessive or prolonged or the tissue is already compromised either mechanically, structurally or biochemically, tissue viability or status may be compromised leading to potential tissue breakdown.

Since pressure and other forces play such an important role in the breakdown of soft tissues it is essential that these parameters should be monitored. It is possible to measure both the pressures at the interface between the tissues and a supporting surface, and the interstitial pressures at some depth within the tissue.

3.2.2 INTERFACE PRESSURE MEASUREMENT

A number of transducers have been developed in order to measure pressure or force at the interface between soft tissues and a supporting surface. Appropriate transducers can measure either pressure over a particular area, or total force independent of area. Pressure transducers operate by means of a number of physical processes including pneumatics, electro-pneumatics, optoelectronics, capacitance, and conductance. The key feature of an interface pressure transducer is that it must be designed in such a way that its presence does not introduce measurement artefacts as a result of its geometry or stiffness. Therefore the optimum transducers must be compliant, flexible, thin and small, in order to measure local pressures. Further desirable features include linearity, low hysteresis and independence from temperature and humidity effects.

In the clinical environment interface pressure measurement has important ramifications in the design of patient support systems which aim to prevent tissue breakdown. As highlighted in Chapter 2, high pressures can be experienced over the sites of bony prominences such as the sacrum, ischial tuberosities and trochanters. Measurement of interface pressures can lead to alleviation of high pressures by modification of support surface or posture. Interface pressure measurement is also important within the stump socket interface associated with lower limb prostheses. Each of these different types of patient support interfaces will experience a range of physical conditions. Thus physical measurement systems, such as interface pressure transducers must be based on individual design specifications.

Within seating clinics the most commonly used interface pressure transducers are the Oxford Pressure Monitor (now Talley Pressure Monitor), the Texas Interface Pressure Evaluator (TIPE), now superseded by the QA measurement system, and the Scimedics single air bladder. These pressure monitors work on pneumatic and electropneumatic principles respectively. An investigation into the accuracy of these pressure transducers was carried out by Reger and Chung [167]. The transducers were used to measure the pressure between a hard ball and a soft surface, a hard ball and a hard surface and between two flat plates. The pressures measured were compared against theoretical values calculated from Hertzian theory on contact mechanics. All

three sensors showed strong positional sensitivity and none were able to detect the peak loads that were predicted, although they all recorded accurate average values over the area of the sensor. Bader & Hawken [9] showed that the Oxford Pressure Monitor had a linear response over a pressure range of 0-260 mmHg (0-34.6 kPa) using a sealed pressure chamber; non-uniformity and positional sensitivity were exhibited when using an indenter to apply pressures to individual air cells.

A number of researchers have used interface pressure transducers to monitor the interface pressures at sites susceptible to soft tissue breakdown on a number of different support surfaces. Table 3-1 identifies the results from these studies showing the pressures experienced at different body sites in clinical situations.

Table 3-1 Mean interface pressure readings at clinically relevant sites.

Reference	Position	Subject Group	Support surface	Greater Trochanter*	IT*	Sacrum*	Heel*
Swain *et al.* [199]	prone	normal	Biwave	59	53	31	80
	prone	normal	Nimbus	49	44	31	79
Swain *et al.* [200]	prone	normal	Quattro	51	43	27	103
			BASE	59	50	32	48
Garber *et al.* [79]	side-lying	SCI		86.0			
	flexion	SCI		86.0			
	extension	SCI		64.8			

* All pressure values are in mmHg.

Bader & Hawken [9] measured the pressures under the ischium and proposed a series of relevant parameters including absolute pressure and maximum pressure gradient. The latter may be of critical importance in determining the degree of tissue distortion, which has been implicated in tissue breakdown and occlusion of blood vessels. Bar [11] investigated the effect of time in combination with interface pressure measurements. Using cumulative frequency distributions, the variation in pressure over the ischial tuberosities, over an extended period of time were investigated and changes attributed to bodily movements, type of cushion and wheelchair motions. This approach of longer term pressure monitoring may be useful in identifying changes in

pressure contours, which will occur due to the viscoelastic nature of both support surfaces and supporting tissues.

Sanders *et al.* [178], investigated the interface conditions in prosthetic sockets. They compared the results of pressure and shear measured in the socket, using a specially designed transducer, with those computed by a finite element model. Shear forces were measured as the resultant of horizontal and vertical forces. There was little agreement between the results of the model and the experimental measurements, which highlights the problems of pressure measurements within the socket and those of mathematical models. The maximum interface shear stresses were experienced during the stance phase, peak normal stresses reaching 1537 mmHg (205 kPa) and shear stresses 405 mmHg (54 kPa).

3.2.3 Interstitial Pressure Measurement

Measurement and understanding of pressure at patient support interfaces is very important and has obvious advantages in the clinical setting. However, it is of equal importance to understand the mode by which these pressures are distributed within the depth of the tissue including the internal pressure gradients, which can lead to tissue deformation and distortion. This is particularly important in tissues which are in close proximity to bony prominences, as there is a compliance mismatch between bone and soft tissues which could potentially lead to high stress concentrations.

A number of transducers are available for invasively measuring interstitial pressures. These include needle manometers, wick catheters and implantable integrated circuit sensors. Wick catheters are considered the most reliable as they are not affected by changes in osmotic pressures which may affect the membrane-type transducers.

An important feature of experiments to determine the distribution of pressure within the tissue is the method used to apply the pressure to the tissue. The two main methods described in the literature utilise either an occlusive cuff or an indenter; the mechanics of these two methods have been investigated by a number of authors.

The use of occlusion cuffs requires a knowledge of the transfer of pressure from the cuff through the tissue. Cristalli & Neuman [40] suggest that pressure is not transmitted

purely hydrostatically and that interstitial pressures will markedly differ from cuff pressures and will be dependent upon tissue properties.

Schock *et al.* [188] used excised pig skin samples to investigate the effect of different indenter geometries on strain distribution measured using grid lines marked on the tissues. He found that spherical indenters produced a strain concentration around the tip of the indenter, whereas flat indenters produced a more uniform strain distribution, vertical deformation of the tissue was greater with the rounded indenter. The strain distributions under the indenters were also found to be dependent upon tissue type, for example, there was a more profound difference between the indenters on fatty tissue than on muscle tissues.

Sacks *et al.* [175] used dimensional analysis to suggest that the important factors to consider when using an indenter to apply an external load include, its diameter, the depth and diameter of the underlying bone, and the tissue deformation properties. He also used Hertzian contact mechanics to design an indenter profile which would provide uniform pressure distribution.

ANIMAL STUDIES

The early studies to relate applied pressures to interstitial pressures were carried out on animals. Reddy *et al.* [164] studied the relationship between external tissue compression and interstitial fluid pressure measured using wick catheters in the foreleg of Yorkshire pigs. The catheter was placed a distance of 2-5 mm into the tissue and pressure was applied using an occlusive cuff. Interstitial pressures at this depth were shown to reach a steady state value of 65-75% of externally applied pressure, which reached maximum values of 200 mmHg (26.66 kPa).

Daniel *et al.* [50-51] measured the transmitted interstitial pressure in the pig using a catheter transducer and compared these values to the applied force. He concluded that pressures are actually greater further away from the indenter and deeper in the tissue corresponding to the occurrence of the greatest tissue damage. This effect has been associated with the fact that muscle is more susceptible to reduction in available oxygen than skin [149].

HUMAN STUDIES

Sangeorzan *et al.* [181] placed a catheter attached to a pressure transducer in the subcutaneous tissues of the lower leg. Both hard and soft sites were tested corresponding to loading over bone and muscle respectively. Pressures up to 125 mmHg (16.66 kPa) were applied via an indenter. The subcutaneous pressures over the bony sites were correspondingly greater than those measured over the soft sites for similar applied pressures.

3.2.4 NON-INVASIVE TECHINIQUES

MODELLING TECHINIQUES

The experimental methods described in Section 3.2.3 are invasive and only capable of measuring pressures at particular points within the tissue. To fully understand the distribution of stress and strain within the tissue due to an applied force, models have been developed which enable spatial representation of the pressure distribution. The accuracy of these models depends upon the validity of the assumptions and the appropriateness of values used for tissue mechanical properties. Techniques have included physical models such as the PVC gel model buttock [33,39] and computer generated finite element models [47,139].

A finite element model of the human buttocks is shown in Figure 3-1, illustrating high pressures at the interface between the bony prominence and the soft tissues adjacent to it.

IMAGING TECHNIQUES

Non-invasive methods of investigating pressure distributions within tissue include measurement of tissue deformation by means of ultrasound and magnetic resonance imaging. These techniques provide greater information on the *in vivo* mechanical characteristics of soft tissue and calculated values for mechanical properties can then be used to improve the accuracy of existing theoretical models.

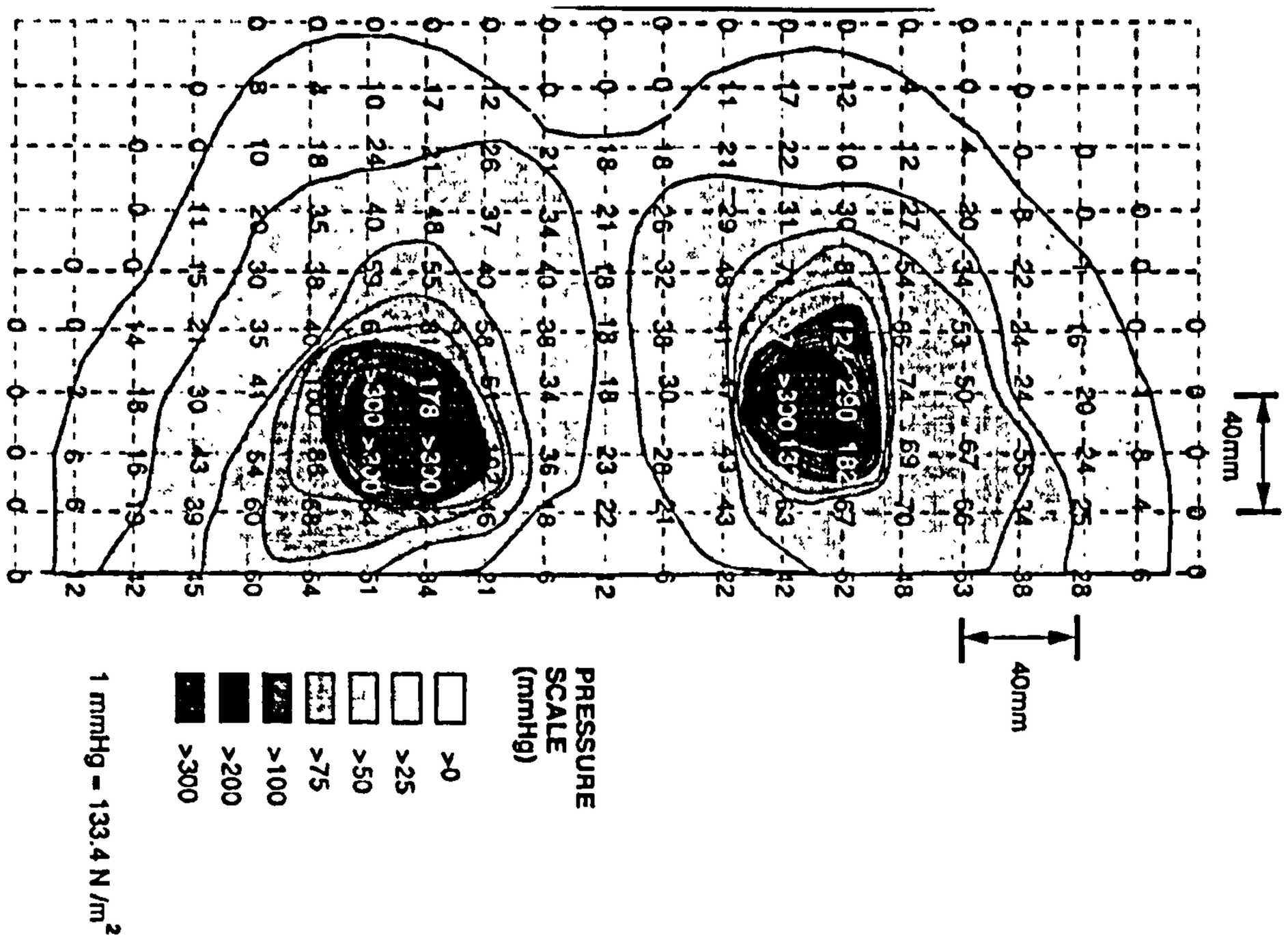

Figure 3-1 FEA model of the human buttock. Adapted from [139]

In a limited study, Reger *et al.* [168] used magnetic resonance imaging to investigate tissue mechanics in healthy and spinal cord injured patients during sitting. An example of the images taken from a female spinal cord injured patient, with flaccid paralysis and a control healthy subject are shown in Figure 3-2.

The healthy subject in Figure 3-2a shows a thick soft tissue layer which reduces in thickness during seating. The paraplegic subject in Figure 3-2b, shows less distinction between muscle and fatty tissue which may be due to muscle atrophy. In addition, there is a greater reduction in tissue thickness during loading as the flaccid tissues are displaced laterally leading to bottoming out of the remaining tissues.

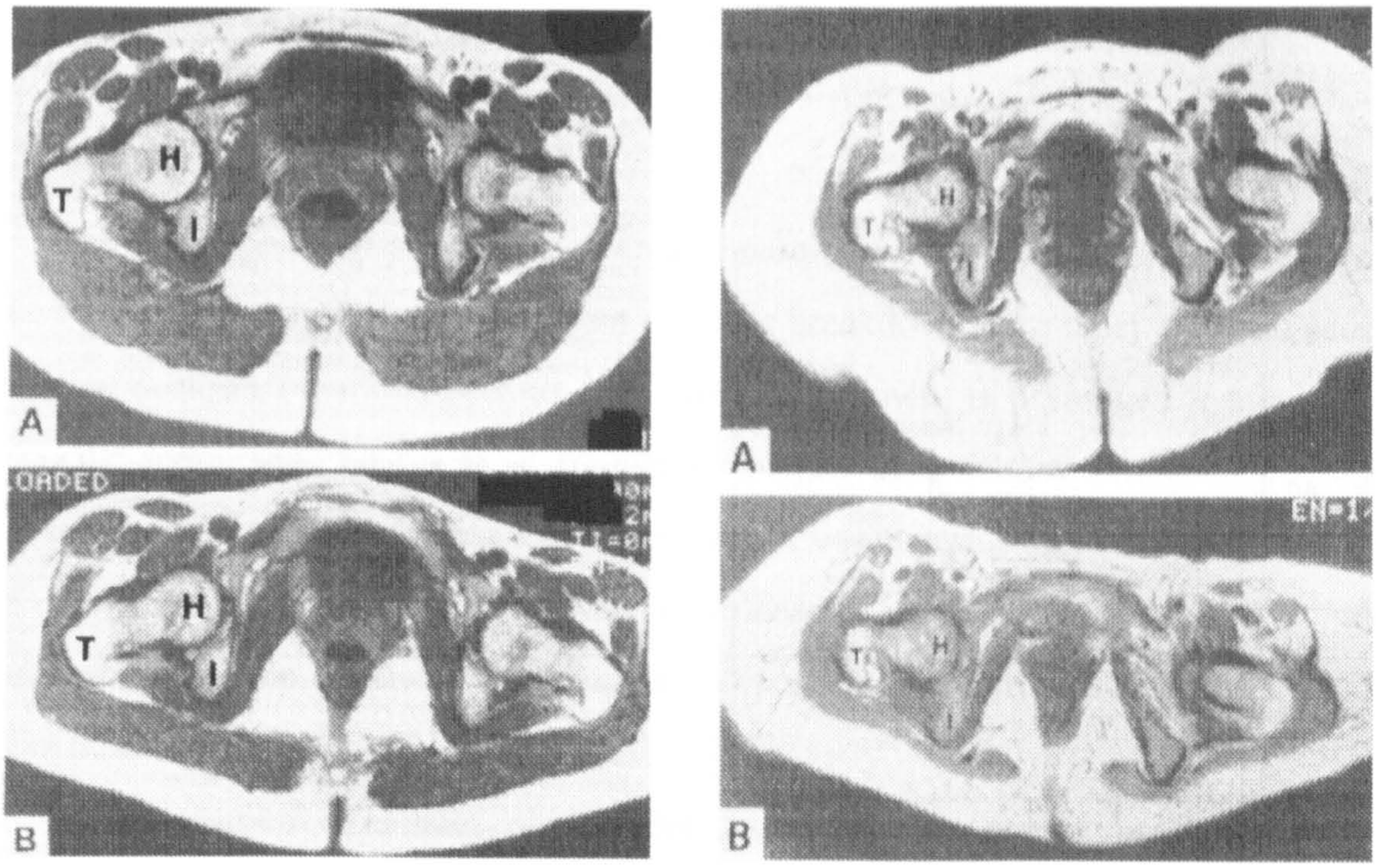

a) Healthy female subject b) Paraplegic female subject

Figure 3-2 Transverse MR images of buttocks near ischial tuberosities. Adapted from [168].
(A) Tissues freehanging, without external support.
(B) Loaded tissues with flat cushion support. T - trochanter, H - head of femur, I - ischium.

Ultrasound has been used to measure both tissue thickness during seating [138] and the seating interface contours [108]. There are inherent problems using ultrasound associated with changes in the acoustic properties of tissues with compression. Until this relationship is established, ultrasound measurements will lead to inaccuracies.

Non-invasive methods for determination of pressure within tissue may also lead to a greater understanding of the transfer of pressure within tissue. Modelling needs to be improved to take account the non-linear and viscoelastic behaviour of tissue before it can achieve its potential.

3.3 TISSUE MICRO-CIRCULATION - ISCHAEMIA AND REPERFUSION

3.3.1 INTRODUCTION

The occlusion of blood flow to an area of tissue leading to ischaemia is believed to be the major factor in the development of tissue breakdown. The most common cause of this occlusion, with respect to soft tissue breakdown, is prolonged loading to a specific tissue site. This is most frequently located over a bony prominence where pressure in the tissue can reach levels in excess of tissue perfusion pressures and cause a reduction in blood flow or ischaemia. Ischaemia can cause disturbances in the metabolism of the cells with a subsequent accumulation of catabolic products which can potentially cause tissue breakdown.

In this section a number of different techniques for measuring tissue micro-circulation are described. These techniques have been employed in pertinent studies, which have examined the effects of loading on tissue micro-circulation and subsequent reperfusion.

3.3.2 TECHNIQUES FOR MEASURING TISSUE MICRO-CIRCULATION

The diversity of techniques available indicates the complexity of measuring different aspects of tissue micro-circulation. Three aspects of micro-circulation which can be measured involve the physical movement of blood cells, heat transport and the oxygen content of blood [201]. Table 3-2 outlines some of the main methods used for measuring tissue micro-circulation with an analysis their relative advantages and disadvantages. Each method will be discussed separately.

Table 3-2 Methods for determining tissue micro-circulation.(✔) denotes yes, (✘) denotes no.

Method	Measurement	Invasive	Continuous	Limitations
Physical Movement				
Radio-isotope clearance	Detection of isotope in blood.	✔	✘	Potentially harmful.
Doppler Ultrasound	Doppler shift in ultrasound signal	✘	✔	Potentially inaccurate
Photoplethysmography	Volume changes in skin flap.	✘	✔	Unable to differentiate between nutritional and non-nutritional blood supply.
Laser Doppler flowmetry	Doppler shift in laser signal	✘	✔	Low penetration, high signal to noise ratio.
Heat Transfer				
Thermography	Temperature changes	✘	✔	Inaccuracies due to skin loss of heat with time.
Oxygenation				
Transcutaneous O_2/CO_2	Gas tension	✘	✔	
Near Infrared Spectroscopy	HbO_2	✘	✔	
Vital Capillary Microscopy	Capillary size.	✘	✔	
Tissue pH/pO_2		✔	✔	
Reflectance spectroscopy	HbO_2	✔	✔	Pigmentation of skin affects reading

Laser Doppler flowmetry utilises the frequency shift of laser light in response to the movement of red blood cells to measure blood flux. However, Liddington *et al.* [124] suggested that red blood cell velocities are a more accurate measurement tool than blood flux. The laser Doppler systems are only linear over very small ranges of red blood cell concentration; it is important to have both the correct signal processing bandwidth cut-off frequency and signal stability to ensure accurate measurement. Movement artefacts due to the relative displacement of the sensor with the skin can also lead to inaccuracies in blood flow measurement at tissue sites involving mobile

skin. Laser Doppler flowmetry is site specific and should be limited to monitoring dynamic blood flow responses to physiologic stimuli at a single site.

Doppler ultrasound works in a similar way to laser Doppler flowmetry, but uses the frequency shift of ultrasound waves rather than light. However, low shift frequencies and high signal to noise ratio can lead to inaccuracies.

Photoplethysmography is an accurate technique which uses changes in tissue volume to determine the blood flow. However, this method requires flaps of skin from which light can be passed through from one side to another; with respect to this restriction the use of plethysmography is limited when considering clinically relevant sites at risk from tissue breakdown.

Temperature techniques can be prone to inaccuracies due to the nature of blood flow in different vessels of the vascular system. For example, the heat from large stores of slow moving blood in veins can give high temperature readings which could be misinterpreted as a region of high blood flow.

Transcutaneous gas tension measurements have been carried out using the diffusion of oxygen across the skin to an electrochemical electrode attached to the skin surface. Evans & Naylor [62-63] recorded negligible values for transcutaneous oxygen tension at normal skin temperatures, but noted that if the skin was heated to 42-45°C higher readings were possible. There are four factors which effect transcutaneous oxygen tensions. These are as follows:

- Rightward shift of oxygen-haemoglobin curve due to heating (Figure 1-6).
- Resistance of skin to O_2 permeability.
- Metabolic consumption of O_2 in skin.
- Effective rate of cutaneous blood flow.

Transcutaneous carbon dioxide tensions are not affected to such an extent by the above factors, due to the fact that there is only a small difference between arterial and venous pCO_2, and CO_2 can diffuse much faster through tissues than O_2. However, during periods of low blood flow, there is likely to be an increase in carbon dioxide and values will deviate from arterial pCO_2. It has been suggested that transcutaneous gas tension measurements are related to microvascular transmural pressures and capillary

blood flow [195-196]. Beran *et al.* [19] suggested that the major regulator of transcutaneous oxygen tension is papillary flow which makes up 80% of measured flow. Transcutaneous carbon dioxide tension, on the other hand, is thought to be regulated by the remaining 20% of deep cutaneous flow. Spence *et al.* [196] has suggested that at low oxygen tensions, for example during ischaemia, the oxygen consumption by certain Clark type electrodes may be a significant proportion of available oxygen supply, which may lead to inaccurate or very low readings. However, transcutaneous pO_2 and pCO_2 measurements have been successfully used as a measure of tissue viability, and in this situation many of the criticisms aimed at the technique are not valid [24,25,55]. It has also been suggested that electrode power consumption can be used as an indication of blood flow [19,64]. As with laser Doppler flowmetry, it may be more accurate to use relative changes in gas tension as a result of different physiological stimuli.

In 1977, Jobsis *et al.* [102] discovered that light with a wavelength between 700 nm and 900 nm penetrates biological tissue more readily than other light. They also discovered that within this spectral range only HbO_2, Hb and cytochrome aa3, a compound consisting of a protein linked to haem, have oxygen dependent absorption changes. This has led to the introduction of spectroscopic methods for measuring blood flow and oxygenation.

There are advantages and disadvantages in all the above systems, the most important factor in using a system for measuring tissue status is the understanding of the parameter being measured. The most accurate measurement technique would combine a number of different methods in order to elucidate as much information as possible.

3.3.3 Effect of Applied Pressure on Tissue Micro-Circulation

The occlusion of blood flow to specific areas of tissue and the resultant ischaemia caused by the application of prolonged or excessive loads has been identified as one of the major contributing factors to the development of tissue breakdown. With respect to this finding, research has been carried out to determine the levels and duration of loading which may be detrimental to tissue status. The desired outcome of this type of

research is to identify threshold levels of load magnitude and duration below which healthy tissue status is not compromised. Table 3-3 shows the key references in the literature which have investigated the effect of load on tissue micro-circulation.

Table 3-3 Research into effect of pressure on tissue micro-circulation.

Reference	Technique	Site	Loading Regime	Subject Group	Comments
Seiler & Stahelin [191]	pO_2	trochanter and quadriceps	136 mmHg (0-18.2 kPa)	Normal	linear relationship between pO_2 and load
Schubert & Fagrell [189]	laser Doppler fluxmetry	sacrum and gluteus maximus	0-110 mmHg (0-14.7 kPa)	Young / Elderly	Greater reduction in flux over sacrum than gluteal region
Bader & Gant [7]	pO_2/pCO_2	sacrum	0-81 mmHg (0-10.8 kPa)	Normal / debilitated	Wide range of pressures required to depress pO_2 below 20 mmHg
Sangeorzan *et al.* [181]	pO_2	tibia, tibialis anterior	0-125 mmHg (0-16.7 kPa)	Normal	Pressure required to bring pO_2 to zero greater over muscle than bone.
Newson *et al.* [147]	pO_2	sacrum, trochanter, thigh	0-150 mmHg (0-20.0 kPa)	Normal	Non-linear relationship between load and pO_2
Bennett *et al.* [17]	photoplethy-smography	thenar prominence	0-120 mmHg (16.0 kPa) with and without shear	Normal	shear decreased the load at which occlusion occurred by 50%.

The initial studies were aimed at investigating the effect of loading on tissue blood flow, overlying hard and soft sites. Seiler & Stahelin [191] and Sangeorzan *et al.* [181], used transcutaneous gas tension monitoring to look at blood flow over the trochanter and quadriceps, and tibia and tibialis major respectively. Both studies showed a greater decrease in the measured oxygen tension over the hard site relative to the soft site in response to a given applied load. Total anoxia ($pO_2 = 0$ mmHg) was demonstrated for

a load of 150 mmHg (19.6 kPa) over the bony site and 525 mmHg (68.7 kPa) over the soft site.

Schubert & Fagrell [189] also looked at differences in blood flow in tissue over hard and soft sites, namely the sacrum and gluteus maximus using laser Doppler flowmetry. Although described as an investigation into the effects of prolonged loading, the temporal nature of the loading cycle, namely loading for 30 s followed by removal and recovery, was more consistent with repeated loading. They noted a slight increase in blood flux up to 30 mmHg (4 kPa) and then a decrease in flux with increasing load. In some subjects the reading decreased to zero over the sacrum. The extent of the fluctuation in the gluteus maximus was not so great and this was attributed to a greater distribution of pressure within the tissue and a greater capacity for compensatory blood flow in this tissue area. By comparison, Newson *et al.* [147] showed similar cut off pressures for tissue over muscle and over bone using transcutaneous oxygen measurement.

Spectroscopic methods have been utilised in recent years to monitor blood flow [69,90,91]. Hampson *et al.* [91], monitored the effect of ischaemia on the blood flow to the muscles of the forearm using near infra-red spectroscopy (NIRS). They compared these measurements to those obtained from transcutaneous oxygen tension measurements. They found that during ischaemia the muscle rapidly consumed O_2, but recovered quickly exhibiting a reactive hyperaemic response when the tourniquet was removed. The transcutaneous O_2 monitor did not detect the rapidity of the consumption of O_2 during ischaemia or subsequent hyperaemia. This was attributed to the dependence of the O_2 monitor on blood flow, whereas the spectroscopic method can detect muscle O_2 delivery and intracellular O_2 independently of blood flow. It should also be noted that the transcutaneous O_2/CO_2 monitor is used to reflect changes in capillary gas tensions rather than muscle gas tensions and, as such, a direct comparison is not truly valid.

More recent techniques include a non-contact laser speckle method to monitor skin blood flow [172]. The laser can penetrate the tissue to a depth of 0.4 mm. So far this method has not been utilised to measure the effect of load on local blood flow.

The majority of the experiments described have employed either methods of measuring oxygenation or blood flow. It has recently become possible to measure partial pressure of carbon dioxide (pCO_2) in addition to partial pressure of oxygen (pO_2). This additional parameter can give information on the nutritional status of the tissue and the effect of pressure on micro-circulation [194]. Bogie *et al.* [24] noted an increase in pCO_2 during loading of sacral tissues in the acute phase of SCI and they have proposed that this accumulation of CO_2 could be harmful. They developed parameters based on the percentage of measurement time that the carbon dioxide tension remained within predetermined bands. These bands were defined as LTC [pCO_2<36mmHg], NTC [36mmHg<pCO_2<44mmHg], and UTC [pCO_2>44mmHg]. These additional parameters could prove useful in the determination of effects of pressure on micro-circulation.

In addition to the micro-circulation of blood and blood gases, the circulation and occlusion of lymph has been studied with respect to tissue breakdown. Miller & Seale [139] proposed that terminal lymph clearance in subcutaneous tissue is a function of externally applied pressure. Using radioactive tracer techniques, they showed that an externally applied pressure up to 60 mmHg (8 kPa) increased lymph clearance but that pressures greater than 75 mmHg (10 kPa) prevented terminal clearance. They hypothesised that the obstruction of lymph clearance may be responsible for tissue breakdown.

The main studies describing investigations into the effect of load on blood flow have involved both normal and susceptible patient groups. With respect to determining threshold levels of load magnitude and duration, it should be noted that in some cases it is difficult to correlate quantitatively the findings from different investigations. However the experiments have been important in identifying qualitative differences between loading regimes and blood flow characteristics with regard to tissue status.

3.3.4 Reperfusion of Blood Supply After Pressure Induced Ischaemia

The ability of an area of tissue to recover from a period of pressure induced ischaemia may be an important factor in the susceptibility to develop subsequent tissue breakdown [133]. Ischaemia-reperfusion injury is an important area of research in

cardiology when applied to heart tissue after a period of ischaemia following a heart attack. After removal of load from tissue a period of reactive hyperaemia is noted, this includes a temporary erythema of the skin as blood supply is restored to the tissue and the oxygen debt recovered. It has been proposed that this increase in blood flow is caused by the action of vasodilators which have accumulated during the period of ischaemia.

A few researchers have measured the reperfusion of blood supply after a period of ischaemia using a number of the techniques to evaluate tissue micro-circulation. Table 3-4 outlines the important research in this area.

Table 3-4 Reperfusion characteristics after pressure induced ischaemia.

Reference	Technique	Site	Subject Group	Comments
Schubert & Fagrell [189]	Laser Doppler flowmetry	sacrum/gluteus maximus	young/elderly	Slower recovery was shown in the elderly group
Meijer *et al.* [136]	Temperature	sacrum, IT	young, elderly (high risk), elderly (low risk)	Slower recovery in high risk group
Hagisawa *et al.* [89]	Reflectance spectroscopy	trochanter	SCI/Normal	Slower recovery in SCI group
Kabagambe *et al* [107]	Trans pO_2	sacrum, hamstring	SCI/Normal	Slower recovery in SCI group
Ewald [64]	Trans pO_2		Young/Adult	
Bader [10]	Trans pO_2/pCO_2	sacrum/IT	SCI/Normal/MS	Two distinct characteristics

Meijer *et al.* [136] proposed that the blood flow recovery time after loading could be used as a measure of susceptibility. They studied a group of elderly patients whose susceptibility was assessed using grading methods. The recovery characteristics of the patients were measured using thermocouples, to monitor changes in skin temperature, and a linear correlation was shown between the recovery characteristics and risk factor. The recovery of blood flow was conveniently described by Equation 3-1.

$$t_r = lt + \tau_u \quad \textit{Equation 3-1}$$

t_r - recovery time, lt - latency, τ_u - time constant of rise.

Hagisawa *et al.* [89] measured the reperfusion and reactive hyperaemic responses using reflectance spectroscopy in both spinal cord injured subjects and normal controls. Pressures of 150 mmHg (20 kPa) were applied to the greater trochanter for periods of 300-900 s, after which the load was removed and reperfusion was recorded over several minutes. Reactive hyperaemia was investigated by applying thumb forces to the area and measuring response. They found that although the reactive hyperaemic response was similar in both groups under investigation, the rate of recovery after loading was significantly slower in the SCI group.

Kabagambe *et al.* [107] used transcutaneous oxygen tension measurements to monitor reactive hyperaemia in both spinal cord injured and normal controls. They also demonstrated that recovery in the spinal cord injured group was significantly slower than that in the controls. In addition, 70% of the spinal cord injured group failed to recover their pre-loaded pO_2 value within 5 minutes of load removal. These results have clear implications in the efficiency of pressure relief regimes in those SCI subjects who are particularly at risk of developing tissue breakdown.

Bader [10] showed two distinct characteristic responses using transcutaneous pO_2 measurements with respect to recovery after repeated loading in both normal control and debilitated subject groups as shown in Figure 3-3.

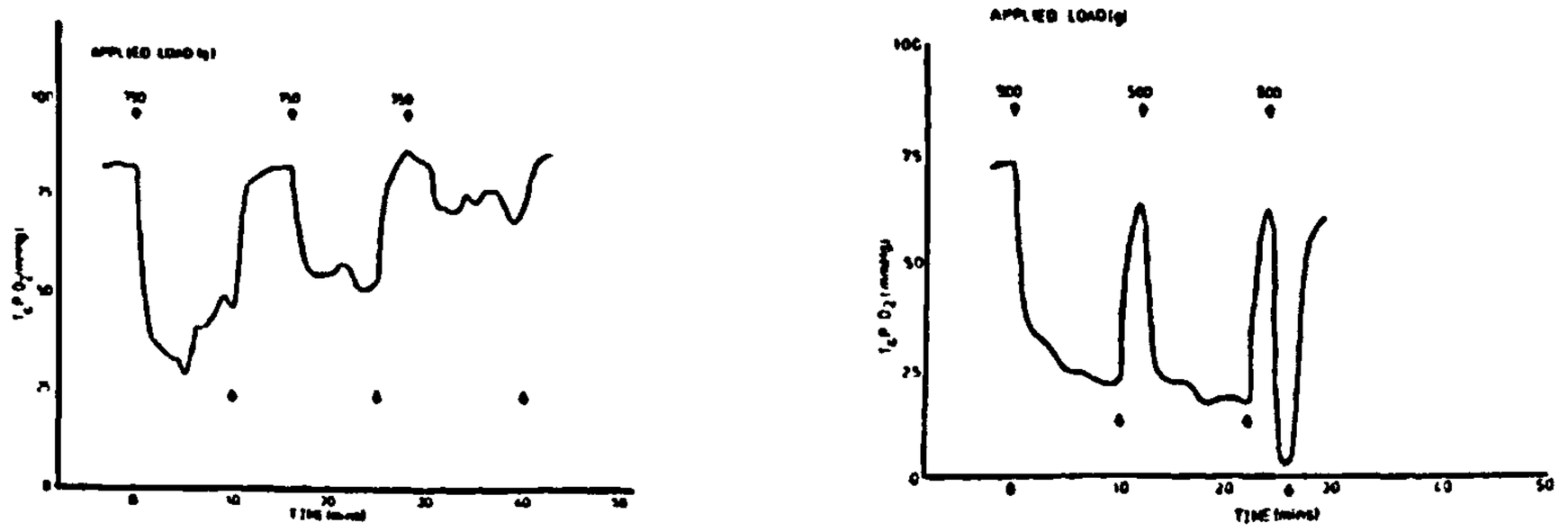

a) normal response b) impaired response

Figure 3-3 Distinct responses to repeated loading and tissue recovery. Adapted from [10].

There are clearly differences in the reperfusion characteristics of blood flow to tissue after a period of pressure induced ischaemia in different patient groups. This may explain why some groups are more susceptible to tissue breakdown than others and lead to predictive screening techniques to identify those patients with specific high risk of developing tissue breakdown. The effect of different load and time regimes has not been comprehensively studied with respect to tissue reperfusion. This approach may be useful in indicating threshold levels at which abnormalities in recovery are initiated.

3.4 Tissue Biochemistry

3.4.1 Introduction

The importance of maintaining blood supply and circulation of other body fluids has been described with respect to the effect of pressure ischaemia on tissue. In addition to ischaemia, a number of different biochemicals have been implicated in the development of tissue breakdown. The biochemical processes which maintain tissue viability are controlled by homeostasis. If this balance is disrupted biochemical pathways can be altered and result in the production of metabolic products which may be immediately damaging to the tissue [173], and the accumulation of these metabolites may lead to tissue necrosis [139]. Ischaemia-reperfusion injury can lead to a decrease in membrane fluidity, inhibition of protein synthesis, blockage of macrophage activity, cross-linking and aggregation of proteins [173]. Methods for identifying these biochemicals and their effect on tissue status would be beneficial in both the overall understanding of the development of tissue breakdown, as well as in the establishment of predictive techniques to identify these processes in specific tissues.

3.4.2 Biochemicals Implicated in Tissue Breakdown

Specific biochemicals implicated in the phenomenon of ischaemia reperfusion injury include chemicals formed during the degradation pathway of adenosine triphosphate (ATP), such as urate and oxygen free radicals. ATP is a ubiquitous, intracellular, high

energy phosphate compound which is involved in intermediate metabolism. The synthesis of ATP is regulated by the availability of oxygen, inorganic phosphate and glucose or fatty acids. ATP is constantly being consumed during normal cellular function for a number of energy requiring reactions which are critical to the maintenance of cell viability. If ATP is consumed too rapidly it will be depleted and an accumulation of adenosine monophosphate (AMP) and adenosine diphosphate (ADP) may occur. The breakdown products of this pathway may include possible harmful oxygen free radicals and urates, the presence of which may be an indicator of energy crisis in cells [75,219].

During prolonged ischaemia, an accumulation of breakdown products is thought to accumulate in the interstitial spaces, these can change capillary permeability and disrupt ionic gradients across cellular membranes leading to changes in the ionic concentrations in interstitial spaces.

Acidotic conditions in the tissues can be potentially dangerous and can arise from increased levels of lactic acid or carbon dioxide. Lactate is the end product of anaerobic, glycolytic activity which may indicate development of tissue breakdown; blood lactate has been used as an indicator of condition in exercise physiology [141], it has also been used as an indicator of damaging occlusion during tourniquet surgery [182].

3.4.3 Invasive Methods of Monitoring Tissue Biochemistry

A number of invasive methods of investigating tissue biochemistry have been employed. For example, Silver [193] used micro-electrodes to measure production of chemicals during hypoxia in tissues, and found a decrease in intracellular pH which could be correlated with an increase in the production of lactate.

Hagisawa *et al.* [90] measured levels of serum creatinine phosphokinase (CPK), inorganic phosphate, and lactate dehydrogenase in pigs during periods of tissue indentation and subsequent load removal. These biochemicals were thought to be possible markers for tissue damage; CPK is normally only found in cardiac or skeletal muscle, its presence in extracellular spaces may indicate leakage caused by muscle damage. Results from the study showed that levels of CPK increased during the period

of recovery after load removal, suggesting that the damage was progressive and delayed. Inorganic phosphate, which reflects the status of cellular metabolism as it relates to the presence of oxygen and ATP, was found to increase during the period of indentation but recovered to normal levels after load was removed. The presence of lactate dehydrogenase could indicate anaerobic respiration resulting in the production of lactic acid. The authors suggested that the levels of these biochemicals could be used to monitor muscle damage due to loading, but emphasised the importance of assessing this proposition on human subjects.

The methods mentioned above are invasive and therefore not ideal as routine screening methods for predicting the potential of patients to develop tissue breakdown.

3.4.4 Non-Invasive Techniques for Monitoring Tissue Biochemistry

There are very few non-invasive methods of monitoring tissue biochemistry in the literature, although nuclear magnetic resonance (NMR) techniques have been employed. Sapega *et al.* [182] used phosphorous NMR imaging to monitor cell bioenergtics by investigating the high energy phosphorous profile during periods of tourniquet ischaemia. This method has potential in the future for the non-invasive monitoring of tissue biochemistry during ischaemia but at the present time the cost is restrictive.

A novel approach for the non-invasive monitoring of tissue status utilises the metabolic activity of the eccrine sweat gland. Human eccrine sweat glands are located in the dermis of the skin, are supplied by cutaneous capillaries and secrete through an opening in the skin surface. Therefore the sweat secreted from these glands has the potential to reflect some of the biochemical processes occurring in the tissue beneath the skin surface as well as being inherently simple and non-invasive to collect. Sweat has been used in the past to diagnose cystic fibrosis [78] , diabetes [211] and peripheral vascular disease [70].

Sweating response can be stimulated using exercise, temperature, iontophoresis and application of chemical activators. These methods have been used to investigate the physiology of the sweat gland under normal and ischaemic conditions.

3.4.5 TECHNIQUES FOR COLLECTION AND ANALYSIS OF SWEAT

A number of different techniques have been developed for the collection of sweat from the skin surface. Some of these methods have been developed to obtain quantitative measures of sweat rate, while others have been designed in order to determine the biochemical composition of the sweat. Table 3-5 outlines some of the main methods that have been described in the literature.

Table 3-5 Techniques for sweat collection.

Reference	Technique	Comments
van Heyningen & Weiner [207]	Oilskin arm bags	Not site specific. Difficult to work out dilution.
Ferguson-Pell *et al.* [73]	Macroduct	Bulky, requires iontophoresis.
Mitsubayashi *et al.* [141]	Direct drippage into tube	Losses due to evaporation.
Polliack *et al.* [157]	Filter paper	Liable to saturation
Tanaka *et al.* [202]	Washdown	Evaporation, contamination.
Fukumoto *et al.* [77]	Body weight change	Non-quantitative
Boisvert *et al.* [27]	Encapsulating chamber	Not applicable for loading.

Clearly, there are a number of problems with some of these collection techniques including contamination, evaporation and dilution. As a result, the majority of the methods described above would not be relevant for use as tissue status indicators.

In order to analyse the composition of sweat a number of different analysis techniques have been described in the literature. These include both quantitative and qualitative methods as summarised in Table 3-6.

Table 3-6 Techniques for analysing sweat composition.

Reference	Compound	Method	Quantitative
Laccourcye *et al.* [120]	l-Lactate	Enzymatic electrode, l-lactate oxidase + O_2 -> pyruvate	✔
Higo & Kamata [95]	Lactic acid	Inelastic tunnelling spectroscopy	✘
Omokhodion & Howard [152]	Trace elements Zn, Cu, Mn, Ni, Cd, Al.	Atomic absorption spectroscopy	✔
Hannon & Quinton [92]	Lactate	Fluorescence microscopy	✔
Faridnia *et al.* [67]	Lactate	Amperometric biosensor	✔
Kondoh *et al.* [114]	d-lactate, Creatinine	HPLC (Jaffes method)	✔
Verde *et al.* [209]	Na^+, K^+	Flame emission photometer	✔
	Ca^{++}, Mg^{++}	Atomic absorption spectroscopy	✔
	Cl^-	Titration	✔
Taylor *et al.* [202]	Lactate, Urea, Urate Chloride	Fluorescence spectroscopy	✔
Mitsubayashi *et al.* [141]	glucose, uric acid	Amperometric biosensor	✔
	Na+, Cl-	Ion selective electrodes	

3.4.6 Effect of Ischaemia on Sweat Gland Function

Relatively few researchers have looked at the effect of ischaemia on sweat gland function, as outlined in Table 3-7. Initial studies showed that ischaemia led to a decrease in sweat gland output in terms of sweat rate [45,162,207]. Randall [162] suggested that this decrease in sweat rate was due to decreased transmission of neurotransmitter across the neuroglandular junction.

Table 3-7 Studies examining the effect of tissue ischaemia on sweat biochemistry.

Reference	Subject	Stimulation	Site & Loading	Duration	Results
Randall [162]	Normal	Thermal	Forearm, biceps, tourniquet-beyond arterial pressure	20-30 min	Decrease in sweat rate with ischaemia
Collins *et al.* [45]	Normal	Acetylcholine, thermal	Forearm, biceps	30 min	Decreased sweat gland activity with ischaemia
Elizonda *et al.* [59]	Normal	Thermal	Forearm, tourniquet beyond arterial pressure	10-15 min	Decreased sweat rate, increased potassium, decreased sodium and chloride.
Polliack *et al.* [157]	Normal	Thermal	Forearm, sacrum, indenter and tourniquet. 150 mmHg	20-55 min	Increase in lactate, urea and chloride with load.
Ferguson-Pell *et al.* [73]	Normal	Iontophoresis	Forearm, indenter. 150 mmHg	30 mins	increase in lactate, and urea, change in sodium.
van Heyningen & Weiner [207]	Normal	thermal, exercise	Whole arm, tourniquet	25 min	Increase in lactate, decrease in sweat rate during ischaemia.

However, when Collins *et al.* [45] repeated these experiments, they injected neurotransmitter directly on to the sweat gland but noted that sweat rate still decreased. They concluded that the decrease was due to a lack of sensitivity of the gland to the neurotransmitter rather than a decrease in transmitter itself. Elizonda *et al.* [59] clarified this finding by the use of localised injections of cholinergic chemicals given before ischaemia. This resulted in a constant, or in some cases, an increase in sweat rate during ischaemia. However, localised heat at the gland site could only increase sweat rate during ischaemia to a limited extent. They proposed that during ischaemia, the local temperature sensitive amplifier was dampened and a decrease in sweat rate during ischaemia was due to failure at the neuroglandular junction.

Van Heyningen and Weiner [207] were the first researchers to comprehensively investigate the composition of sweat during ischaemia. Using tourniquet techniques on

the arm, both electrolyte and non-electrolyte concentrations were measured. A few researchers have followed on from this work [45,73,157] . In terms of the electrolyte concentration of sweat during ischaemia, there have been conflicting reports. Total osmolarity of sweat is shown to increase with ischaemia, suggesting a rise in the ionic content, such as Cl^-, K^+, Na^+ ions. However, the literature reports either, no change [209] , increases [207] or decreases [59] in the ionic content of sweat during ischaemia. Some of these discrepancies may be due to collection methods or means of producing ischaemia. With regard to lactate and urea concentration there is concordance among researchers that ischaemia causes an increase in concentration.

Early researchers used tourniquet methods for inducing ischaemia although this form of loading is not directly relevant in the case of tissue breakdown, due to prolonged uniaxial loading. Only a few researchers have looked at the effect of uniaxial direct loading on sweat biochemistry with respect to determining the effect of loading on tissue status and these investigations were carried out on the forearm [73,157,202].

Polliack *et al.* [157] used filter paper and thermal sweating techniques to collect sweat under an indenter, whereas Ferguson-Pell *et al.* [73] used a Macroduct™ system and iontophoresis of acetylcholine to collect sweat. Polliack *et al.* [157] compared the sweat biochemistry during ischaemia produced by an indenter and an occlusive cuff pressures of 150 mmHg. Sweat was collected for 10 minutes with the cuff and 30 minutes with the indenter the times being controlled by subject comfort. They found a significant difference in the concentration of lactate at the indenter site compared to a control, but no difference at the occlusive cuff site. Ferguson-Pell *et al.* [73] carried out an investigation into whether stimulation technique altered sweat biochemistry. They compared sweat collected by iontophoresis of acetylcholine and sweat collected during heat and slight exercise exposure. They found no significant difference between the samples, though this experiment was only carried out at unloaded sites. Stimulation by iontophoresis must be carried out prior to the period of loading and has a limited effect. Therefore if prolonged periods of loading are to be investigated this may not be the ideal stimulation technique. In addition, the procedure is invasive and difficult to administer and is therefore not ideal as a clinical tool.

Both researchers loaded the forearm for 30 minutes using an applied pressure of 150 mmHg, and both showed significant increases in lactate, which returned to normal levels during a subsequent reperfusion period of 30 minutes [73] and 10 minutes [157]. Polliack *et al.* [157] also investigated sweat responses at clinically relevant sites, i.e. at the sacrum and ischial tuberosities during wheelchair sitting and found a similar result.

Taylor *et al.* [202] investigated the control levels of sweat taken from a number of relevant unloaded sites, namely the sacrum, ischium, forearm and calf. This study reported the greatest sweat rates occurring at the sacrum and ischium.

Although the above studies have looked at the effect of occlusion on sweat gland function in terms of secretion rate and sweat composition, only Polliack *et al.* [157] investigated sweat gland function and ischaemia at sites relevant to tissue breakdown. However, a full investigation of the effect of different magnitudes and durations of loads at clinically relevant sites has yet to be undertaken.

3.5 FT-Raman & FT-IR Tissue & Sweat Analysis

Vibrational spectroscopy has been utilised in wide variety of modes from the measurement of blood oxygenation [91], to the study of biological compounds [52,206] and the investigation of human skin [216-217]. Raman and infrared spectroscopy are used to discern the vibrational modes of molecules; the techniques are complimentary though the selection rules for each are fundamentally different. Infrared spectroscopy utilises the absorption of IR wavelength light in molecules with various vibrational and rotational modes. Absorption of IR radiation is governed by the Beer-Lambert Law given by Equation 3-2.

$$A = \log\left(I_o / I\right) = a.\,b.\,c \quad \textit{Equation 3-2}$$

A - absorbance, I_o - intensity of transmitted light, I - intensity of incident light, a - absorptivity, b - path length, c - concentration.

The Raman process is a scattering effect and results from a change in molecular polarisability during excitation. The excitation energy is monochromatic, and the molecules exhibit both elastic and inelastic scattering. During inelastic scattering, a small number of molecular bonds undergo excitation but on relaxation, they return to a different vibrational level, thus emitting a photon of a different frequency to the incident light. The frequency shift is known as the Raman shift and is described by Equation 3-3.

$$h\nu = h\nu' + \Delta E_{vib} \quad \textit{Equation 3-3}$$

Williams *et al.* [216-217] stated that for biological macromolecules Raman bands are generally sharper than the corresponding IR bands. In addition, the intensity of Raman scattering is directly proportional to the concentration of the scattering species, whereas IR absorbance is not linearly proportional to concentration.

The Raman microprobe has been used to identify biological inclusions in histological sections. Dhamelincourt [52] and Truchet *et al.* [206] described the development of the MOLE (molecular optical laser examiner) which was developed to investigate very small samples which have a characteristic Raman signal. They identified spectra of uric acid and its sodium and potassium salts, xanthine and guanine in vertebrate concretions; these purine derivatives would also be expected to be found in human sweat. The conclusion of the study was that the microprobe was capable of detecting compounds, non-destructively and at the microscopic level which could be potentially very useful for determining sweat metabolites.

3.6 Summary

This chapter has described a number of methods of measuring soft tissue status, utilising pressure, blood flow and oxygenation and tissue biochemistry. The ideal measurement techniques for tissue status monitoring are non-invasive, pain-free and continuous. It would also be of benefit to examine whether different techniques provide a similar assessment of soft tissue status. These objectives can be achieved by the use of transcutaneous oxygen and carbon dioxide tension, and sweat biochemistry

measurements, and as such these methods were selected for this work as the most relevant non-invasive tissue status measuring techniques.

3.7 Aims & Objectives

Tissue breakdown is an expensive and painful problem, and has been discussed in the previous chapters with respect to aetiology and treatment. It is clear from the literature that there is no conclusive method for predicting those subjects at greatest risk from developing tissue breakdown. This chapter has highlighted several methods for determining a number of parameters of soft tissue status. Two of these methods - transcutaneous gas tensions and sweat biochemistry measurement - have been selected to investigate the response of soft tissue to prolonged loading. The aim of this thesis is to explore the potential of these techniques as predictive indicators of soft tissue status. This will be achieved by the following means:

- Comprehensive validation of the two non-invasive techniques and development of standard operating procedures for temporal studies.
- Simultaneous use of the techniques to measure soft tissue status of healthy volunteers during sacral loading for extended time periods.
- Evaluation of the techniques in two susceptible patient groups to assess feasibility in soft tissue screening.

4. EXPERIMENTAL MATERIALS & METHODS

4.1 INTRODUCTION

It is clear from the literature review that a range of techniques are available for determining various aspects of soft tissue status. The main aim of this thesis is to investigate the effect of different loading regimes on soft tissue status, by means of non-invasive measurement techniques. The techniques which have been selected are transcutaneous oxygen and carbon dioxide gas tension monitoring and sweat biochemistry measurement both of which will be detailed in the present chapter.

4.2 TRANSCUTANEOUS GAS TENSION MEASUREMENT

4.2.1 INTRODUCTION

Transcutaneous monitoring of O_2 and CO_2 tensions has been validated as a method of investigating tissue status both experimentally [147-148] and clinically [24-26]. The technique is continuous and non-invasive and therefore fulfils the requirements of the ideal tissue status transducer [73]. For the following experimental investigations, a transcutaneous blood gas tension monitor (Model TINA, Radiometer AS, Copenhagen, Denmark) was used in conjunction with a combined oxygen and carbon dioxide electrode (Model D481, Radiometer AS).

4.2.2 THEORY OF OPERATION

The principle of transcutaneous oxygen and carbon dioxide monitoring relies on the diffusion of the blood gases through the uppermost layers of the skin. Abernathy [1] noted that skin released small amounts of carbon dioxide and Baumberger and Goodfriend [16] demonstrated that the oxygen released from the skin could be measured in a surrounding fluid. Transcutaneous oxygen electrodes were developed by Evans & Naylor [61-63] who showed that vasodilation beneath the electrode increased perfusion

and diffusion of oxygen. More recently, carbon dioxide electrodes have also been developed. A typical combined O_2/CO_2 electrode is shown in Figure 4-1.

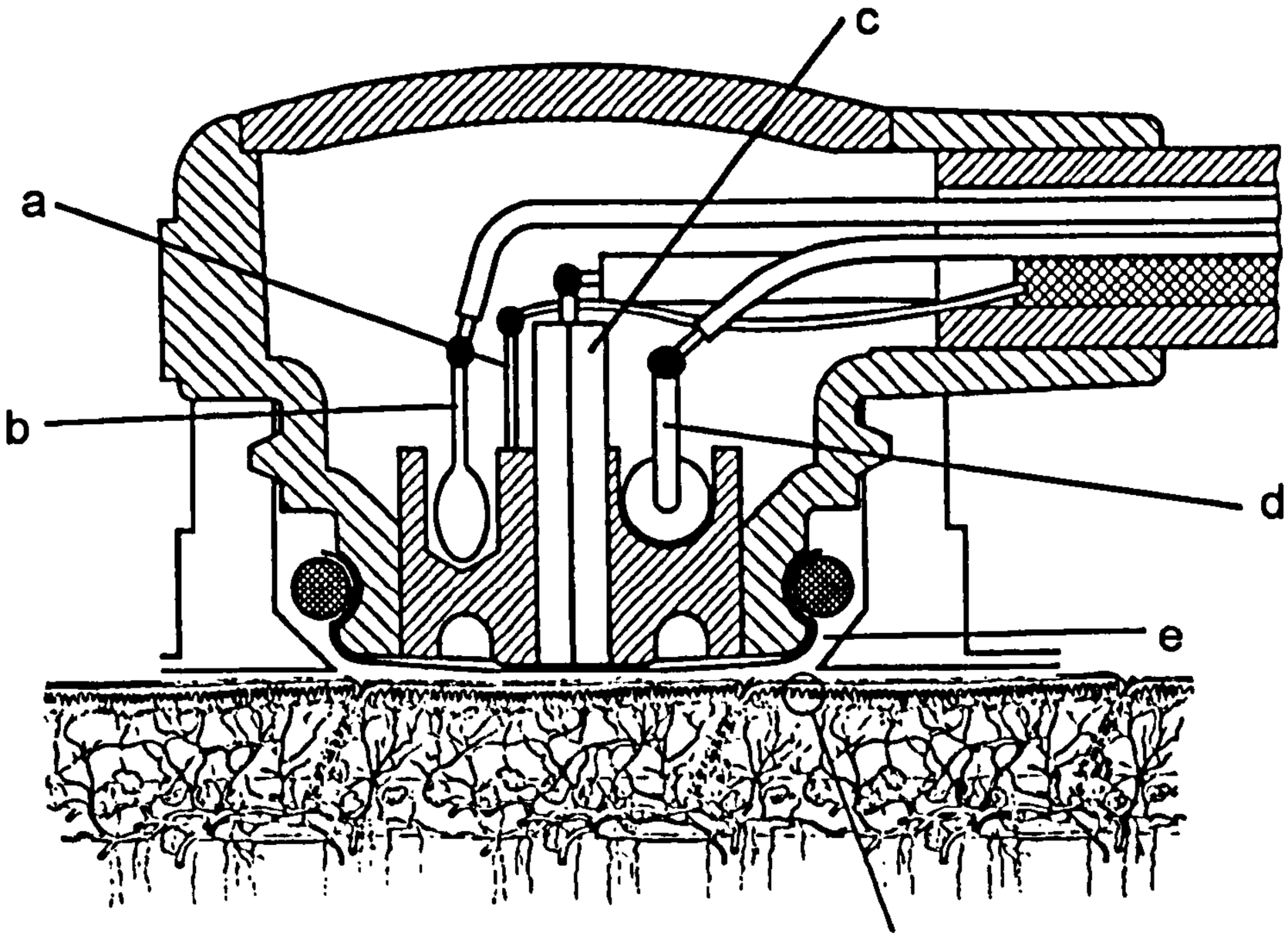

Figure 4-1 Diagram of the combined oxygen and carbon dioxide electrode
a) and b) pO_2 electrochemical cell
c) and d) pCO_2 electrochemical cell
e) electrode membrane

Partial pressure of oxygen (pO_2) is measured using a sensor based on the Clark electrode, consisting of a silver/silver chloride electrochemical cell with a buffered potassium chloride electrolyte solution. The cathodic reaction is shown by Equation 4-1 and the voltage generated is linearly proportional to the oxygen tension, pO_2.

$$O_2 + 2H_2O + 4e^- \Leftrightarrow 4OH^-$$

Equation 4-1

The physiological significance of pO_2 measured at the skin surface is shown in Figure 4-2. The oxygen tension is increased by the heating action of the electrode so that oxygen tension in the capillaries is higher than that in arterial blood. This effect is counteracted by the metabolism of oxygen in the skin which reduces the tension measured at the surface by the transcutaneous oxygen electrode.

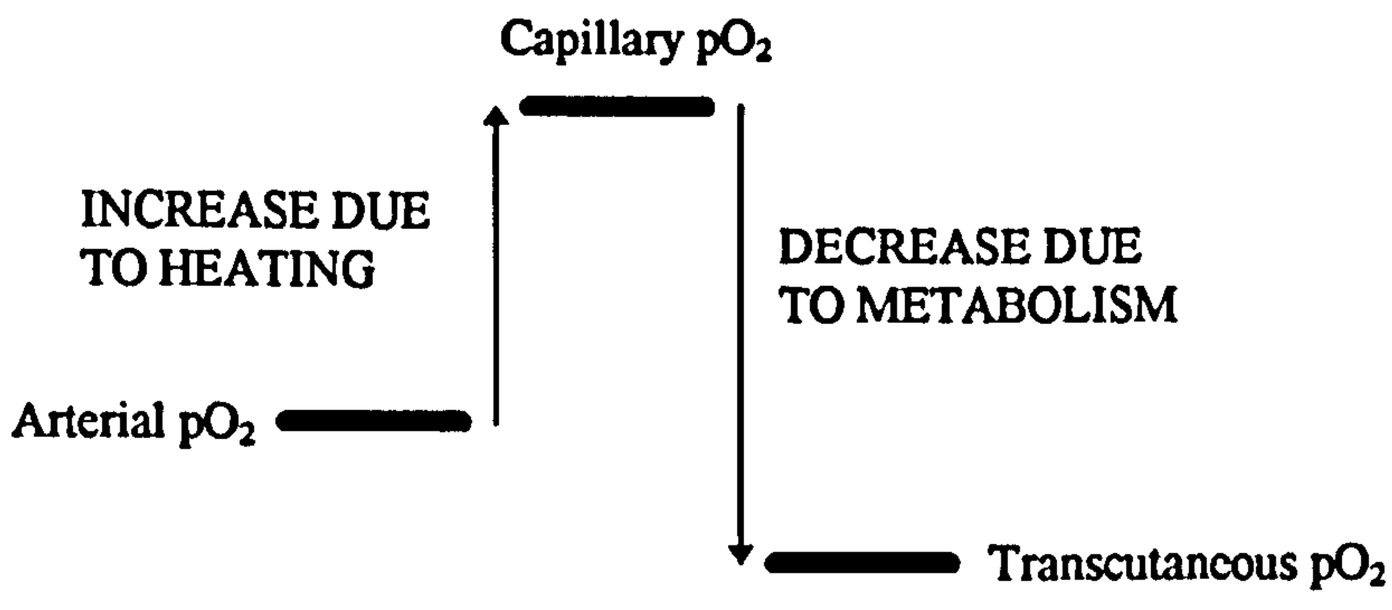

Figure 4-2 The physiological significance of oxygen tension measurements.

The transcutaneous carbon dioxide sensor is based on the Stow-Severinghaus pH electrode, comprising of a glass pH electrode with a concentric silver/silver chloride reference electrode. The appropriate electrochemical reaction is given by Equation 4-2. Carbon dioxide diffuses from the skin and reacts with water to form carbonic acid, the voltage difference generated is proportional to the negative logarithm of the carbon dioxide tension, pCO_2.

$$CO_2 + H_2O \Leftrightarrow H_2CO_3 \Leftrightarrow H^+ + CO_3^-$$

Equation 4-2

The physiological significance of the carbon dioxide tension is shown in Figure 4-3. The pCO_2 is increased by both the heating action and the metabolism in the dermal layers of the skin. In order to account for this increase in pCO_2 a calibration factor must be used, as indicated in Equation 4-3.

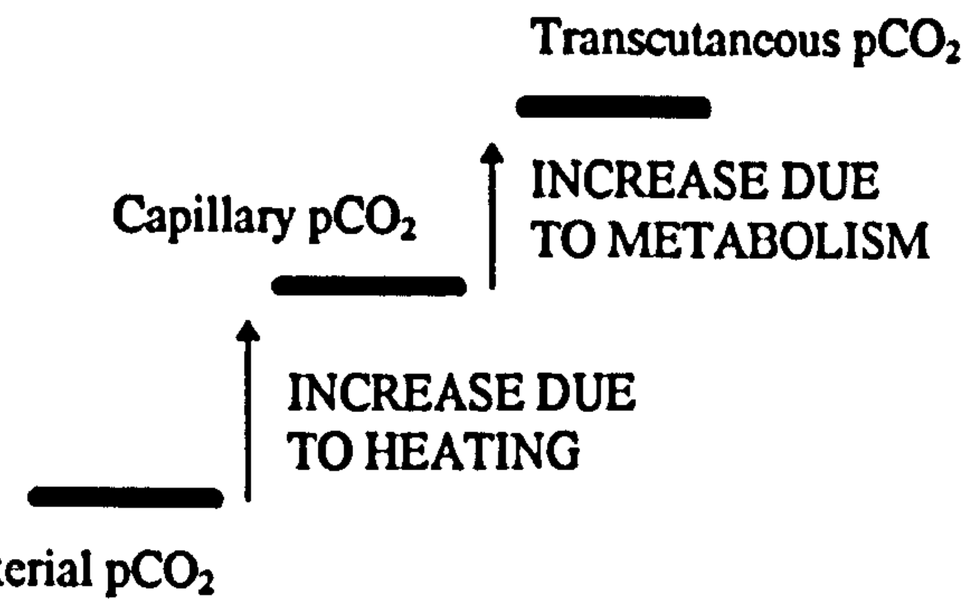

Figure 4-3 The physiological significance of transcutaneous carbon dioxide tension.

$$pCO_{2(37°C)} = \left[pCO_{2(T)} \Big/ 10^{0.021(T-37°C)} \right] - 4mmHg$$

Equation 4-3

T - selected electrode temperature

4.2.3 CALIBRATION OF THE ELECTRODE

The combined electrode was calibrated prior to usage following a standard procedure. Calibration was performed using a standard calibration gas composed of 5% CO_2 and 20.9% O_2. The partial pressure of the gases depends on the barometric pressure, and at extremes of temperature and humidity the calibration values are corrected using Equation 4-4.

$$pO_{2(cal)} = (B - pH_2O(t) * RH) * XO_2$$

$$pCO_{2(cal)} = (B - pH_2O(t) * RH) * XCO_2$$

Equation 4-4

B - barometric pressure, *RH* - relative humidity, $pH_2O(t)$ - saturated water vapour pressure at ambient temperature, XO_2 , XCO_2 - mole fraction of oxygen and carbon dioxide in atmospheric air.

For an atmospheric pressure of 760 mmHg,

$pO_2 = 159\ mmHg$

$pCO_2 = 38\ mmHg$

4.2.4 DATA COLLECTION

The output from the transcutaneous gas tension monitor could be recorded during experiments using the in built printer, or alternatively collected via the RS232 port into a computer ASCII file. By collecting the digital output of the monitor a record can be kept of oxygen and carbon dioxide tension, power, electrode temperature and time. The digital output from the transcutaneous gas tension monitor was read into a data file using Procomm (Microsoft Corporation, USA) software. This data file was converted to a delimited text file using a QBasic program, the details of which can be found in Appendix A.

4.2.5 STANDARD OPERATING PROCEDURE

Transcutaneous oxygen and carbon dioxide gas tensions were measured using the following procedures:

- Transcutaneous Gas Tension Monitor re-membraned and calibrated with standard gas.
- Excess hair removed with a razor from the measurement site, which is then cleaned and dried with alcohol and water.
- Electrode fixation ring attached to site and filled with 5 drops of contact solution (1,2-propanediol and deionised water).
- Electrode temperature selected. 43-45°C is generally considered to be adequate to produce maximal vasodilation in adults.
- Equilibration period of 10-15 minutes required until the electrode records a steady state value of between 40-100 mmHg for oxygen and 30-80 mmHg for carbon dioxide.
- Sample values taken throughout collection period, sampling frequency is dependent upon experimental protocol.

4.3 SWEAT COLLECTION AND ANALYSIS TECHINIQUES

4.3.1 INTRODUCTION

In order to carry out the objectives of this study, sweat samples were collected from various sites and analysed. The measurement of metabolites and ionic substances in sweat may reflect biochemical processes in the underlying tissue providing markers of tissue status or viability. The sites of interest include the sacrum, ischium and the residual limb tissue of the lower limb amputee. One of the most important features of the sweat collection technique was that it did not distort the tissue interface as a result of the physical nature of the collection device. It was also important that after sweat collection accurate quantitative analysis of composition and volume could be undertaken. This section describes the sweat collection and analysis techniques used in the subsequent experimental work.

4.3.2 SWEAT COLLECTION

As described in Section 3.4.5, a number of sweat collection techniques exist including the Macroduct, filter paper, wash down and direct drippage into a test tube. For the present work filter paper collection was utilised. The major advantages of this technique are that it is cheap, allows quantitative composition and volume analysis, and has minimal thickness, so tissue distortion is reduced at a loaded measurement site.

The sweat was collected on Whatman Cellulose (1Chr) chromatography paper (Whatman Paper Ltd, Maidstone, Kent, UK). This inert paper comprises of 100 per cent cotton lint and has been designed specifically for clinical application. Individual sweat collection pads were cut to either 40 mm diameter circles, or annuli with an outer and inner diameter of 40 mm and 12 mm respectively. The water retention per unit area of the paper was measured at 245.87±5.2 g/m^2. This corresponds to a maximum retention of 309 mg of sweat for the circular pads and 281 mg of sweat for the annular pads.

The pads were stored in 30 ml screw capped 'Universal' conical bottomed tubes (Bibby Sterilin Ltd, Stone, Staffs, UK). Spacers were manufactured from the tops of small glass bottles, and were placed at the bottom of the tube; each contained five to

seven 2 mm holes drilled into the top. The tube, spacer and collection pad were weighed using an analytical balance prior to sweat collection. In addition, the sweat pad was covered with an impermeable, hydrophobic, polypropylene sheet which minimised evaporation of sweat during the collection period. The sweat pad and polypropylene cover were adhered to the skin using Blenderm® (3M Healthcare, Loughborough, UK) surgical tape, a clear, impermeable, hypoallergenic tape.

After collection the pad was removed with tweezers and replaced in the container. The bottle was re-weighed in order to determine the quantity of sweat collected. The sample was then frozen at -20°C prior to subsequent biochemical analysis.

4.3.3 Sweat Sample Preparation

On the day of biochemical composition analysis, the sample was thawed and diluted with 5 volumes of distilled water. The tubes were then agitated and centrifuged at 3000g for 10 minutes to ensure that all the sweat was removed from the pad and collected in the conical bottom of the container. The spacer prevented the collection pad from coming into contact with the eluted sweat. Recovery of sweat from the collection pad has been shown to be between 95-106% [158].

4.3.4 Sweat Composition Analysis

For this study, sweat lactate, urea, chloride and urate were measured spectroscopically using a Cobas FARA II Analyser (Roche Products, Welwyn Garden City, UK). The centrifugal analyser utilises a high intensity xenon flashlight source with a holographic grating monochromator, which enables selection of any desired wavelength of light in the range 285 nm to 760 nm. A schematic diagram of the optical set up of the machine is shown in Figure 4-4.

Light of the desired wavelength for analysis is split using a beam splitter. Ten percent of the light is directed to a dark field reference photodiode to compensate for flash intensity variation. The remaining ninety percent of light passes through the photometer lens and through one of the 30 separate reaction units (Figure 4-5) which comprise the annular cuvette rotor, containing the sweat samples and the specific reaction reagents. The light then passes through a series of 4 band pass filters to a

photodiode, where it is converted to an electrical signal whose intensity is a measure of the absorbance. The absorbance is a function of the concentration of the metabolite in the sample.

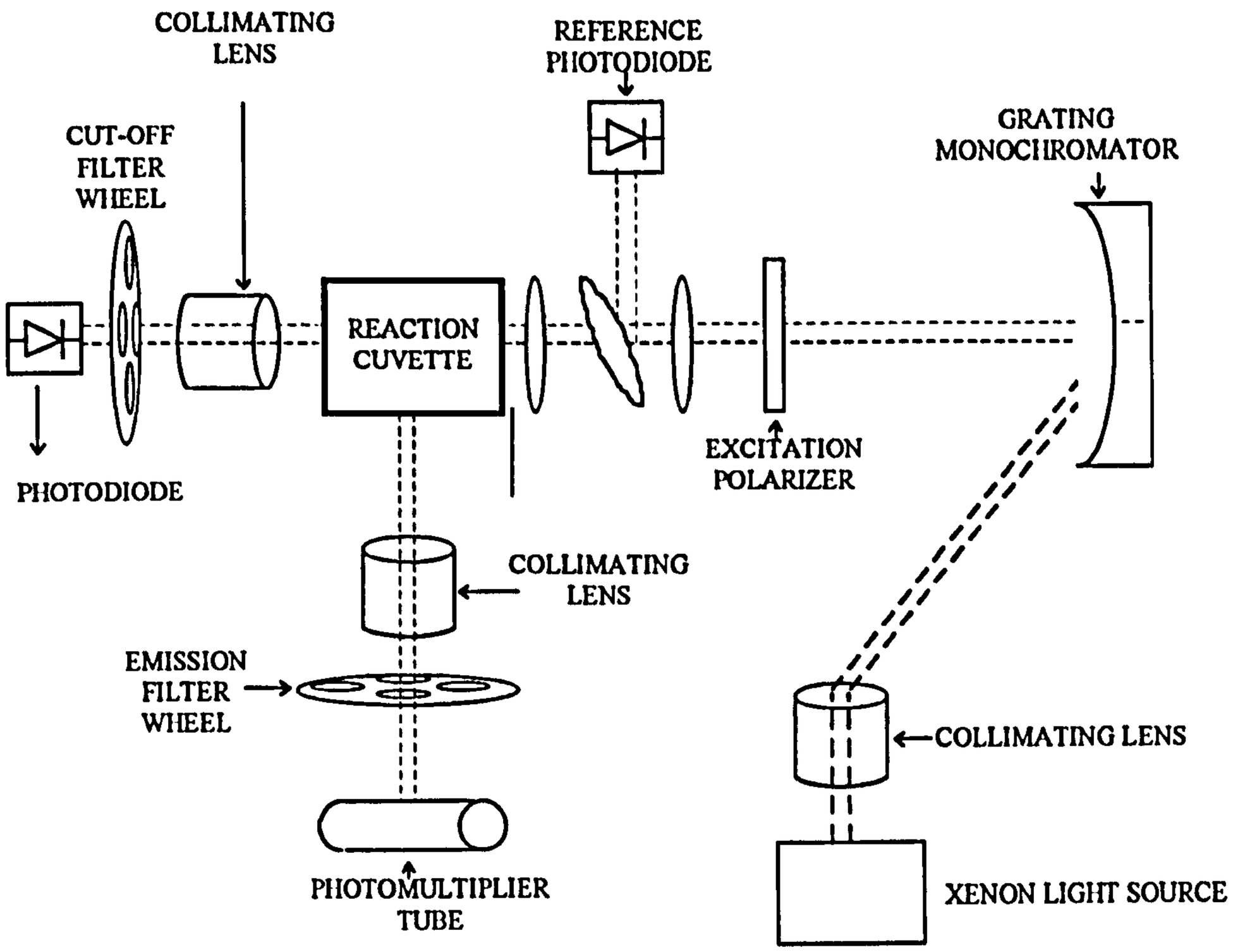

Figure 4-4 Schematic diagram showing components of the COBAS FARA spectrophotometer.

The sample and reagent are mixed in the reaction segment by centrifugal force. Each test is carried out in duplicate, with 2 controls and 2 blanks (one air, one water). The number and nature of the calibrants and controls are dependent on the specific metabolite being analysed. The controls comprised of various dilutions of lipholysed calf serum (Randox Laboratories, Co Antrim) and two different control solutions were used, Randox High (Multisera Elevated) and Randox Low (Multisera Normal).

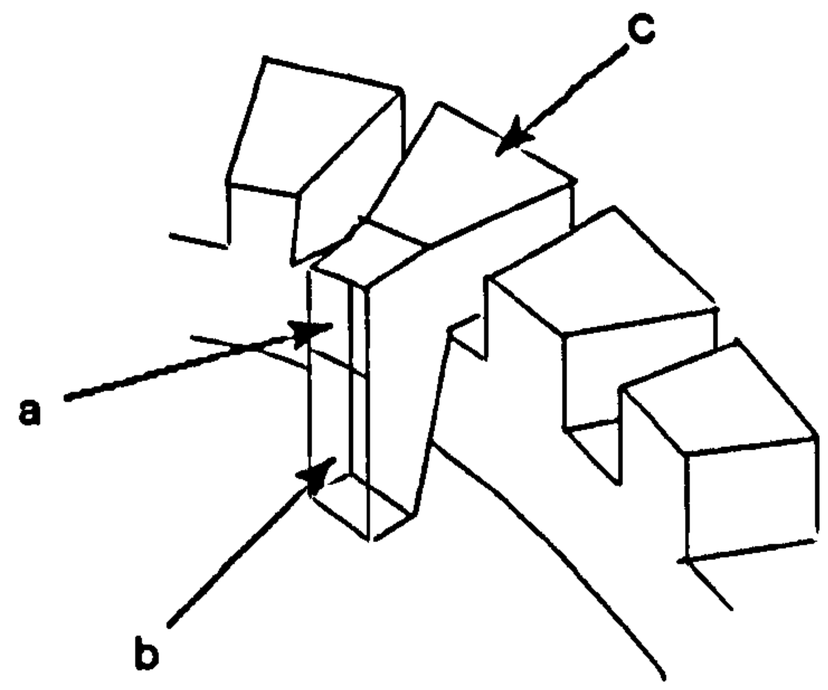

Figure 4-5 Schematic diagram of reaction cuvette.
a) sample segment, b) start reagent segment, and c) reagent segment.

SWEAT LACTATE

Sweat lactate was analysed using the lactate dehydrogenase method [84]. The reagent comprised the co-enzyme nicotinamide adenine dinucleotide (NAD^+) and a buffer solution containing glycine, hydrazine hydrate and ethylenediamene tera-acetic acid (EDTA) (Boehringer Mannheim UK, Lewes, UK). The reaction followed Equation 4-5 and the concentration of lactate present in the sample was proportional to the production of NADH.

$$L\text{-}lactic\ acid \xrightarrow{LDH} pyruvate + 2H^+$$

$$H^+ + NAD^- \Leftrightarrow NADH \qquad \textit{Equation 4-5}$$

4 µl of diluted sweat was incubated with 300 µl of reagent for 1 minute at 25°C. 10 µl of lactate dehydrogenase (LDH) was added and the readings were taken at the endpoint of the reaction after 12.5 min at 340 nm. The reaction was calibrated with 5 mmol/l lactic acid solution and the controls were Randox High and Randox Low.

SWEAT UREA

Sweat urea was analysed using a urease/glutamate dehydrogenase method [203]. Using the BUN (blood urea nitrogen) kit (Sigma Chemicals, UK) the reaction followed those described in Equation 4-6.

$$urea + H_2O \xrightarrow{urease} 2NH_3 + CO_2 \xrightarrow{H_2O} NH_4^+ + CO_3^-$$

$$2NH_4^+ + 2(2-oxo-glutarate) + 2NADH \xrightarrow[dehydrogenase]{glutamate} 2glutamate + 2NAD^+ + 2H_2O$$

Equation 4-6

5 µl of diluted sweat and 50 µl of reagent were incubated at 37°C and the absorbance changes over 2 minutes measured at 340 nm were recorded, these represented changes in concentration of NAD. The reaction was calibrated with 2, 4, 6, 8 mmol/l solutions of urea and the controls were Randox Low and 1:2 Randox Low solution.

SWEAT CHLORIDE

Sweat chloride was measured by the mercuric thiocyanate method [76]. 300 µl of chloride colour reagent (Nycomed, UK), and 30 µl of sample are mixed and absorbance change over 3 minutes at 37°C are measured at 480 nm. 2, 4, 8 mmol/l aqueous solutions of sodium chloride were used as calibrants. 1:11 Randox Low and 1:22 Randox Low were used as controls.

SWEAT URATE

Sweat urate was measured using the oxidation of uric acid to allantoin in the presence of uricase and a glycine buffer. The reaction followed that shown in Equation 4-7

$$Uric\ Acid + 2H_2O + O_2 \xleftrightarrow{uricase} Allantoin + CO_2 + H_2O_2$$

Equation 4-7

50 µl of diluted sweat was incubated with 100 µl of buffer at 37°C for 30 sec. 4 µl of uricase reagent (Sigma, UK) was added and the absorbance change at 292 nm measured which was proportional to the urate concentration.

The accuracy of the Cobas FARA has been calculated using the controls Randox High and Randox Low. Table 4-1 shows the mean and coefficient of variation of the measurements.

Table 4-1 Accuracy of sweat metabolite measurement.

Metabolite	Control	Mean (mmol/L)	CV
Lactate	Randox High	8.54	1.05%
	Randox Low	2.29	0.62%
Urea	Randox Low	5.59	0.96%
	1:2 Randox Low	2.82	1.73%
Chloride	1:11 Randox Low	8.65	0.66%
	1:22 Randox Low	4.66	0.89%

A miminum sweat quantity of 50µl was required to ensure that assays were carried out within their sensitivity ranges. Sweat samples not exceeding this quantity failed to provide sufficient volume for analysis of all constitiuents.

4.3.5 Standard Operating Procedure

Sweat collection and analysis measurements were carried out using the following procedures:

- Before use collection pad, spacer and bottle weighed using an analytical balance.
- Skin site washed and dried with alcohol and distilled water
- Collection pad placed on tissue site, covered with impermeable membrane and tape.
- Following collection, pad removed using tweezers, ensuring that any excess sweat is well mopped up from the skin surface.
- Collection pad replaced in tube as quickly as possible to prevent evaporation.
- Sweat quantity evaluated using a gravimetric technique. If sweat amount does not exceed 50 mg (50 µl) pad discarded.
- Sweat sample stored at -20°C until analysis.
- Sample thawed and diluted with 5 volumes of distilled water.
- Analysed for lactate, urea, chloride and urate.
- Results of analysis multiplied six fold to give metabolite concentration.

4.4 PRESSURE APPLICATION - INDENTER

4.4.1 INTRODUCTION

The majority of the experiments described in Chapters 5, 6 and 7 relied on the use of a pressure indenter to produce ischaemia. In terms of tissue breakdown at the site of a bony prominence the indenter approach is more practical and provides a more relevant model than that of the tourniquet cuff.

4.4.2 THEORY OF INDENTATION

The pressure under a cylindrical indenter has been previously modelled using Equation 4-8 [104].

$$p = p_o\left(1 - \left(r/a\right)^2\right)^n$$

Equation 4-8

p - local pressure, p_o - mean pressure, r - distance from centre, a- radius of indenter.

For a uniform pressure n = 0, for uniform normal displacement n = $-^1/_2$, for Hertzian pressure distribution n = $^1/_2$. For a rigid flat indenter, resting on a flat semi-infinite homogenous elastic body, there is uniform normal displacement i.e. n = $-^1/_2$, and therefore the pressure beneath the indenter can be modelled using Equation 4-9 [204].

$$p = p_o\left(1/\sqrt{1 - \left(r/a\right)^2}\right)$$

Equation 4-9

p - local pressure, p_o - mean pressure, r - radial distance from centre line, a - radius of indenter

To investigate the pressure distribution under the indenter, Figure 4-6 shows a plot of local pressure divided by average pressure, against distance from centre line of indenter. It indicates that the local pressure is fairly constant under most of the indenter, but increases dramatically at the edge of the indenter where r/a values exceed 0.9.

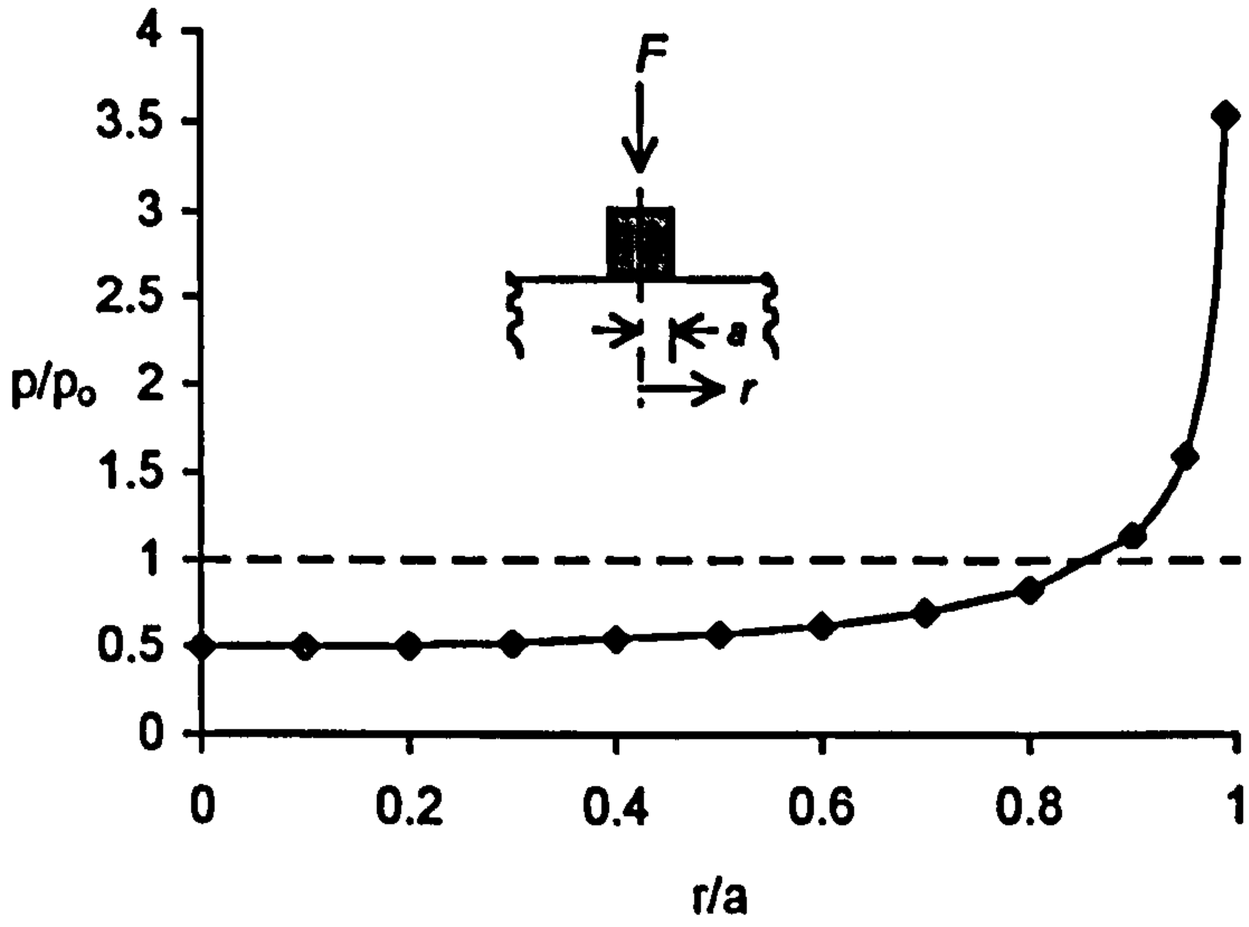

Figure 4-6 Pressure distribution beneath a flat, rigid indenter.

Brunski *et al.* [29] developed a finite element model to determine the load distribution under different shaped indenters. Their model showed that for a spherical tipped indenter the load distribution was almost Hertzian, while for a flatter indenter, a similar distribution to that shown in Figure 4-6 was apparent. Sacks *et al.* [175] demonstrated using dimensional analysis how to produce a profile for an indenter which would provide an approximately uniform pressure distribution. However, it was noted that a different profile would be necessary for each individual as well as for each different load applied. This approach is clearly impractical and as a result, for the present work, a cylindrical indenter has been designed with rounded edges to reduce high pressures at the edge of the indenter. In addition, all applied loads are quoted as the theoretical applied pressure given by the Equation 4-10.

$$P = \left(F/\pi a^2\right)$$

Equation 4-10

The deformation of tissue beyond the edge of the indenter can be modelled using Equation 4-11 for uniform displacement beneath the indenter [104].

$$\bar{u}_z = 2\left(1 - \nu^2/E\right) p_o a \sin^{-1}\left(a/r\right)$$

Equation 4-11

Figure 4-7 shows the tissue deformation around the indenter using this model.

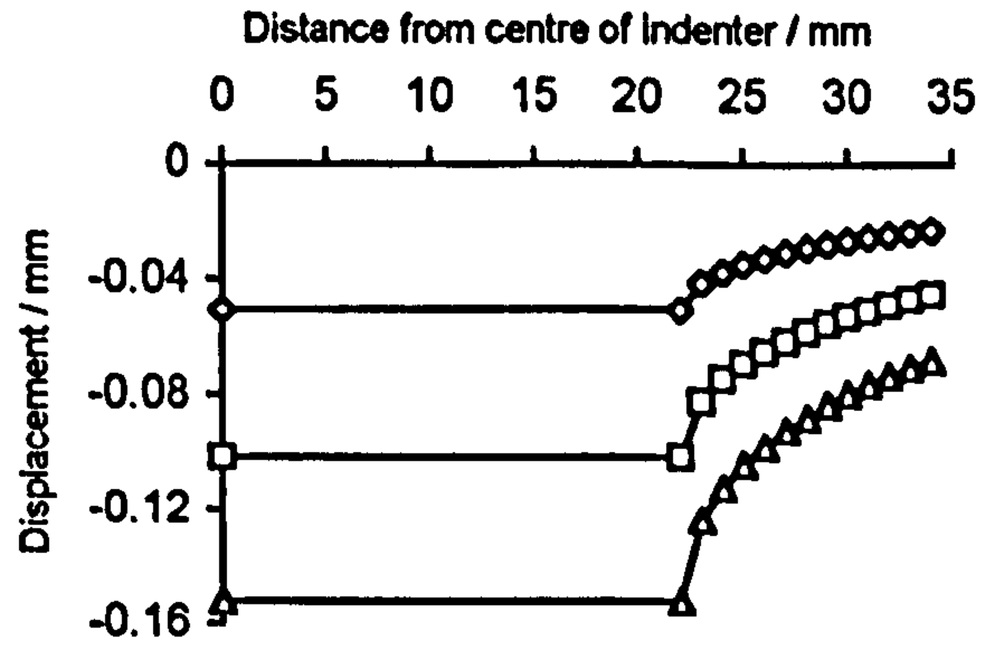

Figure 4-7 The predicted displacement of soft tissues at the edges of a 44 mm diameter flat rigid indenter at three applied pressures. Using E=2.76 MPa, v=0.49 [13].
(◇) 40 mmHg, (□) 60 mmHg, (Δ) 120 mmHg.

This model is limited by the assumptions of the material properties of the tissue, but again it highlights the large deformation gradients associated with high pressures at the edge of the indenter. These gradients were reduced by including a rounded edge to the indenter.

4.4.3 DESIGN SPECIFICATION

A new indenter was designed for the present study. It was based on an indenter previously designed to incorporate a gas tension electrode [8], with an outside diameter of 32 mm and rounded edges. However, for the present work the indenter diameter was increased to enable a sufficient area to accomodate an annular sweat pad capable of absorbing in excess of 100 mg of sweat. Figure 4-8 shows the design of the indenter incorporating a universal joint allowing free movement during loading and a removable segment which facilitated positioning of the gas tension electrode. It was manufactured from Perspex in order that the contact area of the tissue could be visualised during the loading experiments. Figure 4-9 shows the equipment for the combined sweat collection and gas tension measurements. To enable maximum area for sweat collection the electrode fixation rings were trimmed to give an outside diameter of 14 mm.

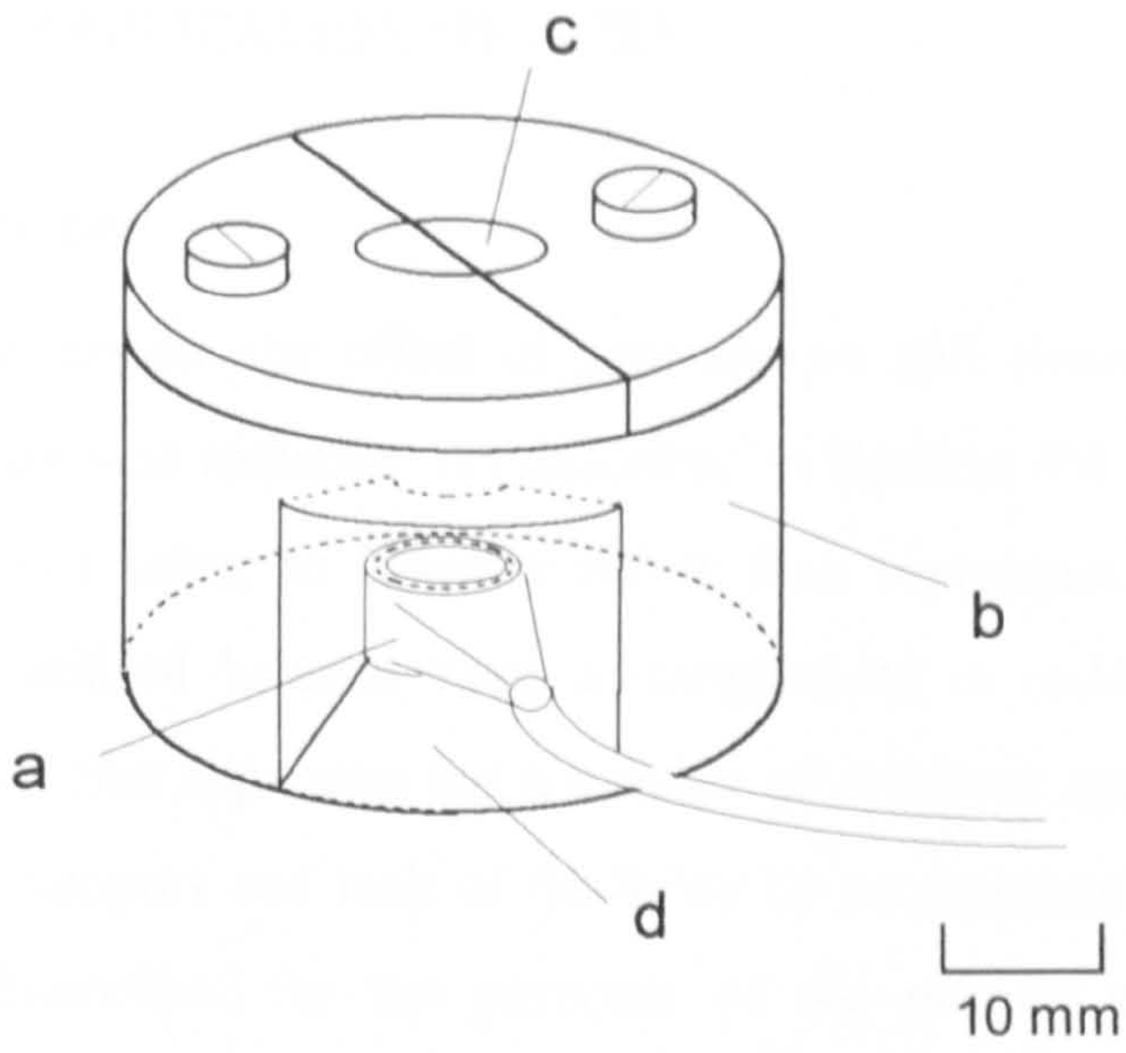

Figure 4-8 Schematic diagram of indenter modified for sweat collection and gas tension measurement.
a) combined electrode, b) perspex indenter, c) universal joint, d) removable segment

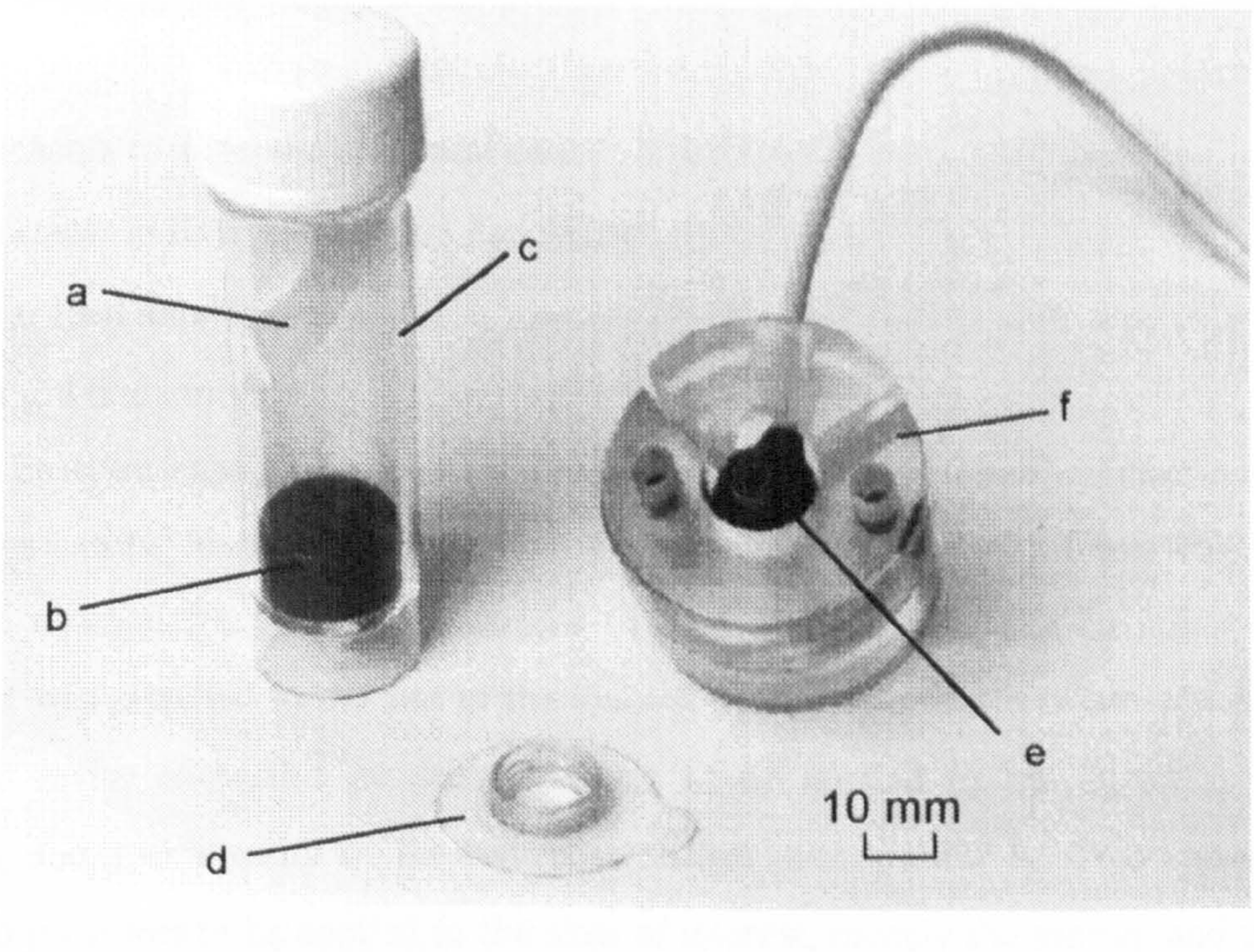

Figure 4-9. Combined sweat collection and gas tension measurement equipment.
a) sweat collection pad, b) spacer, c) 'Universal' container, d) fixation ring, e) O_2/CO_2 electrode, f) indenter

4.5 PRESSURE APPLICATION DEVICES

4.5.1 INTRODUCTION

In order to investigate the effect of pressure on soft tissue status a system for pressure application was required. As described in Section 4.4 the experiments were generally carried out using an indenter rather than tourniquet techniques. Previous researchers have utilised balance beam arrrangements in order to provide uniaxial pressure. However, this apparatus has a number of disadvantages including instability due to the tripod support and lack of flexibility to accomodate the sacral tissue in a prone position. Therefore, for the purposes of the present work a new pressure application device was designed.

4.5.2 DESIGN SPECIFICATION

The design specification for the pressure application device included the following factors:-

- Attachable to a standard hospital bed.
- Adjustable in three orthogonal directions.
- Linear load application
- No rigid body motion.

The pressure application device is illustrated in Figure 4-10 and engineering design drawings can be found in Appendix A. The bearing consisted of a linear ball race to provide minimal friction during transfer of load from loading pan to indenter. The indenter was attached to the end of the loading pan by means of a universal joint. The loading device allowed a constant pressure to be applied to the indenter, via the loading pan; the linearity of the device is shown in Appendix A. This arrangement allowed pressures to be applied to the sites of interest, namely the sacrum and in some cases the forearm, whilst subjects lay prone on a hospital bed. This ensured that the clinical relevance of the project was kept at the forefront of the investigations.

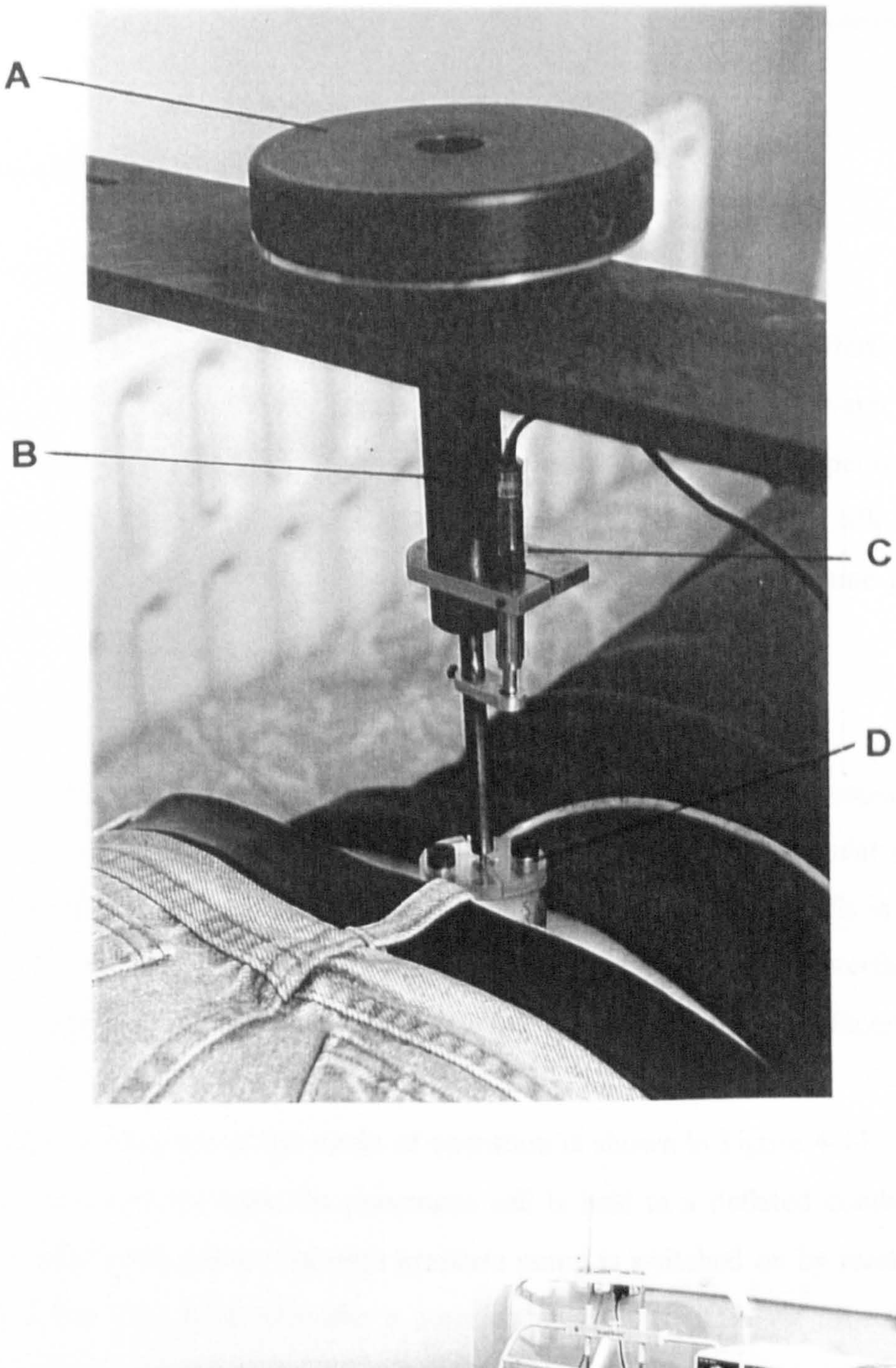

Figure 4-10 Pressure application device attached to a hospital bed.
A - load and loading pan, B - linear bearing, C - LVDT, D - indenter.

4.6 INTERFACE PRESSURE MONITORING

4.6.1 INTRODUCTION

A number of interface pressure monitors are available employing different operating principles such as capacitance, strain gauges, electropneumatics and water filled sacs, these have been discussed in Chapter 3. The monitors used for the experiments in this thesis were the commercially available Talley Mk III and the Oxford Mk II Pressure Monitor (Talley Group Ltd, Romsey, Hants), both employing the same principle of operation.

4.6.2 PRINCIPLES OF OPERATION

The OPM II and the TPM III comprise a matrix of 12 and 96 cells respectively. The cells are 20 mm in diameter and are arranged either in a 4 x 3 rectangular matrix with 28 mm distance between centres or in a large sheet containing the cells in a designed array. The cells are highly flexible and therefore do not distort the interface surfaces which is especially important when dealing with highly compliant surfaces associated with the soft tissue support interface.

A systemic diagram of the mode of operation is shown in Figure 4-11. At the start of each measurement cycle the pneumatic cell is held in a deflated condition by the vacuum side of the pump. The high pressure pump is switched on by means of an air control valve. The pump provides a constant mass of air flow via a needle valve in order to inflate the cell. When the pressure in the cell equals the external pressure, the cell begins to open and, as a consequence, the volume of the system increases and the rate of pressure increase with time is effectively reduced. This rate of pressure change is continuously monitored by a microprocessor and when it changes, the pressure is recorded and the control valve is switched back to vacuum in order to deflate the cell. The maximum pressure limit is 310 mmHg (41.32 kPa) for the OPM II and 246 mmHg (32.80 kPa) for the TPM III. The frequency of readings is in excess of 2 Hz and is dependent upon applied pressure, pump characteristics and measurement mode. Both cell matrix and single cell monitoring can be achieved in modes of instant, average, maximum or minimum pressures.

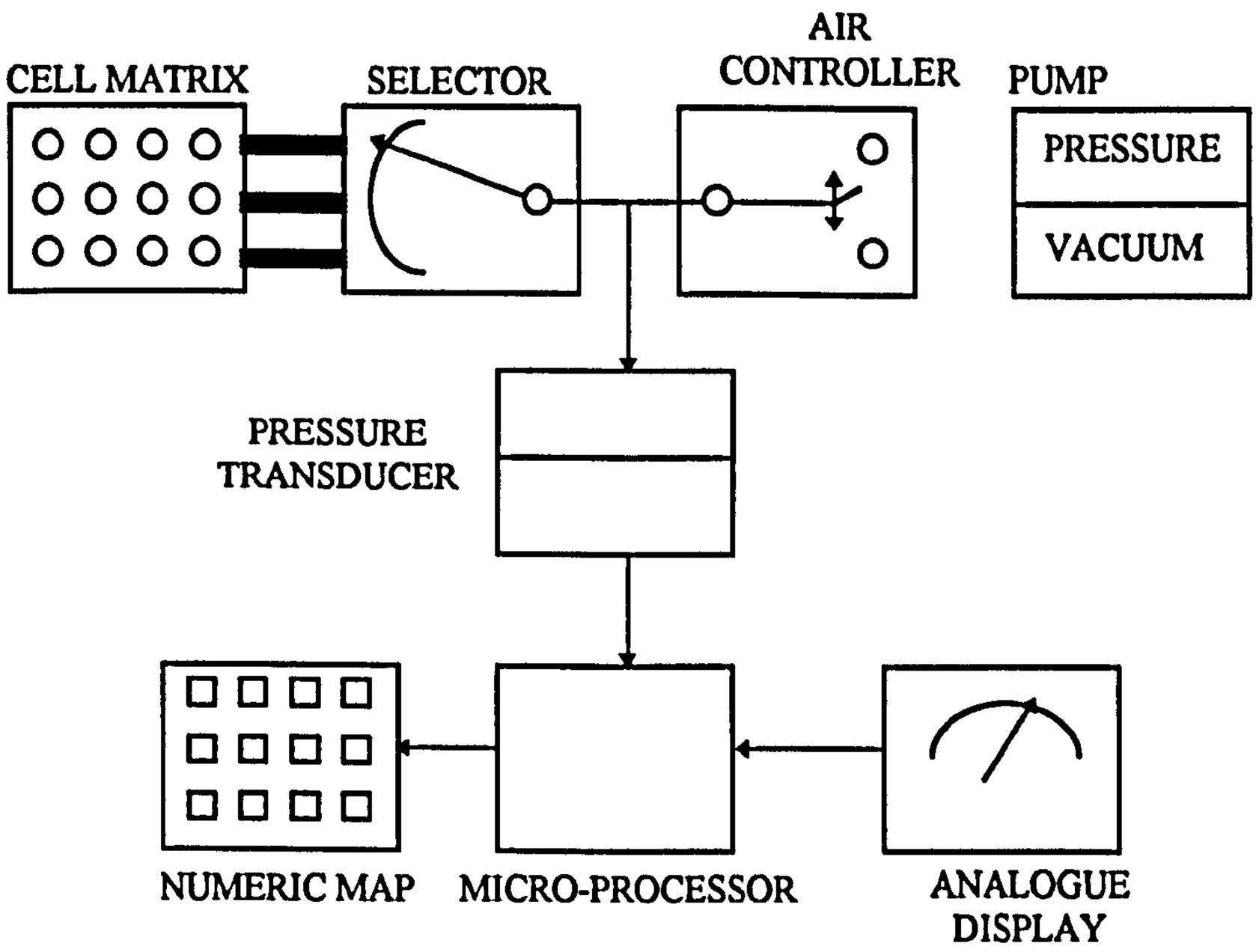

Figure 4-11 Schematic diagram showing components of the Interface Pressure Monitor.

4.7 TISSUE DEFORMATION MEASUREMENT

4.7.1 INTRODUCTION

The mechanical characteristics of soft tissue, such as stiffness and viscoelasticity, may give some indication of status and integrity with respect to its ability to carry load and to recover fully after the load is removed. Tissue is a viscoelastic material and therefore time is an important parameter in the characterisation of tissue response to load. In order to measure soft tissue deformation a linear voltage displacement transducer (LVDT), one of the most common forms of displacement transducer was used in conjunction with the loading device and indenter to measure tissue deformation.

4.7.2 DESIGN SPECIFICATION

The LVDT (D5/200AG, RDP, UK) consisted of three electrical coils, one for energisation and the other two for receiving signals, and a moveable nickel iron core.

The LVDT was driven by a sine wave and the output amplitude and phase were directly proportional to the position of the core with respect to the receiving coils. A phase sensitive detector was required to demodulate the output signal. The advantages of this non-contact type of transducer are that they do not suffer from wear such as associated with potentiometers and they provide infinite resolution and high accuracy and linearity. Figure 4-12 shows the experimental set up for the tissue deformation measurements using the LVDT.

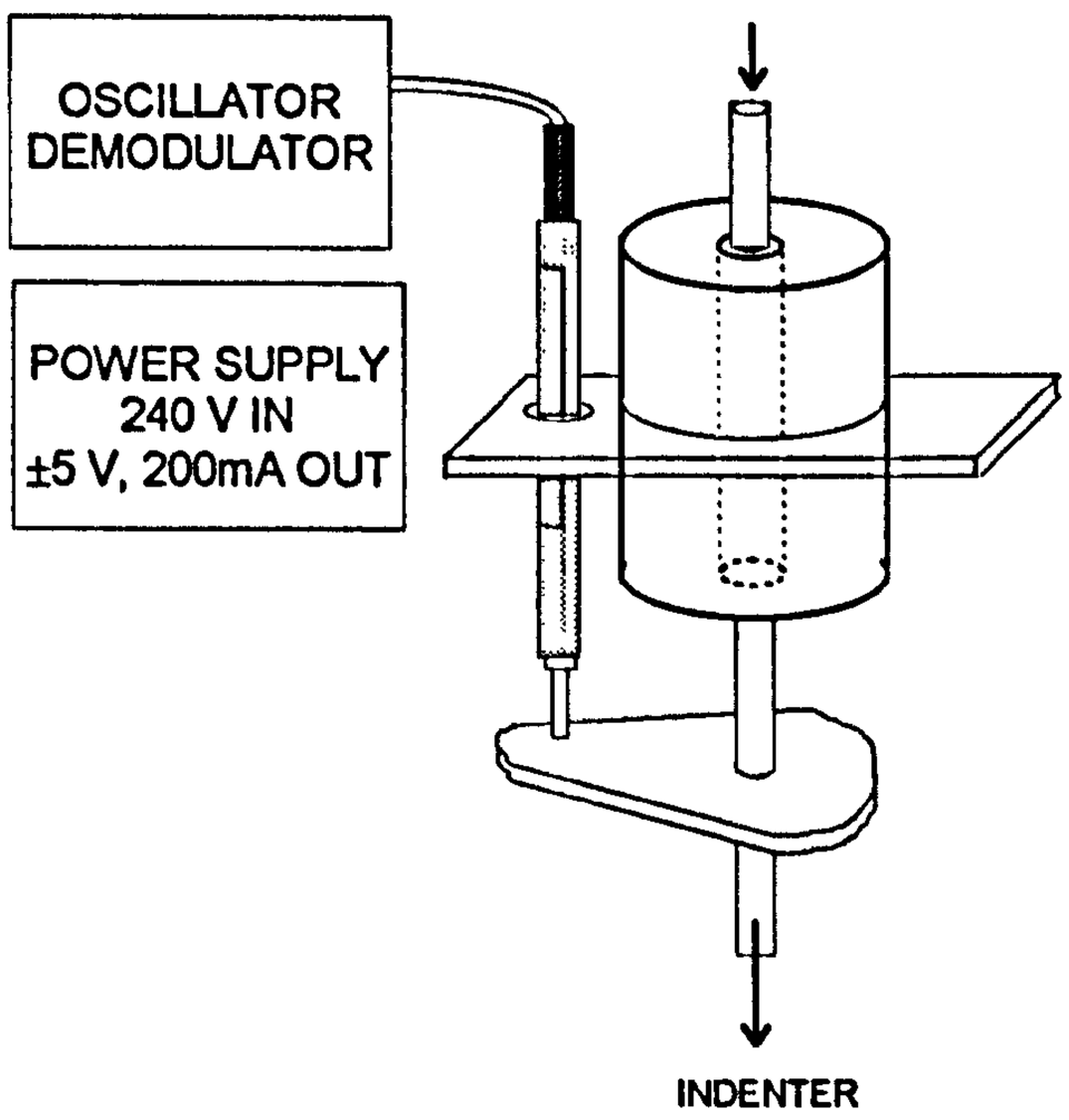

Figure 4-12 Experimental apparatus for measuring tissue deformation.

4.7.3 CALIBRATION

In order to investigate the response of the LVDT over its range of 11.5 mm, it was calibrated using incremental displacements using a series of slip gauges each with a nominal thickness of 0.12 mm (Appendix A). The results indicated a linear response over the displacement range (Figure A1).

4.7.4 SIGNAL ANALYSIS

During tissue deformation measurements at the sacrum, the signal data was filtered to remove artefacts due to subject respiration. A low pass Butterworth digital filter was designed for a sampling frequency of 0.166 Hz and a cut off frequency of 0.0415 Hz using Equation 4-12. An example of the filtered data is shown in Figure 4-13.

$$Y_n = (a_o X_n) + (a_1 X_{n-1}) + (a_2 X_{n-2}) + (b_1 Y_{n-1}) + (b_2 Y_{n-2}) \qquad \textit{Equation 4-12}$$

where $a_0 = 0.25$, $a_1 = 0.5$, $a_2 = 0.25$, $b_1 = 0$, $b_2 = 0$

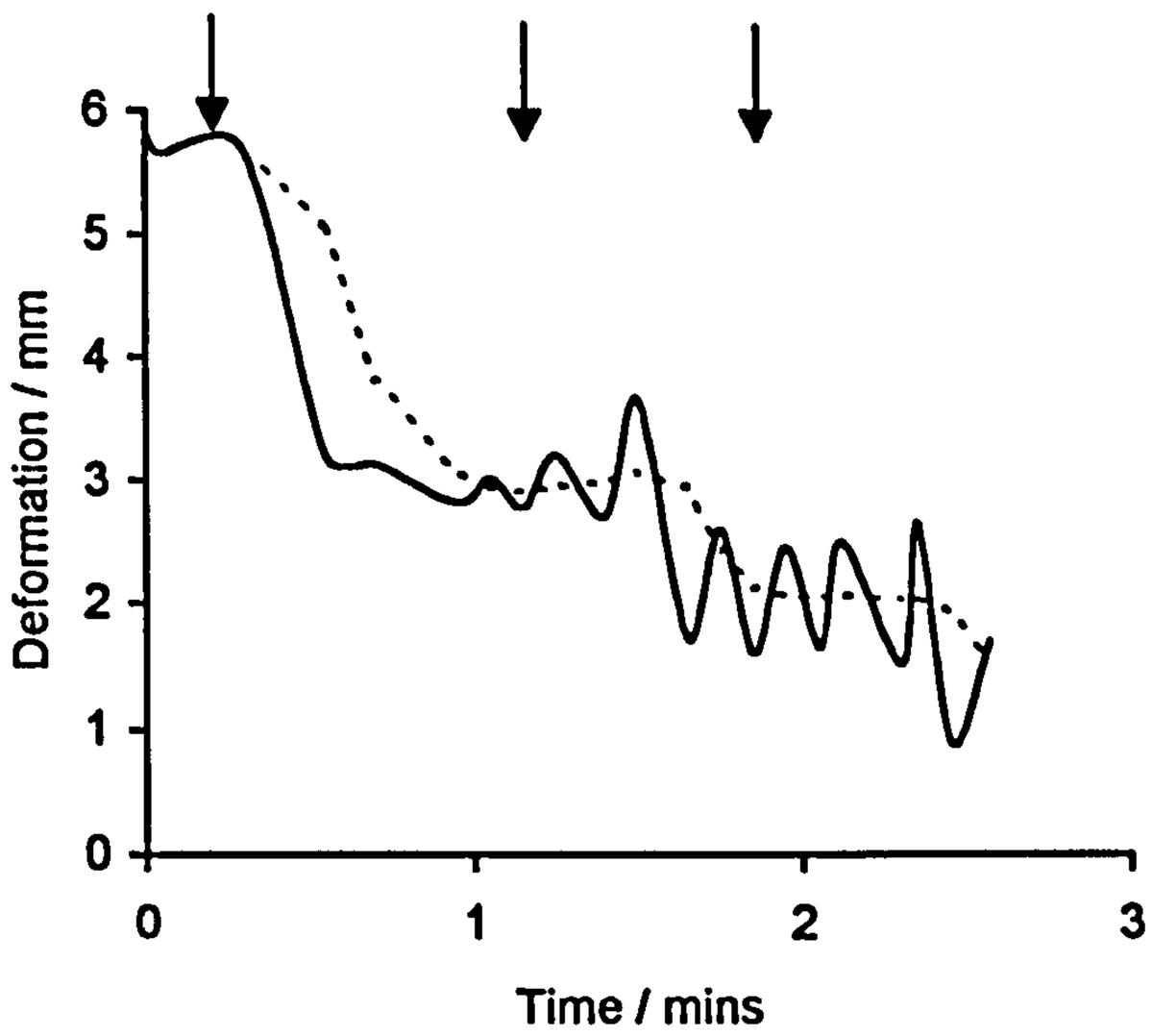

Figure 4-13 Filtered tissue deformation data. (↓) denotes application of load, (-----) filtered data, (—) actual data.

4.8 SUMMARY

The techniques described in this chapter were available for subsequent investigation of prolonged loading on soft tissue status in both healthy controls and clinically relevant patient groups.

5. Development of Gas Tension Parameters and Loading Protocols

5.1 Introduction

Transcutaneous oxygen tension measurement has been used successfully in a number of studies to measure tissue viability in both normal healthy volunteers and particular patient groups [6-10,24-25,55-56,64,107,147-148,181,191,194]. More recently transcutaneous carbon dioxide tension monitoring has been possible, although there are more limited reports of the use of this technique in the measurement of tissue status [24-25,].

This chapter describes the establishment of some experimental protocols, with regard to transcutaneous O_2 and CO_2 tension measurement and loading techniques, which will be adopted in the main experiments described later in this thesis. In addition, the chapter derives a series of novel parameters which characterise tissue status during prolonged loading with respect to oxygen and carbon dioxide tension.

5.2 Effect of Electrode Temperature on Steady State Gas Tension Measurements

Transcutaneous gas tension measurements rely on producing maximal vasodilation in the tissues beneath the electrode. This state facilitates the diffusion of oxygen and carbon dioxide from capillaries through the upper layers of the skin which is subsequently detected by the electrochemical sensor at the skin surface. The main aim of this experiment was to investigate the effect of electrode temperature on steady state oxygen and carbon dioxide tensions. The experiment was carried out on two healthy volunteers (female age 25 years), and two skin sites were investigated namely the volar aspect of the forearm, a hirsute site, and the heel, a glabrous site.

The standard operating procedure for the transcutaneous monitor described in Section 4.2.5 was generally followed, although the electrode was set to a range of temperatures between 37°C to 45°C; a steady state measurement was taken after 15 minutes. Each measurement site was repeated a maximum of 5 times. The electrode

position was adjusted slightly between readings to minimise the possibility of permanent reddening or skin erythema. The results of the steady state oxygen and carbon dioxide tensions measured at each electrode temperature and skin site are illustrated in Figures 5-1 and 5-2.

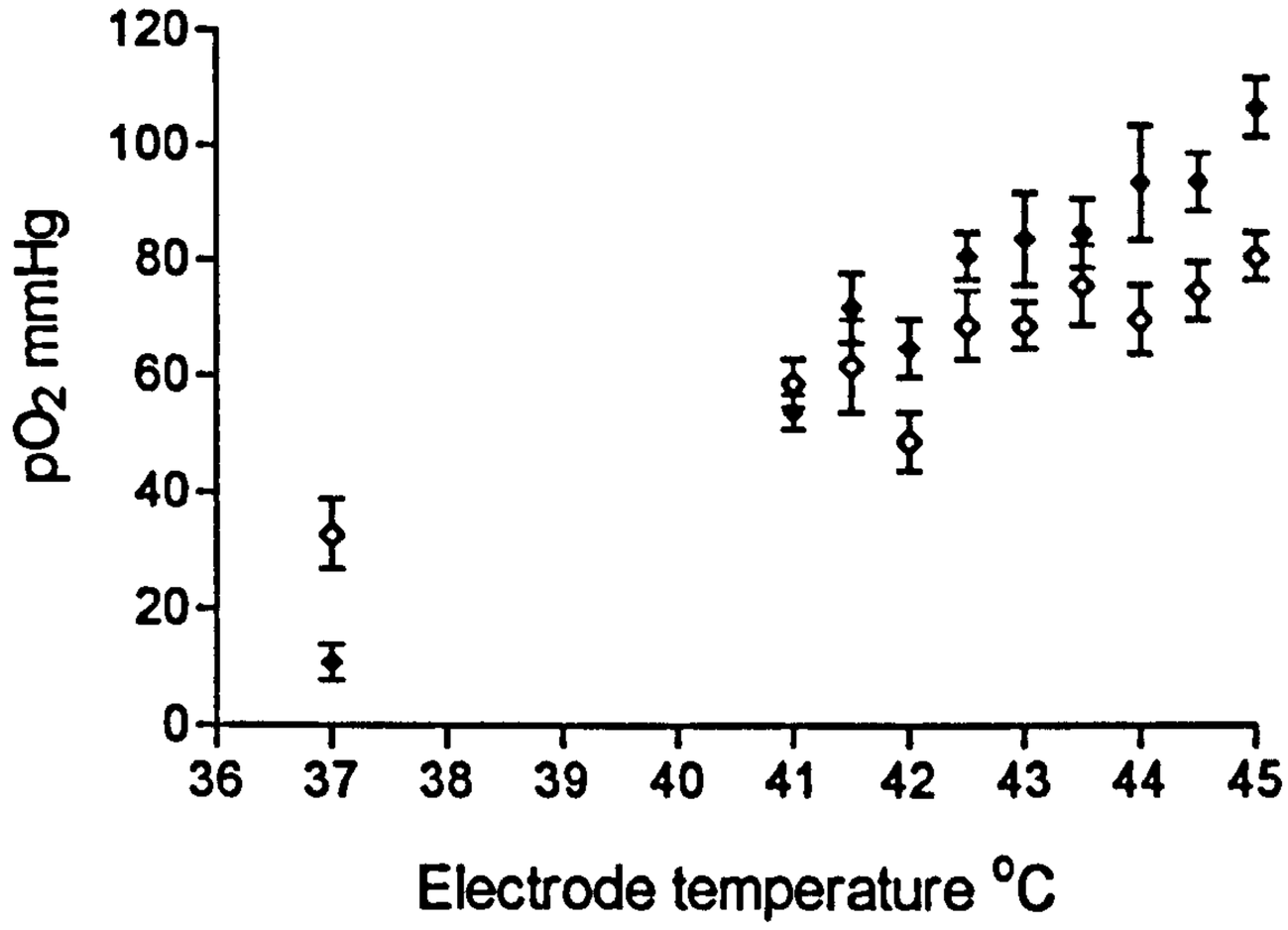

Figure 5-1 The effect of electrode temperature on transcutaneous oxygen tension measured at the volar aspect of the forearm (◆), and the heel (◊). Error bars denote standard deviation.

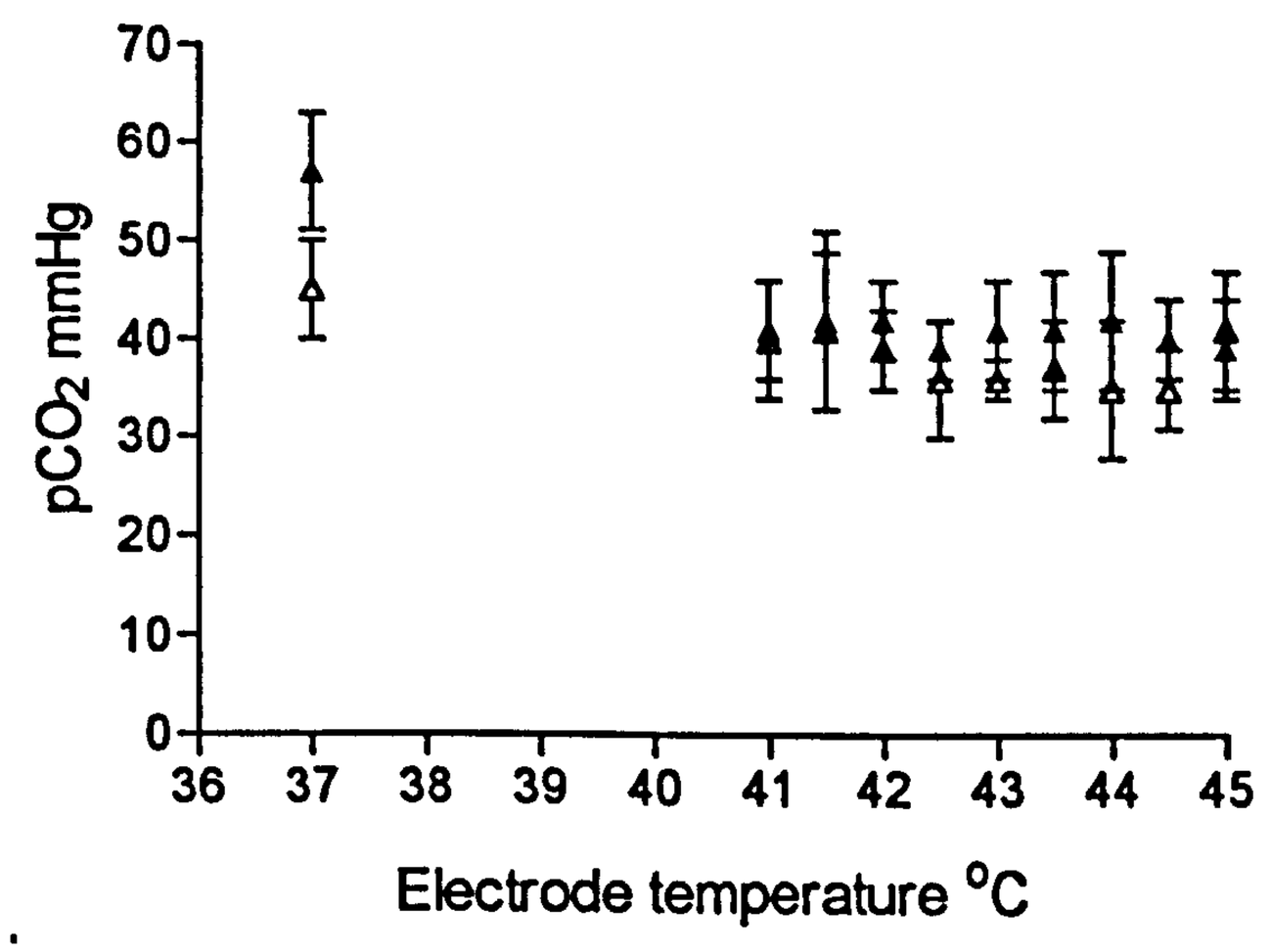

Figure 5-2 The effect of electrode temperature on transcutaneous carbon dioxide tension measured at the volar aspect of the forearm (▲), and the heel (Δ). Error bars denote standard deviation.

It is clear from Figure 5-1 that for an increase in electrode temperature there is a corresponding increase in steady state oxygen tension at both skin sites. The steady state oxygen tension at the hirsute skin site is higher than that measured at the glabrous site at temperatures above 37°C. Transcutaneous oxygen tension measurements are affected by two major factors as described in Section 3.3.2; the rightward shift in the oxygen-haemoglobin dissociation curve (Figure 1-6) with temperature and the metabolism in the upper layers of the skin. The lower O_2 tension values in the glabrous skin may be explained by the thicker skin at this sites, which may inhibit the diffusion of oxygen through the skin to the sensor to a greater extent than in the thinner hirsute skin. The effect of the metabolism of the skin may account, to a much smaller extent, for the difference between the hirsute and glabrous skin oxygen tension readings, since the upper layers of the epidermis are not metabolically active.

It appears from Figure 5-2 that the electrode temperature has a less significant effect on steady state carbon dioxide tensions. Transcutaneous carbon dioxide measurements are less affected by the above factors, this is supported by the results in Figure 5.2 which show that steady state pCO_2, although slightly elevated at 37°C remains fairly constant over the temperature range of 41°C to 45°C.

As a result of these findings, subsequent experiments were carried out at 44.5°C, a temperature which was sufficiently high to ensure maximal vasodilation without causing irreversible erythema or even skin burns.

5.3 Effect of Loading Technique on Transcutaneous Gas Tension

Previous studies have generally employed one of two main loading methods to induce pressure ischaemia in soft tissue *in vivo*. These involve use of a tourniquet or occlusive cuff [207] and the use of an indenter [72,58]. The occlusive cuff can be used to induce ischaemia in a whole limb, or to apply a hydrostatic load to the enclosed soft tissues. The indenter effectively applies a uniaxial compressive load to the tissue site.

The aim of the current investigation was to determine the effect of three loading techniques on the measured transcutaneous gas tensions. The three loading techniques are shown in Figure 5-3 corresponding to

a) Tourniquet ischaemia, with the electrode downstream from the occlusive cuff.

b) Hydrostatic pressure, with the electrode beneath the occlusive cuff.

c) Direct uniaxial compression, with the electrode incorporated into the indenter.

The tourniquet ischaemia was produced with the aid of a sphygmomanometer (Duplex Hand Model, Accoson, UK). The indenter was the model described in Section 4.4.

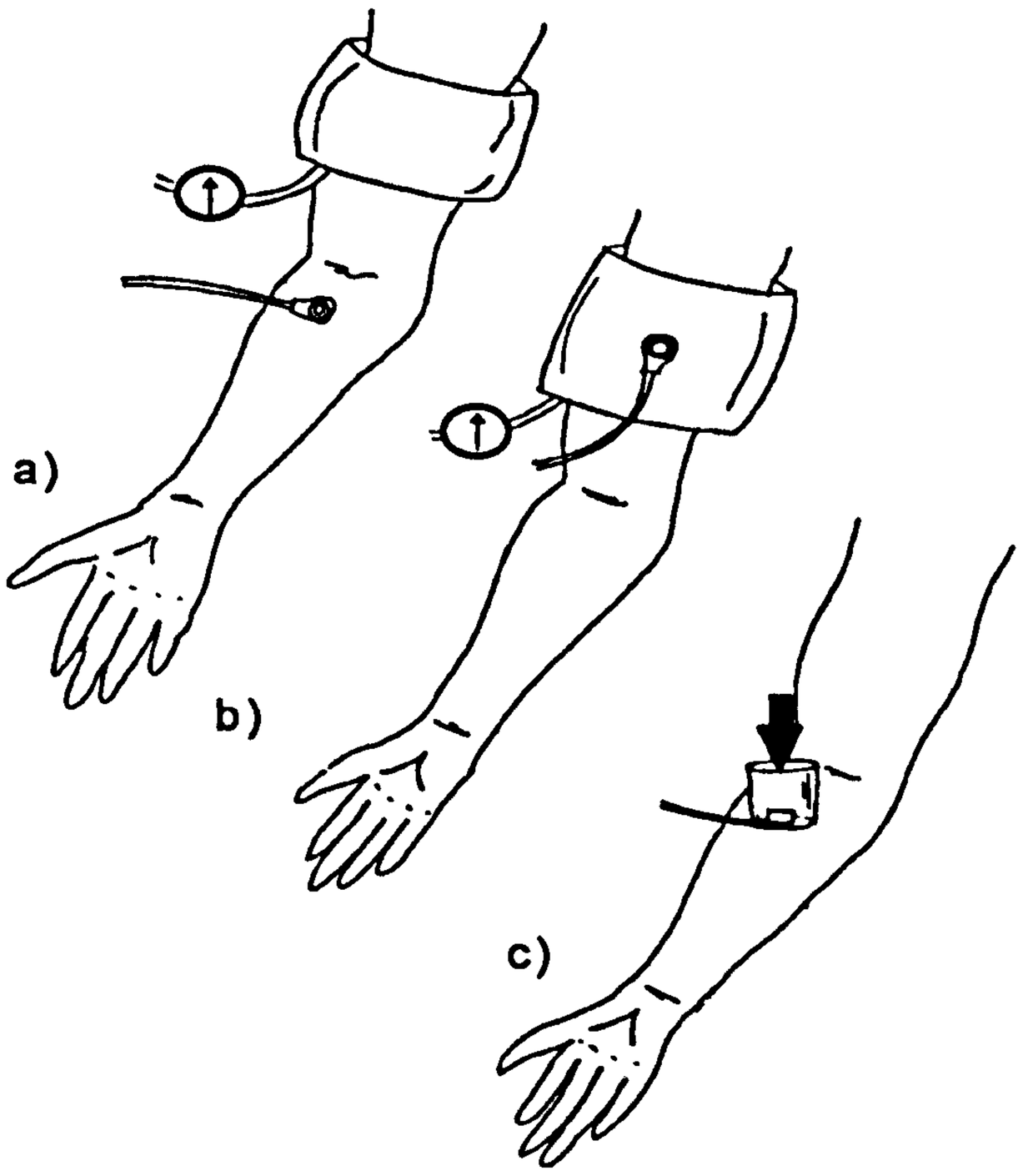

Figure 5-3 Methods of inducing pressure ischaemia in soft tissue
a) tourniquet occlusion, b) hydrostatic pressure, c) direct uniaxial compression.

The experiments were carried out on the forearm of a healthy volunteer, and the standard operating procedure (Section 4.2.5) for transcutaneous gas tension measurement was followed using an electrode temperature of 44.5°C. A pressure of 80 mmHg (11.3 kPa) was applied via both the sphygmomanometer cuff, and through the

indenter. Although it is recognised that this pressure is still below systolic pressure, it was felt to be sufficient to induce a reduction in blood flow or partial ischaemia due to occlusion of smaller blood vessels. The gas tensions were recorded for a maximum of ten minutes, as periods in excess of this caused subject discomfort during tourniquet loading.

The oxygen and carbon dioxide tensions during the experimental test period are shown for each loading technique in Figures 5-4 and 5-5 respectively. Indenter and hydrostatic loading showed a rapid decrease to a pO_2 level of 40 mmHg (5.33 kPa), representing an approximate 60% reduction of the initial unloaded level. By contrast, tourniquet loading showed a more gradual decline in oxygen tension, reducing by only about 20% of the initial unloaded pO_2 level after 10 minutes.

There is a similar difference in pCO_2 response to the three loading techniques (Figure 5-5). Tourniquet loading produced little change in pCO_2, whereas both hydrostatic and uniaxial compression showed a monotonic increase in carbon dioxide tension, which reached values of approximately 80 mmHg (11.3 kPa) after 10 minutes.

Due to the finite size of the electrode and its relative inflexibility, the hydrostatic loading regimen may have been more representative of uniaxial compression with the pressure applied to the electrode rather than equally to all the surrounding tissue. This would explain the similar results obtained for both the hydrostatic and uniaxial compression loading regimes. This situation would be altered if the electrode was set flush within the sphygmomanometer cuff.

It is clear from the results of this experiment that tourniquet ischaemia showed a very different response to that of direct uniaxial compression, in terms of transcutaneous oxygen and carbon dioxide tensions. The tourniquet ischaemia model is more relevant to situations where whole limb ischaemia is experienced, for example, in peripheral vascular disease. Uniaxial compression loading is more relevant to the manner of loading that would be expected to cause tissue breakdown in the pressure sore situation, whereby a bony prominence and/or non-conforming support surface produces high localised pressures which cause tissue ischaemia.

As a consequence, direct uniaxial compression applied through an indenter was employed on subsequent investigations.

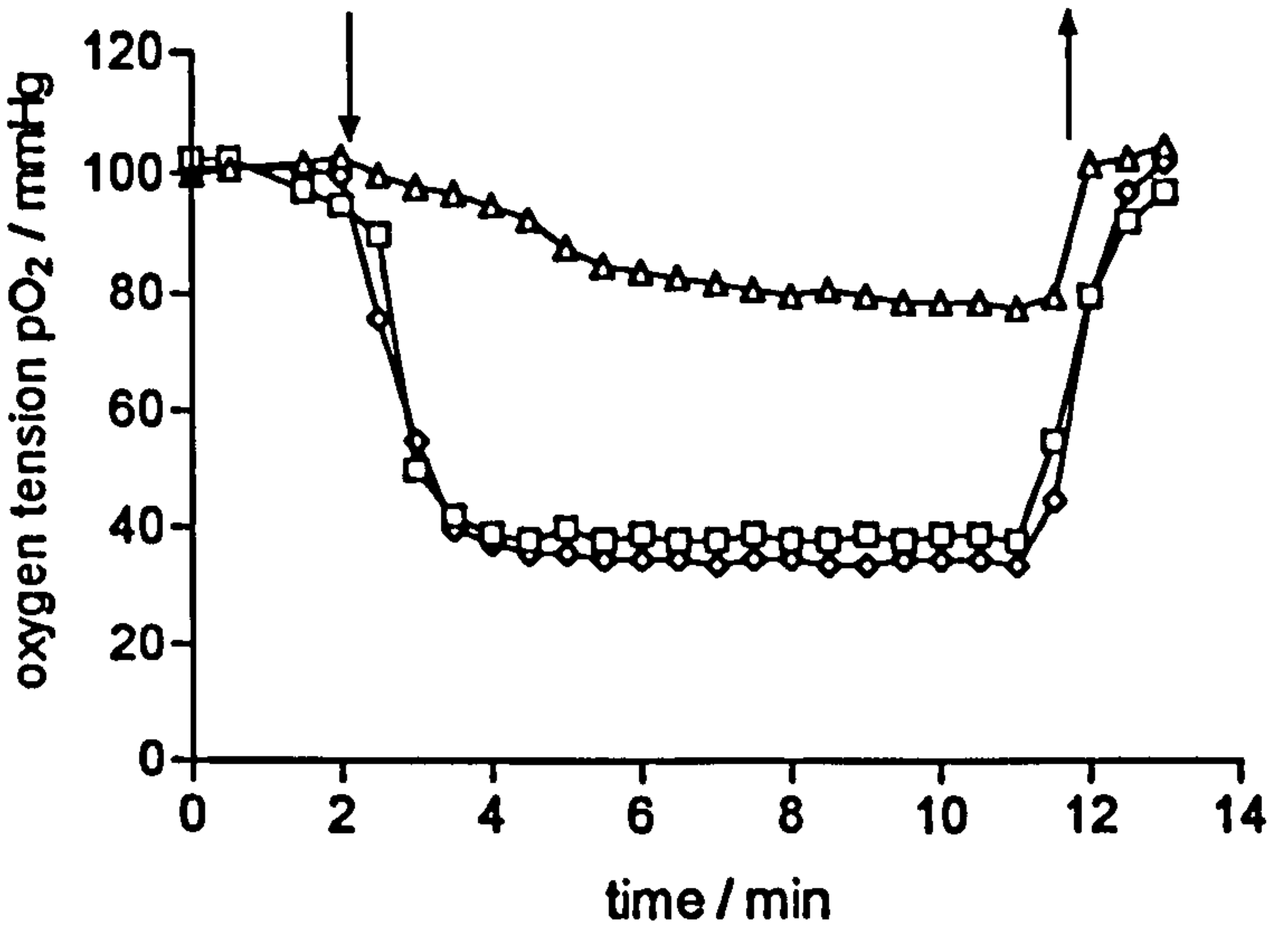

Figure 5-4 Transcutaneous oxygen tension measured at the forearm under different loading techniques.
(Δ) downstream from cuff, (□) beneath cuff, (◊) beneath indenter.
↓ indicates load application, ↑ indicates load removal.

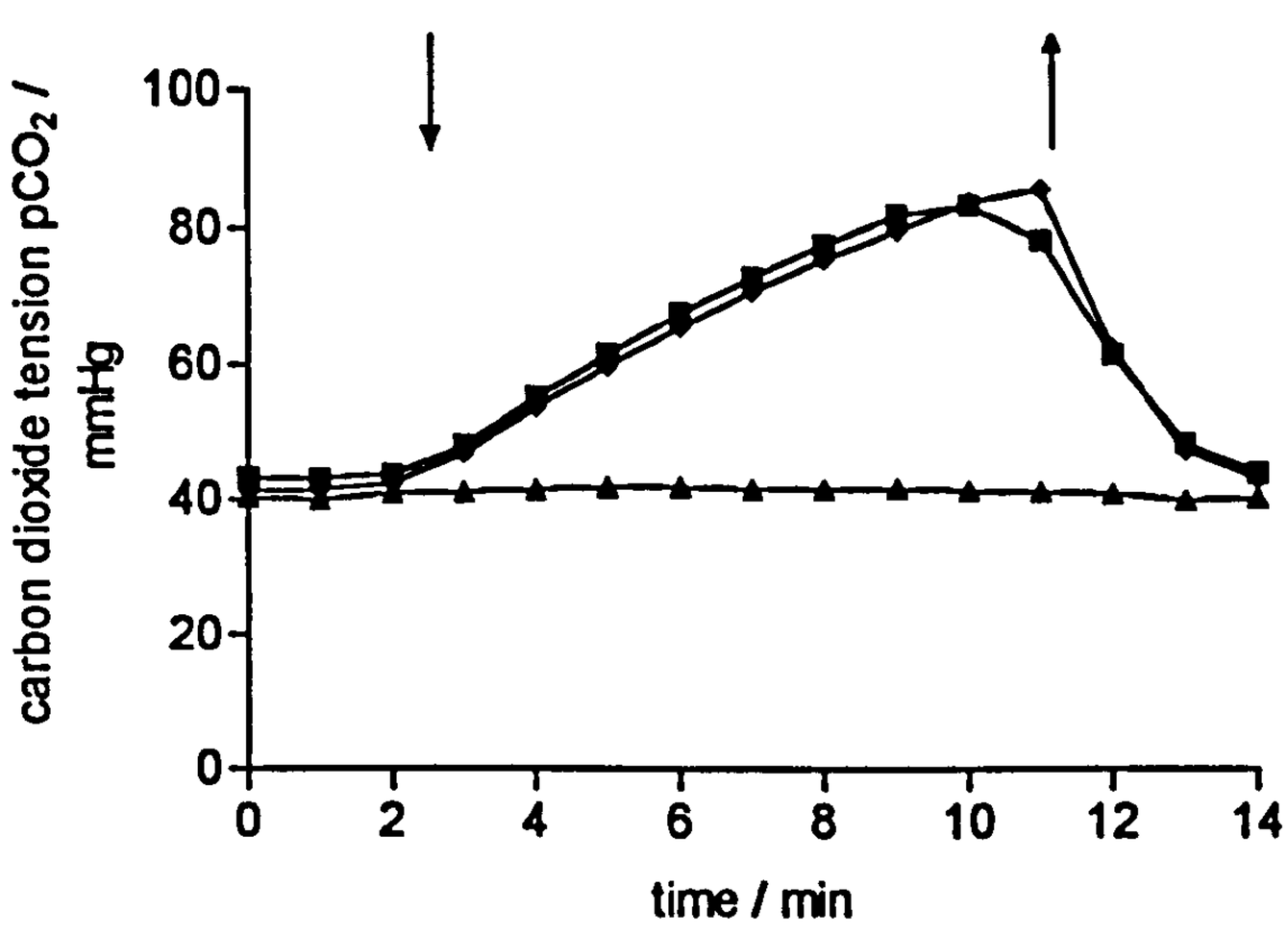

Figure 5-5 Transcutaneous carbon dioxide tension measured at the sacrum under different loading techniques.
(▲) downstream from cuff, (■) beneath cuff, (◆) beneath indenter.
↓ indicates load application, ↑ indicates load removal.

5.4 Effect of Pressure on Gas Tension Measurements.

This experiment investigated the effect of different applied pressures on gas tensions and interface pressures measured at the sacrum of healthy volunteers. In addition, some new parameters are derived to quantify some aspects of soft tissue status. The indenter and pressure application device described in Sections 4-4 and 4-5 were used in conjunction with the combined oxygen and carbon dioxide gas tension electrode to investigate the effect of different applied pressures on gas tensions at the sacrum of 7 healthy, male volunteers (mean age 24.5 years). Prior to application of the gas tension electrode, the interface pressure at the sacrum beneath the indenter was measured for a number of different applied pressures using the Talley Pressure Monitor described in Section 4-6. The standard operating procedure for gas tension measurement was followed (Section 4.2.5) and following equilibration the indenter was placed over the electrode and one of three pressures (40, 80 and 120 mmHg) was applied to the sacral tissues for a period of ten minutes (Figure 4-10).

Pressure Measurement

A series of increasing loads were applied to the sacrum via the pressure application device and at each load an average of 10 scans was calculated. The loads were then removed and the pressures measured again. The graph in Figure 5-6 shows the average interface pressure measured at each applied pressure for the seven individuals.

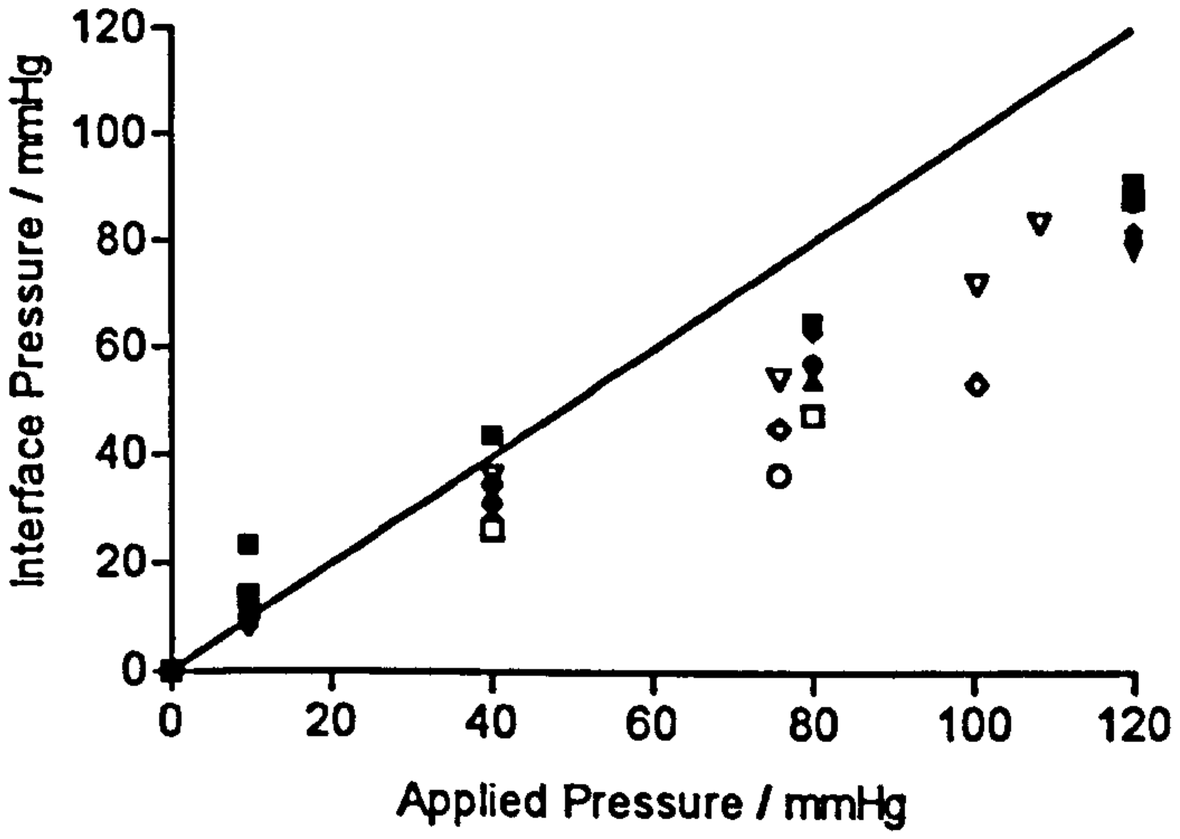

Figure 5-6 Relationship between applied pressure and interface pressure measurements at the sacrum. Symbols represent individual subjects.

It is clear from this graph that there is a correlation between applied pressure and interface pressure, although the interface pressure is always slightly underestimated by the theoretical applied pressure. Applied pressures of 40, 80 and 120 mmHg have been selected as a clinical relevant range for the main experimental work in this thesis; 40 mmHg would be considered an acceptable pressure in a clinical situation, whereas 120 mmHg would be considered unacceptably high [9,98,115].

OXYGEN TENSION

The oxygen tension readings were normalised to initial unloaded values and a parameter defined as % reduction in pO_2 was derived. This parameter is calculated using Equation 5-1.

$$\%\ reduction\ in\ pO_2 = \frac{pO_{2(initial)} - pO_{2(test)}}{pO_{2(initial)}} * 100 \qquad \textit{Equation 5-1}$$

Figure 5-7 shows a typical response of O_2 tension to various applied pressures during the loaded phase. Table 5-1 shows the mean and standard deviation for the % reduction in pO_2 for each applied pressure for the 7 subjects tested.

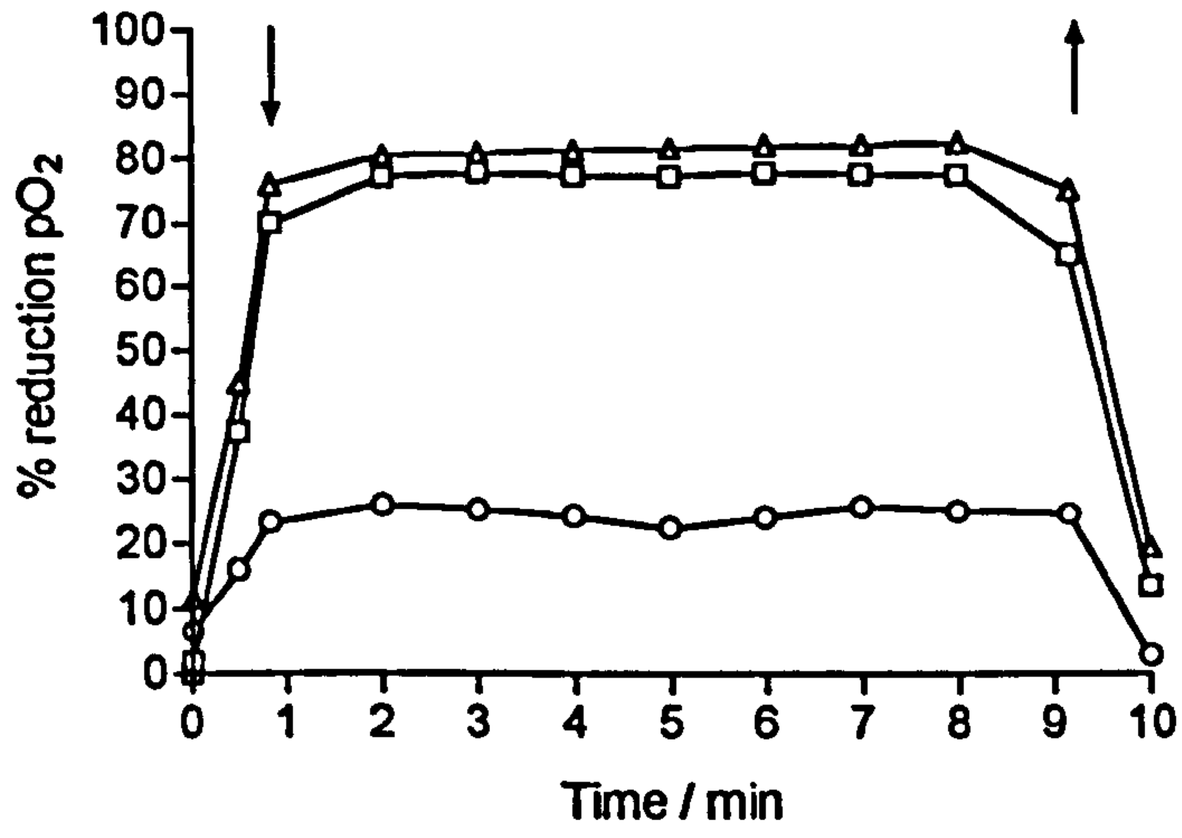

Figure 5-7 Typical curves for percentage reduction in transcutaneous oxygen tension measured at the sacrum for three different applied pressures.
(O) 40 mmHg, (□) 80 mmHg, (Δ) 120 mmHg.
↓ indicates load application, ↑ indicates load removal.

Table 5-1 % reduction in pO_2 values measured at the sacrum of healthy subjects during the loaded phase at three applied pressures.

% reduction in pO_2	40 mmHg	80 mmHg	120 mmHg
Mean	25.89	77.58	82.88
SD	24.95	8.27	6.24

The results indicate that there is a wide variability in measured O_2 tension at 40 mmHg, whereas at the higher pressures this is greatly reduced. It is apparent that at applied pressures in excess of 80 mmHg there is a dramatic reduction, up to 80%, in pO_2 from initial values, suggesting a large reduction in blood flow.

CARBON DIOXIDE TENSION

A typical graph showing the carbon dioxide response to the three applied pressures is shown in Figure 5-8. It was noted that three distinct responses were apparent which are conveniently listed as:-

- *Mode 1* - a minimal change in pCO_2 from steady state value of 40 mmHg (5.33kPa).
- *Mode 2* - an elevation in pCO_2 reaching a steady state value between 50 and 60 mmHg (6.66 - 8.0 kPa).
- *Mode 3* - a continuous increase in pCO_2 over the 10 minute loading period to values in excess of 80 mmHg (10.66 kPa).

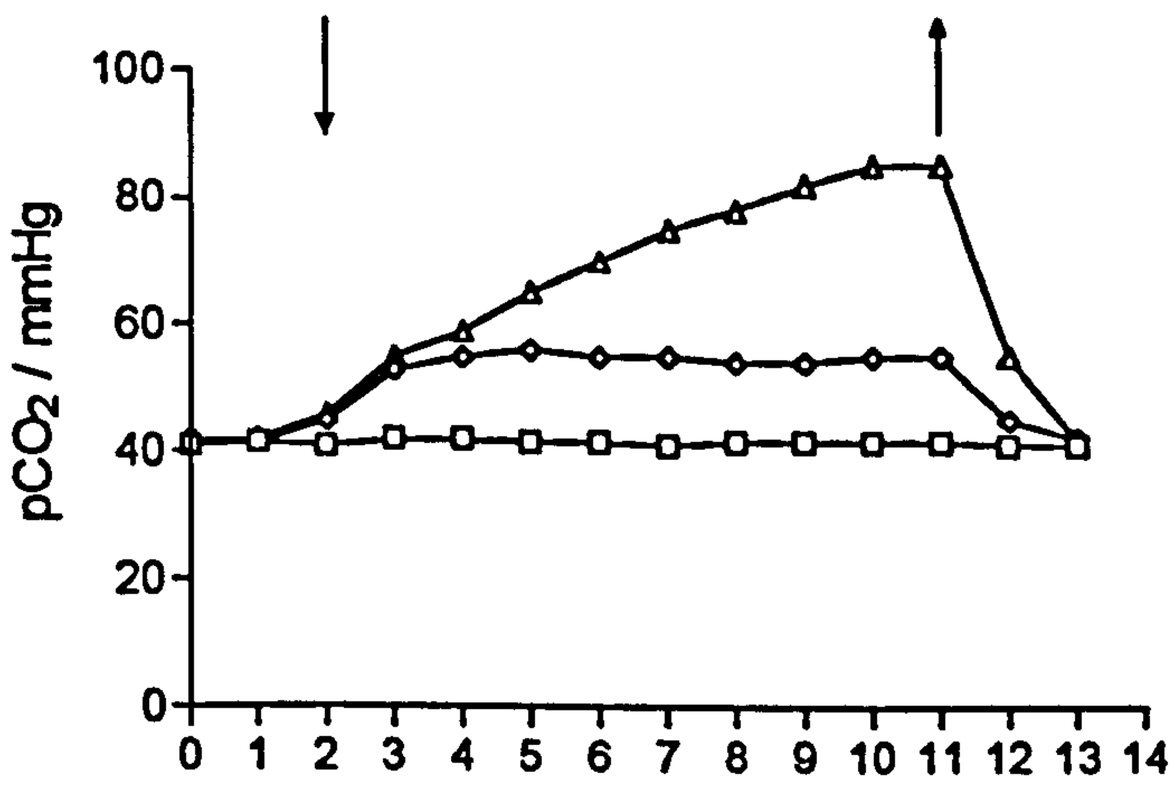

Figure 5-8 Typical transcutaneous carbon dioxide tension responses measured at the sacrum for three different applied loads
(□) 40 mmHg *(Mode 1)*, 80 mmHg (◊) *(Mode 2)*, (Δ) 120 mmHg *(Mode 3)*.
↓ indicates load application, ↑ indicates load removal.

The Mode 3 response has previously only been described by a few authors [24-25]. Table 5-2 shows the distribution of the three modes of carbon dioxide response for each applied load in the 7 subjects tested. It is clear from the table that Mode 1 was associated with applied pressures of 40 mmHg, whereas Modes 2 and 3 were associated with applied pressures in excess of 80 mmHg.

Table 5-2 Distribution of carbon dioxide tension modes measured at the sacrum of healthy subjects during the loaded phase at three applied pressures.

CO_2 tension mode	40 mmHg	80 mmHg	120 mmHg
Mode 1	7	-	-
Mode 2	-	2	-
Mode 3	-	5	7

In order to quantify the pCO_2 response, two further parameters were defined. The first is based on an approach described by Bogie *et al.* [24], using pre-defined limits of carbon dioxide tension based on normal levels [32]. The time during which the pCO_2 level exceeded 50 mmHg was calculated as a percentage of the total duration of the applied pressure. This parameter, as illustrated in Figure 5-9a, effectively distinguishes between the Mode 1 response and the Mode 3 response. The alternative parameter is calculated from the integration of the pCO_2 curve above the initial unloaded pCO_2 level and using a normalised time axis to derive the area denoted by A in Figure 5-9b.

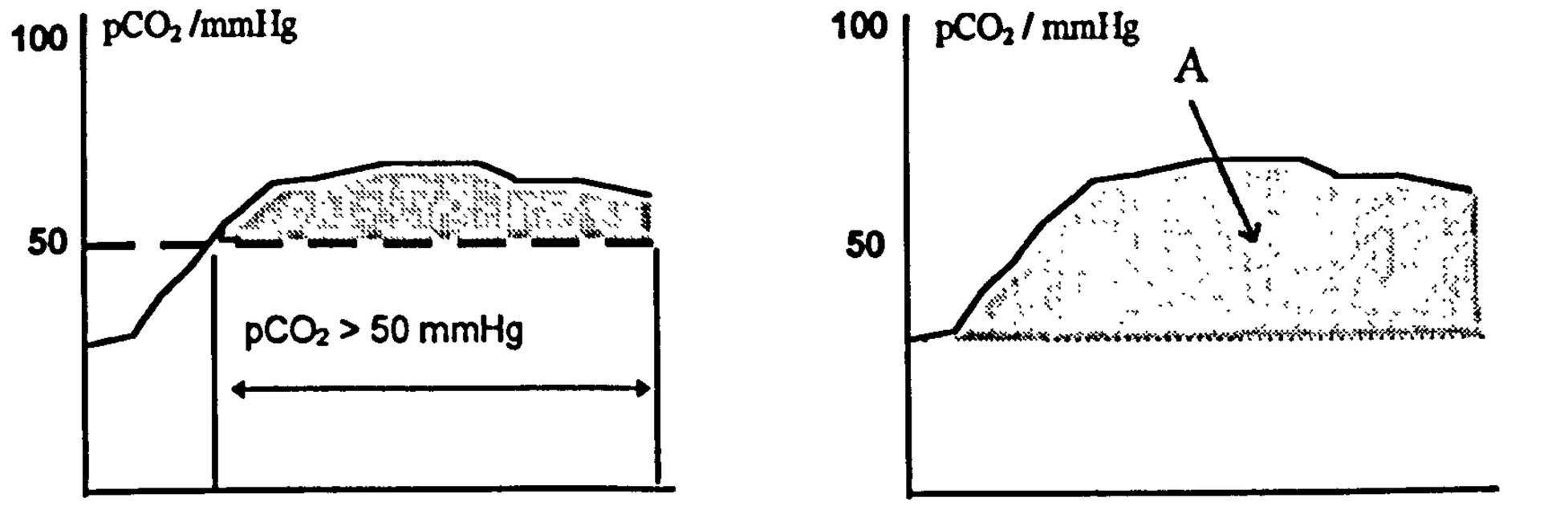

Figure 5-9 Diagrammatic representation of the two derived parameters for describing pCO_2 tension.
a) percentage time when pCO_2 is greater than 50 mmHg,
b) area, A, underneath the pCO_2 - % time curve

Table 5-9 details the results obtained for the 7 subjects with respect to these further parameters.

Table 5-3 Mean and standard deviations for the derived carbon dioxide tension parameters measured at the sacrum of healthy volunteers during the loaded phase at three applied pressures.

Applied Pressure	% time > 50 mmHg	Area under pCO_2 curve
40 mmHg	0.0 ± 0.0	563.4 ± 181.7
80 mmHg	73.6 ± 11.0	2843.7 ± 2233.6
120 mmHg	87.2 ± 8.1	6178.2 ± 2052.4

5.5 Reperfusion Measurement using Gas Tension Monitor

The ability of the blood supply to reperfuse an area of tissue, which has previously been subjected to pressure induced ischaemia, may be of equal importance in terms of soft tissue breakdown to the original extent of the ischaemia. Reperfusion was assessed in an extension to the experiment described in Section 5.4, in which the applied pressures were removed after a 10 minute period and both the transcutaneous pO_2 and pCO_2 levels were monitored during 5 minutes of reperfusion.

Figure 5-10 shows the pO_2 as a percentage of the initial unloaded value, after the removal of the load. It is clear that the time taken to restore pO_2 to the initial unloaded values is dependent on the extent of the pressure induced insult.

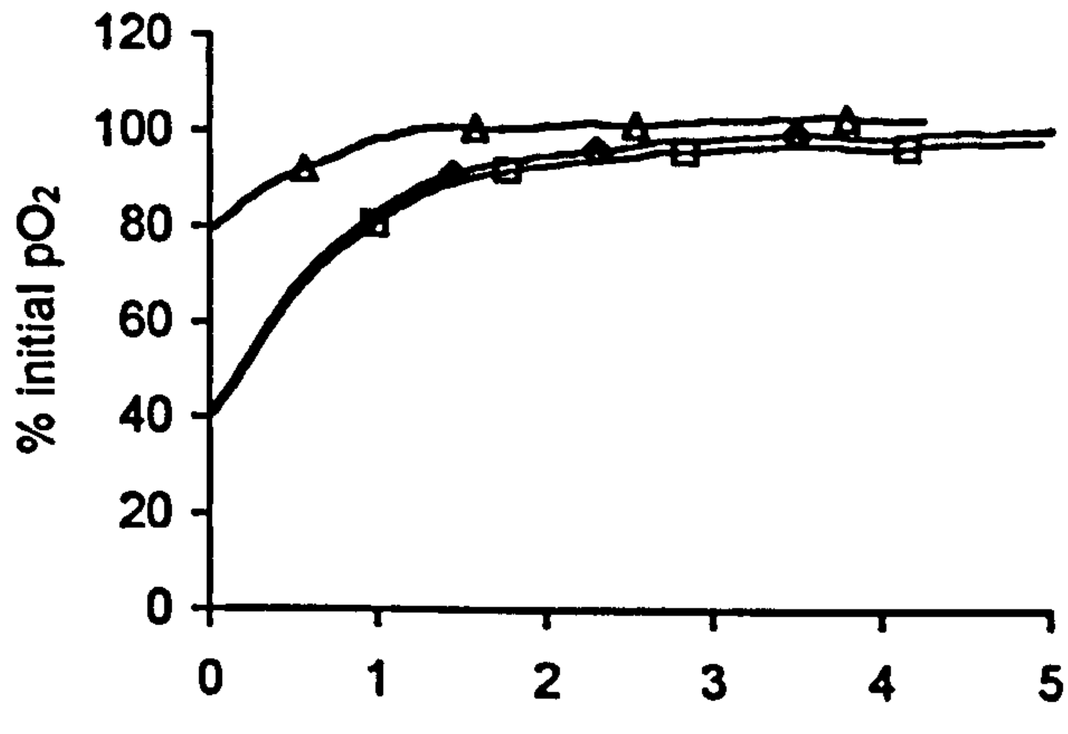

Figure 5-10 Typical pO_2 reperfusion characteristics after loading at the sacrum for 10 minutes. (Δ) 40 mmHg, (◊) 80 mmHg, (□) 120 mmHg.

In order to quantify reperfusion, a parameter was defined based on the half time for recovery of pO_2 given by Equation 5-2.

$$t_{[1/2]} = t_{\left[\left(\frac{T_f - T_i}{2}\right) + T_i\right]} \qquad \textit{Equation 5-2}$$

$t_{1/2}$ - half time, T_f - final pO_2, T_i - pO_2 during loading phase.

This parameter was found to increase with applied pressure as indicated in Figure 5-11. This suggests that for greater applied pressures, the time required for reperfusion of blood supply is increased.

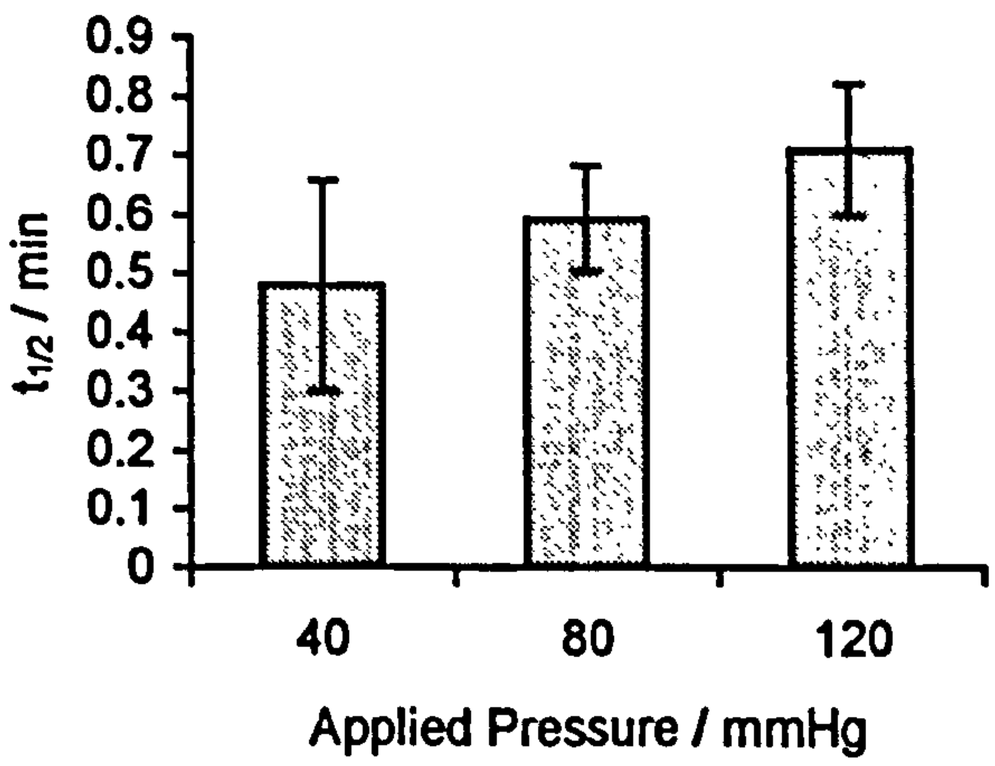

Figure 5-11 The effect of applied pressure at the sacrum on the reperfusion half time paramcter. Error bars denote standard deviation.

A number of researchers have suggested that impairment of the reperfusion response may be an indicator of susceptibility to tissue breakdown [89,107,137]. It should be noted that reperfusion and reactive hyperaemia are distinct physiological processes. Indeed, reactive hyperaemia can not be measured using transcutaneous gas tension measurements at the chosen temperature of 44.5°C, as maximal vasodilation is required to promote efficient gas diffusion. At a lower electrode temperature of 37°C, however, it has been suggested that transcutaneous oxygen tension values can reflect the reactive hyperaemic response [64], although pO_2 values at this temperature will not reflect arterial levels.

5.6 SUMMARY

Transcutaneous gas tensions have been used by a number of researchers to provide an indicator of tissue viability [8,24,56]. This chapter has established some important protocols which will be used in the main experimental chapters of this thesis. These findings are described below:-

- An electrode temperature of 44.5°C is required to promote maximal vasodilation without causing discomfort.
- Pressure ischaemia is most representatively produced via loading through an indenter.
- Applied pressures of 40, 80 and 120 mmHg ill be used.

In addition, a number of parameters have been derived which will be used in the subsequent experimental investigations into the effect of applied pressure on soft tissue status. The main derived parameters of this chapter are summarised as follows:-

- Oxygen tensions are described as a percentage reduction in oxygen tension from initial unloaded pO_2 values.
- Carbon dioxide tensions are described using one of three parameters
  - ⇒ % time $pCO_2 > 50$ mmHg
  - ⇒ Area under normalised pCO_2 curve
  - ⇒ Mode 1, Mode 2 or Mode 3 response.

6. TEMPORAL CHANGES IN THERMALLY INDUCED SWEAT

6.1 INTRODUCTION

The analysis of sweat collected at soft tissue sites experiencing pressure induced ischaemia can be used as a measurement of tissue status. Previous studies involving the sweat pad technique have examined discrete collection periods of between 10 minutes and 9 hours [158-159,202]. Previous researchers have characterised the repeatability of these measurements in single individuals [45,158,207] however, the measurement of the temporal profile in the basal and loaded states, for both sweat rate and sweat metabolite concentration has not been established. The two experiments in this chapter were carried out to establish temporal relationships for thermally stimulated eccrine sweat. The experiments were carried out on sweat collected from the loaded and unloaded sacrum of healthy volunteers during consecutive intervals over an extended time period.

6.2 TEMPORAL CHANGES IN UNLOADED THERMAL SWEAT COMPOSITION

6.2.1 MATERIALS & METHODS

Each test was performed in a physiological chamber controlled at a temperature of 36°C and relative humidity of 35% in addition each experiment was conducted at a similar time of the day. The subjects entered the chamber and sat down on a chair that did not require pressure to be applied to the sacral region; immediately circular sweat pads, of 40 mm diameter, were attached to their sacrum following the procedure described in Section 4.3.5. This first pad was removed after a period of 20 minutes and the area was cleaned with an alcohol swab prior to application of a second pad which was affixed for a 30 minute period. This procedure was repeated for a further three 30

minute periods amounting to a total assessment period of 140 minutes, with sweat collected over 5 separate intervals. Each sweat sample was analysed biochemically to determine the concentrations of three metabolites namely, lactate, urea and chloride, using the procedures described in Section 4.3.4.

6.2.2 RESULTS

A total of 10 healthy, non-smoking volunteers with a mean age of 28 years was involved in the experiment as detailed in Table 6-1. This table also contains full details of the amount of sweat collected during each period.

Table 6-1 Time course of sweat collected at the unloaded sacrum for a group of healthy subjects.

			Sweat Amount / mg				
Subject	**Sex**	**Age**	**0-20 min**	**20-50 min**	**50-80 min**	**80-110 min**	**110-140 min**
1	M	23	49.9	74.0	146.6	59.1	84.1
2	M	25	43.8	90.1	290.6	302.7	305.6
3	M	24	25.4	38.5	68.0	58.6	42.4
4	F	24	24.1	93.9	120.6	131.5	66.2
5	M	24	29.0	91.0	204.5	163.1	58.8
6	F	29	15.7	40.8	44.6	21.0	28.3
7	M	41	161.4	234.8	208.5	203.1	230.0
8	M	23	201.9	188.8	77.2	122.3	53.0
9	M	23	127.6	241.4	208.6	202.6	217.3
10	F	25	218.0	236.3	231.9	273.5	238.5
Median			*46.85*	*92.45*	*175.55*	*147.30*	*75.15*
			NS	NS	NS	NS	

A Mann-Whitney U test shows no statistically significant difference, at the 5 per cent level, between the sweat rates at each consecutive collection period. However, close examination of the sweat collection profiles over the 140 minute period suggested two sweating responses. Typical examples of the resulting sweat rates are presented in Figure 6-1. These may be most conveniently described as:-

- *Mode A*- a low initial sweat rate followed by a sharp increase, as exhibited by subjects 1, 2, 4, 5, 7 and 9.

- *Mode B* - a fairly constant sweat rate over the collection period, as exhibited by subjects 3, 6 and 10.

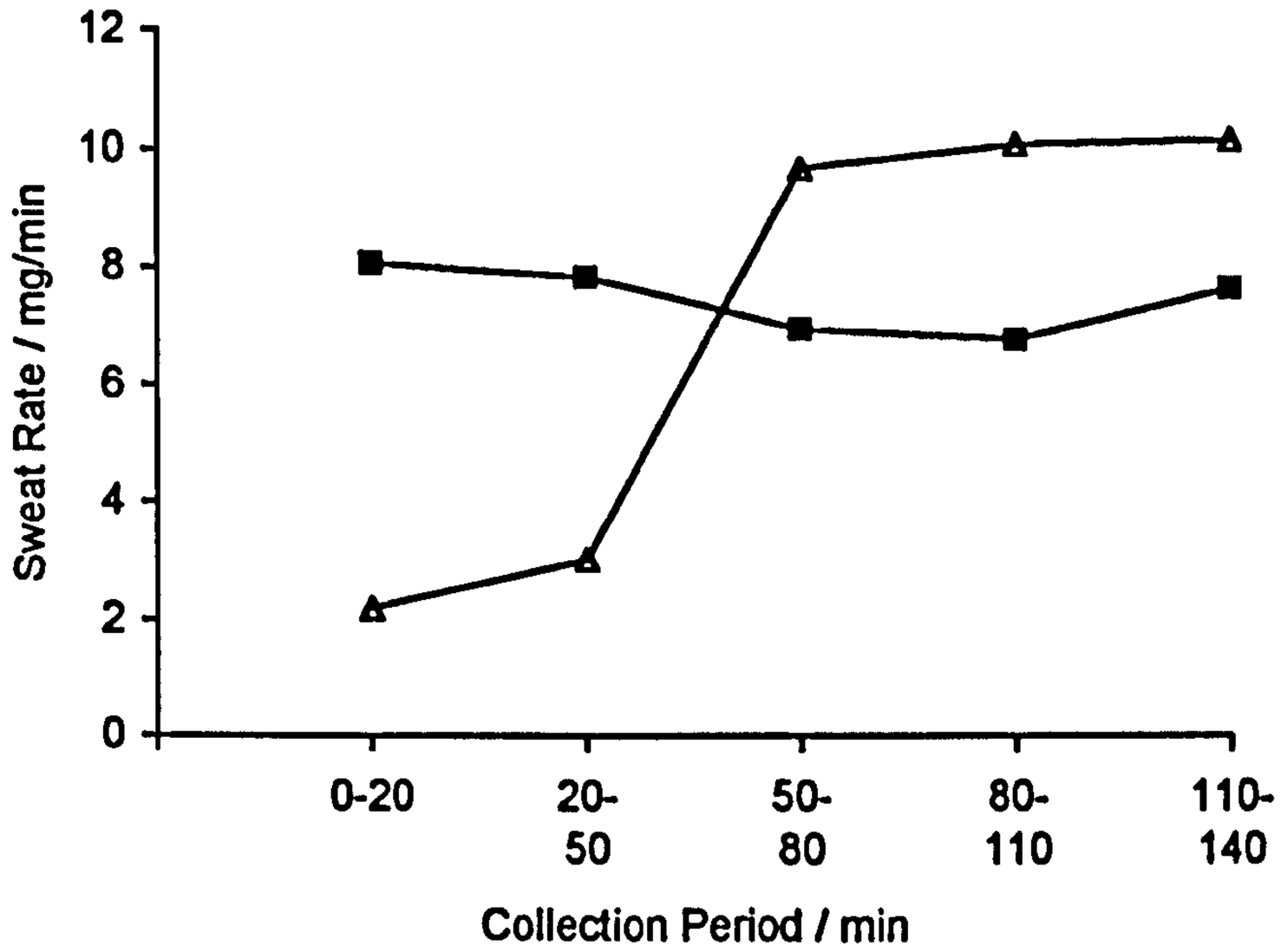

Figure 6-1 Typical graphs of sweat rate during five consecutive collection periods. Sweat rates are calculated as the weight of sweat collected in mg divided by the period of time collected in minutes. Mode A (Δ), Mode B (■).

The individual results of the biochemical analysis are shown in Tables 6-2 to 6-4, with the median values for each of the collection periods. The differences between the median values were analysed using the Mann-Whitney U test, a p value of less than 0.05 was considered to be statistically significant.

The graphs in Figures 6-2 to 6-4 show the relationship between the sweat metabolite concentration and collection period. The symbols represent the data from the four subjects (7-10) who provided a sufficient quantity of sweat throughout the duration of the experiment. As has previously been discussed in Section 4.3.5, the minimum amount of sweat required for complete biochemical analysis is 50 mg. Consequently, it can be seen that in 6 cases during the first collection period and in 2 cases (subjects 3 and 6) during the entire test period the sweat collected did not exceed this minimum value.

Table 6-2 Summary of measurement of lactate concentration in thermally stimulated sweat collected at the sacrum in five consecutive collection periods.

	Lactate Concentration / mmol/L				
Subject	**20 minutes (1)**	**30 minutes (2)**	**30 minutes (3)**	**30 minutes (4)**	**30 minutes (5)**
1	X	X	15.18	X	X
2	X	19.83	38.28	24.3	21.42
3	X	X	X	X	X
4	X	15.09	16.95	20.63	8.07
5	X	32.28	27.45	28.89	22.5
6	X	X	X	X	X
7	45.24	23.85	20.7	18.87	18.57
8	35.49	21.48	17.01	21.6	21.75
9	33.27	20.73	18.42	17.04	16.14
10	30.96	19.86	22.65	14.58	15.57
Median	*34.38*	*20.73*	*19.56*	*20.63*	*18.57*
		p<0.05	NS	NS	NS

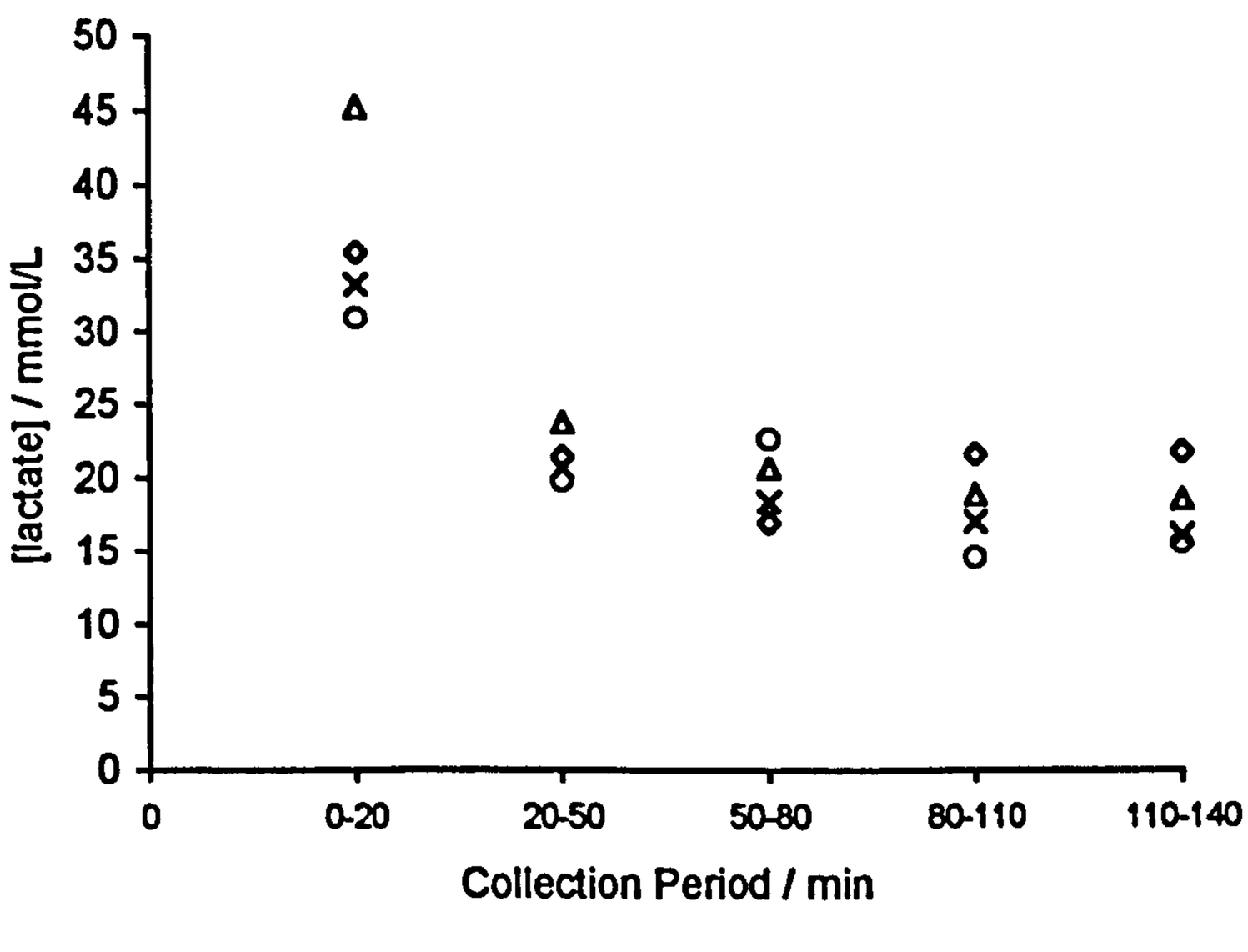

Figure 6-2 Lactate concentration in four separate subjects collected in consecutive periods over a total time of 140 minutes.

Table 6-3 Summary of measurement of urea concentration in thermally stimulated sweat collected at the sacrum for five consecutive collection periods.

	Urea Concentration / mmol/L				
Subject	**20 minutes (1)**	**30 minutes (2)**	**30 minutes (3)**	**30 minutes (4)**	**30 minutes (5)**
1	X	X	9.51	X	X
2	X	11.64	14.52	5.47	14.79
3	X	X	X	X	X
4	X	6.36	6.24	9.45	4.61
5	X	22.04	18.57	18.33	14.64
6	X	X	X	X	X
7	25.02	12.36	11.01	9.09	9.03
8	21.6	16.32	13.23	18.0	18.87
9	29.55	15.54	13.89	12.96	12.9
10	28.74	16.77	13.91	12.5	12.9
Median	*26.88*	*15.54*	*13.56*	*12.5*	*12.9*
	p<0.05	NS	NS	NS	

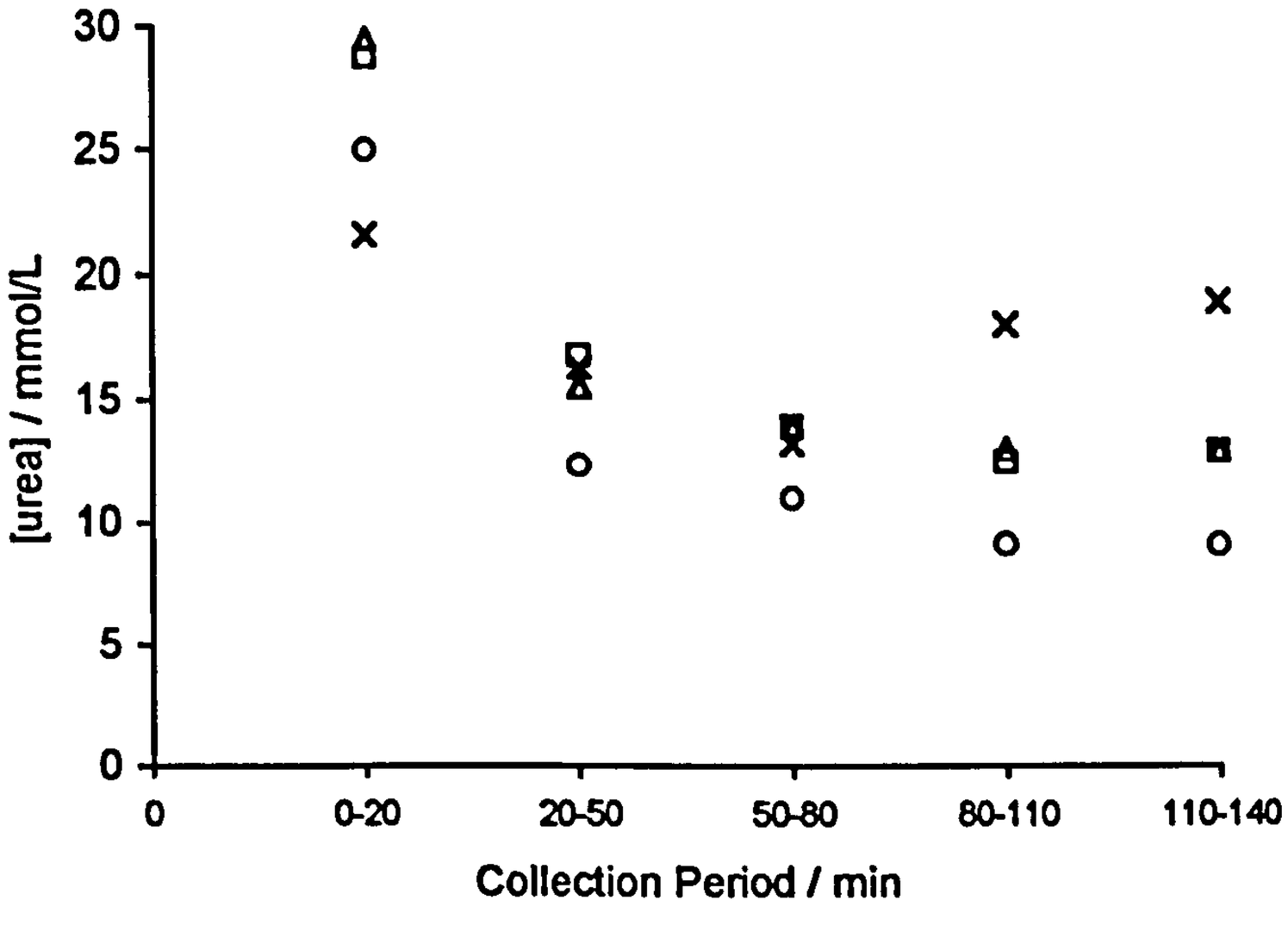

Figure 6-3 Urea concentration in four separate subjects collected in consecutive periods over a total time of 140 minutes.

Table 6-4 Summary of measurement of chloride concentration in thermally stimulated sweat collected at the sacrum for five consecutive collection periods.

	Chloride Concentration / mmol/L				
Subject	**20 minutes (1)**	**30 minutes (2)**	**30 minutes (3)**	**30 minutes (4)**	**30 minutes (5)**
1	X	X	32.61	X	X
2	X	21.21	29.76	36.45	28.71
3	X	X	X	X	X
4	X	13.14	13.8	27.78	10.17
5	X	22.38	22.17	23.46	20.37
6	X	X	X	X	X
7	23.16	13.80	12.60	15.51	15.03
8	14.79	10.08	10.83	15.24	17.61
9	25.2	14.43	14.52	15.15	17.76
10	24.48	16.2	23.46	19.17	24.18
Median	*23.82*	*14.43*	*18.35*	*19.17*	*17.76*
	└— p<0.05 —┘	└— NS —┘	└— NS —┘	└— NS —┘	

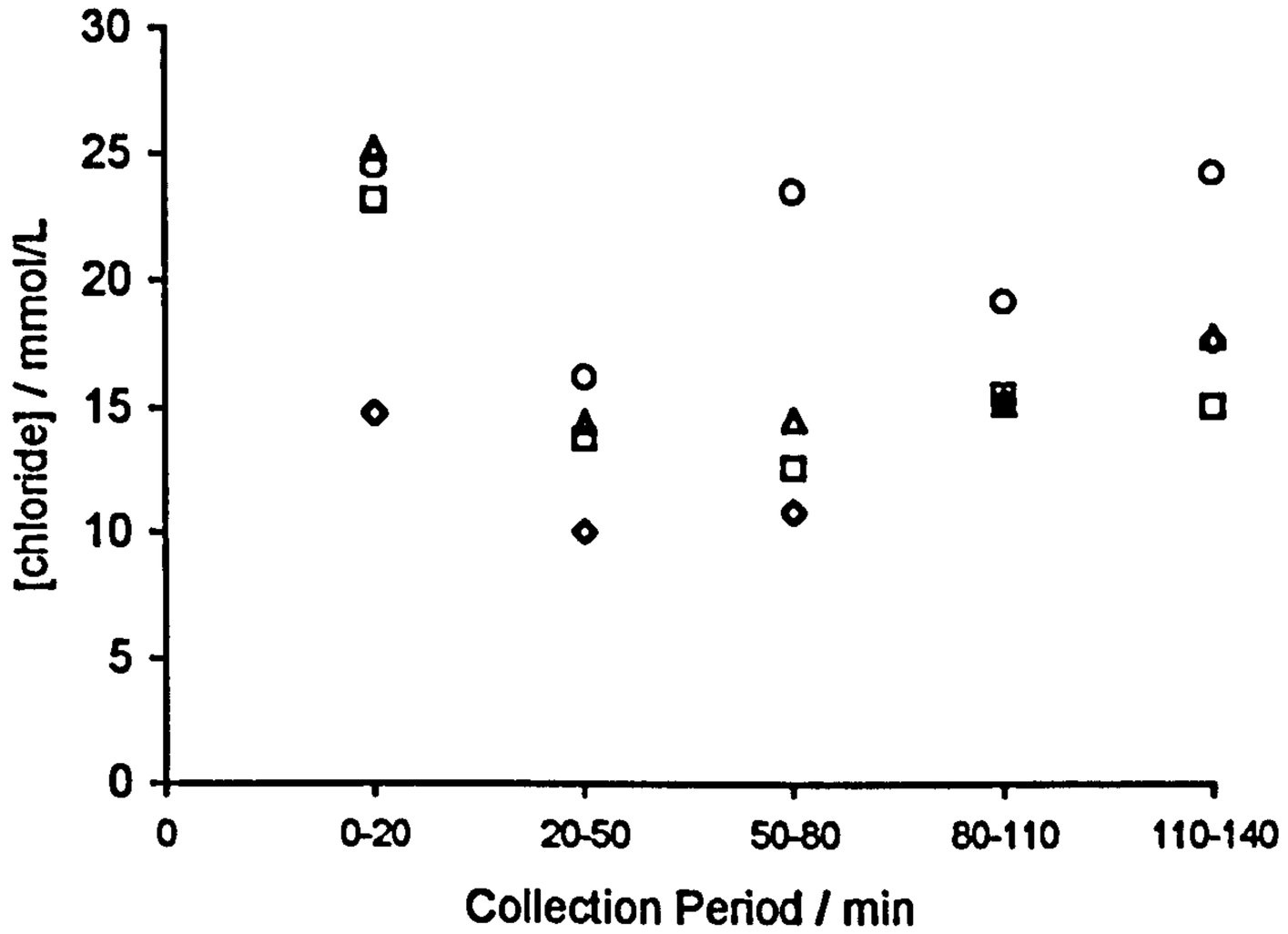

Figure 6-4 Chloride concentration in four separate subjects collected in consecutive periods over a total time of 140 minutes.

It is clear from the results that the sweat collected in the first 20 minute collection period has a statistically significantly higher concentration of all three measured metabolites, lactate, urea and chloride than in subsequent collection period. However, there was shown to be no significant differences between any of the sweat metabolite concentrations collected during the following four consecutive test periods.

6.2.3 DISCUSSION

In the cases where measurement was possible, the elevated concentrations of lactate, urea and chloride in the first collection of thermally induced sweat confirms the unsubstantiated findings of other researchers [2,213]. The phenomenon has been attributed to either insufficient cleansing of the skin prior to collection [213], or the presence of a small but concentrated amount of sweat within the duct of the sweat gland which is secreted as the temperature rises during the initial collection period [2].

Another important consideration involves the fact that in 60% of the cases, metabolite concentration was not analysed due to the limited sweat rate exhibited by these subjects in the initial 20 minute period. Both these findings suggest that a minimum acclimatisation period of 20 minutes is required before measurable levels of metabolite concentrations could be estimated in the thermally stimulated sweat samples.

This experiment also examined the effects of the long term collection of sweat. Following the initial period both the amount of sweat and the concentration of its metabolites did not change significantly over the extended time period. This suggests that following acclimatisation it is appropriate to collect sweat up to a maximum period of 2 hours. However, beyond this time collection may be inappropriate as it may reflect changes in sweat gland output due to fatigue [119]. Analysis of sweat beyond this time period would be difficult to interpret, especially if factors associated with pressure induced ischaemia were to be assessed.

6.3 Temporal Changes in Sweat Collected from Loaded and Unloaded Sites

6.3.1 Introduction

The previous experiment involving unloaded sweat established two time constraints namely, a 20 minute acclimatisation period and a total subsequent collection period of 120 minutes. With consideration of these findings a further experiment was conducted to examine the temporal changes in sweat biochemistry at loaded sites.

6.3.2 Materials & Methods

For this experiment each subject was required to equilibrate for 20 minutes in the physiological chamber at 36°C (35% RH). Each subject then adopted the prone position on a standard King's Fund hospital bed, a position which enabled load to be applied to the sacral tissues using the bed mounted pressure application device shown in Figure 4-10.

Prior to sweat collection interface pressures and tissue deformation were measured at the sacrum of 6 volunteers, for a number of applied pressures using the Talley Pressure Monitor (Section 4.6) and the tissue deformation equipment (Section 4-7). The results of these investigations are detailed in Appendix B.

After the equilibration period a first pair of sweat pads was attached at adjacent sites on the sacrum, designated the test pad and the control pad. The indenter was placed over the top of the test sweat pad and a pressure of 80 mmHg was applied through the indenter. The first pair of pads were removed after 30 minutes, both sites cleaned with an alcohol swab, and replaced immediately by a second pair of fresh sweat pads. At the end of the third 30 minute period the sites were again cleaned and two sweat pads attached. However, during this fourth 30 minute period no load was applied to the test site. This represented a sweat collection during a 30 minute period of reperfusion. Sweat rates and sweat metabolite concentrations are represented as the ratio between loaded and unloaded values an approach which eliminates differences in the individual nature of sweating.

6.3.3 RESULTS

A total of 8 healthy non-smoking volunteers with a mean age of 26 years was used for this experiment. The sweat rates for loaded and unloaded sites at each consecutive collection period are shown in Table 6-5. This data highlights the wide range of values for the amount of sweat collected in the time periods and therefore the sweat rates. There were also clear differences between the values collected at both loaded and unloaded sites for the same individual.

Table 6-5 Temporal changes in thermally stimulated sweat rates at loaded and control sites near sacrum.

	Sweat Amount / mg							
	0-30 min		30-60 min		60-90 min		90-120 min	
Subject	Loaded	Control	Loaded	Control	Loaded	Control	Reperf.	Control
1	35.8	41.8	36.0	87.5	56.5	140.7	182.3	116.0
2	59.6	81.4	80.3	64.1	28.3	21.5	51.0	19.1
3	109.4	29.5	123.8	230.5	113.2	225.5	256.4	159
4	106.3	100.1	38.2	30.9	18.3	37.4	40.7	17.3
5	4.3	6.7	2.2	11.1	2.7	11.1	10.8	8.6
6	174.5	109.4	117.4	139.5	67.4	114.5	149.8	38.3
7	166.2	117.1	186.3	195.8	129.7	164.4	-	-
8	39.6	72.7	45.4	80.8	41.3	118.6	86.2	44.3

The temporal changes in the sweat rate, presented as a ratio of that collected from the experimental and control sites, are shown in Figure 6-5. This ratio approach permits each individual to act as their own control and, consequently, a comparison can be made between sweat rate response to loaded and unloaded conditions. A Mann-Whitney U test was used to test significance of differences between sweat rate ratios in consecutive collection periods. It is clear from the graph that during the first collection period (0-30 min) there is a mean sweat rate ratio above unity suggesting that sweat rate at the loaded site is greater than that at the unloaded site. However, the variation during this collection period is quite large, and for four subjects control sweat rates are higher. During the subsequent 2 collection periods (30 to 60 minutes and 60 to 90 minutes), the sweat rate at the loaded site is lower than that at the control site,

suggesting a suppression of the sweating response during the period of loading. The results of the statistical analyses show that there was no statistically significant difference, at the 5 per cent level, between the sweat rate ratios in the first three collection periods.

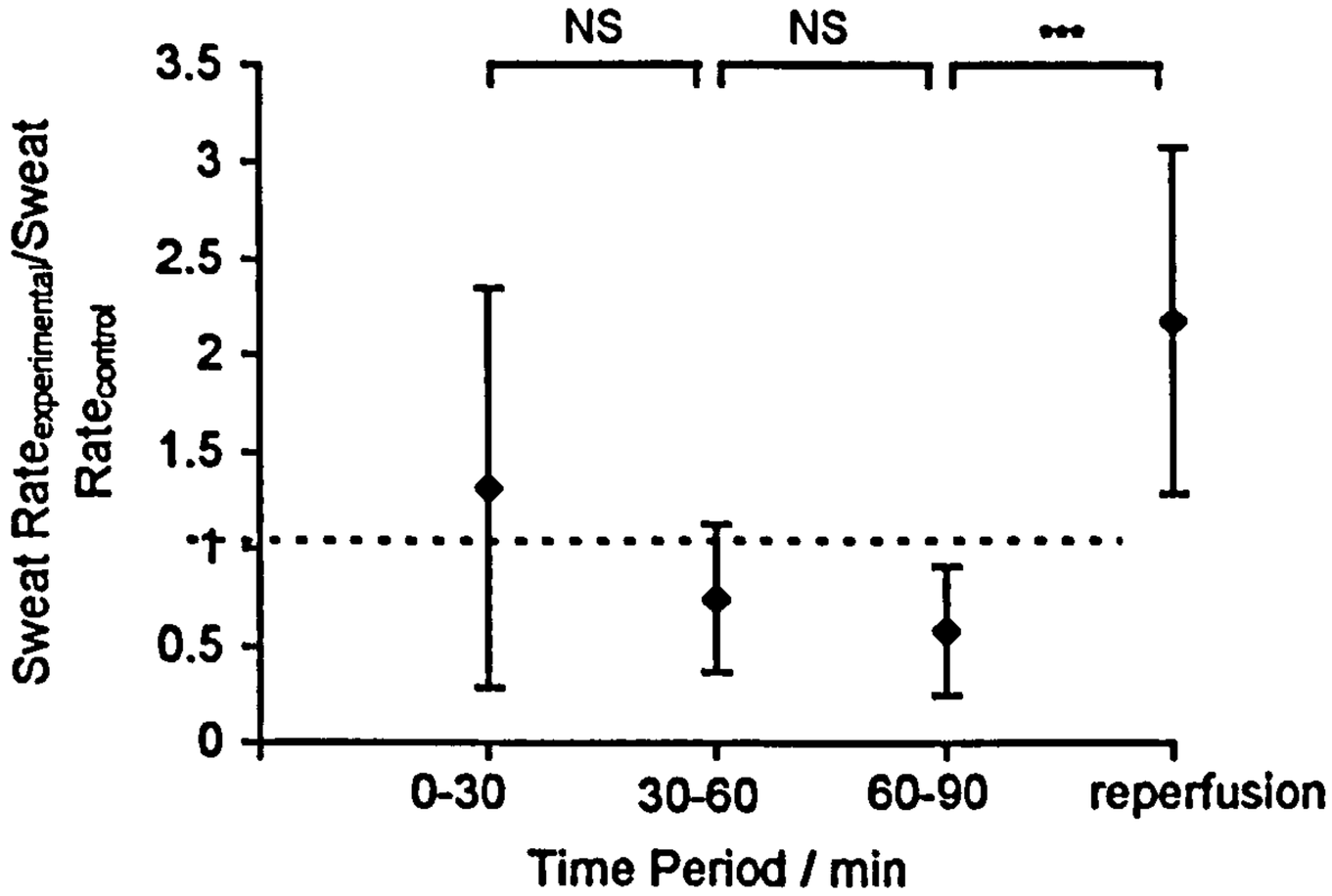

Figure 6-5 Mean sweat rate ratios measured during four distinct periods of loading or reperfusion. Error bars indicate ± 1 s.d. *** ($p<0.001$)

However, during the reperfusion period, the sweat rate ratio is significantly higher ($p<0.001$) and has a mean value of 2.25 suggesting that the sweat rate at the previously loaded site is in excess of that at the adjacent control site during the reperfusion period. In addition, the absolute sweat rates at the loaded site during both loaded and subsequent reperfusion periods can be compared using the Wilcoxon rank pair test. A significantly higher sweat rate ($p<0.05$) is shown at the site during reperfusion compared with the sweat rate during the final loaded period. This finding is analogous to the reactive hyperaemia response exhibited by the increase in blood flow above basal levels, in an area of tissue in which blood flow has been previously occluded.

The sweat samples, which weighed in excess of 50 mg were analysed for lactate, urea and chloride using the analysis techniques described in Section 4.3.4. The results of the biochemical analysis are shown in Tables 6-6 to 6-8 and a graphical representation of the mean ratios of sweat metabolite concentrations at the experimental site compared to the control site is shown in Figure 6-6 to 6-8.

Table 6-6 Temporal changes in lactate concentration of thermally induced sweat at unloaded and loaded sites at the sacrum of healthy volunteers..

	Lactate Concentration mmol/L							
Time	**0-30 min**		**30-60 min**		**60-90 min**		**90-120 min**	
Subject	**Loaded**	**Control**	**Loaded**	**Control**	**Loaded**	**Control**	**Reperf.**	**Control**
1	X	X	X	30.39	29.37	20.49	26.55	33.75
2	80.37	68.94	42.99	22.26	X	X	41.04	X
3	31.26	X	33.18	20.16	21.9	20.07	14.46	18.36
4	152.52	120.48	X	X	X	X	X	X
5	X	X	X	X	X	X	X	X
6	93.06	49.86	59.01	48.99	31.41	24.12	42.75	46.08
7	72.54	59.7	45.09	34.26	47.55	37.08	X	X
8	X	47.43	42.63	31.53	37.23	24.81	24.39	30.18

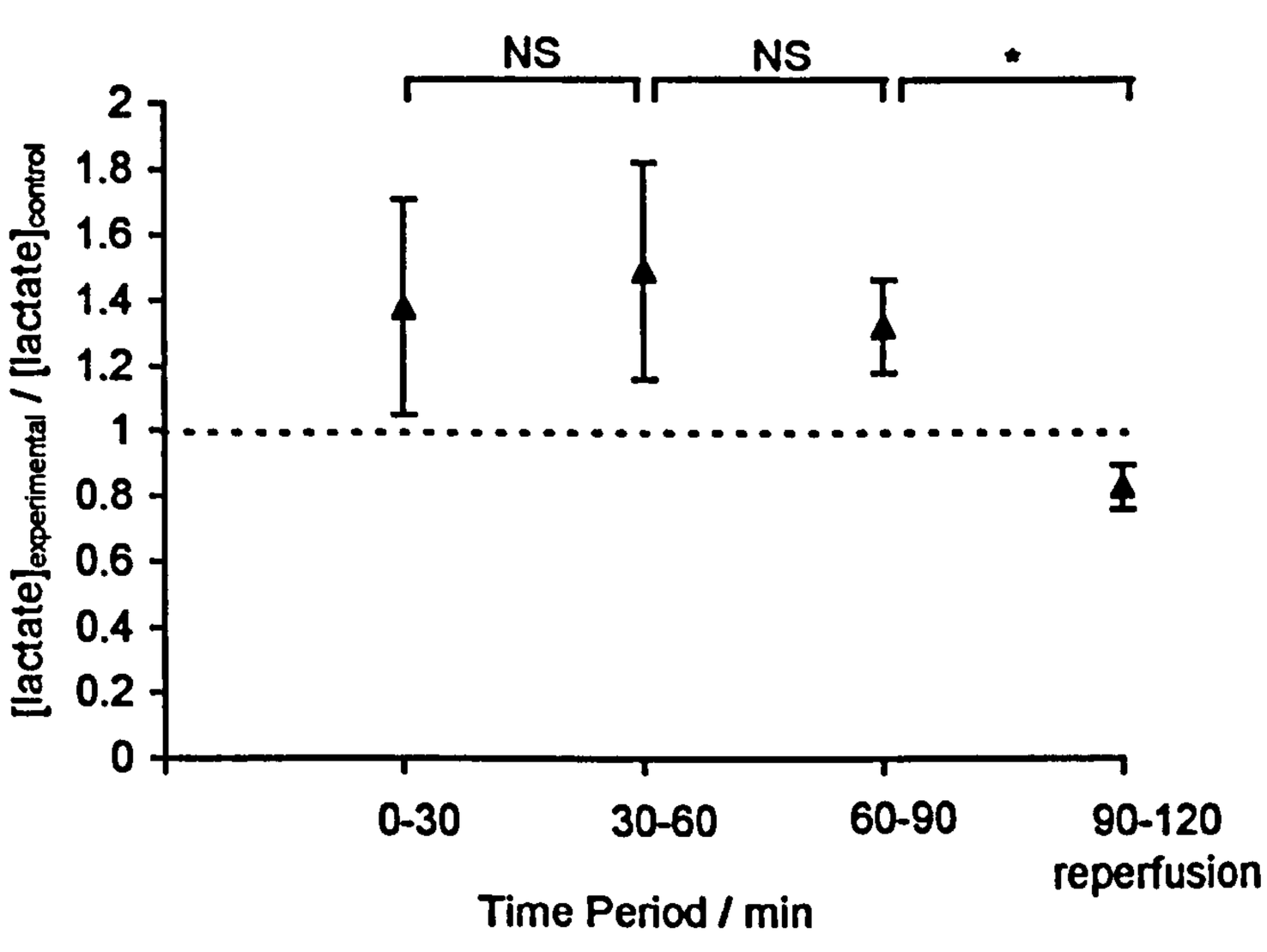

Figure 6-6 Mean ratios for sweat lactate concentration measured during four distinct periods of loading or reperfusion.
Error bars indicate ± 1 s.d. * ($p<0.05$)

Table 6-7 Temporal changes in urea concentration of thermally induced sweat at loaded and unloaded sites at the sacrum of healthy volunteers.

	Urea Concentration mmol/L							
Time	**0-30 min**		**30-60 min**		**60-90 min**		**90-120 min**	
Subject	**Loaded**	**Control**	**Loaded**	**Control**	**Loaded**	**Control**	**Reperf.**	**Control**
1	X	X	X	18.69	16.62	10.59	13.83	13.29
2	78.63	63.48	38.07	22.98	X	X	37.41	X
3	26.79	X	14.16	14.08	13.98	12.99	9.03	11.76
4	73.56	56.91	X	X	X	X	X	X
5	X	X	X	X	X	X	X	X
6	48.42	24.03	29.70	24.27	16.11	13.29	20.61	23.67
7	40.23	30.69	22.29	17.43	21.6	18.0	X	X
8	X	19.86	14.85	13.47	14.55	10.65	9.99	12.96

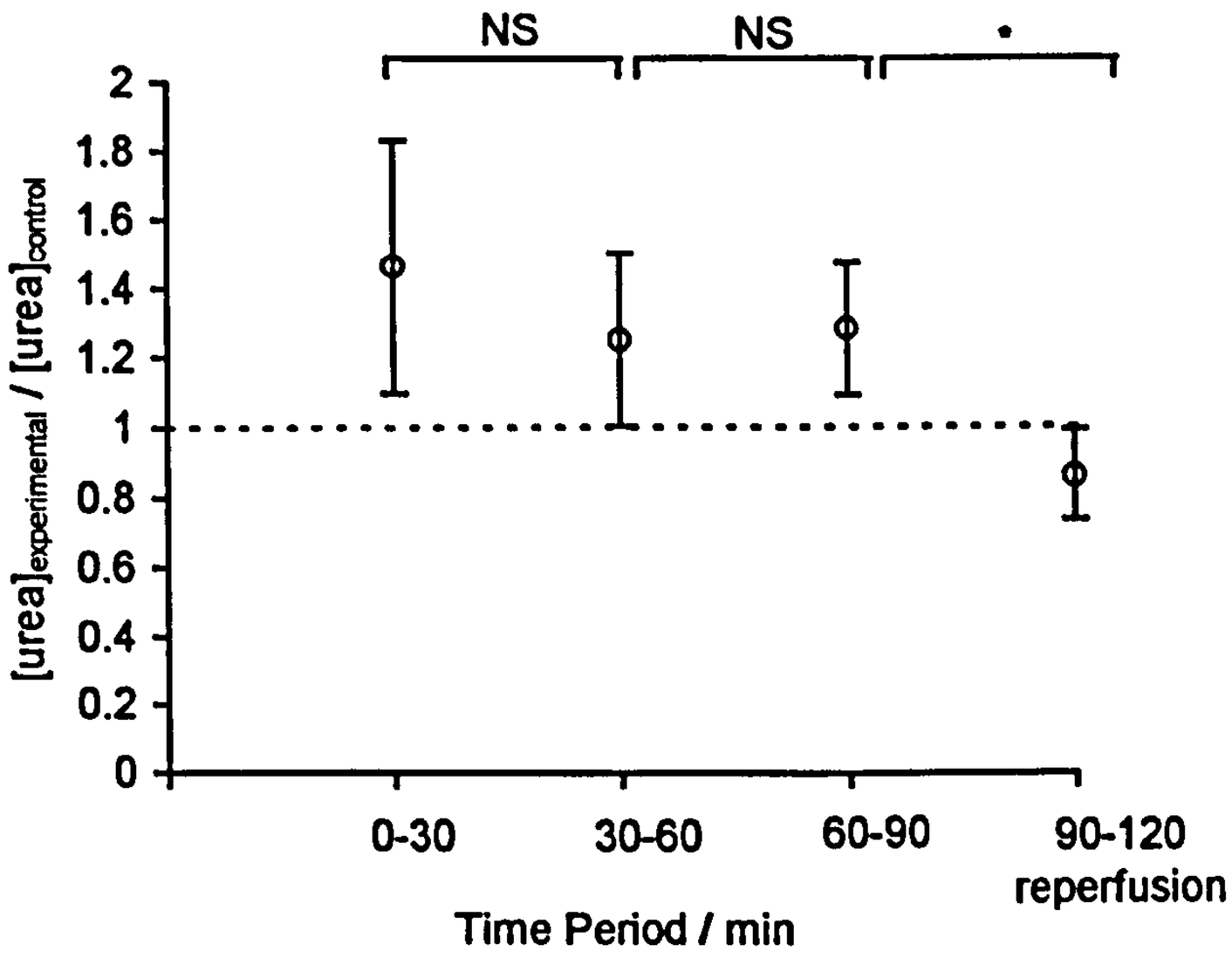

Figure 6-7 Mean ratios for sweat urea concentration measured during four distinct periods of loading or reperfusion.
Error bars indicate ± 1 s.d. * ($p<0.05$)

Table 6-8 Temporal changes in chloride concentration of thermally induced sweat at loaded and unloaded sites at the sacrum of healthy volunteers.

	Chloride Concentration mmol/L							
Time	**0-30 min**		**30-60 min**		**60-90 min**		**90-120 min**	
Subject	**Loaded**	**Control**	**Loaded**	**Control**	**Loaded**	**Control**	**Reperf.**	**Control**
1	X	X	X	19.89	25.68	16.98	21.30	22.35
2	104.91	92.64	59.31	43.47	X	X	74.25	X
3	26.64	X	30.33	14.55	20.25	17.19	18.90	24.99
4	94.26	82.41	X	X	X	X	X	X
5	X	X	X	X	X	X	X	X
6	30.54	18.48	22.17	17.58	14.91	9.87	16.95	29.61
7	52.29	43.05	37.98	27.00	42.24	38.40	X	X
8	X	42.15	41.52	30.90	49.74	34.11	41.34	41.37

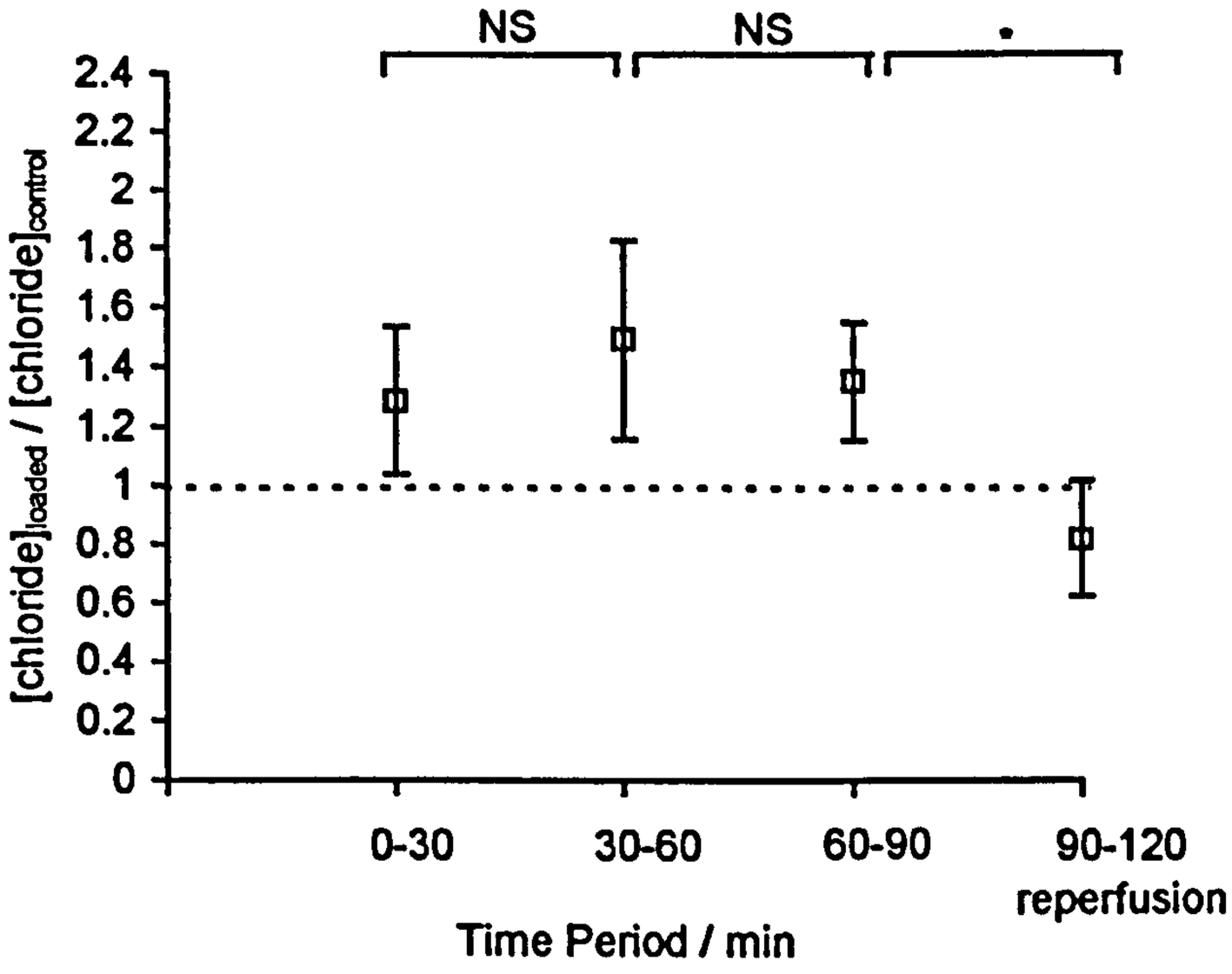

Figure 6-8 Mean ratios for sweat chloride concentration measured during four distinct periods of loading or reperfusion.
Error bars indicate ± 1 s.d. * ($p<0.05$)

In all periods up to 90 minutes the loaded sites yielded increased sweat metabolite concentrations, as reflected in a mean ratio greater than unity. A comparison between each consecutive pair of ratio data was performed using the Mann-Whitney U test. During the loaded period there was found to be no statistical significant difference, at the 5 per cent level between the ratios for each of the three metabolites. However, during the reperfusion period, there was a statistically significant difference ($p<0.05$) between reperfusion sweat metabolite ratios and those in the immediate preceding loading period.

6.3.4 Discussion

The effect of applied pressure on sweat biochemistry has two major effects. A reduction in sweat rate and an increase in sweat metabolite concentrations. These findings have been previously established for single collection periods [158,207]. However, the present study has illustrated that the elevation in sweat lactate, urea and chloride was continuous throughout the 90 minute duration of the experiment and a analysis revealed no statistical difference between metabolite ratios of loaded and unloaded sweat for each of the three 30 minute collection periods (Figures 6-6 to 6-8). This supports the hypothesis that it is feasible, if not always practical, to collect a single sweat sample from a loaded site for a period up to 90 minutes.

Following the 90 minute period of pressure induced ischaemia a 30 minute of reperfusion was monitored and sweat collected. During this period the sweat metabolite ratios return to a level just less than unity, suggesting that the sweat collected from the previously loaded site has a metabolite concentration approaching the control levels. Such a finding has also been reported by other researchers measuring the effect of loading on sweat metabolite concentration at the volar aspect of the forearm [73,157].

Figure 6-9 shows the combined results of the sweat metabolite concentrations collected during loaded, control and reperfusion periods. Again this trend suggests that sweat metabolite concentration follows a similar course to blood flow during a period of reperfusion following pressure induced ischaemia. Thus sweat metabolite

concentrations may be used as an indicator of the ability of tissue to recover from pressure insult.

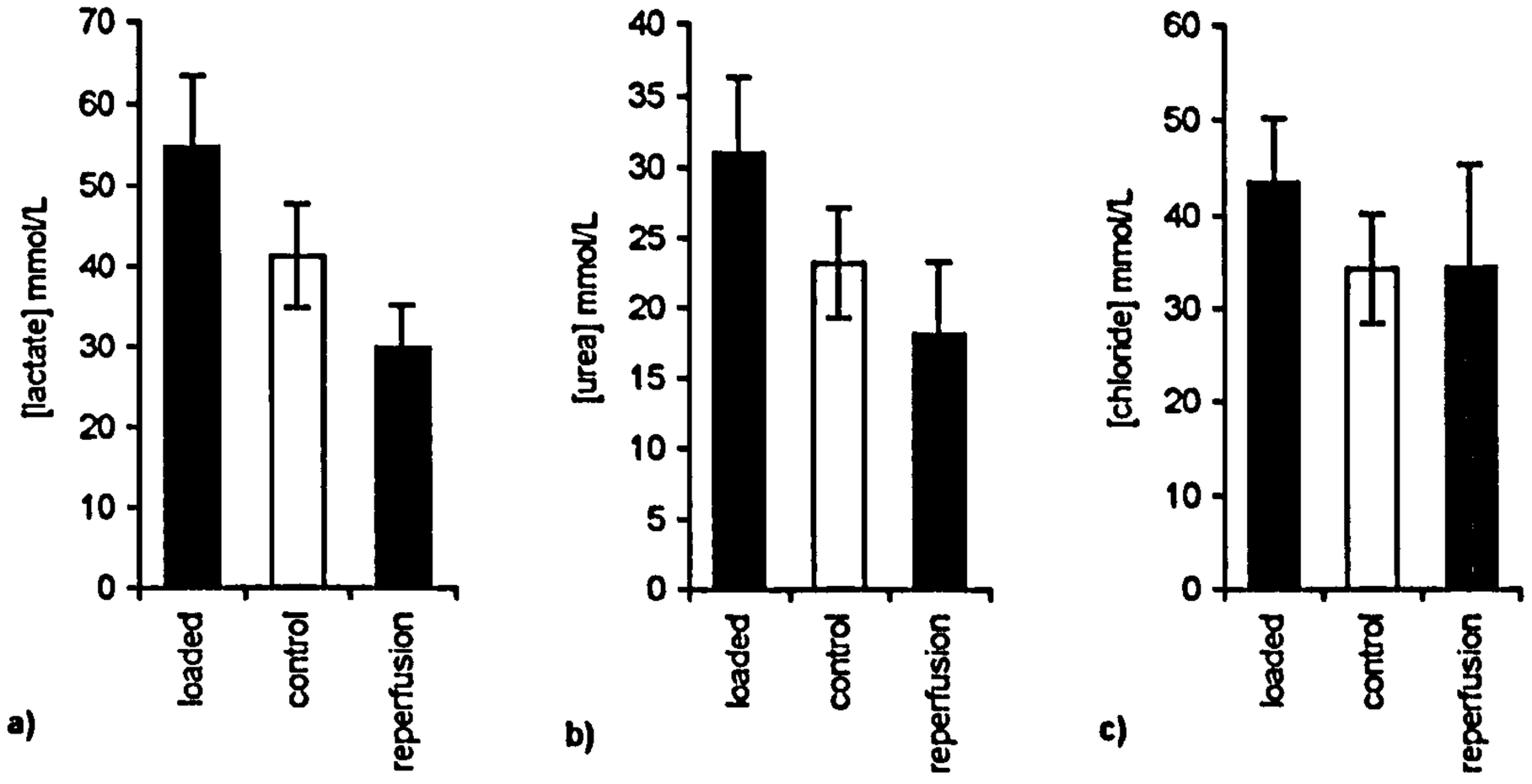

Figure 6-9 Mean sweat metabolite concentrations during three distinct collection periods, a) lactate, b) urea, c) chloride.
■ loaded (*n=15*), □ control (*n=16*), and □ reperfusion (*n=5*). Error bars denote s.e.m.

6.4 SUMMARY

The experimental investigations described in this chapter have verified some important experimental details and information about the temporal nature of thermally stimulated eccrine sweat. The important findings of this experimental chapter are listed below.

- An acclimatisation period of 20 minutes is required prior to thermally stimulated sweat collection, to enable sufficient sweat rate and stable sweat metabolite concentration.
- Pressure induced ischaemia leads to a decreased sweat rate and increased sweat metabolite concentration; these findings are consistent over an extended time period up to 90 minutes.
- Validation that a single sweat collection can be made for periods up to 90 minutes in both loaded and unloaded tissue sites

- Sweat rate and metabolite concentration ratios provide a normalised parameter of sweat biochemistry.
- Sweat biochemistry measurements, both sweat rates and sweat metabolite concentrations, are sensitive to reperfusion of blood flow after a period of ischaemia.

7. COMBINED SWEAT BIOCHEMISTRY & GAS TENSION MEASUREMENTS

7.1 INTRODUCTION

In Chapters 5 and 6 two independent techniques for measuring soft tissue status, namely transcutaneous blood gas tension and sweat biochemistry measurement, were separately investigated. The aim of this chapter is to utilise, simultaneously, both techniques in order to measure the effect of pressure and time on soft tissue status.

This chapter utilises a site of clinical relevance, the sacrum, which is a soft tissue area overlying a bony prominence, and a common area for tissue breakdown. Transcutaneous gas tensions and sweat metabolites have been measured over a series of different applied pressures and times.

7.2 METHODS & MATERIALS

A total of 14 healthy, non-smoking volunteers, 9 male and 5 female, were used in the following investigation. The mean age of the male volunteers was 26.7 years (range 23-41 years) and the mean age of the female volunteers was 27.6 years (range 22-36 years).

All experiments were carried out in a temperature and humidity controlled physiological chamber (36°C, 35% RH) at a similar time each day. The chamber temperature and humidity were monitored throughout the experiments.

The experimental protocol is described schematically in the flow chart in Figure 7-1. Subjects entered the room and adopted a prone position on a standard King's Fund hospital mattress and bed. During the 20 minutes temperature acclimatisation, two oxygen/carbon dioxide electrodes (Model D841, Radiometer Copenhagen Ltd, Denmark) were placed on adjacent sites at the sacrum and allowed to equilibrate as described in Section 4.2.5. After equilibration for both temperature and gas tension electrodes, annular sweat pads, with internal and external diameters of 12 mm and 42 mm respectively, were applied to the skin around both gas tension electrodes. The

pressure was then applied via the indenter and the bed mounted pressure application device, as described in Section 4.5 and shown in Figure 4-10.

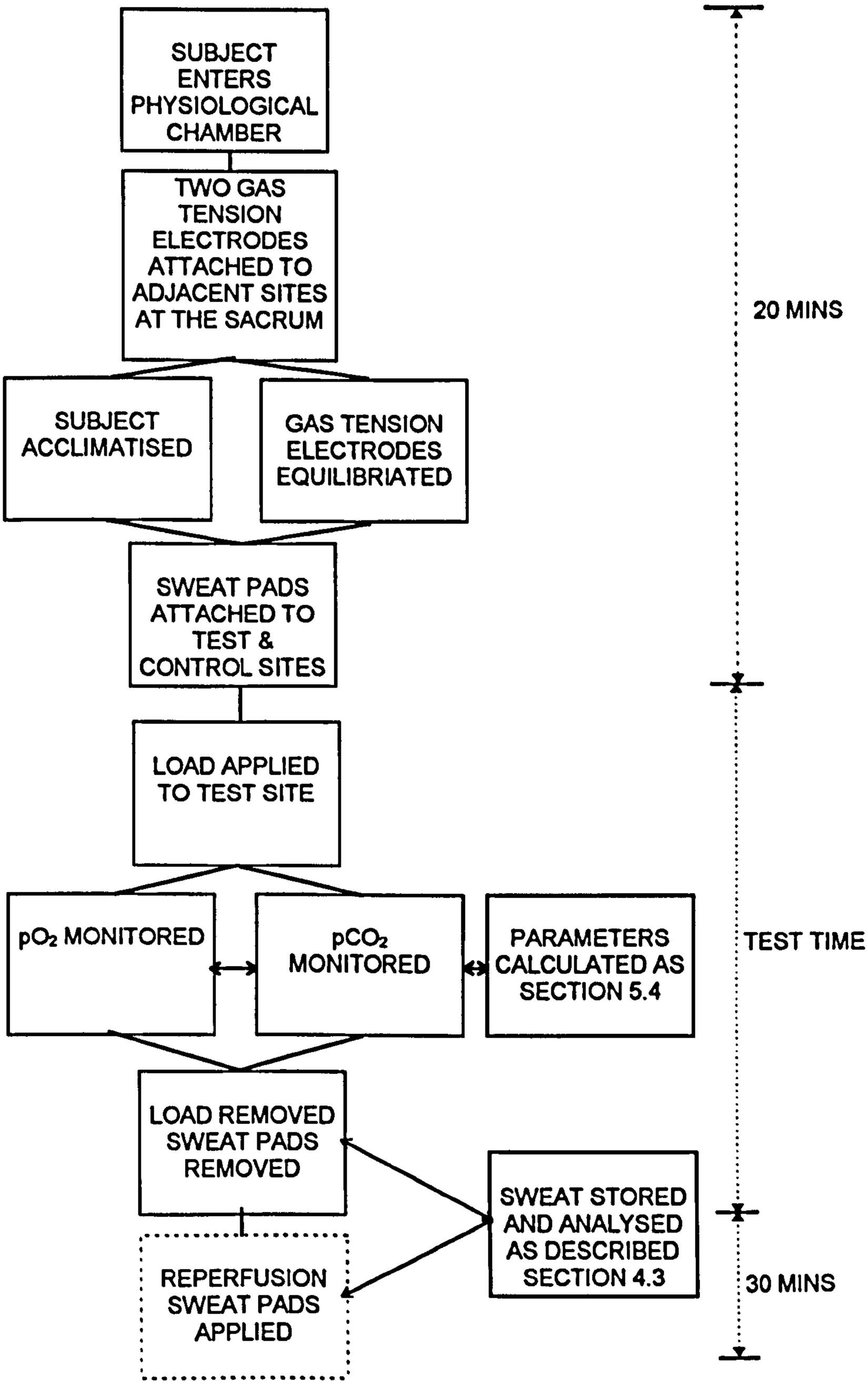

Figure 7-1 Flow diagram showing experimental procedure for combined transcutaneous gas tension and sweat biochemistry measurements.

After the prescribed time, the sweat pads were carefully detached from the skin surface with tweezers. Any excess sweat was mopped up with the pad which was then placed into the pre-weighed container for subsequent analysis for lactate, urea, chloride and urate following the assays described in Section 4.3.4.

The test matrix of applied pressure and times is detailed in Table 7-1, with *n* representing the total number of complete data sets that were obtained for each test. In some cases, less than 50 µl of sweat were obtained at one site which precluded further analysis.

Table 7-1 Experimental design for investigating the effect of pressure and time on soft tissue status.

	Time of Loading			
Applied Pressure	**30 mins**	**45 min**	**60 min**	*Total*
40 mmHg	n = 2	-	n = 8	*10*
80 mmHg	n = 3	n = 5	n = 4	*12*
120 mmHg	n = 4	n = 4	n = 6	*14*
Total	*9*	*9*	*18*	*36*

7.3 Data Analysis

In order to examine the results of this study, a number of parameters were calculated for each subject. Appropriate statistical analyses were carried out on the group values.

Oxygen tensions were calculated as a percentage reduction in pO_2 during the loading period compared to initial value, as described in Section 5.4. Two parameters were used to describe carbon dioxide values. The first is based on an approach used by Bogie *et al.* [24], whereby the percentage of the total loaded period that pCO_2 values remained above a threshold of 50 mmHg was calculated, as described in Section 5.4. The second approach is based on integration of the pCO_2 response over a normalised time period. A range of parameters reflecting the sweat metabolite concentrations were also calculated. These included:-

i. Absolute concentrations at loaded and unloaded sites

ii. A concentration ratio at each pair of sites, which enabled each individual to act as their own control.

Non-parametric statistics were used to analyse data, using the Wilcoxon Rank for paired data, the Mann-Whitney U test for unpaired data, and Spearman coefficient for correlations. Statistical significance levels were defined as * ($p<0.05$), ** ($p<0.01$), and *** ($p<0.001$).

7.4 Results

The results section is most conveniently divided into two parts. The first part describes the effect of applied pressure on the individual measurement techniques i.e. gas tensions and sweat biochemistry, whilst the second provides a comparison between the measurement techniques. Full tabulated results for each test subject can be found in Appendix C.

A Individual Measurements of Tissue Status

7.4.1 Effect of load on Transcutaneous Gas Tensions

Transcutaneous oxygen and carbon dioxide tensions were measured at both loaded and control sites during the pressure induced ischaemia. The effect of applied pressure on measured gas tensions is shown in Figures 7-2 and 7-3.

Figure 7-2 shows the relationship between percentage reduction in pO_2 from the control value and applied pressure measured at the sacrum for all three time periods, 30, 45 and 60 minutes. It is clear from the graph that even applied pressures as low as 40 mmHg (5.33 kPa) produce a significant reduction in pO_2 values. This reduction reaches a value of 80% when the applied pressures were 80 mmHg (10.66 kPa), although no subsequent reduction was achieved at the maximum applied pressure of 120 mmHg (15.98 kPa).

Figure 7-3 shows the relationship between applied pressure and carbon dioxide tension. Figure 7-3a shows the pCO_2 response as the parameter, percentage of time carbon dioxide tension is greater than 50 mmHg.; it is clear from the graph that for an applied pressure of 40 mmHg (5.33 kPa), an average of only 20% of the loading time is spent above 50 mmHg. However, at pressures of 80 mmHg and greater, the parameter reaches a constant at a value of approximately 80% of the loading time spent above 50 mmHg.

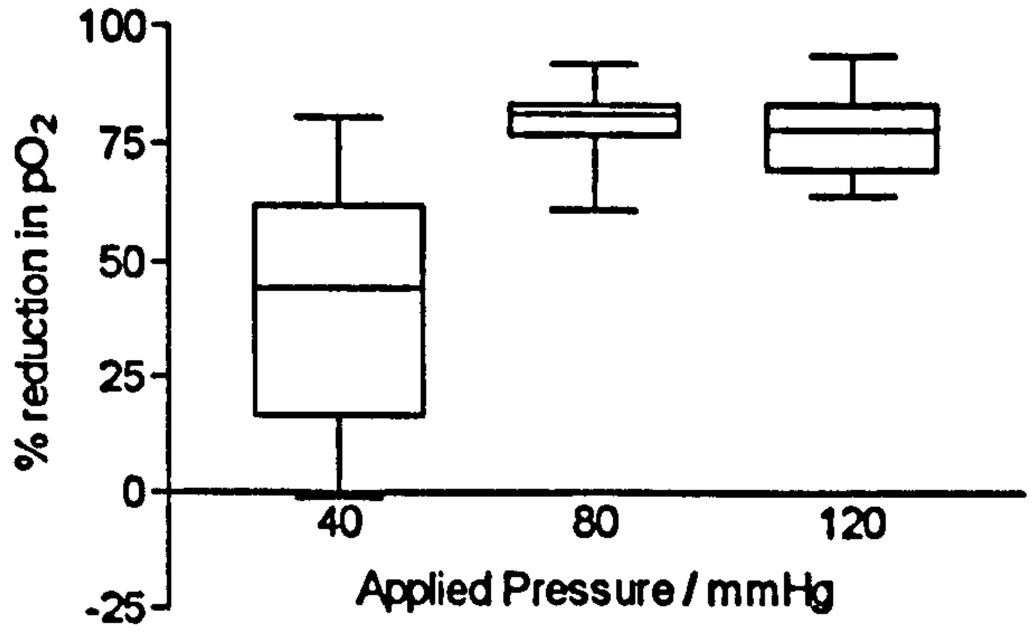

Figure 7-2 The effect of applied pressure on the percentage reduction in pO_2 levels at the sacrum. Boxes show 25th to 75th percentile and whiskers denote range of data.

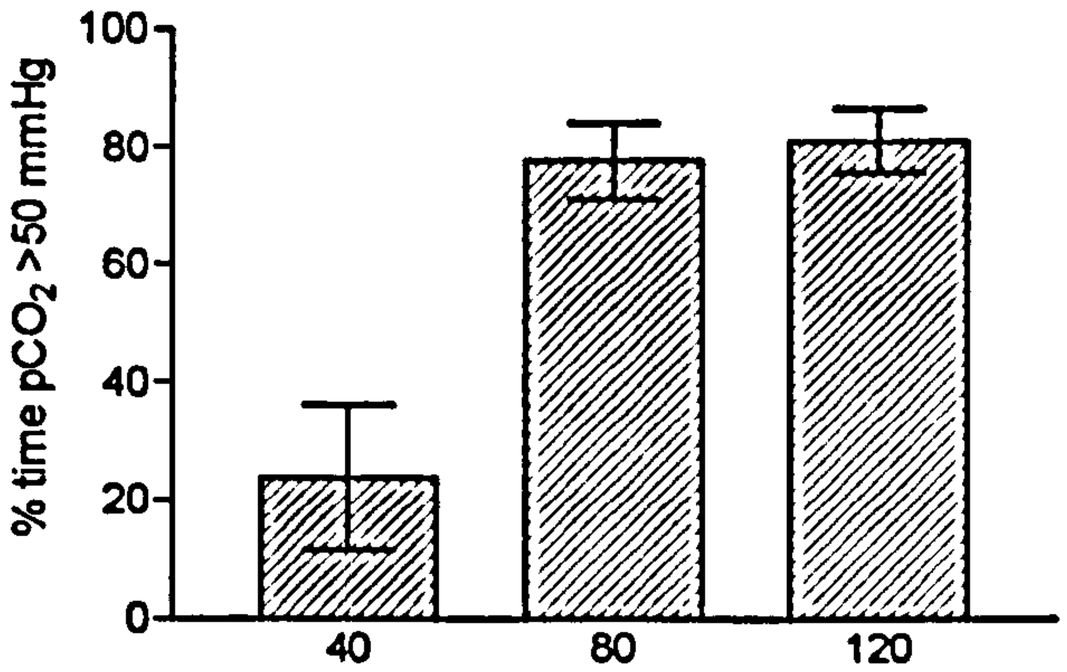

a)

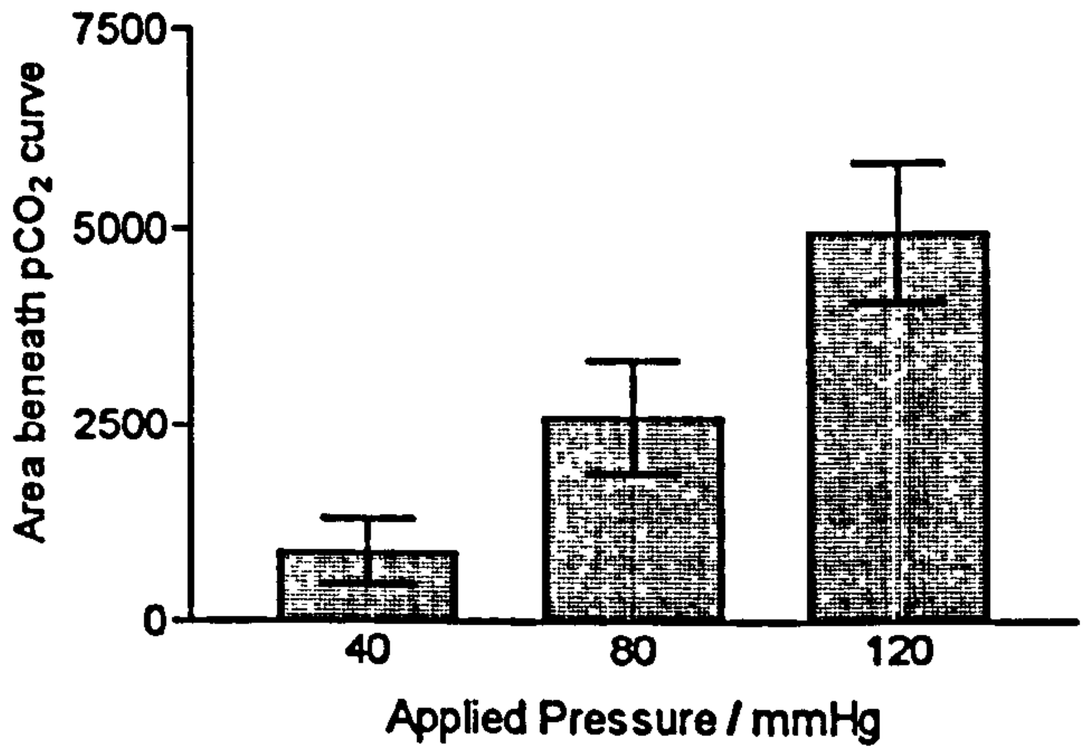

b)

Figure 7-3 Effect of applied pressure on pCO_2 measured at the sacrum, represented by
a) Percentage time that pCO_2 remained above 50 mmHg.
b) Area beneath pCO_2 curve.
Error bars denote s.e.m, for n values see Table 7-1.

These results suggests that for a large proportion of loading period, carbon dioxide tension is elevated above values that would generally be considered normal [32]. Figure 7-3b shows the relationship between applied pressure and area under the pCO_2 curve; for this parameter there appears to be a monotonic increase in value with applied pressure.

7.4.2 Effect of Time on Sweat Biochemistry

The employment of different loading periods in the test matrix permitted the investigation of the effects of time on sweat metabolite concentration for each applied pressure. Figure 7-4 presents the values of both lactate and urea ratio, calculated from the metabolite concentration of sweat collected at the loaded site and control sites, against applied pressure for each of the three time periods. Any differences between the lactate and urea ratios at each time period for the three separate applied pressures was examined using the Mann-Whitney U-test.

Although the data was limited in number for many of the cases, the results of this analysis suggest that there is no significant difference between the levels of both sweat lactate and sweat urea collected over different time periods. As a result of this finding, the data from these three time periods have been combined in all subsequent analyses.

7.4.3 Effect of Pressure on Sweat Biochemistry

The graphs in Figures 7-5 to 7-8 show the relationships between the four sweat metabolite concentrations and the applied pressure. The first graph in each pair shows the mean values of the absolute sweat metabolite concentrations at the loaded site compared to the mean values for all measurements at the control site. The second graph of each pair shows the loaded:unloaded ratio at the three separate applied pressures.

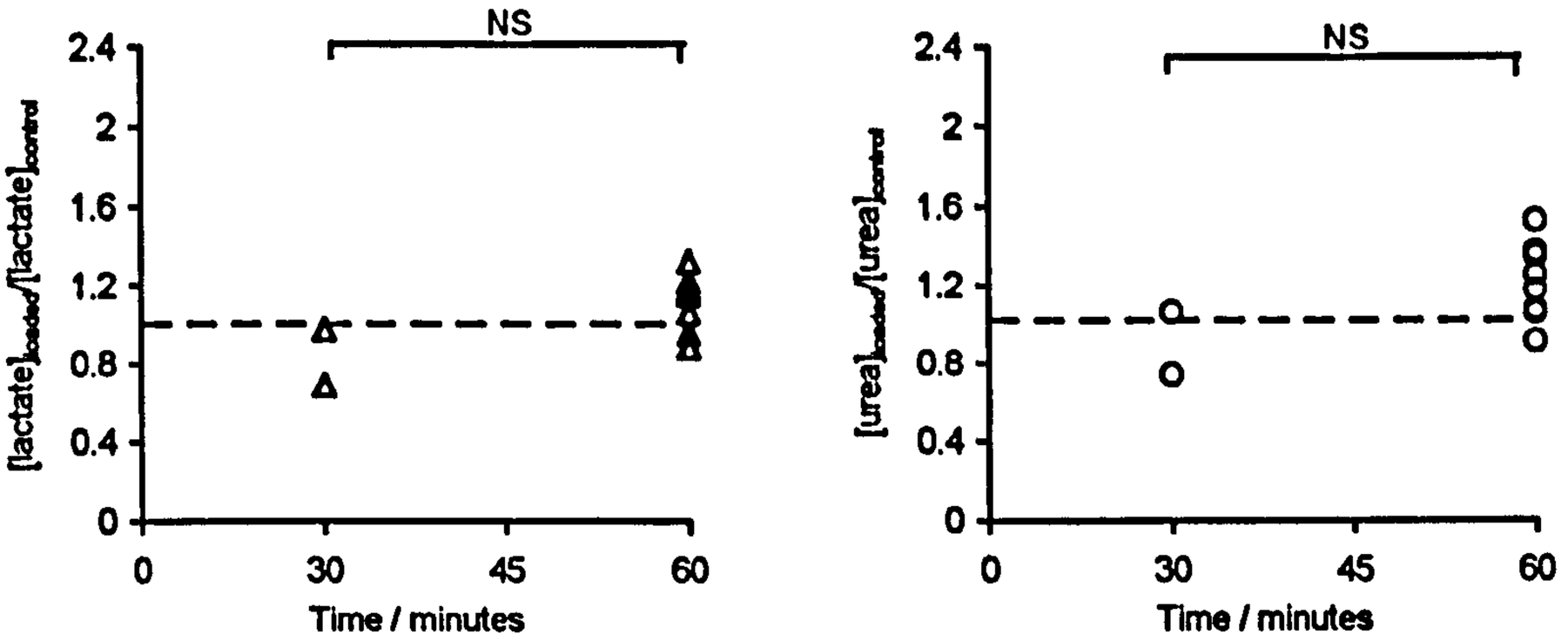

a)

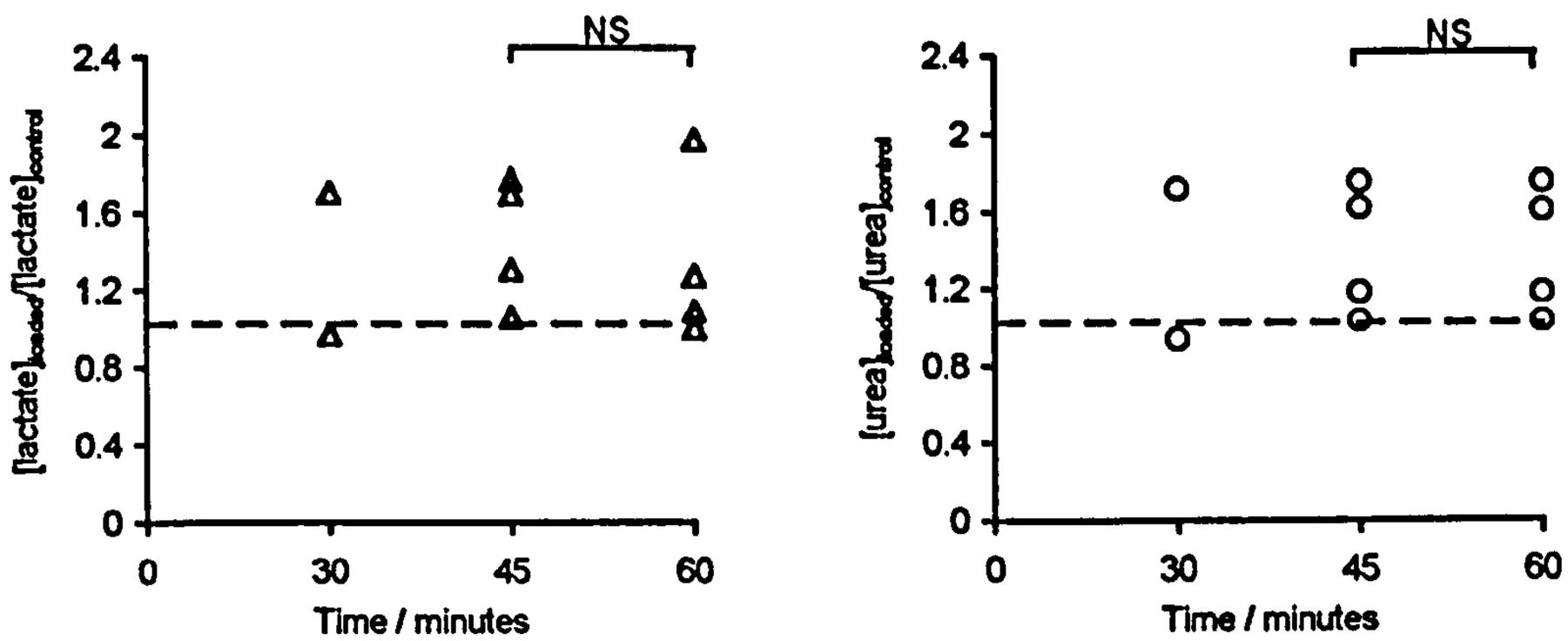

b)

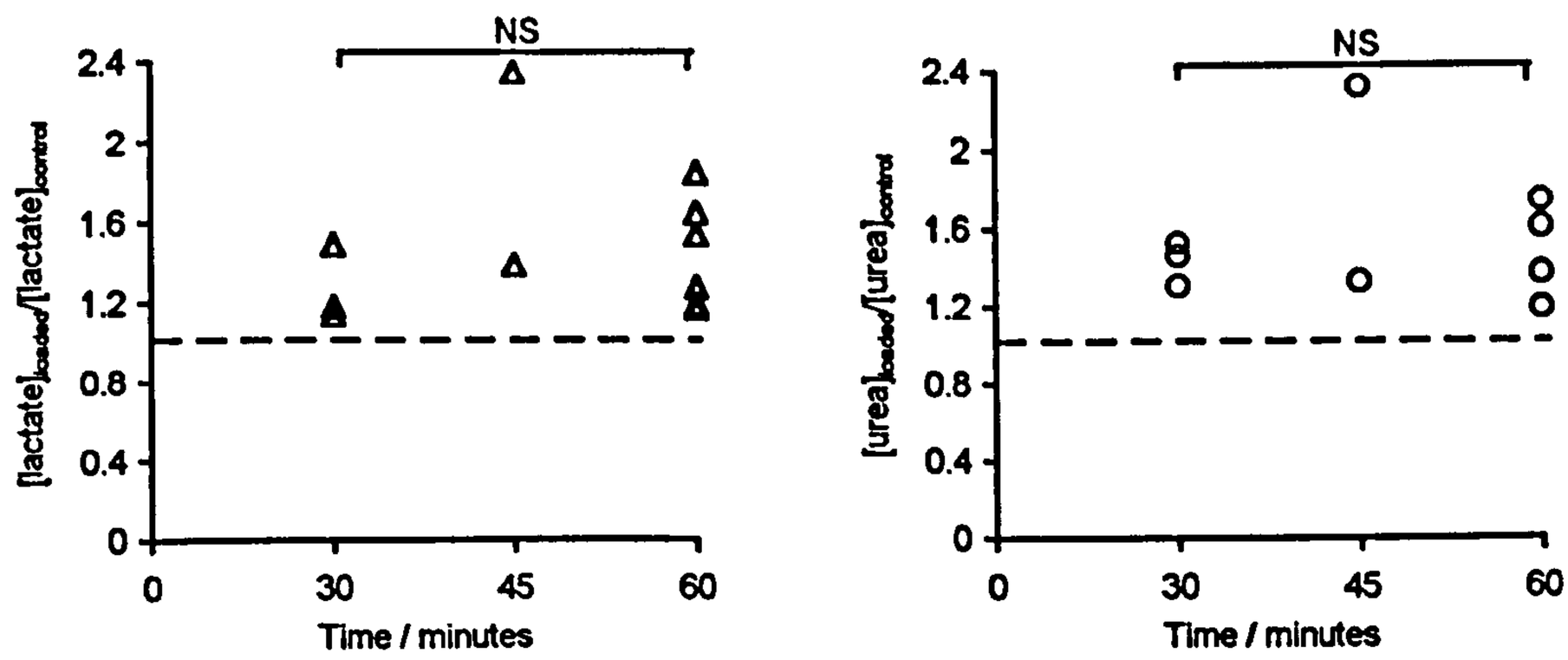

c)

Figure 7-4 Effect of collection time on sweat lactate and sweat urea concentration.
a) 40 mmHg,
b) 80 mmHg,
c) 120 mmHg applied pressure.

Using the Wilcoxon Rank test for paired data, the relationship between the sweat collected at the loaded and unloaded sites for each applied pressure was investigated with a summary of the results presented in Table 7-2.

Table 7-2 Table showing statistical significance of sweat metabolite data at different applied loads using Wilcoxon Rank Test for all time periods.

Metabolite	40 mmHg	80 mmHg	120 mmHg
Lactate	NS	$p<0.01$	$p<0.01$
Urea	$p<0.05$	$p<0.01$	$p<0.01$
Chloride	NS	$p<0.05$	$p<0.01$
Urate *	-	-	-

* Denotes that lack of sample data precluded rigorous statistical analysis.

It is clear from the results that a significant increase in sweat lactate and chloride concentrations is exhibited at applied pressures greater than 40 mmHg, whereas sweat urea concentration shows an elevation at applied pressures of 40 mmHg and above. In addition, a linear regression model was applied to the ratio data using the Spearman correlation coefficient. Statistically significant correlations were shown for the relationship between lactate, urea and chloride sweat concentration ratios and applied pressure.

Although there was insufficient data to statistically analyse the urate response, it appears from the graph in Figure 7-8b that urate ratio is also elevated at applied pressures greater than 80 mmHg.

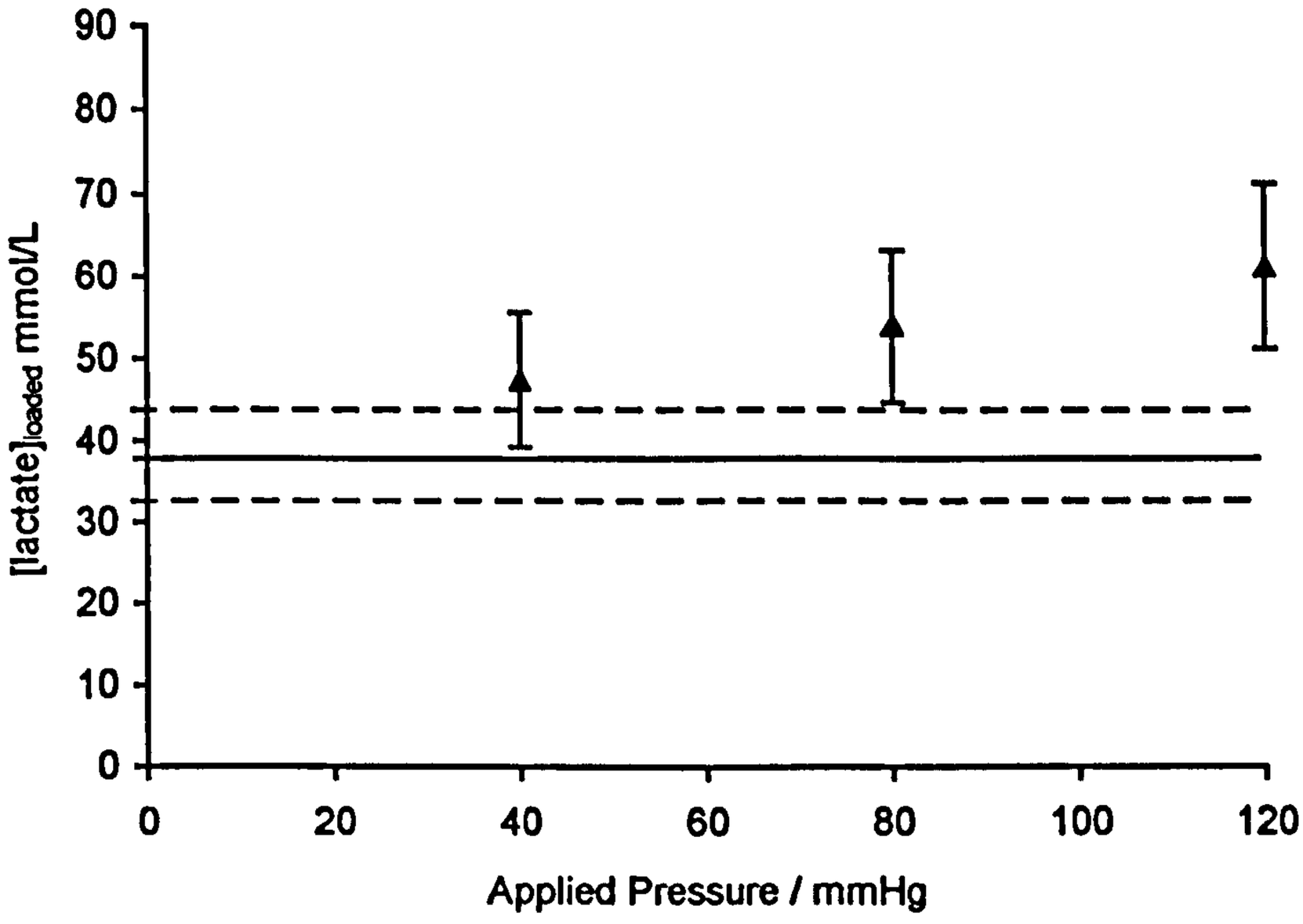

a)

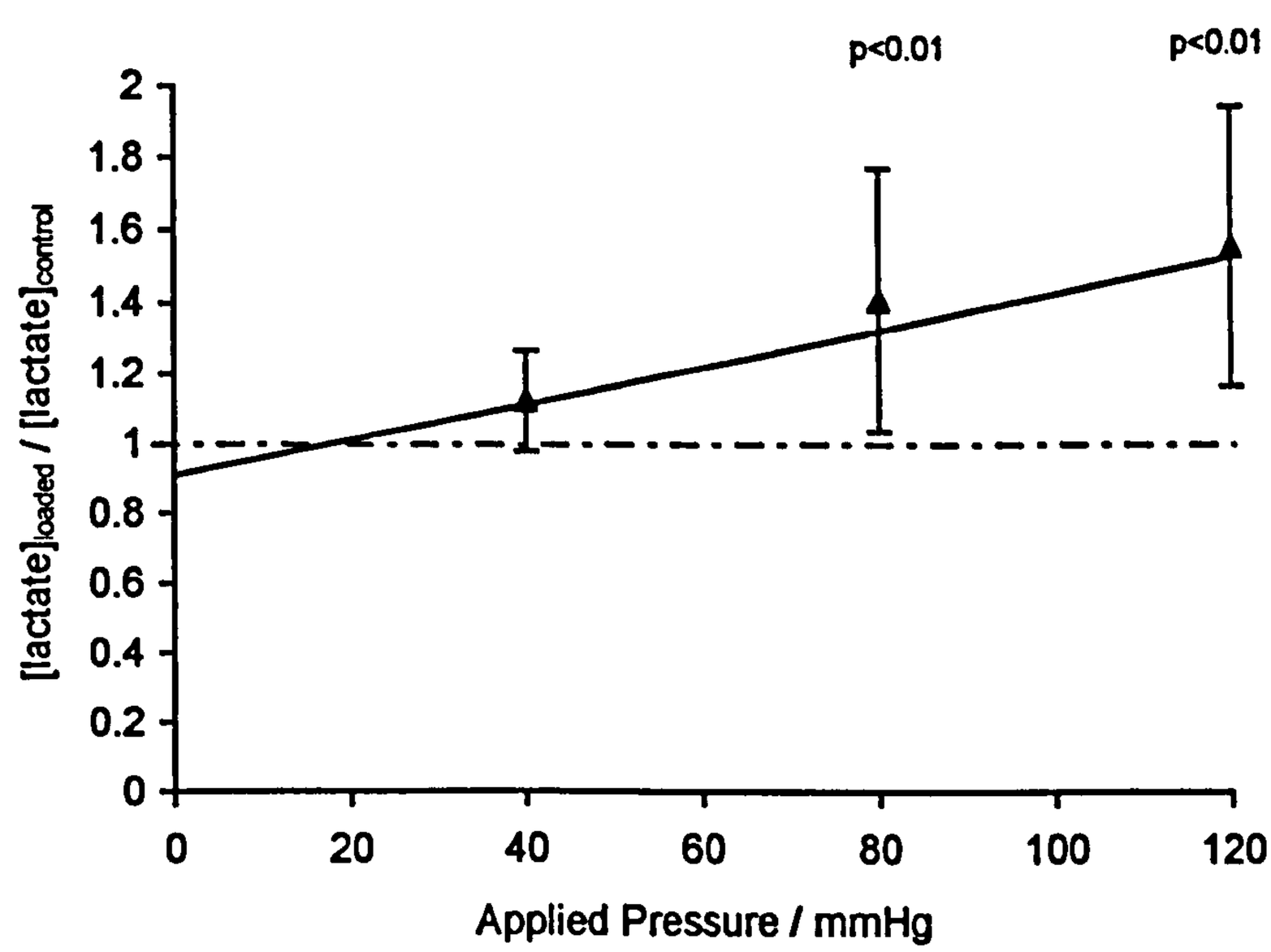

b)

Figure 7-5 The effect of applied pressure on sweat lactate concentrations
a) mean sweat lactate concentrations at the loaded sacrum, superimposed mean (——) and s.e.m (– – –) lactate concentration at the unloaded site.
b) ratio of sweat lactate concentration at loaded versus unloaded sites. (- — -) ratio of unity.
Linear regression model $y=0.0051x+0.909$ $r=0.48$ **
Error bars denote s.e.m, for n values see Table 7-1..

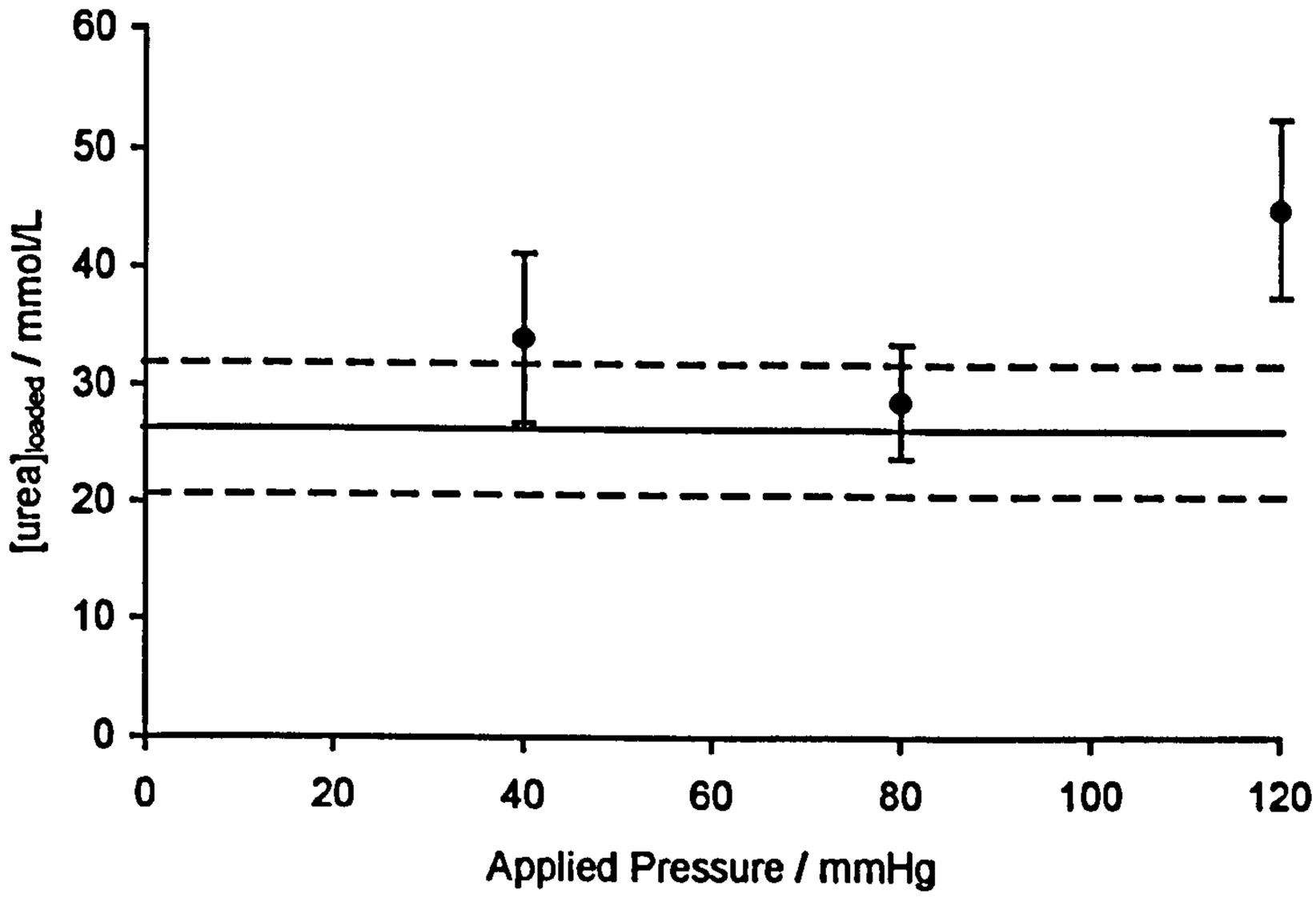

a)

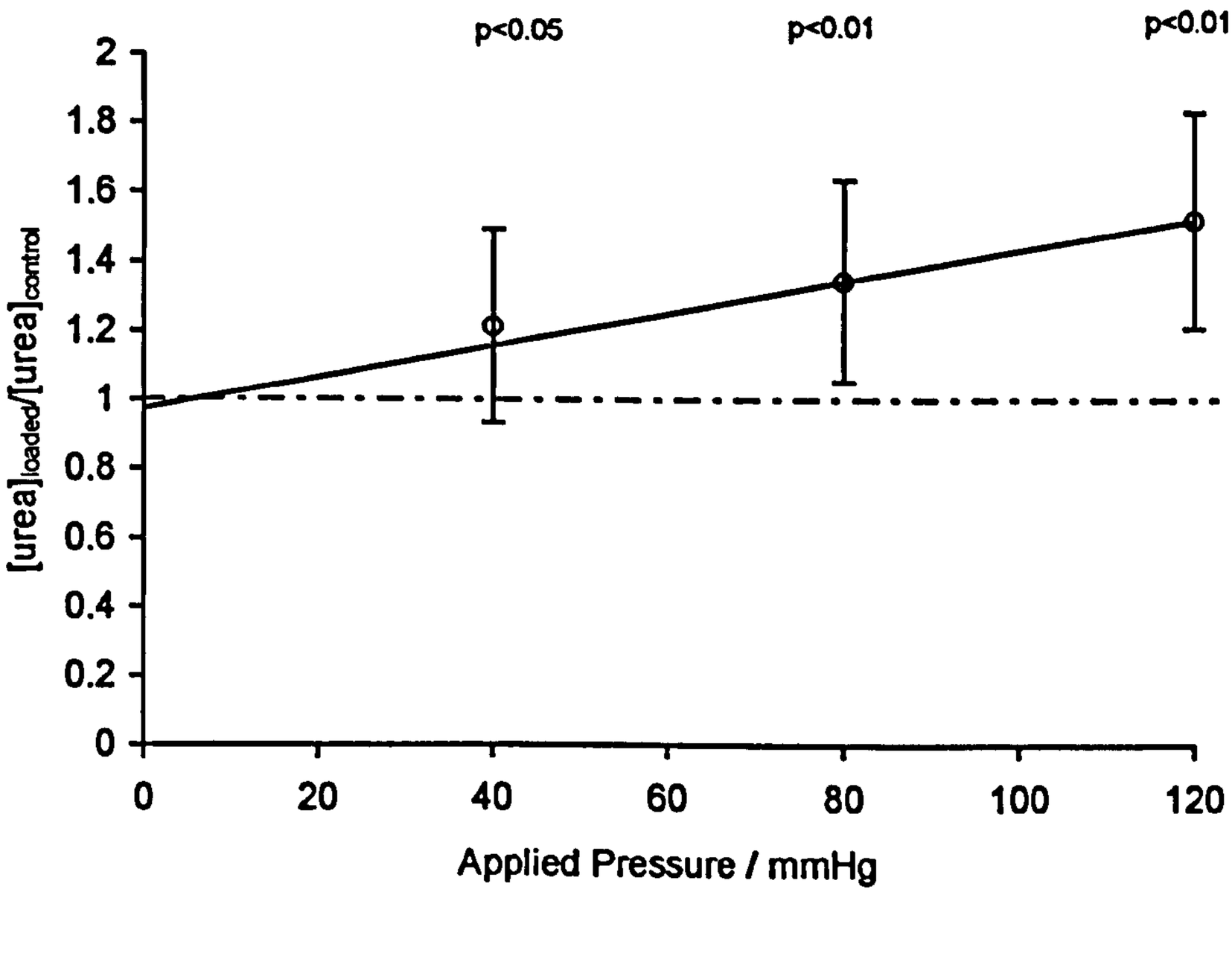

b)

Figure 7-6 The effect of applied pressure on sweat urea concentrations
a) mean sweat urea concentrations at the loaded sacrum, superimposed mean (——) and s.e.m (– – –) urea concentration at the unloaded site.
b) ratio of sweat urea concentration at loaded versus unloaded sites. (- — -) ratio of unity.
Linear regression model $y=0.0046x+0.975$ $r=0.48$ **
Error bars denote s.e.m, for n values see Table 7-1.

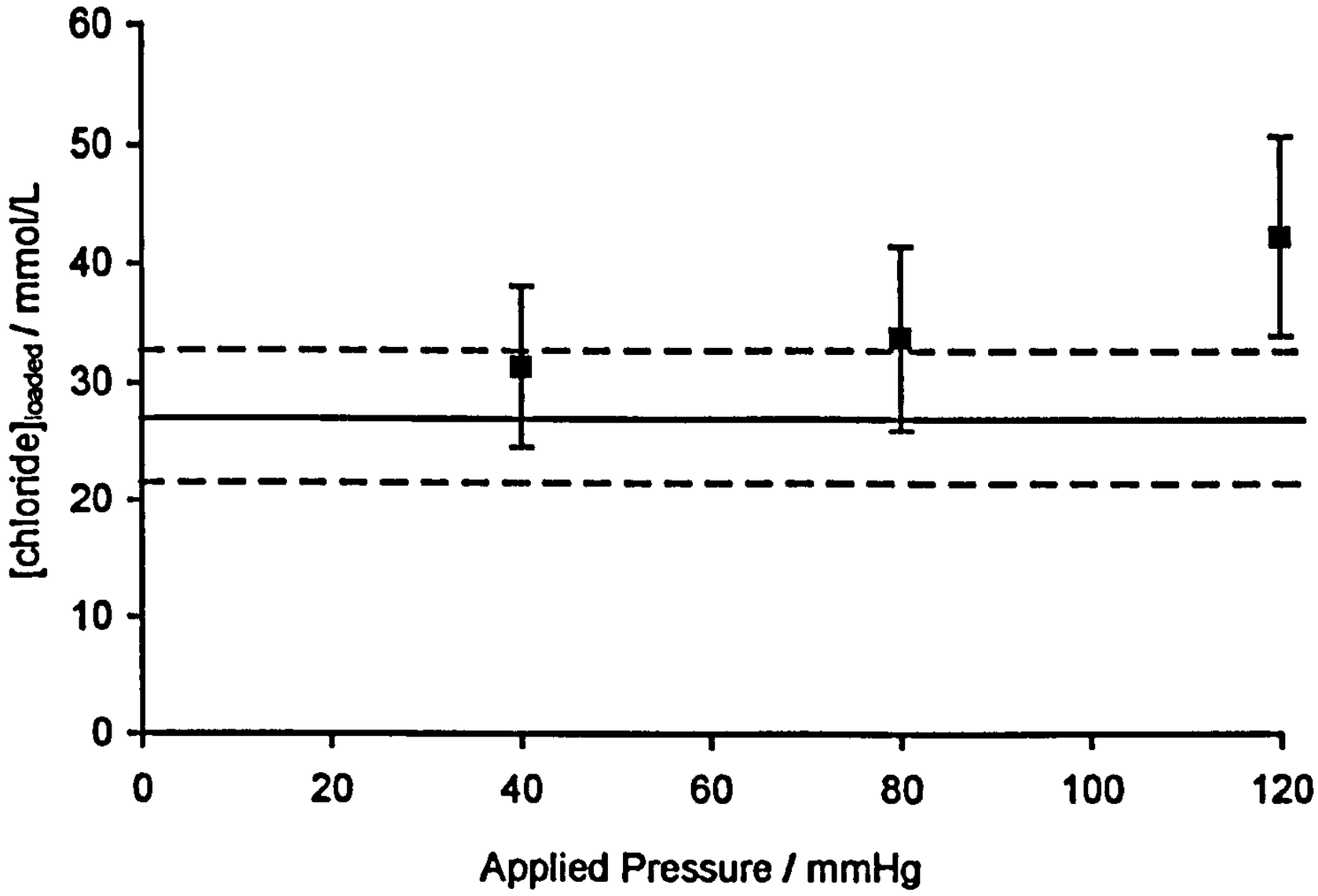

a)

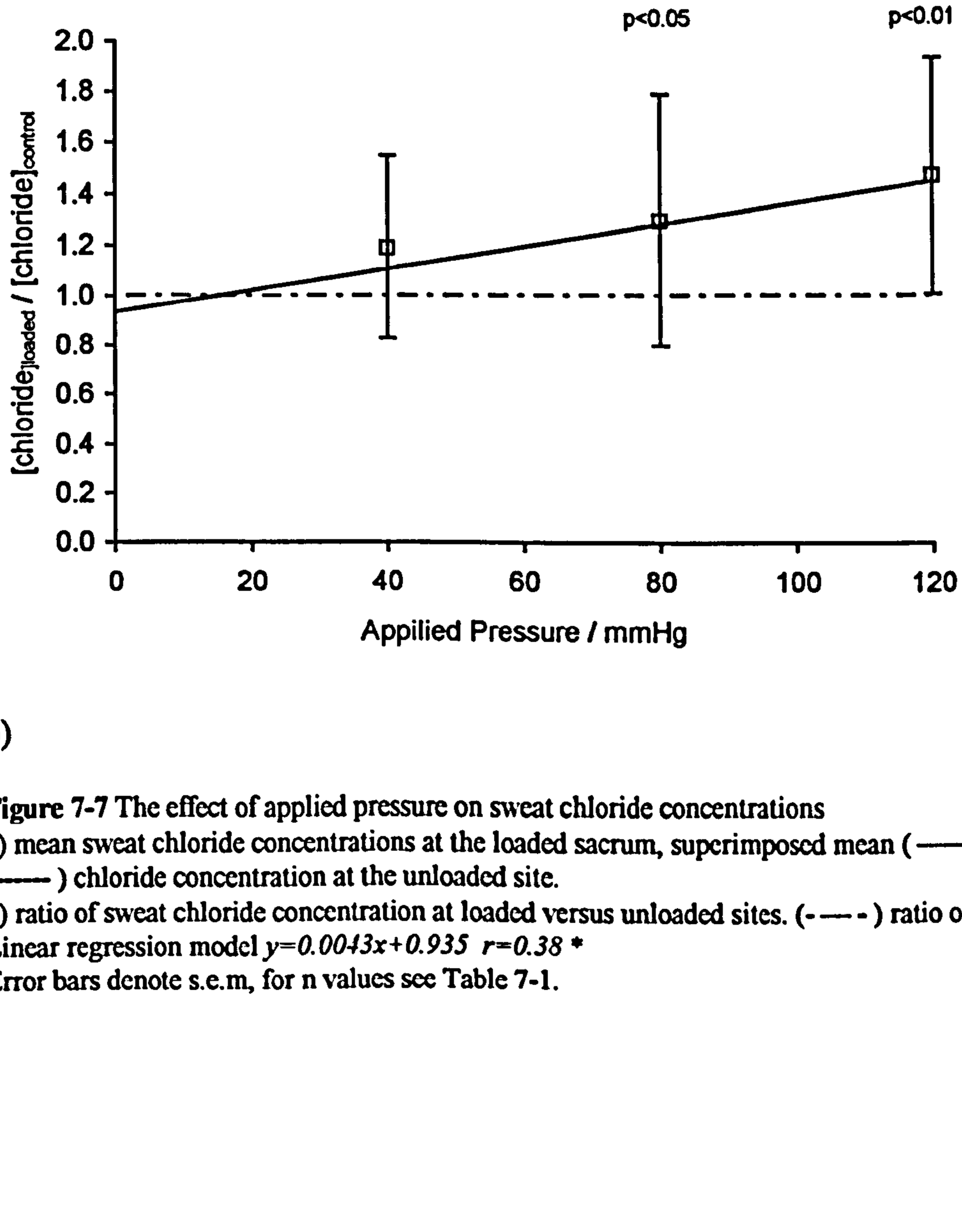

b)

Figure 7-7 The effect of applied pressure on sweat chloride concentrations
a) mean sweat chloride concentrations at the loaded sacrum, superimposed mean (——) and s.e.m (– – –) chloride concentration at the unloaded site.
b) ratio of sweat chloride concentration at loaded versus unloaded sites. (- — -) ratio of unity.
Linear regression model $y=0.0043x+0.935$ $r=0.38$ *
Error bars denote s.e.m, for n values see Table 7-1.

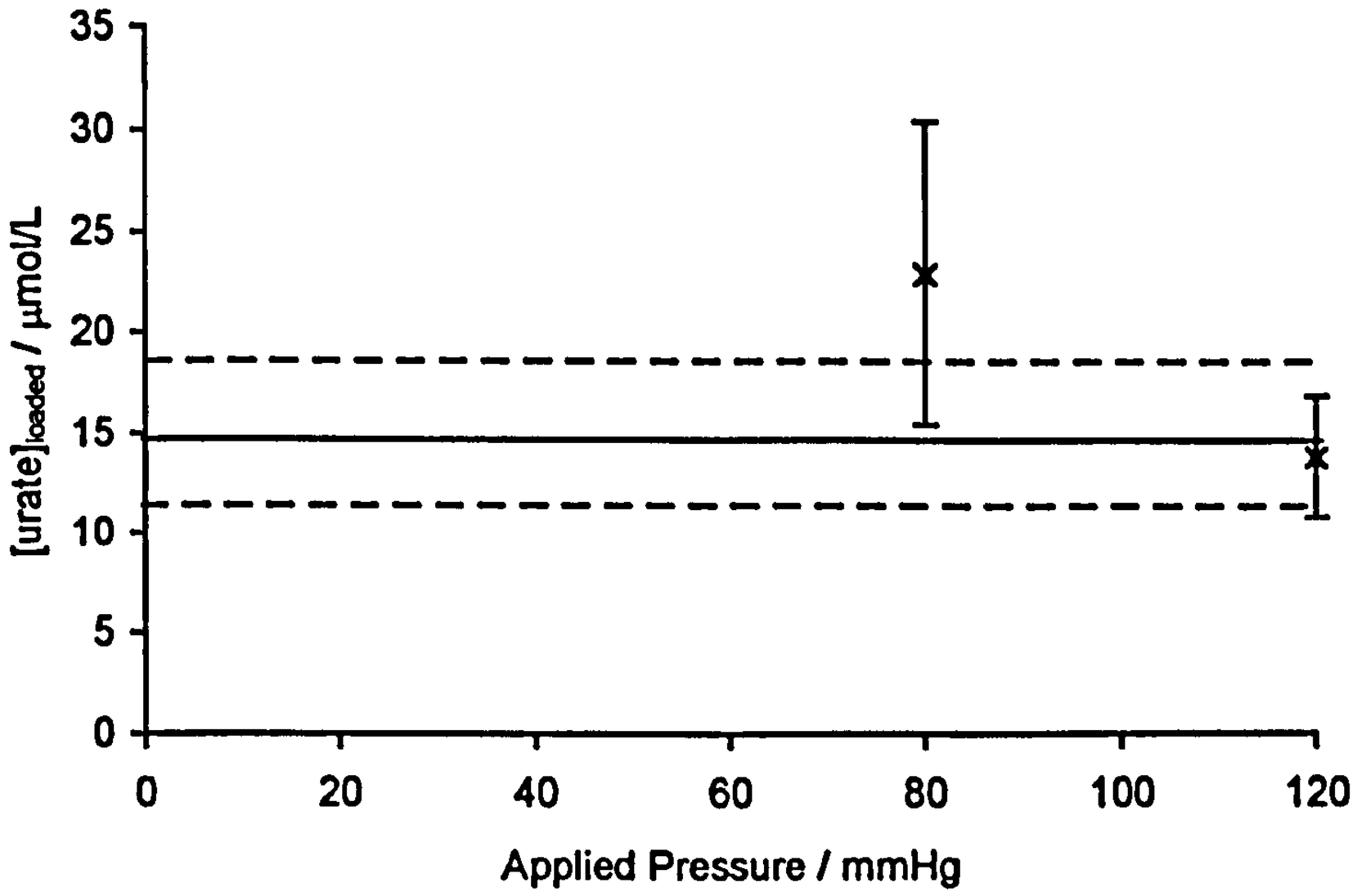

a)

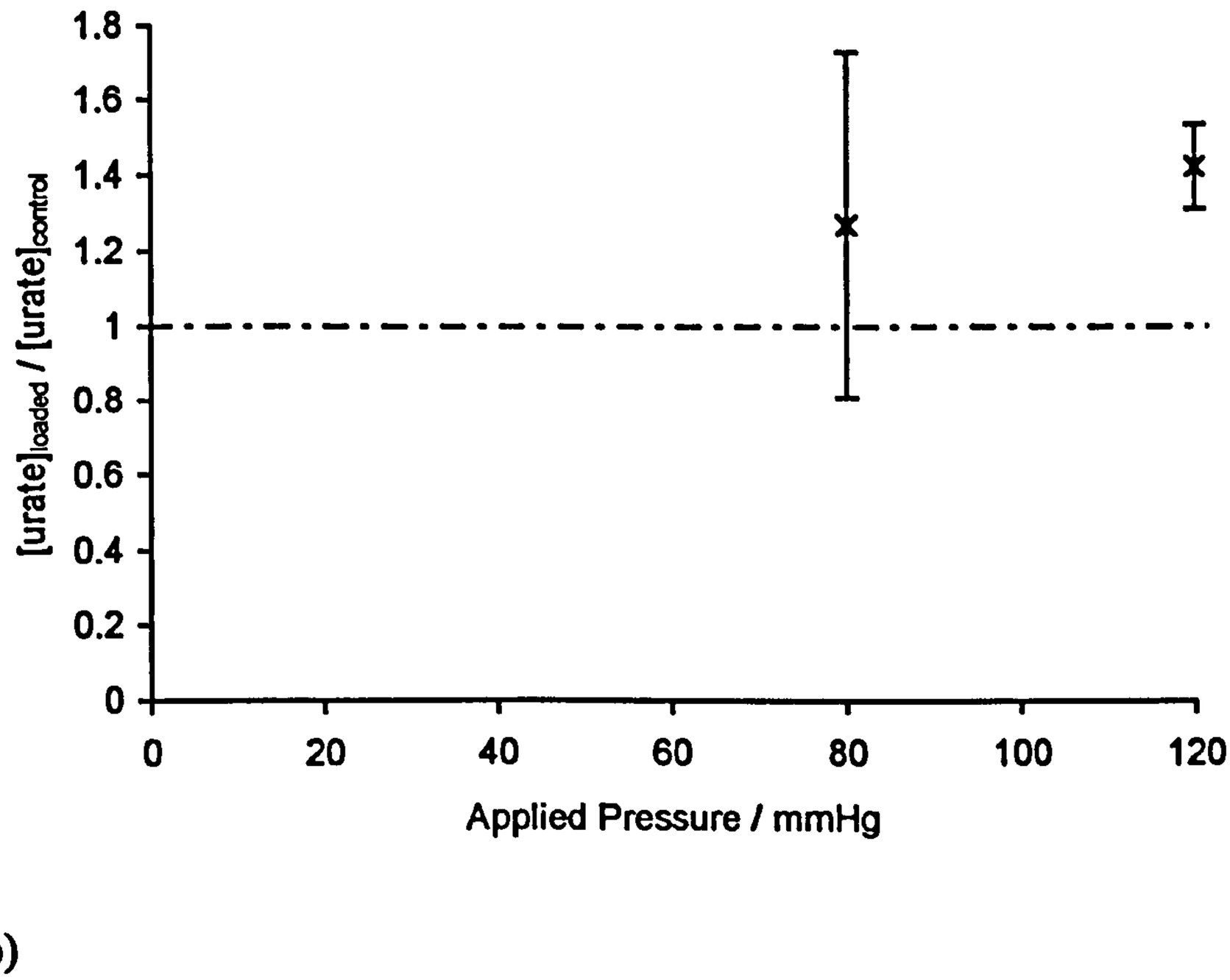

b)

Figure 7-8 The effect of applied pressure on sweat urate concentrations
a) mean sweat urate concentrations at the loaded sacrum, superimposed mean (——) and s.e.m (——) urate concentration at the unloaded site.
b) ratio of sweat urate concentration at loaded versus unloaded sites. (- — -) ratio of unity.
Error bars denote s.e.m, for n values see Table 7-1.

B COMPARISON BETWEEN PARAMETERS OF SOFT TISSUE STATUS

7.4.4 TRANSCUTANEOUS OXYGEN & CARBON DIOXIDE TENSION

The combined transcutaneous electrode permits continuous monitoring of both oxygen and carbon dioxide tensions throughout the experimental period. Examination of the associations between these two measures reveals some interesting trends. The data is hence presented in two distinct forms (Figures 7-9 and 7-10).

Figure 7-9 shows the frequency distribution of median oxygen tension at the loaded sites for each of the three modes representing carbon dioxide response, as described in Section 5-4. Clear trends are revealed namely, the Mode 3 pCO_2 response was always associated with a median pO_2 of less than 30 mmHg. By contrast, Mode 1 and Mode 2 pCO_2 responses were associated with a median pO_2 of greater than 30 mmHg in 57% and 67% of cases respectively.

Figure 7-10 shows the percentage reduction in pO_2 plotted against the percentage time pCO_2 exceeds 50 mmHg during the assessment period. Close examination of this data reveals some distinctive trends, based upon a threshold level of 60% reduction in pO_2 from the unloaded values, as indicated by a dashed line in Figure 7-10. It is clear that in all cases where this threshold level is not exceeded, the corresponding values of pCO_2 are consistently below 50 mmHg. In contrast, above this threshold value, the pCO_2 values were generally above 50 mmHg for a significant proportion of the loaded period. Indeed, in only one subject out of the 21 cases, was a significant reduction in median pO_2 (about 80%) not associated with a pCO_2 level which exceeded 50 mmHg.

7.4.5 SWEAT BIOCHEMISTRY & OXYGEN TENSION

The employment of simultaneous measurement techniques permitted the comparison between parameters derived for an individual test. Transcutaneous oxygen tensions and sweat biochemistry were measured at the sacrum under a variety of loading regimes. The absolute concentrations of sweat lactate and sweat urea at both the loaded and unloaded sites are plotted against the corresponding median pO_2 at each site and illustrated in Figures 7-11 and 7-12 respectively.

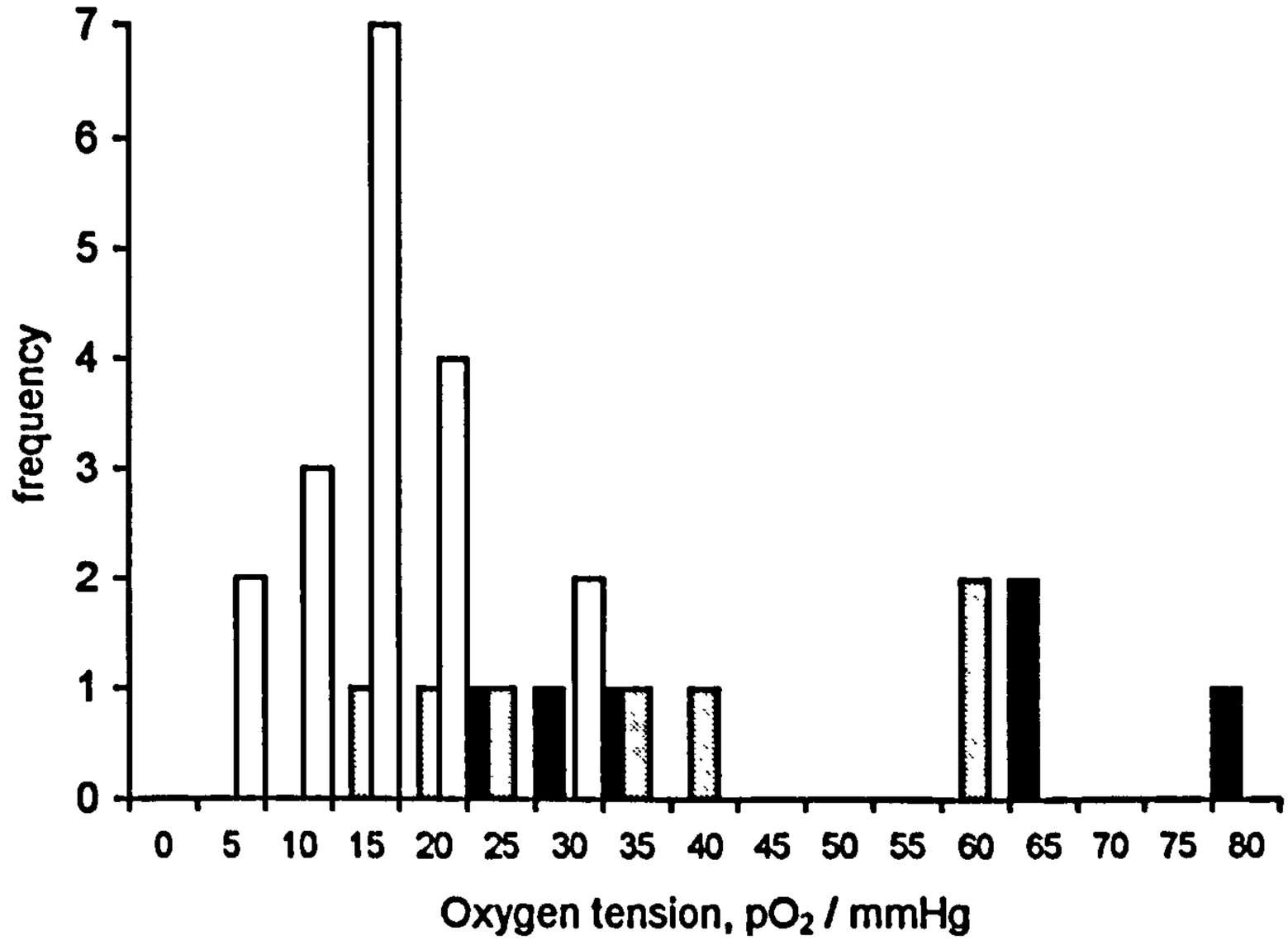

Figure 7-9 Frequency distribution of median oxygen tension for each mode of carbon dioxide response.
(■) Mode 1, (□) Mode 2 and (□) Mode 3.

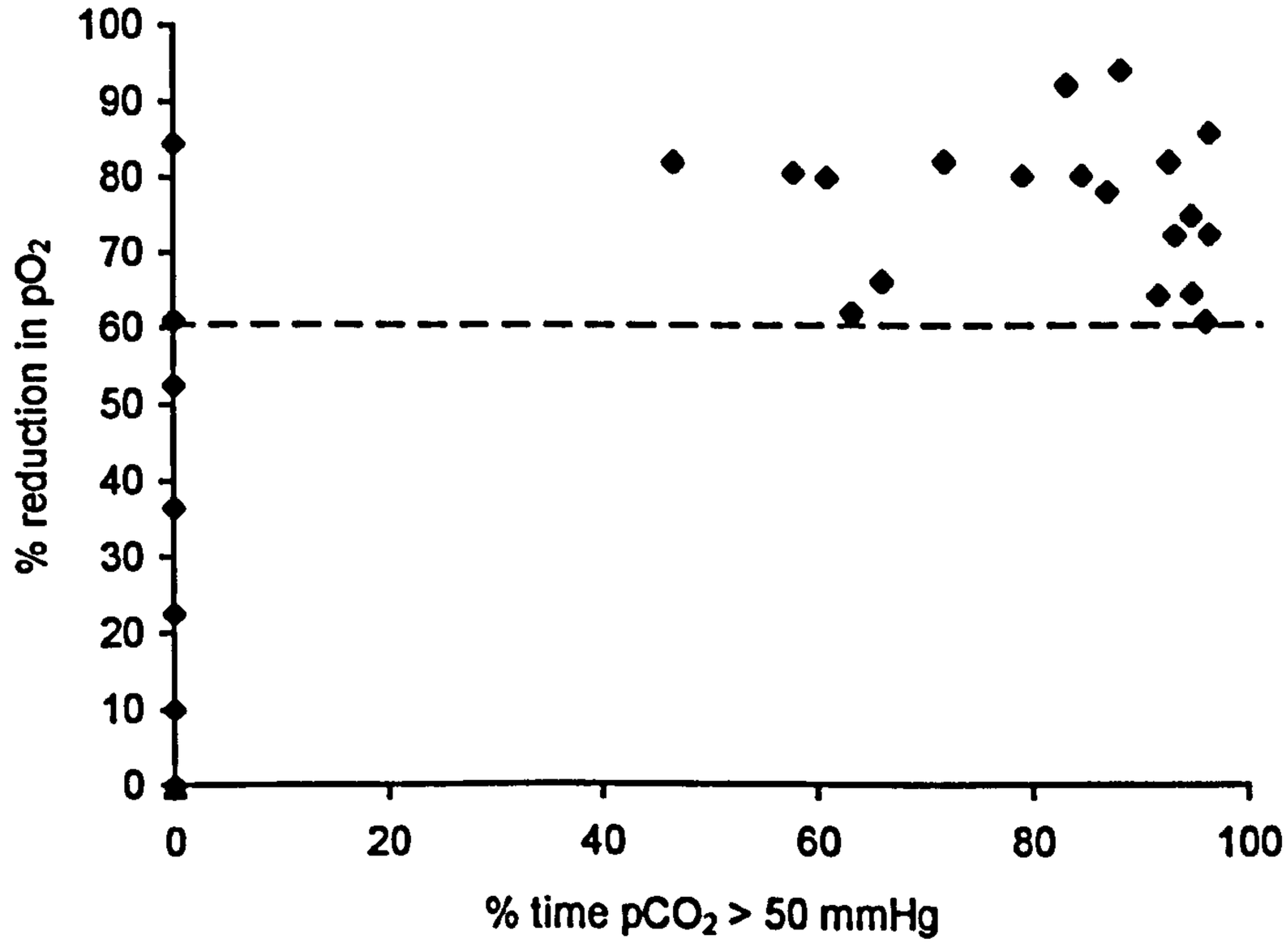

Figure 7-10 Relationship between median pO_2 tension and % of time pCO_2 exceeds 50 mmHg.

Both graphs indicate that for loaded sites, there are low values of median pO_2 which are generally associated with elevated levels of metabolite concentrations. Indeed the results strongly suggest an inverse relationship between median pO_2 values and sweat lactate and urea concentrations.

Furthermore, the data can be presented using the derived parameters of percentage reduction in oxygen tension and loaded:unloaded sweat metabolite concentration ratio (Figures 7-13 and 7-14). The data highlights some interesting relationships and can be effectively divided into two regions, separated by the 60% threshold of reduction in oxygen tension. Linear models can be tested for the data in both regions. For reductions in pO_2 up to 60% there appears to be no correlation between either sweat lactate or urea and pO_2 value. However, above the 60% threshold there are positive correlations between sweat lactate and sweat urea ratio and percentage reduction in pO_2, which are both statistically significant at the 1 per cent level.

7.4.6 Sweat Biochemistry & Carbon Dioxide Tension

The corresponding relationship between the two parameters derived from the carbon dioxide response (Figure 5-9) and ratio values for sweat lactate and urea are presented in Figures 7-15 and 7-16. Although there is considerable scatter in the data, the results suggest that an increase in area below the pCO_2 - time curve is associated with elevated ratio values for both sweat lactate (Figure 7-15) and sweat urea (Figure 7-16). Indeed, the associated linear models have found the relationship to be statistically significant at the 5% and 1% level respectively.

Figure 7-17 and 7-18 show the relationship between the sweat metabolite ratios and the percentage time at which pCO_2 exceeds 50 mmHg. This data appears to be approximately bimodal in form with the pCO_2 parameter exhibiting data at 0% and between 37 and 90%. Those subjects falling into the latter group largely produce a sweat metabolite ratio, for both lactate and urea, in excess of 1.0, up to a maximum value of 2.4. However some subjects, representing 20% and 23% of the total for lactate and urea respectively, showed an elevated metabolite level at the loaded site without an associated increase in pCO_2.

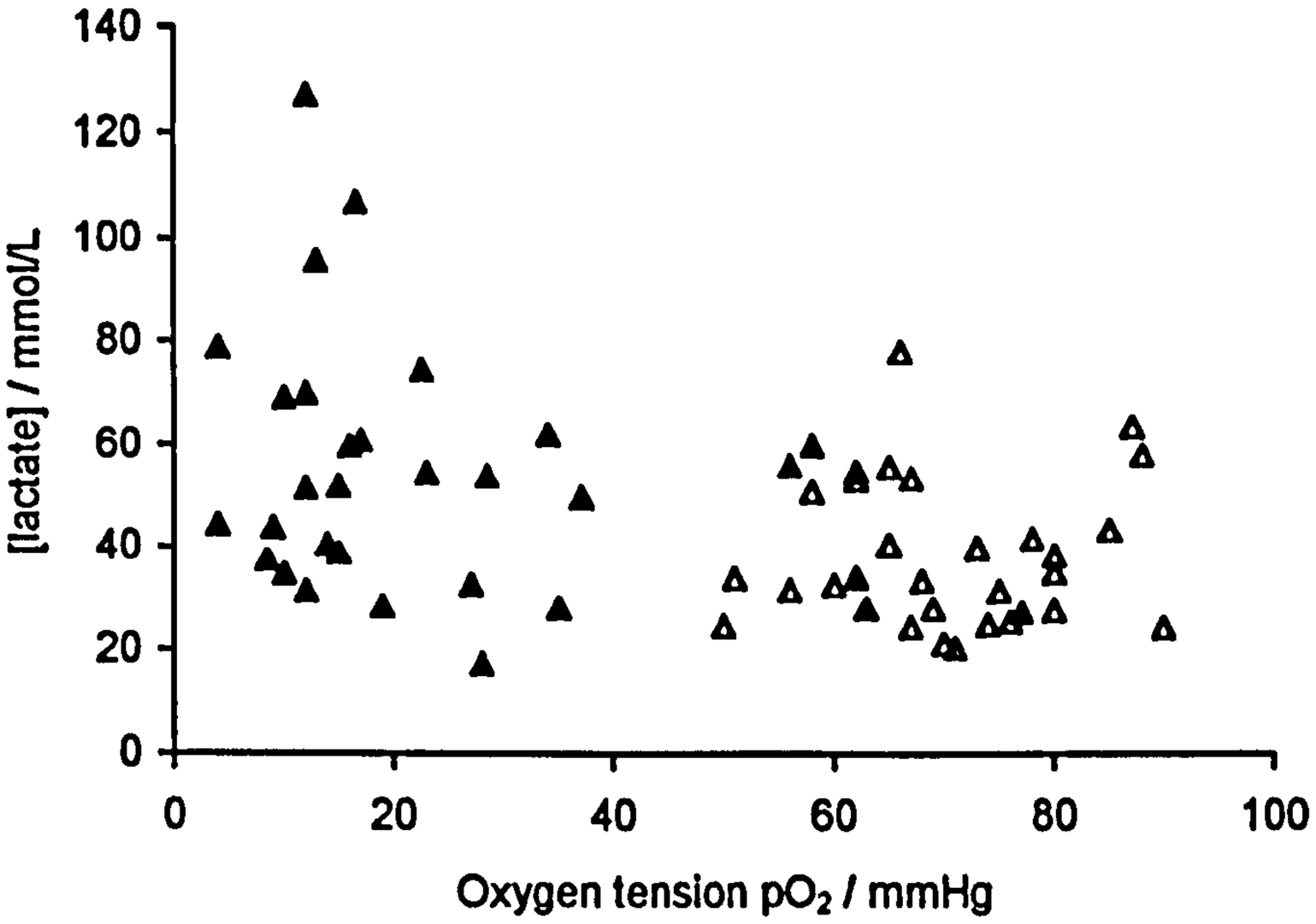

Figure 7-11 The relationship between sweat lactate concentrations and median values for oxygen tension (pO_2) for individual measurements.
(▲) loaded sites, (Δ) unloaded sites.

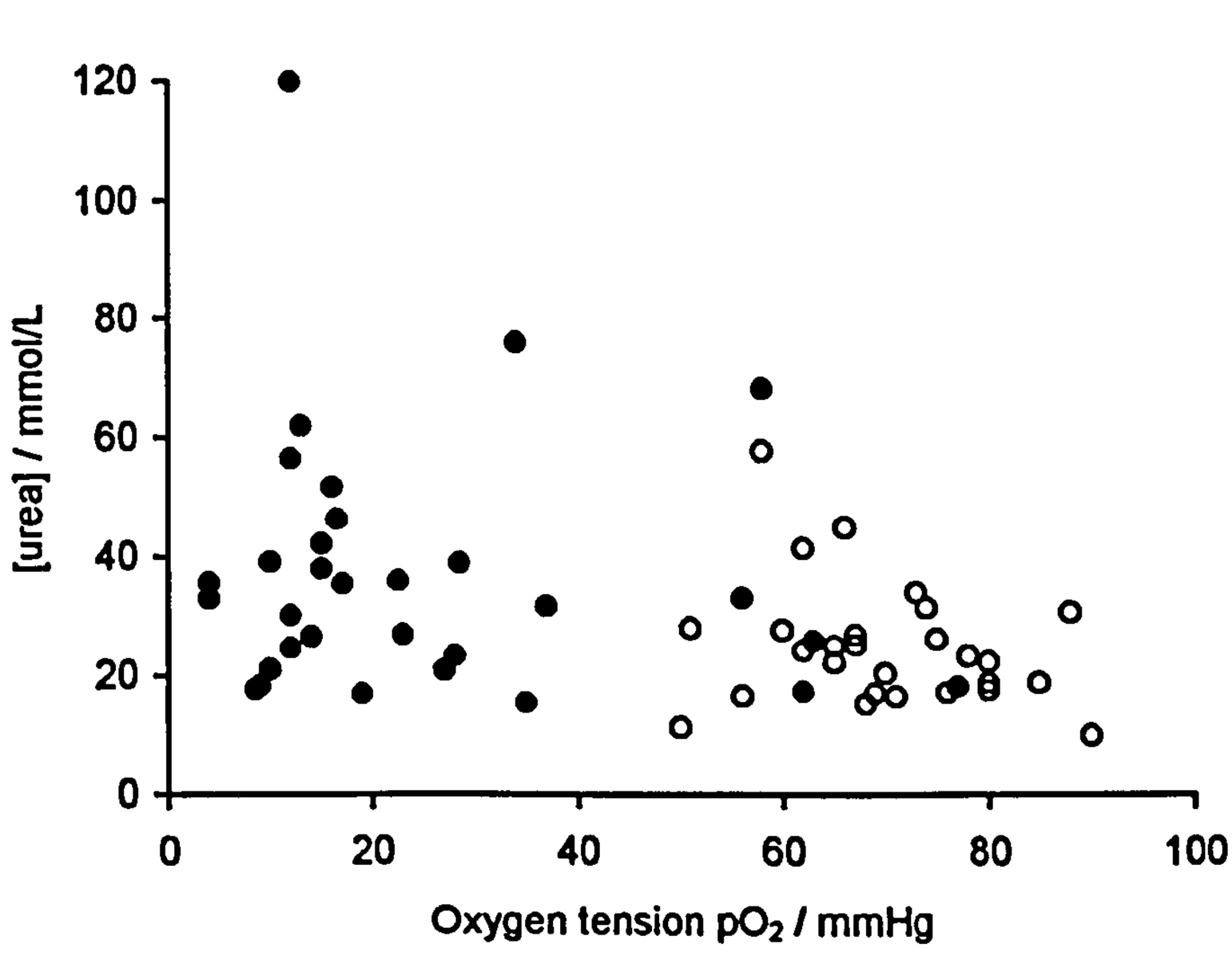

Figure 7-12 The relationship between sweat urea concentrations and median values for oxygen tensions (pO_2) for individual measurements.
(●) loaded sites, (○) unloaded sites.

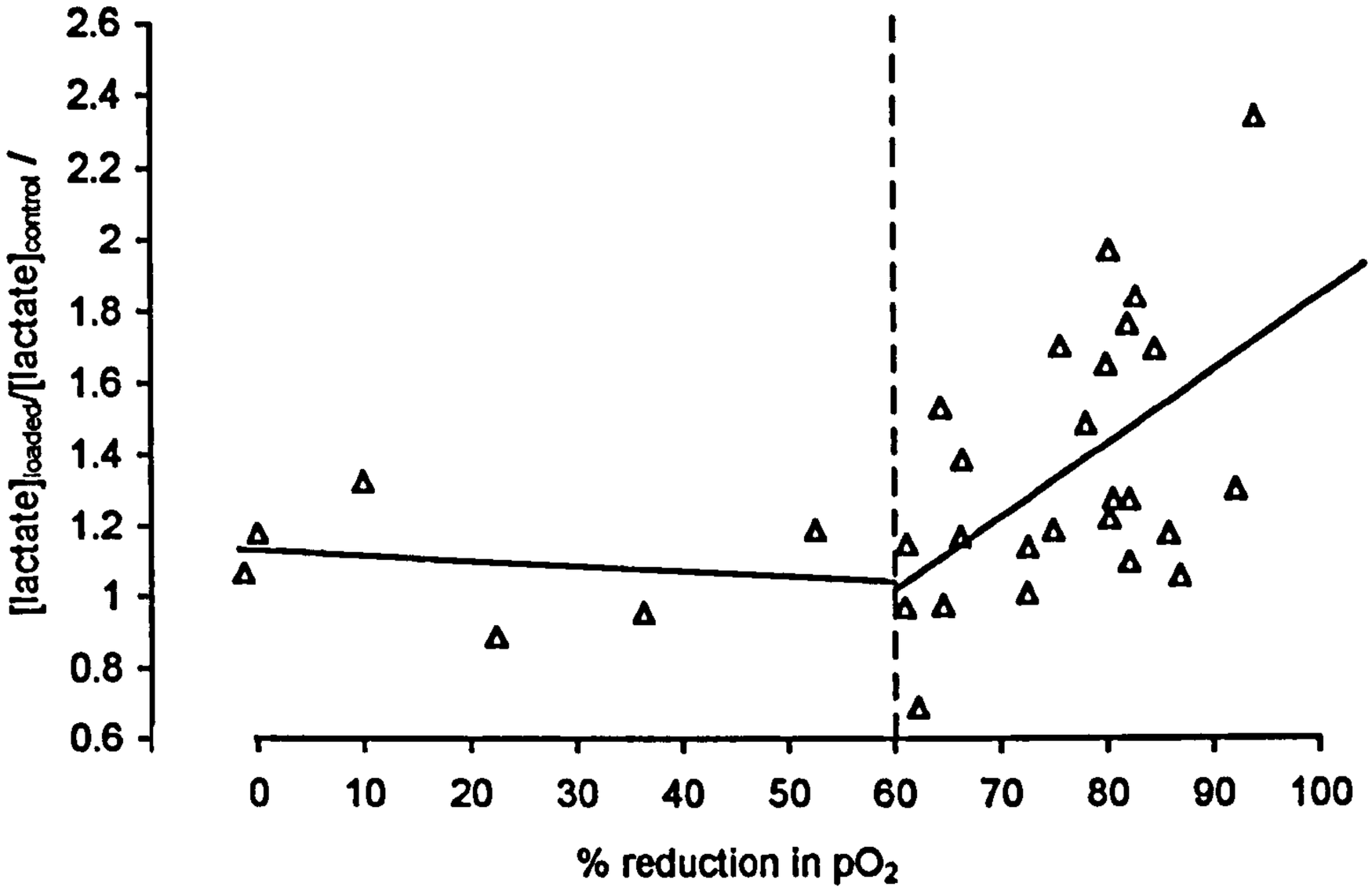

Figure 7-13 The relationship between ratio of sweat lactate concentration and the percentage reduction in pO_2 levels as a result of sacral loading on individual subjects.
Linear model at % reduction in pO_2 > 60% *y=0.02x-0.21 r =0.53* **,
Linear model at % reduction in pO_2 < 60% *y=-0.0013x+1.12 r=0.175.*

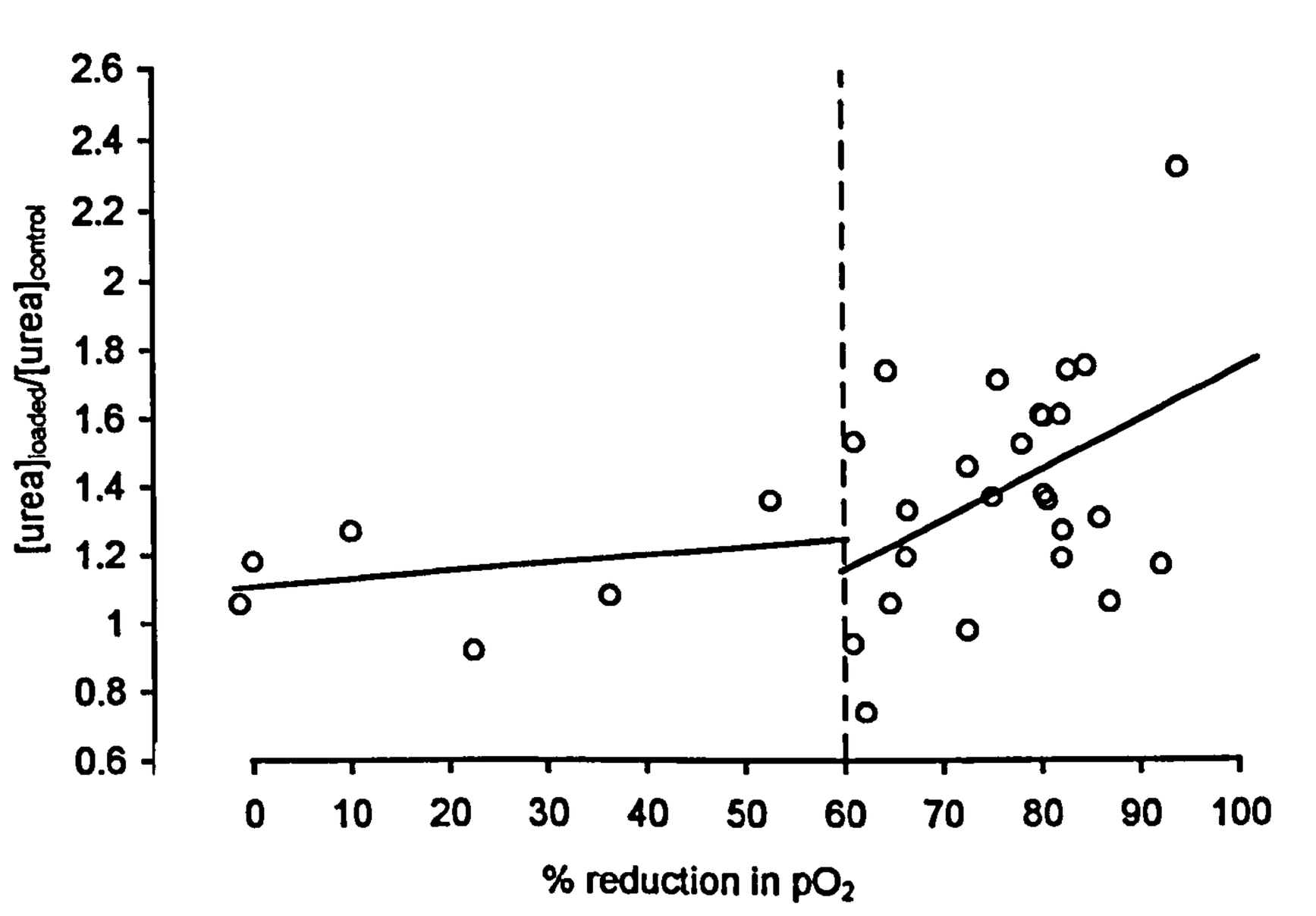

Figure 7-14 The relationship between ratio of sweat lactate concentration and the percentage reduction in pO_2 levels as a result of sacral loading on individual subjects.
Linear model at % reduction in pO_2 > 60% *y=0.015x+0.28 r=0.48.* **,
Linear model at % reduction in pO_2 < 60% *y=0.0023x+1.09 r=0.312.*

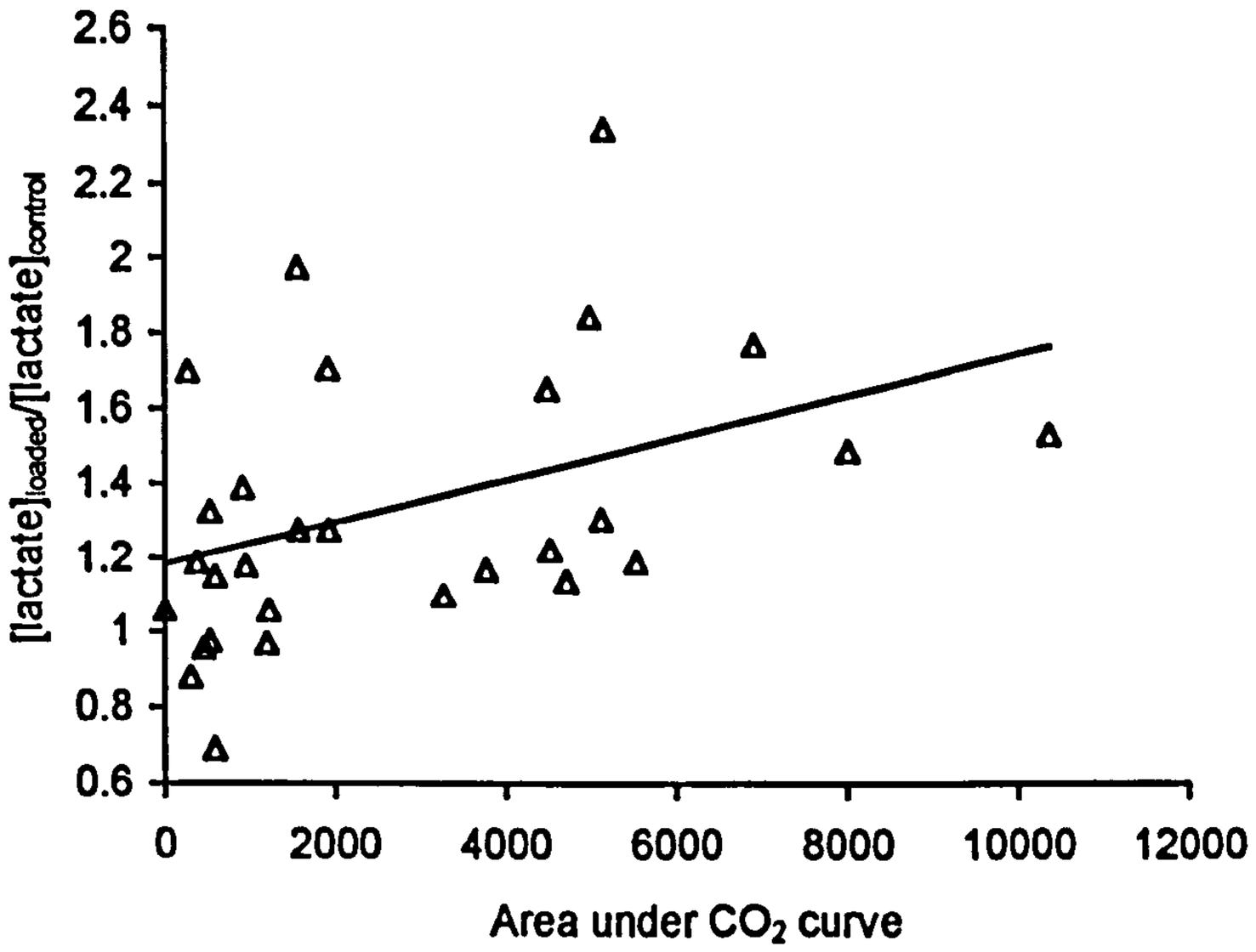

Figure 7-15 The relationship between area under pCO_2 time curve and sweat lactate ratio for sweat collected at loaded and unloaded sites at the sacrum.
Linear model $y=6*10^{-5}x+1.18$, $r=0.41$ *

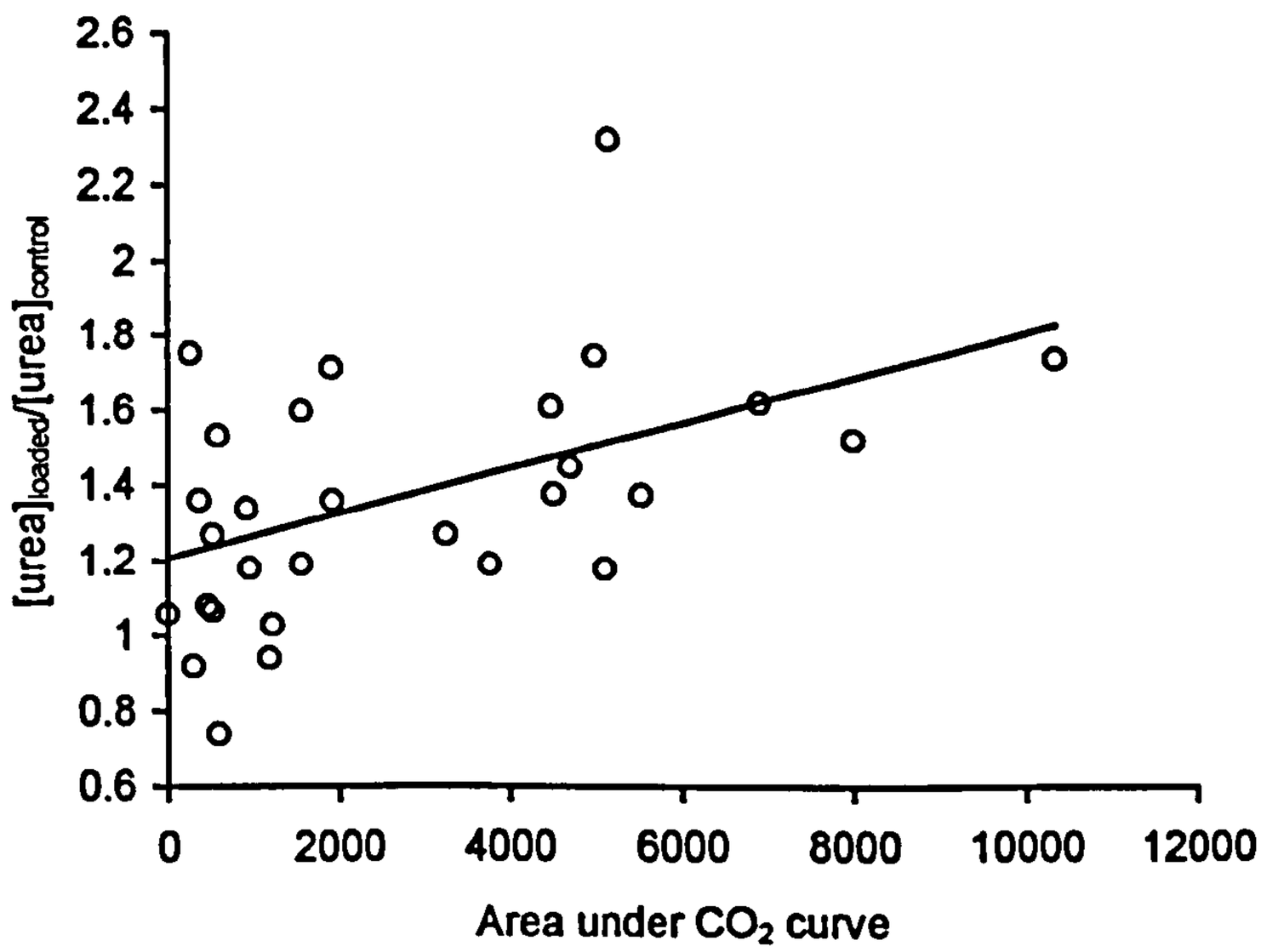

Figure 7-16 The relationship between area under pCO_2 -time curve and sweat urea ratio of sweat collected at loaded and unloaded sites at the sacrum .
Linear model $y=6*10^{-5}+1.2$, $r=0.49$.**

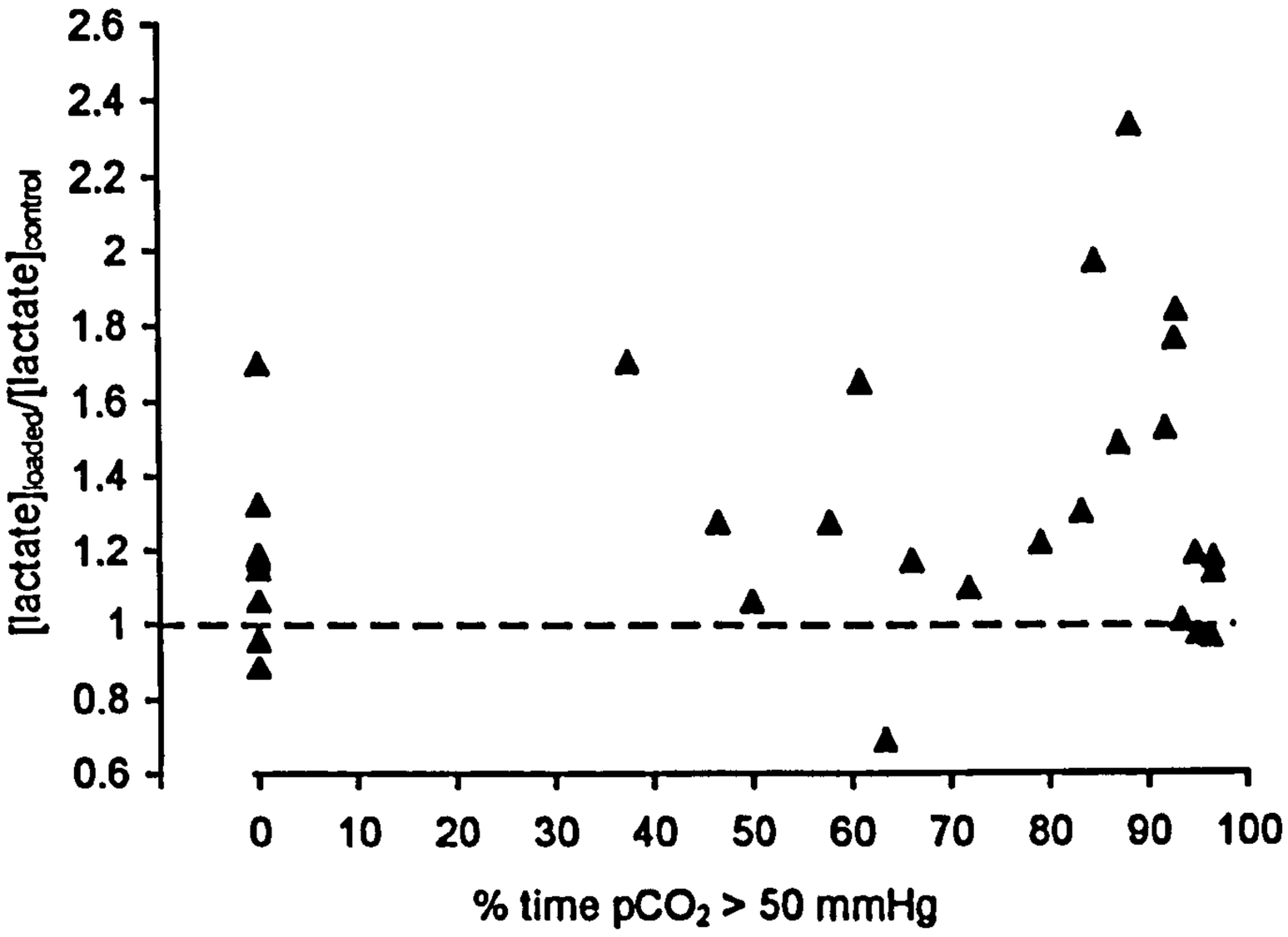

Figure 7-17 The relationship between sweat lactate ratio and percentage time pCO_2 exceeded 50 mmHg.

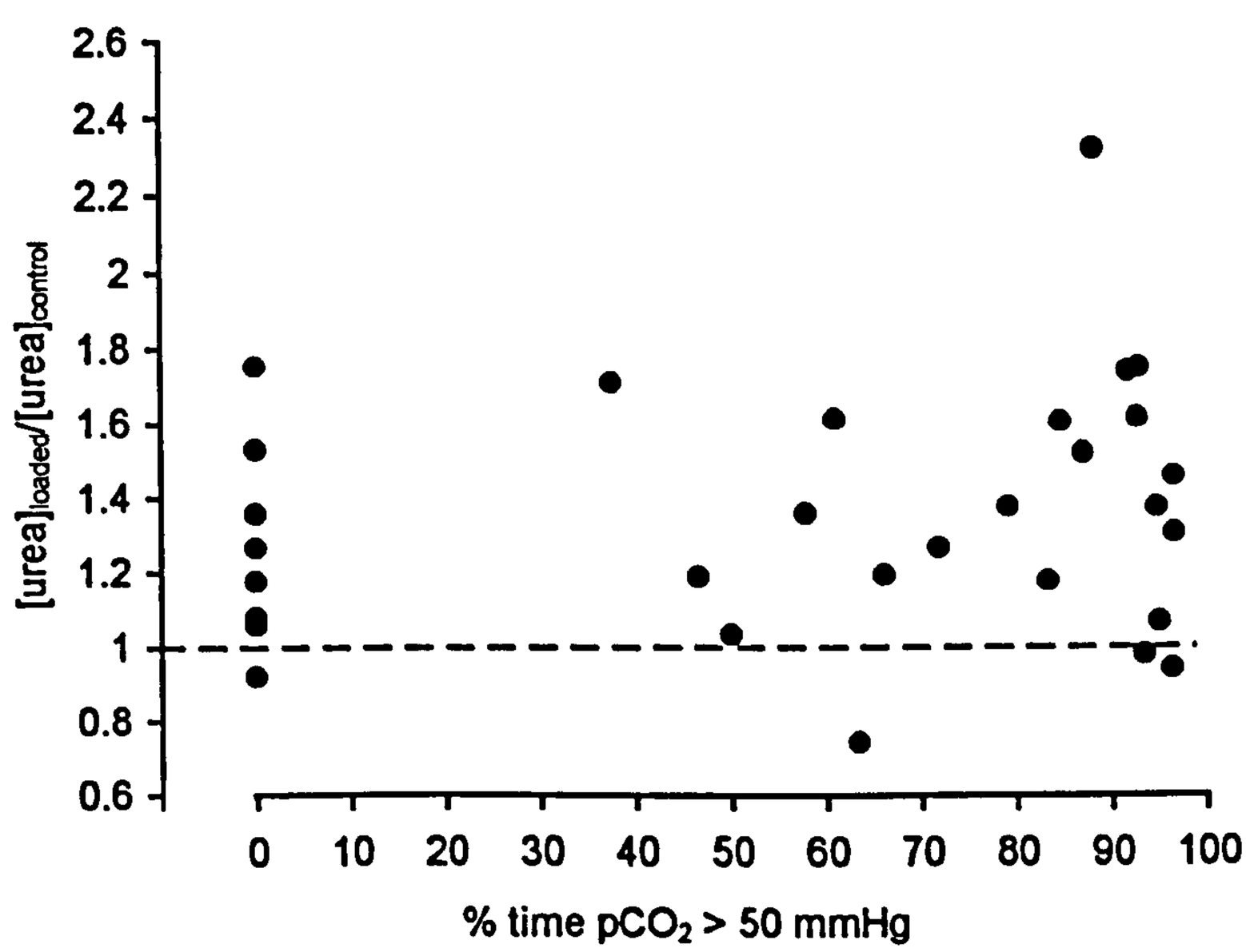

Figure 7-18 The relationship between sweat urea ratio and percentage time pCO_2 exceeded 50 mmHg.

7.5 DISCUSSION

7.5.1 EFFECT OF APPLIED PRESSURE ON GAS TENSIONS

The graphs in Figures 7-2 and 7-3 highlight distinct responses in terms of both transcutaneous oxygen and carbon dioxide tensions and applied pressure. A number of researchers have previously reported a decrease in pO_2 with applied pressure [147,175,191]. Newson *et al.* [147] showed a reduction to negligible values of pO_2 with applied pressure at the sacrum of approximately 120 mmHg, although the physiological significance of zero readings has been questioned [196]. Newson demonstrated a sigmoidal relationship between pO_2 and applied load, at low loads there was little change in pO_2 levels, whereas at higher loads there was a rapid decrease in pO_2 [147]. This finding was at variance with the linear reduction in pO_2 reported by Seiler & Stahelin [175]. The present results in Figure 7-3 suggest some similarity with the two previously reported findings with a plateau reached at 80-90% reduction in pO_2 from its initial value. Transcutaneous oxygen tension gives an indication of the degree of ischaemia present in the tissue [55-56] and since ischaemia is one of the major aetiological factors in the development of tissue breakdown it is a very important measure to be monitored. However, to date no threshold value has been quoted below which tissue damage may occur.

The response of transcutaneous carbon dioxide tension to applied pressure could be approximated to one of the three distinct forms as described in Figure 5.9b. Carbon dioxide tensions can give an indication of blood flow and 'wash-in and wash-out' of the tissue gas [24]. An increased pCO_2 reading suggests that an accumulation of CO_2 has occurred due to the inability of circulating blood to remove the excess gas levels in the tissues. Indeed, the results in Figure 7-3 suggest that at loads above 40 mmHg a substantial accumulation of CO_2 may develop. This could be potentially damaging to soft tissue leading to localised conditions of low pH. This damage will be enhanced if there is an associated accumulation of toxic waste products, as a direct result of compromise to the lymph supply in loaded tissues [118].

The combination of oxygen and carbon dioxide tensions shows the inter-relationship between these two measures of tissue status. There are only a few previous studies, which have examined the relationship between transcutaneous levels of oxygen and carbon dioxide tensions in loaded tissues [24-25]. Bogie *et al.* [24] indicated an inverse relationship, namely a reduction in pO_2 associated with elevated levels of pCO_2, in the ischial tissues of spinal cord injured subjects. In the present study, a threshold value for pO_2 reduction was demonstrated below which there was no accumulation of carbon dioxide (Figure 7-10). This threshold value at 60 % reduction from unloaded pO_2 values could be recommended as a safe limit of tissue compromise, above which damage could occur. It is also interesting to note that one or two subjects exhibits a very low pO_2 without the corresponding increase in pCO_2. The present results suggest the importance of measuring pCO_2 in tissues subjected to applied pressures and support the previous suggestions that the pCO_2 response may be used as an important marker of susceptibility of tissue breakdown [10].

7.5.2 Effect of Applied Pressure on Sweat Biochemistry

It is clear from the graphs in Figures 7-5 to 7-8 that the application of pressure to the sacrum alters the sweat biochemistry at loaded sites. In particular, increases in sweat lactate, urea, urate and chloride are shown at loads greater than 40 mmHg. These results are in general agreement with previous researchers who have used similar techniques for uniaxial loading though with limited pressure and time regimes [73,157-158].

Sweat lactate, urea and urate significantly increased with increasing applied pressure. The presentation of sweat metabolite ratios appear to eliminate the wide variation in basal values of the metabolite concentrations. Elevations of sweat lactate, urea and urate may reflect tissue metabolic status. Sweat lactate and urea may reflect ischaemia and resulting anaerobic metabolism of the sweat gland itself or underlying tissues [132,157,212]. Whereas elevated levels of urate may be an indication of the depletion of cellular energy and cell crisis [75,157].

Sweat chloride concentrations are very variable and can be altered by dietary intake of NaCl [31]. Chloride concentrations showed an increase at loaded sites with applied

pressure (Figure 7-7). This finding can be explained by a decrease in ability of the sweat gland duct to reabsorb chloride during periods of high applied pressure, or as a result of changes in the osmotic gradients within the distorted tissues. Due to its variable nature, further analysis of this particular metabolite was not carried out.

7.5.3 Combination of Gas Tension and Sweat Biochemistry Measurements

By studying the relationship between gas tensions and sweat biochemistry, two independent measurements of soft tissue status are effectively combined to examine any possible correlation between them. This approach effectively eliminates the level of applied pressure, which may not accurately represent the degree of induced ischaemia, as individuals undoubtedly respond differently to the same applied pressure as reflected in the variability of the data (Appendix C and Figures 7-2 to 7-8).

Figures 7-13 and 7-14 highlight the relationship between transcutaneous oxygen tension and sweat biochemistry measurements at the loaded sacrum. Above a threshold of 60%, there is a significant positive correlation between percentage reduction in pO_2 and sweat lactate and urea ratio concentrations, indicating that at low oxygen tensions there is a corresponding increase in lactate and urea concentrations. The ischaemia, reflected by the reduced pO_2 may lead to anaerobic metabolism of the sweat gland, which results in an increased production in lactate [45]. Indeed, the nature of the sweat lactate and pO_2 relationship, with a clear threshold level, is consistent with a change in metabolism of the sweat gland when O_2 supply becomes critical. At this stage, lactate production would rise rapidly because anaerobic metabolism produces much less energy per unit of substrate, so takes place at a high rate in an attempt to fill the energy gap. The altered metabolism of the sweat gland may also reflect other changes in biochemical processes in the underlying tissues.

There is also evidence of a correlation between pCO_2 levels and sweat lactate and urea concentrations (Figures 7-15 to 7-18), indicated by a statistically significant correlation between sweat lactate and urea concentrations and area beneath the pCO2-time curve. Elevated levels of pCO_2 indicate that the mechanism of wash-in and wash-

out of CO_2 is not functioning, leading to an accumulation of CO_2 and possibly other waste products. This accumulation of waste products which are not removed by circulating blood may be demonstrated by the increased levels of urea and lactate in the sweat.

7.6 SUMMARY

The results of the present experiment indicate that the two non-invasive tissue status monitoring techniques have been successfully combined to simultaneously measure different aspects of tissue status at a site often prone to soft tissue breakdown. Furthermore there is strong evidence to suggest that the techniques are complementary and provide additional valuable information on the biochemical processes occurring during prolonged loading in healthy subjects.

The major findings of this chapter include:

- A relationship between pO_2 and pCO_2 levels in loaded tissue based on a threshold level of 60% reduction in pO_2.
- Above the 60% threshold, a linear correlation between pO_2 reduction and sweat lactate and urea ratios.
- A linear correlation between area beneath the pCO_2 time curve and sweat lactate and urea concentrations.

8. CLINICAL STUDY

8.1 INTRODUCTION

Having established the potential of the two complementary non-invasive techniques to assess tissue status in healthy subjects, it was considered appropriate to assess their applicability to relevant patient groups.

The first patient group consisted of subjects who had been hospitalised following injury to their spinal cord and were undergoing a period of rehabilitation. The second group consisted of patients who had undergone unilateral lower limb amputation and were fitted with an artificial prosthesis. The amputation population may be classified in a variety of ways depending on level of activity, age and underlying pathology. In the present study two such groups were investigated, designated the general and the athletic amputee population.

In order to assess the feasibility of this method of soft tissue assessment in a clinical setting specific protocols were drawn up for each group. Results are analysed and a critical appraisal of the relevance of the techniques in a clinical setting are presented in the discussion section.

8.2 SPINAL CORD INJURED POPULATION

8.2.1 CLINICAL BACKGROUND

The spinal cord injured (SCI) population are particularly susceptible to tissue breakdown due to a number of intrinsic and extrinsic factors as described in Chapter 2. Lack of mobility, long periods of time spent in prone or seated positions, changes in circulation and tissue properties all lead to an increased incidence of tissue breakdown in this subject group [88].

During the initial period after spinal cord injury, patients enter a phase known as spinal shock. This stage is characterised by an altered pattern of reflex activities; one consequence of this alteration is a reduction of vasomotor tone which can reduce blood flow to skin and subcutaneous tissues [85]. The reduction in blood pressure

associated with the decrease in vasomotor tone combined with decreased tissue resistance and paralysis, may play a part in the increased susceptibility to tissue breakdown during this phase [85].

Sudomotor or sweating responses in the spinal cord injured can be altered during the initial period of injury, as described in Section 1.3.9. Alterations can include excessive reflex sweating, or cessation of thermoregulatory responses.

The aim of this investigation was to determine the validity of the tissue status measurement techniques in spinal cord injured patients.

8.2.2 Prevalence and Incidence of Spinal Cord Injury

There is an incidence of spinal cord injury of 15-20 cases per million of the population, and a prevalence of 300-600 cases per million of the population in the United Kingdom [85]. In recent years, the increased life expectancy of spinal cord injured subjects due to improved treatment and understanding of the associated problems, has lead to an increased prevalence. One important outcome of this extended life expectancy is the increase in the number of elderly spinal cord injured subjects who have problems associated with both ageing and the injury itself.

8.2.3 Support Surfaces

One of the major methods of preventing tissue breakdown is the use of pressure relieving support surfaces. A number of pressure relieving mattresses were described in Section 2.9, for the wheelchair bound patient and a number of support cushions are also available. These include air filled, water filled, gel and foam cushions. Each support cushion has its own advantages and disadvantages. For example, foam cushions tend to deteriorate and should be changed frequently, whilst air filled cushions are only effective if inflated to the correct level for the individual patient. In addition, the nature of the support cushions will inevitably influence temperature and humidity at the interface. Gel cushions tend to maintain local skin temperature, foam cushions tend to increase it, while water filled cushions tend to decrease skin temperature. Moreover, water filled cushions induce the highest humidity levels at the skin interface compared to gel and foam cushions [26].

8.3 Soft Tissue Status Measurements in the Spinal Cord Injured Population

8.3.1 Subject Selection & Data

All the subjects selected for this study were in attendance at a seating clinic at the National Spinal Injuries Centre, Stoke Mandeville Hospital, Aylesbury, UK. Nine male patients in the sub-acute phase following spinal cord injury were selected, on the basis that they had been observed by the therapists to sweat on occasions. The subjects had all previously attended the clinic and received an initial assessment for a support cushion. Table 8-1 outlines the relevant subject data.

Table 8-1 Summary characteristics of spinal cord injured subjects included in experimental study.

Subject	Age	Level of Injury	Time since injury	Blood Pressure mmHg	Frankel Grade	Support cushion	History of Sores
1	40	C7	14 wk.	128/90	B	Jay Active	no sores
2	30	T11	49 wk.	130/80	A	Foam + Jay Active	no sores
3	73	T10	21 wk.	150/100	C	4 inch Foam	no sores
4	36	C6	21 wk.	-	A	Jay Medical	sacral, occipital, heel sores on admission
5	21	C4	35 wk.	-	A	Jay Medical	sacral, occipital sores on admission
6	25	T12	17 wk.	-	A	Jay Active	no sores
7	46	C4/5	52 wk.	-	A	Jay Medical 100	sacral sore on admission
8	41	C5	29 wk	-	C	Jay 2	no sores
9	37	T6/7	60 wk	120/90	A	Jay 2	ischial sore present on admission

The definitions of Frankel Grade are given as

- *A* - No motor or sensory function
- *B* - No motor but some sensory preservation
- *C* - Useless motor function preserved
- *D* - Useful motor function preserved
- *E* - Normal functions with or without minor neurological deficit.

8.3.2 EXPERIMENTAL PROTOCOL

The protocol for this investigation was approved by the relevant hospital ethical committee. The investigation included three independent measures of tissue status involving interface pressures, transcutaneous gas tensions and sweat biochemistry measurements. The former two techniques were introduced in research studies to assess the viability of tissues of both acute [24] and sub-acute [25] SCI subjects. These are now routinely employed by therapists in standard clinical prodeures involving all patients attending the seating clinic at the centre. The present experiemntal protocol was based on patient attendance at the clinic and was designed to provide minimal disruption to the normal routine. All investigations were carried out at room temperature within the hospital wards and the seating clinic. Informed consent was obtained from each patient prior to investigation, a consent form is shown in Appendix D.

The sweat was collected over three distinct collection periods, control, loaded and reperfusion for a period of 60 minutes. The sweat was collected from clinically relevant sites namely, the sacrum and the ischium. For the initial control collection period the subjects were visited on the ward, by the investigator, and a 40 mm circular sweat pad was applied to the ischium and/or sacrum and covered with the impermeable membrane, following the standard operating procedure described in Section 4.3.5. The subject adopted a side lying or prone position in order to avoid pressure on the sweat pad. After a period of 60 minutes the control pad was removed and the subject transferred to his wheelchair and proceeded to the seating clinic.

At the seating clinic, the subject transferred to an examination table where a combined transcutaneous gas tension electrode was attached to the ischium with the leg held at 90° flexion. This technique has been shown to give optimal positioning of the electrode over the bony prominence when the subject returns to a seated position [24]. A 48 cell pressure matrix of the Talley Pressure Monitor was placed over the support cushion of each subject in order to monitor the interface pressures under the seated buttocks. The subject was then carefully positioned back on the cushion in the wheelchair and the normal seating position was adopted. The interface pressures were

measured over 10 scans and the average for each cell recorded. The subject was asked to perform pressure relief exercises, as prescribed by the therapist, and the effect on pO_2 and pCO_2 was recorded. After the assessment the combined electrode was removed and a second sweat collection pad was applied to the ischium and/or sacrum. The subject then returned to the chair and remained seated for a further 60 minutes.

At the end of this loaded collection period the sweat pad was removed and a third, reperfusion pad was applied to the ischium and/or sacrum. The subject then returned to bed adopting a side lying or prone position to ensure the sweat pad was unloaded. This pad was left in position for a further 60 minutes. Sweat pads were re-weighed and stored frozen until subsequent biochemical analysis as described in Section 4.3.4.

8.3.3 Results

Gas Tension Measurements

The transcutaneous gas tensions measured at the ischium were analysed and a summary of the results are shown in Table 8-2. For each subject, unloaded equilibrium pO_2 and pCO_2 values are shown along with the median pO_2 tension recorded during the seated period. The carbon dioxide mode during seating was recorded corresponding to the definitions detailed in Section 5.4.

Table 8-2 Transcutaneous gas tensions measured at the ischium of spinal cord injured subjects.

Subject	Unloaded O_2 mmHg	Unloaded CO_2 mmHg	Loaded O_2 mmHg	Loaded CO_2 Mode
1	88	39	< 5	3
2	80	32	< 5	1
3	78	25	< 5	1
4	79	33	12	1
5	50	39	< 5	3
6	84	35	6	1
7	75	45	19	3
8	65	50	< 5	3
9	32	45	< 5	3

A number of subjects demonstrated very low pO_2 readings at the ischium during seating. However, these values were observed to return to normal unloaded levels during the period of pressure relief carried out by the subject, which lasted on average 90 seconds. Interestingly, the spinal cord injured population demonstrated either a Mode 1 or Mode 3 carbon dioxide response to applied loading at the ischium. In addition, subjects who showed an initial unloaded pCO_2 value that was in excess of 39 mmHg demonstrated a Mode 3 response, whereas those with an unloaded pCO_2 value less than 39 mmHg demonstrated a Mode 1 response. None of the subjects exhibited a depressed pCO_2 value during loading, as was reported in a previous study involving spinal cord injured subjects [25].

Sweat Collection

Subjects 1, 2 and 3 had sweat collection pads placed at the ischium during the three collection periods, whereas subjects 4 to 9 had sweat pads attached to both the sacrum and the ischium. However, none of the nine subjects provided a sweat sample in excess of 50 mg for any of the three collection periods. Indeed, no sweat was detectable on the sweat pads, for the majority of the subjects. As a result no biochemical analysis of the sweat samples was possible.

Pressure Measurement

The interface pressure measurements between the buttocks of the seated subject and their normal support surface were monitored, as part of the assessment carried out at the seating clinic. A typical contour map of the mean interface pressure measured at each of the 48 cells is shown in Figure 8-1. Clearly there are areas of high pressures, exceeding 100 mmHg, which appear to correspond to the locations of the ischial tuberosities.

The frequency distribution of the mean interface pressures of each cell measured for each individual subject are shown in Figure 8-2. It should be noted that the rigidity of the electrode resulted in interface pressure recordings in excess of 246 mmHg beneath the electrode. Since these pressures are not representative of the actual situation, the

pressures indicated by the cell beneath the electrode has been eliminated. These represent the range of pressures experienced over the whole buttock region. The ideal support cushion would provide a surface over which load is uniformly distributed in order to prevent areas of high pressure, especially over bony prominences. In addition, high pressure gradients caused by uneven pressure distributions are likely to cause tissue distortion which can be more damaging than pressure alone [174].

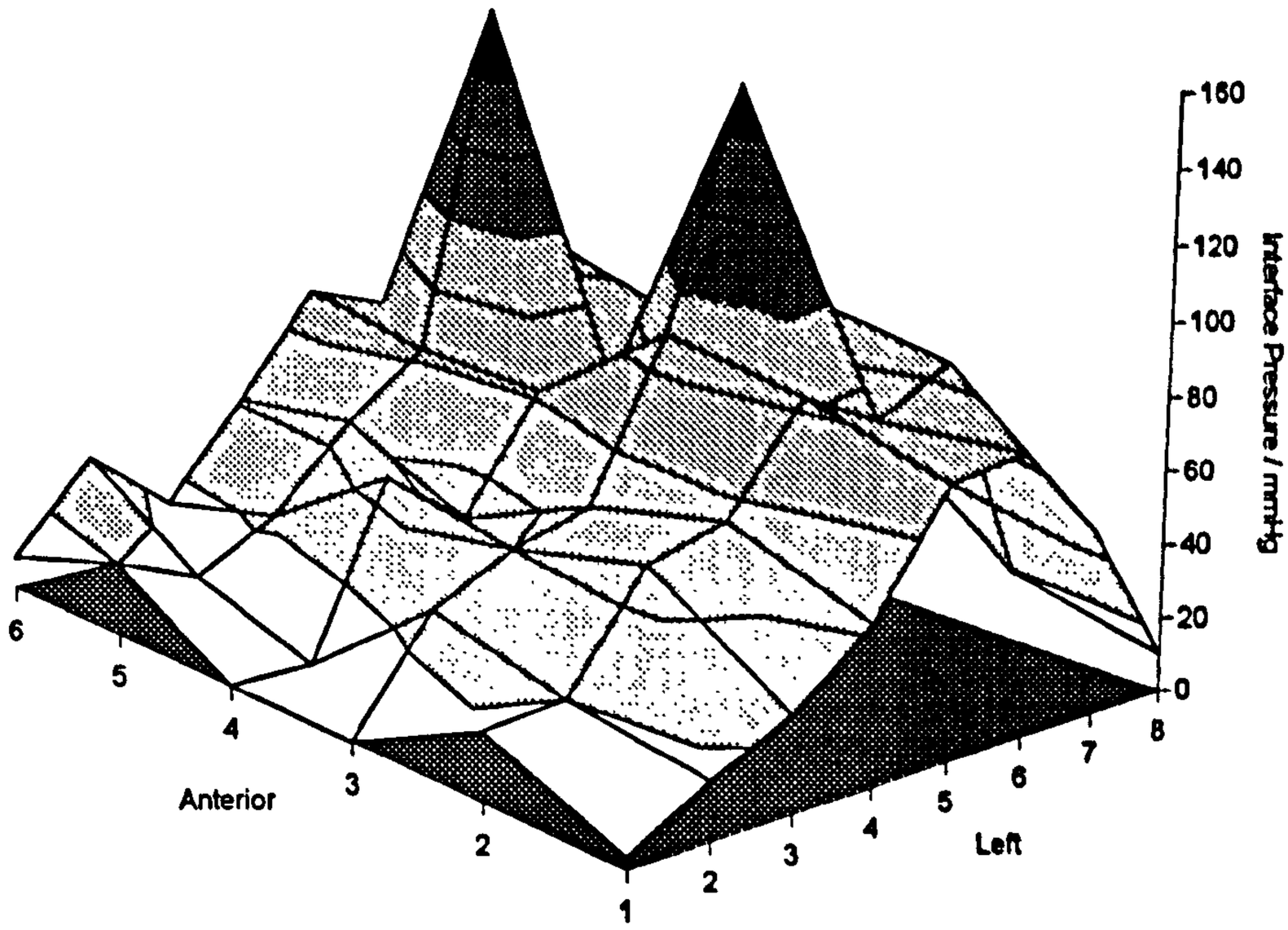

Figure 8-1 Typical contour map showing interface pressures measured under the buttocks of a seated spinal cord injured subject (Subject No 7 supported on a Jay Medical cushion).

Subjects 5 and 8 show a fairly uniform pressure distribution, with a modal values of 40 and 50 mmHg respectively and in addition, no pressures were recorded in excess of 90 mmHg. By contrast, subjects 1, 6 and 9 show a bimodal distribution, and Subject 4 shows a skewed distribution. It has been suggested that the use of pressure distributions can give additional information to seating specialists [11].

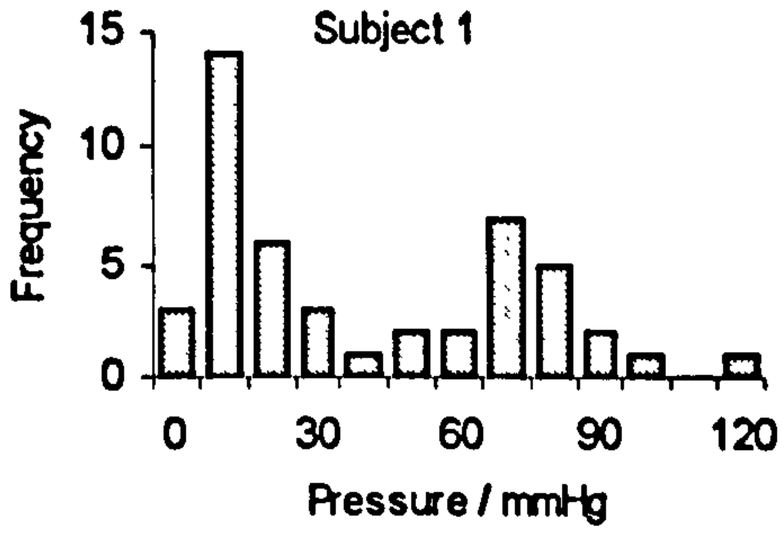

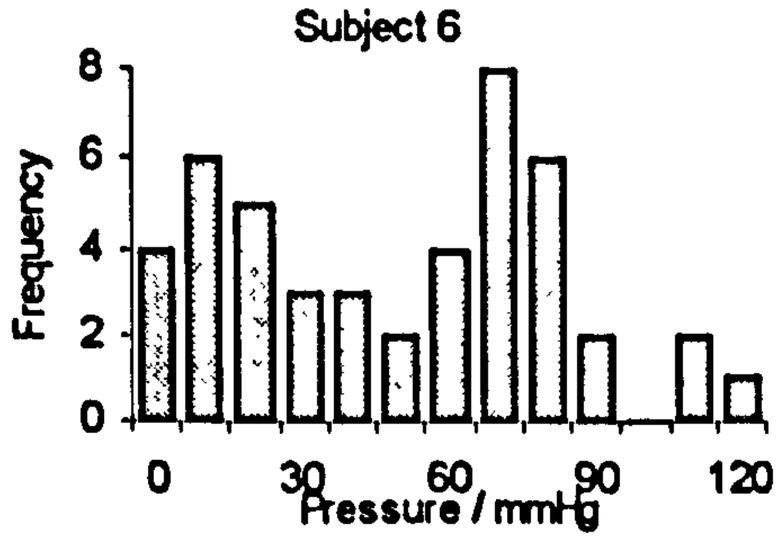

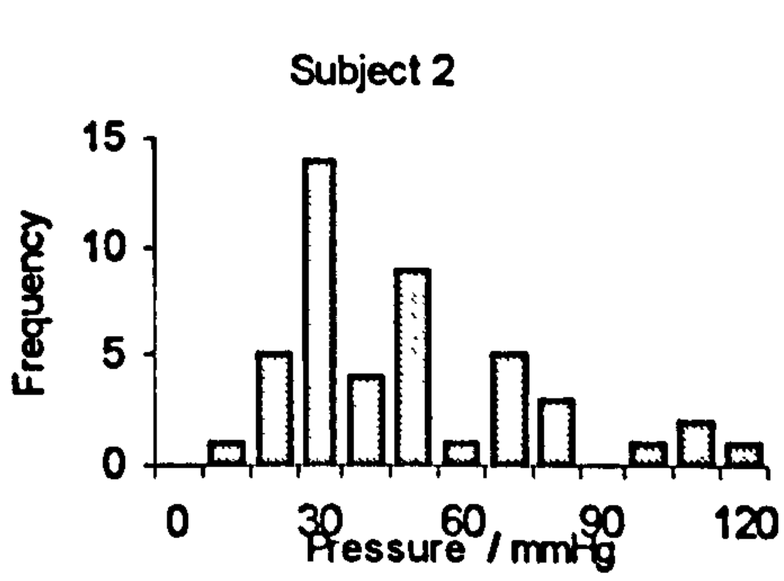

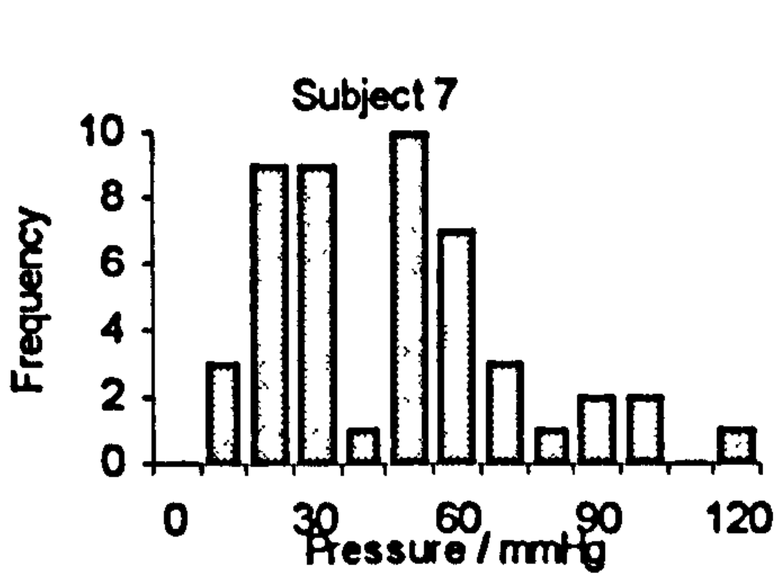

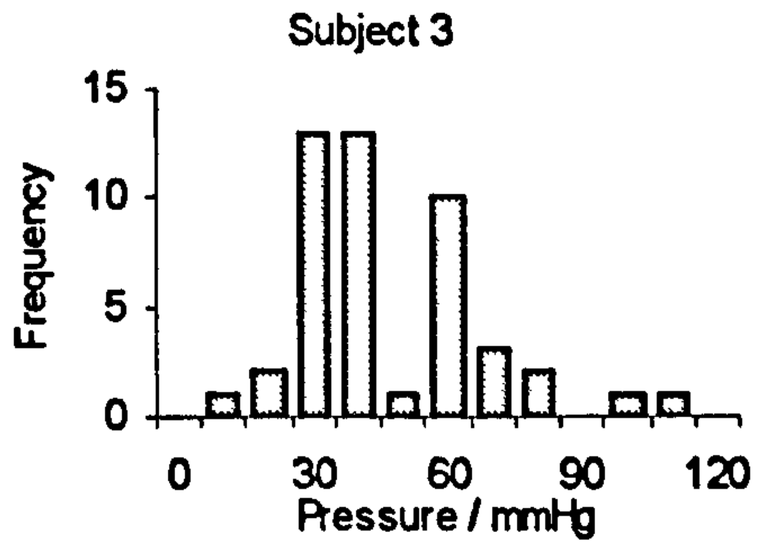

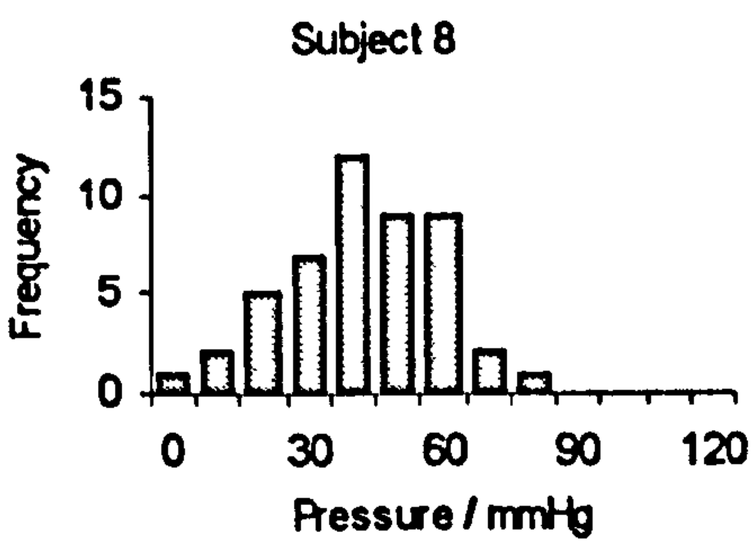

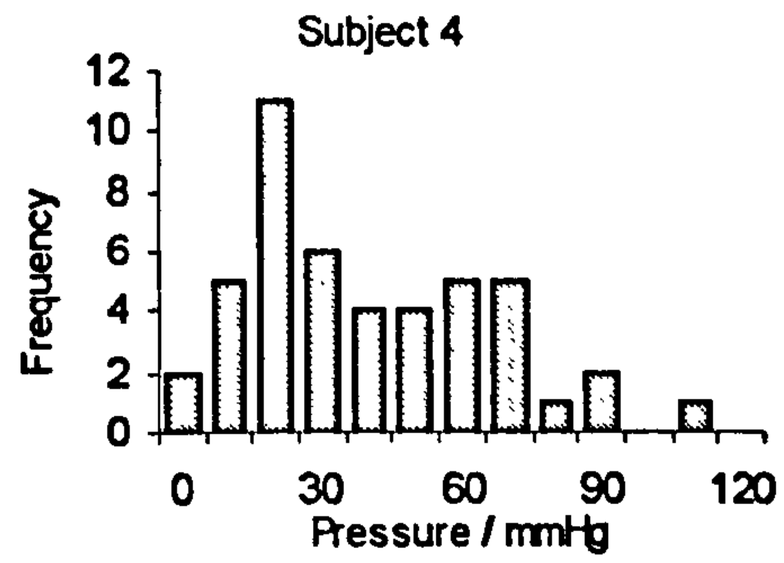

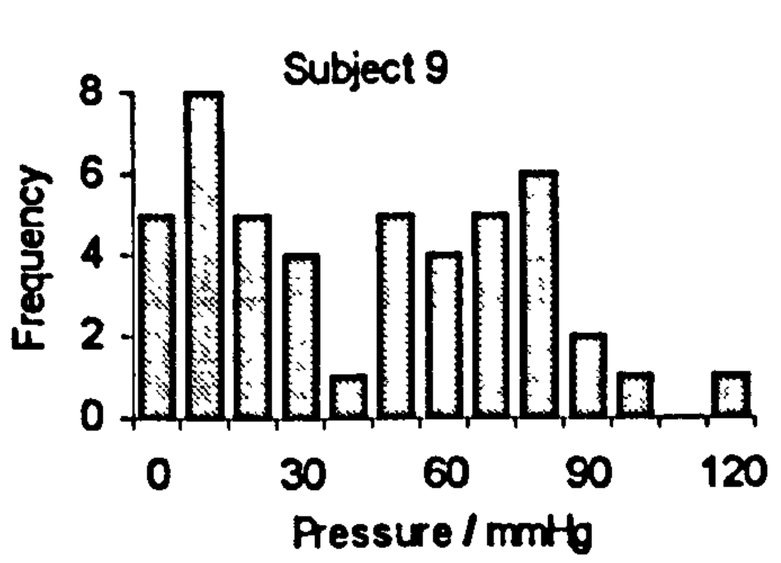

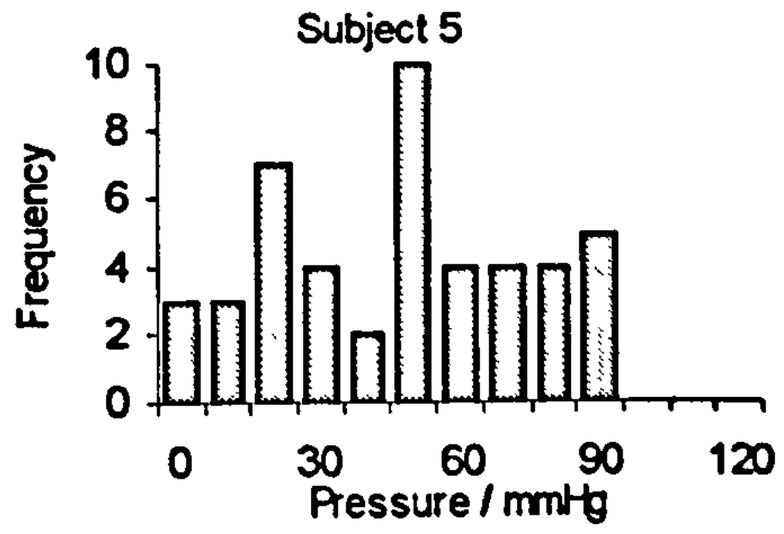

Figure 8-2 Frequency distributions of interface pressure under the buttocks of seated spinal cord injured subjects.

8.4 DISCUSSION

Transcutaneous gas tensions have been successfully used as a measure of tissue status in the spinal cord injured population within seating clinics [25]. In addition, transcutaneous oxygen measurements have been used to indicate a delayed reactive hyperaemic response in spinal cord injured subjects [107]. The results obtained from the present study are discussed further in Section 9.3.1

It is clearly evident that there was very little sweat yielded from the subjects during any of the three 60 minute collection periods. This obviously has serious implications for the use of sweat biochemistry measurements as an indicator of soft tissue status in this subject group. There are a number of possibilities to explain the low sweat yields:

- The relatively low environmental temperatures within the hospital environment (22°C), may have inhibited sweat response. However, subjects were requested to wear as much clothing as was comfortable in order to promote sweating.
- The altered sudomotor response as a result of the spinal cord injury itself [85], especially below the level of the lesion where the sweat was collected.

Although the current method of sweat collection and analysis was not appropriate in this subject group, certain modifications could be made to the procedure, which might yield an improved sweat output. These include a more sensitive analysis technique or the use of iontophoresis sweat stimulation techniques. It may also be useful to repeat the current procedure on a similar group of immobile or wheelchair bound subjects who do not have altered thermoregulatory response, for example, subjects with multiple sclerosis.

8.5 LOWER LIMB AMPUTEE POPULATION

8.5.1 CLINICAL BACKGROUND

Many amputee subjects suffer from problems associated with adverse physical and chemical conditions at the interface between stump tissues and the socket of a lower limb prosthesis [123]. In extreme cases tissue breakdown can occur, which causes

distress and limits the function of the prosthesis, namely normal weight bearing activities. The enclosed environment of the socket is likely to become saturated in the form of sweat and excessive moisture can lead to maceration of stump tissues. Indeed, in one survey, 70% of respondents reported excessive sweating associated with skin problems [96].

The aim of this study was to determine the validity of measuring tissue status at various sites located within the prosthetic socket.

8.5.2 Incidence of Amputation

The incidence of amputation in the United Kingdom has been reported at being 46 per 100,000 of the population, however, the incidence and reason for amputation is greatly dependent upon both age and sex [123,166]. Within the elderly population 90% of amputations are the result of arterial occlusive disease, including diabetes, and there is parity between the number of males and females undergoing amputation. However, within the younger age group the most common reason for amputation is trauma, with 40% of cases involving road traffic accidents (RTA). Interestingly, 80% of these cases are the result of accidents occurring on 2 wheeled vehicles, and this trend is reflected in the 2.5:1 ratio between males and females requiring amputation in the younger age group. In third world countries there is a much higher incidence of amputation as a result of trauma, rather than disease [145]; and with 2,000 injuries per month as a result of land mines this disparity is likely to increase.

8.5.3 Designs of Common Lower Limb Prostheses

There are a number of different types of prosthesis used as a replacement for an amputated limb; their common purpose is to restore the function of the residual limb. In order to regain function, the weight of the body is distributed over an area of tissue, which might not be optimally designed for this purpose. Prostheses are generally classified according to level of amputation, namely above knee (AK) or trans-femoral, and below knee (BK) or trans-tibial, each of which has specific functional properties and design features.

The below knee (BK) prosthetic socket contains and supports the residual limb during weight bearing and is designed to transmit forces from the limb to control placement of the foot. Early BK sockets consisted of a thigh corset, which distributed forces to the thigh and were generally open ended which often resulted in oedema in the tissues at the distal end [166]. The patella tendon bearing socket (PTB) designed in the 1950's, ensures that the greatest proportion of load bearing is taken on the patella tendon. The basis of this design is that the tendon is more capable of carrying high loads without damage, due to its relative avascularity and ability to withstand high tensile forces; it should be noted that in this situation the patella tendon will actually be exposed to compressive forces. Liners are most commonly used with new stumps and where the residual limbs may have thin skin coverage, particularly over bony prominences. Sockets can be worn without a liner for mature stumps which have good tissue coverage, the main advantage being that this is more hygienic and less bulky. The main anatomical markers of the below knee residual stump and socket are shown in Figure 8-3.

The principles of an above knee (AK) prosthetic socket involve contouring to ensure that stabilising pressures are applied to skeletal structures rather than functional muscle tissues. The socket should also allow for changes in the dimensions of the stump when muscles are either activated or at rest. The ischial seat provides the major weight bearing area, through the ischium and the gluteus maximus, medially and laterally respectively. The lateral wall of the socket provides a surface against which the femur can react to maintain medio-lateral pelvic stability and the medial wall provides uniform pressure to the adductor muscles. The main anatomical sites of the above knee residual stump and socket are shown in Figure 8-4.

The ICEROSS (Icelandic Roll On Roll Off Socket System) prosthesis consists of a silicon rubber sleeve which provides suspension and an outer plastic shell, which establishes the supporting interface between the prosthesis and sleeve. This socket system is attached to the shank of both above knee and below knee prostheses. The silicon sleeve is soft and pliable and when rolled over the stump provides total contact. The design of the total contact socket has several advantages [166] including

- an aid for venous return to prevent oedema
- an increased surface area for weight bearing
- an aid for sensory feedback.

In addition, the longitudinal displacement of the tissue is thought to provide additional stabilisation and reduce the pistoning effect. The adhesion between the sleeve and the skin effectively limits sliding motion to between the sleeve and the socket, thus reducing frictional forces on the skin.

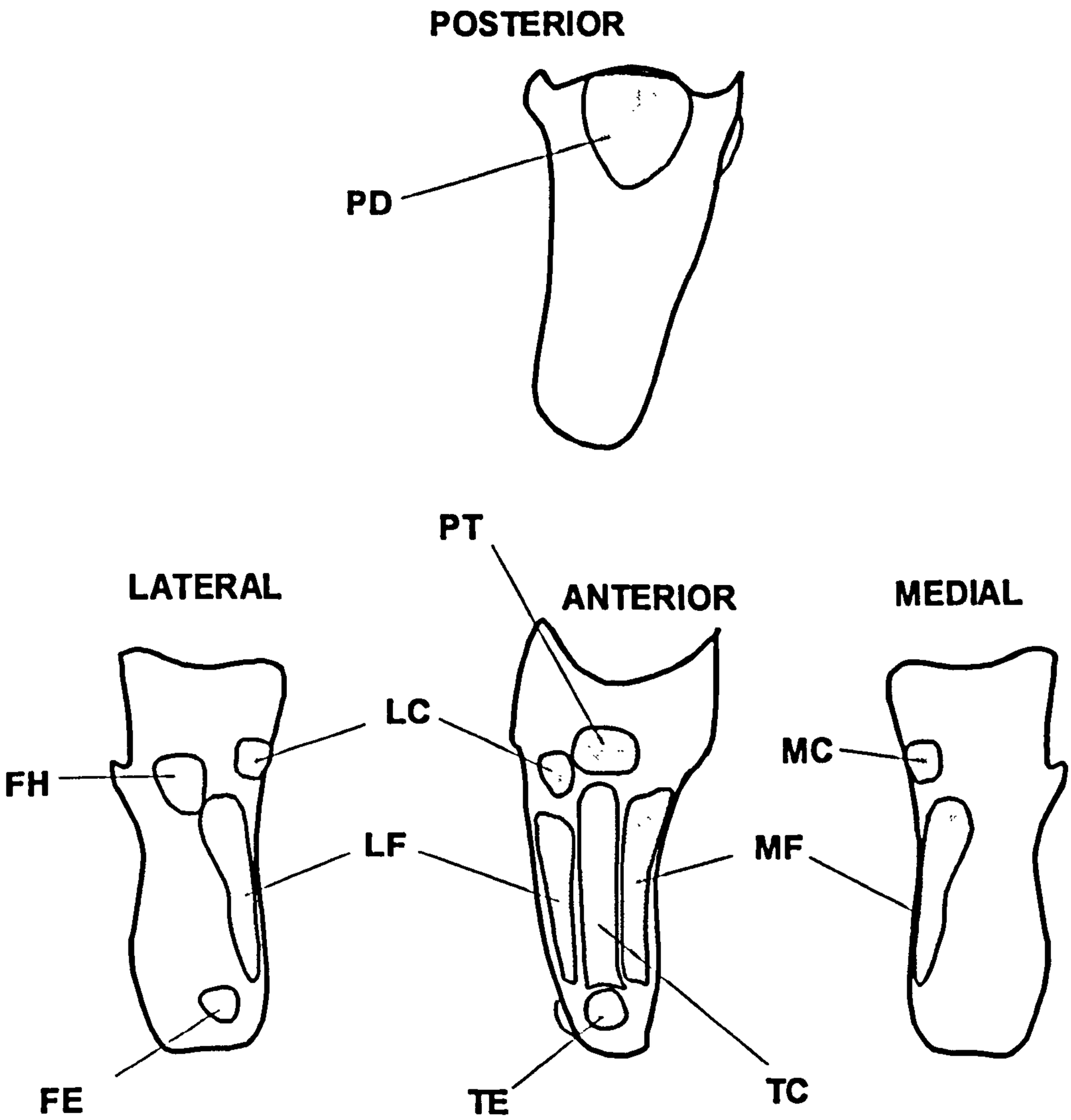

Figure 8-3 Anatomical landmarks of the below knee (BK) socket.

PD - popliteal depression, PT - patella tendon, FH - fibular head, LC - lateral condyle, MC - medial condyle, LF - lateral tibial flare, MF - medial tibial flare. FE - fibular end, TE - tibia end, TC - tibial crest.

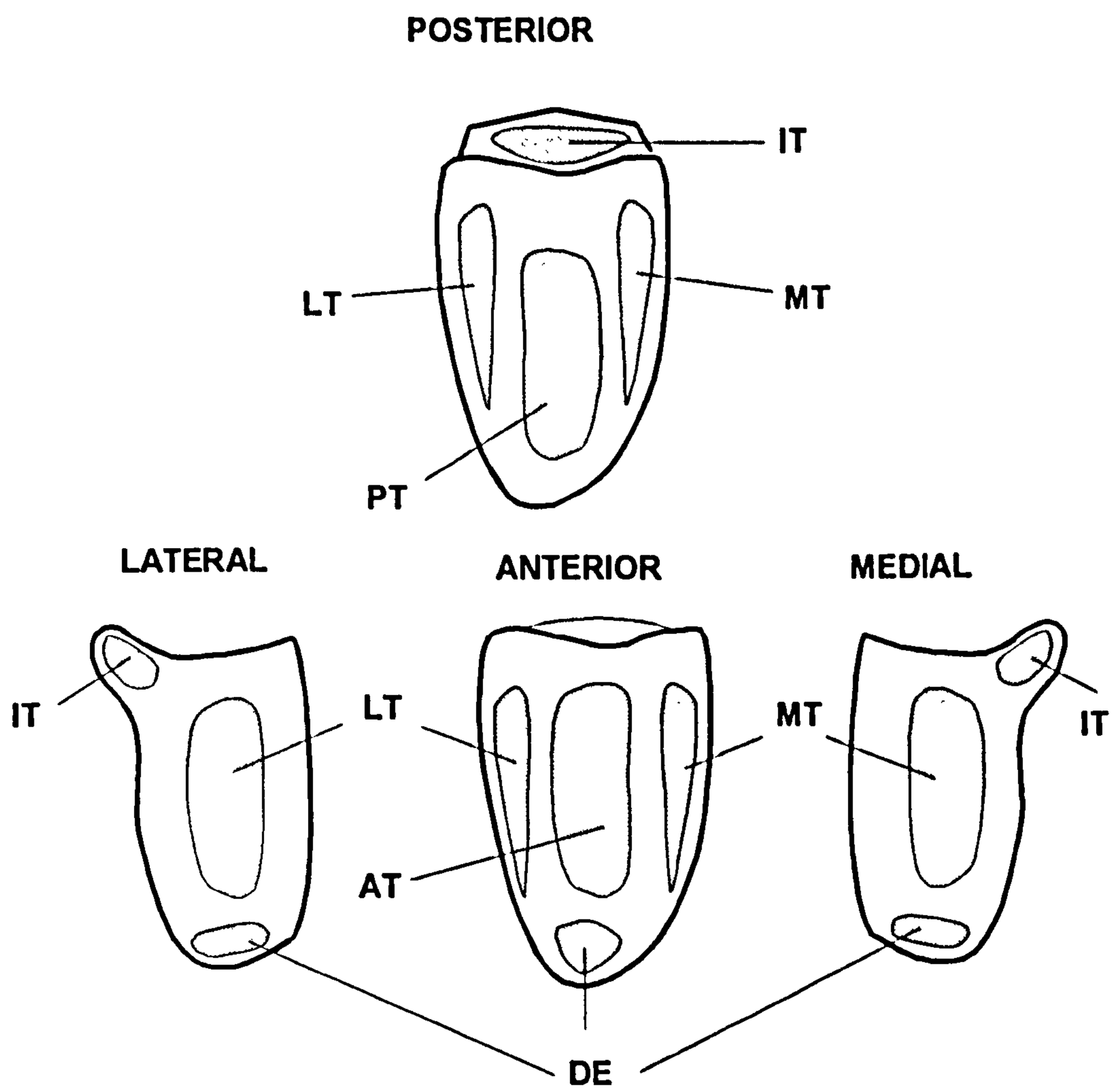

Figure 8-4 Anatomical landmarks of the above knee (AK) socket.

IT - ischial tuberosity, LT - lateral thigh, MT - medial thigh, AT - anterior thigh, PT - posterior thigh, DE - distal end

8.5.4 Sports and Amputation

The amputee who partakes in sporting activity experiences a wide range of additional problems to those of the general prosthesis wearer. The nature of high

activity can lead to higher and more repetitive stresses being transferred by the prosthesis to the residual stump tissues. Specially designed prostheses are available for sporting activities, but the design improvements have concentrated on the shank of the prosthesis to improve weight and movement characteristics rather than on the socket, where many tissue problems can occur. A study by Kegel [109] involving physically active lower limb amputees highlighted the problems associated with the residual limb during exercise, the results of her questionnaire are summarised in Table 8-3.

Table 8-3 Problems associated with the residual limb during exercise. Adapted from [109].

Problem	Occurrence
Soaked in sweat	46%
Pain	26%
Sores	26%
Fatigue	20%
Swelling	17%
Cramp	8%
Miscellaneous	7%

8.6 Sweat Analysis in the Socket of the General Amputee Population

8.6.1 Subject Selection & Data

All subjects selected for this experiment were patients at the King's Healthcare Rehabilitation Centre who had been fitted with a lower limb prosthesis following an assessment by a prosthetist. The subjects had all responded to a questionnaire compiled by an MSc student, Liz Moore and had reported excessive sweating or skin problems in the residual stump tissues. The main exclusion criteria for the study was amputation as a result of arterial occlusive disease, including diabetic neuropathy, smokers and female patients who might be pregnant.

In total 12 subjects, 4 female and 8 male, with a mean age of 47 years (range 21-75 years) were included in the study. Individual subject data is detailed in Table 8-4. Each

subject was informed of the details of the study and asked to sign a consent form which is located in Appendix D.

Table 8-4 Summary of general amputee subjects involved in sweat analysis study.

No.	Age	Sex	Level	Reason for amputation	Date of amputation	Weight/ kg	Type of Socket
1	34	F	BK	Trauma	28/6/92	104.8	Leather in plastic shell
2	21	M	AK	Trauma	20/3/95	55.0	ICEROSS
3	53	F	BK	Congenital	27/10/59	47.6	Leather socket, thigh corset
4	75	M	BK	Trauma	-	-	Leather socket, thigh corset
5	60	M	BK	Trauma	8/3/91	103.9	Plastic with liner
6	73	M	AK	Trauma	27/8/93	66.7	Quadrilateral/ waist belt
7	27	F	BK	Congenital	31/12/69	88.9	Plastic with liner / ICEROSS
8	54	M	BK	Trauma	19/6/89	69.8	Plastic with liner
9	54	M	AK	Trauma	30/12/48	69.8	Plastic suction
10	34	M	BK	Trauma	4/6/81	94.3	Plastic with liner
11	25	M	BK	Trauma	25/10/94	69.8	ICEROSS
12	55	F	BK	Trauma	-	63.5	Leather socket in plastic shell

8.6.2 Experimental Protocol

The protocol for this investigation was approved by the relevant hospital ethical committee. Prior to each investigation the socket was removed from the amputee (doffed) and a visual assessment of the stump was made in order to identify bony prominences and areas of high weight bearing. The subject was also asked to point out any specific areas of previous tissue breakdown.

An assessment of the interface pressures at specific stump sites were made using the Oxford Pressure Monitor (Mk II, Talley Group Ltd, Romsey, UK). A single pressure cell was attached to each site of interest on the stump using Micropore ® (3M Healthcare, UK) to prevent movement. The prosthesis was then replaced (donned) by the subject, who was requested to stand adopting a normal base of gait, weight bearing

evenly through both feet. The interface pressures were recorded and the average of 10 scans calculated for each site.

The subject returned to the seat and doffed the prosthesis in order to remove the pressure cells. 40 mm diameter sweat collection pads were placed on the stump at identical sites corresponding to the pressure measurements, in addition control pads were placed on the medial or lateral thigh. Each sweat pad was covered with flexible impermeable membrane to prevent evaporation and sealed with Blenderm ® surgical tape. In Subject 1, in addition to the standard sweat pad, a commercial wound dressing (Release ® , Johnson & Johnson, UK) which claimed enhanced moisture absorption properties and a one way liner, was employed for a second session of sweat collection.

The subject then donned the prosthesis and walked on a computerised treadmill at a brisk pace for as long as possible without causing discomfort. The treadmill speed was recorded throughout the experiment. The subject was requested to continue walking for a period of 20 minutes, sufficient to produce sweating within the stump, although no undue pressure was placed on the subject to attain or exceed this time.

After the period of treadmill walking the subject returned to the seat and doffed the prosthesis. The sweat pads were removed using tweezers taking care to mop up all sweat beneath the impermeable cover. The sweat pads were placed in the plastic containers weighed and frozen for subsequent biochemical analysis, using the assays described in Section 4.3.4 for lactate, urea and chloride.

Subjects 4, 6 and 7 had recently been prescribed an ICEROSS socket in addition to their conventional socket. These subjects were requested to repeat the protocol wearing the ICEROSS socket, to enable comparison between the two socket types.

In addition, subjects 5, 6, 7 and 9 presented for re-investigation on a second occasion, the walking protocol was replicated and sweat pads applied to identical sites.

8.6.3 RESULTS

The complete results including interface pressure measurements, walking protocol, amount of sweat collected and, where appropriate, metabolite concentrations are detailed for each subject in Table 8-5.

Table 8-5 Summary of assessment of stump socket interface of general amputees walking on a treadmill.
* indicates which samples were analysed for sweat metabolites

SUBJECT 1, *WALKING SPEED 0.7 KM/H, DURATION 15 MIN. SOCKETS [1], SESSIONS [1]*

Notes	Site	Pressure mmHg	Sweat Amount mg	Lactate mmol/L	Urea mmol/L	Chloride mmol/L
Convent.	patella tendon	174 ± 10	43.0	-	-	-
BK	distal end	> 350	61.2*	52.71	27.6	60.9
	medial condyle	0	10.3	-	-	-
Relcase ®	patella tendon		11.7	-	-	-
pad	distal end		19.7	-	-	-

SUBJECT 2, *WALKING SPEED 1.2 KM/H, DURATION 20 MIN. SOCKETS [1] , SESSIONS [1]*

ICEROSS	distal end	213.9 ± 55	12.5	-	-	-
AK	IT	111 ± 6.7		-	-	-
	groin	60.4 ± 23	33.3	-	-	-
	lateral mid thigh	53 ± 4.1	10.9	-	-	-

SUBJECT 3 *WALKING SPEED 1.1 KM/H, DURATION 20 MIN. SOCKETS [1], SESSIONS [1]*

Convent.	patella tendon	7.8 ± 2	33.5	-	-	-
BK	distal end	22.3 ± 2		-	-	-
	groin	39.4 ± 2	13.3	-	-	-
	20 mm medial to fib head	19.5 ± 3.9	36.0	-	-	-

SUBJECT 4 *WALKING SPEED 0.4 KM/H, DURATION 6 MIN. SOCKETS [2] SESSIONS [1]*

ICEROSS	patella tendon	27 ± 3.6	14.4	-	-	-
BK	distal end	177.6 ± 6	28.8	-	-	-
	mid thigh	20 ± 0.4	21.5	-	-	-
Leather Socket	patella tendon	16 ± 0.7	24.0	-	-	-
BK	distal end	15 ± 0.2	32.9	-	-	-
	mid thigh	78 ± 2.1	22.2	-	-	-

SUBJECT 5 *WALKING SPEED 0.5 KM/H, DURATION 20 MINS. SOCKETS [1] SESSIONS [2]*

Session 1	patella tendon	17 ± 1	161.1*	39.03	18.72	35.91
Convent.	distal end	196.5 ± 1	56.8*	18.12	32.85	144.72
BK	cut end tibia	137 ± 0.8	39.9	-	-	-
	medial thigh	0	16.0	-	-	-
Session. 2	patella tendon	100 ± 13	27.6	-	-	-
Convent.	distal end	215 ± 5		-	-	-
BK	cut end tibia	> 350	31.0	-	-	-

SUBJECT 6 *WALKING SPEED 1.1 KM/H, DURATION 12 MINS. SOCKETS [2] SESSIONS [2].*

Prosthesis	Site	Pressure mmHg	Sweat Amount mg	Lactate mmol/L	Urea mmol/L	Chloride mmol/L
Session 1	cut end femur	79 ± 5.6	38.9	-	-	-
ICEROSS	IT	58.8 ± 2	8.7	-	-	-
AK	groin	125 ± 5	6.5	-	-	-
Session 1	cut end femur	6.6 ± 0.7	23.5	-	-	-
Convent.	IT	> 350	8.4	-	-	-
AK	groin	329 ± 8.4	10.4	-	-	-
Session 2	cut end femur		323.9*	40.95	22.62	36.51
ICEROSS	IT		259.0*	46.8	24.27	39.99
AK	groin		39.1	-	-	-
Session 2	cut end femur		-	-	-	-
Convent.	IT		9.8	-	-	-
AK	groin		9.8	-	-	-

SUBJECT 7 *WALKING SPEED 1.4 KM/H, DURATION 15 MINS. SOCKETS [2] SESSIONS [2].*

Session 1	distal end	239 ± 4.5	20.8	-	-	-
ICEROSS	patella tendon	107 ± 12	177.2*	43.32	19.02	59.76
BK	medial thigh	135 ± 7.5	75.8*	28.62	13.73	29.59
Session 1	distal end	39 ± 0.8	84.3	35.07	16.26	59.13
Convent.	patella tendon	180 ± 12.2	21.4	-	-	-
BK	medial thigh	146 ± 0.8	15.6	-	-	-
Session 2 ICEROSS	patella tendon		265.1*	13.53	13.91	33.43
Session 2	distal end		72.4*	12.18	9.39	81.00
Convent.	patella tendon		164.6*	19.68	9.72	27.30
BK	medial thigh		102.3*	21.33	10.41	33.66

SUBJECT 8 *WALKING SPEED 1.0 KM/H DURATION 10 MINS. SOCKETS [1] SESSIONS [1]*

Convent.	patella tendon	102 ± 5	8.8	-	-	-
BK	cut end tibia	246 ± 17	9.7	-	-	-
	fib head	295 ± 11	8.1	-	-	-
	back of knee	76 ± 10	7.5	-	-	-

SUBJECT 9 *WALKING SPEED 1.2 KM/H, DURATION 20 MINS. SOCKETS [1] SESSIONS [2]*

Session. 1	cut end femur	20 ± 2	23.1	-	-	-
Convent.	anterior thigh	70 ± 4	10.2	-	-	-
AK	IT	80 ± 5	125.0*	25.77	19.41	54.45
Session 2	cut end femur	47 ± 4	10.5	-	-	-
Convent.	anterior thigh	112 ± 3	3.3	-	-	-
AK	IT	68 ± 2	113.3*	27.84	23.70	63.90

SUBJECT 10 *WALKING SPEED 1.4 KM/H, DURATION 25 MINS. SOCKETS [1] SESSIONS [1]*

Prosthesis	Site	Pressure mmHg	Sweat Amount mg	Lactate mmol/L	Urea mmol/L	Chloride mmol/L
Convent.	patella tendon	126.8 ± 12	15.7	-	-	-
BK	medial condyle	287 ± 17	139.2*	31.62	22.14	24.43-
	distal end	270 ± 28	150.5*	25.77	26.16	24.12
	mid thigh	0	34.6			

SUBJECT 11 *WALKING SPEED 1.2 KM/H DURATION 15 MINS. SOCKETS [1] SESSIONS [1]*

ICEROSS	patella tendon	310 ± 4		
BK	distal end	316 ± 3	28.6	
	cut end tibia	>350	12.8	
	fib head	300 ± 5		

SUBJECT 12 *WALKING SPEED 1.1 KM/H DURATION 12 MINS. SOCKETS [1] SESSIONS [1].*

Convent.	patella tendon	152 ± 6		
BK	cut end tibia	259 ± 8	11.0	
	distal end	169 ± 11	5.5	
	fib head	247 ± 14	5.5	

PRESSURE MEASUREMENT

It is evident from the interface pressure measurements made within the amputee sockets that large variations in pressure are recorded both within a single collection period and, where carried out, on subsequent occasions. These changes can be attributed to small postural changes during the collection period, and to inability to place the pressure cells in an identical site on during subsequent measurements. Some of the inherent difficulties in using the interface pressure monitor for measuring within sockets are described in the discussion section of this chapter (Section 8.8.1). For this experiment the interface pressure measurements were used to give an indication of relative pressures experienced within the socket; it is interesting to note that the patella tendon site, which is supposed to be a high pressure bearing area in below knee sockets did not always exhibit high pressures.

SWEAT COLLECTION AND ANALYSIS

It is clear from the amount of sweat collected that not all subjects provided sufficient sweat for analysis during the collection period. In fact, only subjects 1, 5, 6, 7, 9 and 10 produced sweat samples in excess of the minimum threshold level of 50 mg required for subsequent analysis. For these subjects, the sweat metabolite concentrations may be presented in relation to the tissue sites, as illustrated for lactate and urea in Figures 8-5 and 8-6. It is clear that there is a wide variability in metabolite concentrations, both within and between sites for the 6 subjects. In view of these individual variations, it is most appropriate to describe the results for each subject separately.

Subject 1 showed a lactate concentration of 52.71 mmol/L at the distal end of her residual stump which would be considered elevated from normal values. This coincides with a high pressure, mean value in excess of 350 mmHg which would suggest that the area could be ischaemic. Chloride concentration was also high, although urea concentration was not noticeably so.

Subject 5 provided sweat samples in excess of 50 mg at both the patella tendon and the distal end of the stump. Sweat lactate concentration was higher at the patella tendon compared to the distal end, whereas for urea and chloride concentrations the opposite was observed. The subject showed a low interface pressure and a high sweat rate at the patella tendon.

Subject 7 was investigated on two separate occasions and with 2 different sockets. It is interesting to note that on the first occasion the sweat lactate and urea concentration was higher with both sockets than on the second occasion, which highlights the need for reliable control sweat samples which were not always possible to collect. This subject consistently showed a high sweat rate at the patella tendon. However, sweat lactate concentrations were variable, though there was a trend to elevated levels at the patella tendon, which is typically a high load bearing area of the socket. Indeed average pressures of 107 mmHg and 180 mmHg were recorded at this tissue site.

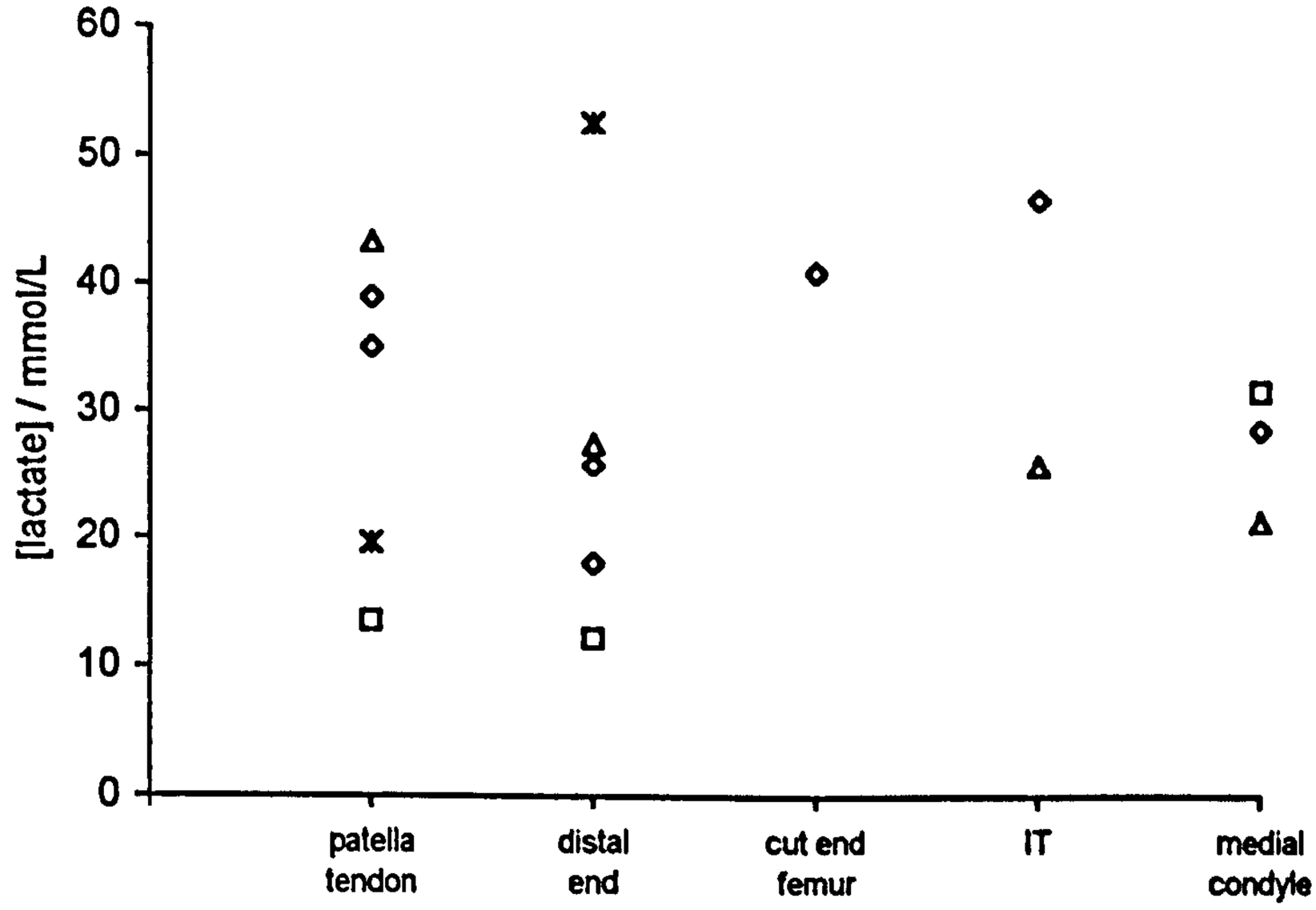

Figure 8-5 Lactate concentration of sweat collected from various sites within the lower limb amputee prosthetic socket. Symbols represent individual subjects.

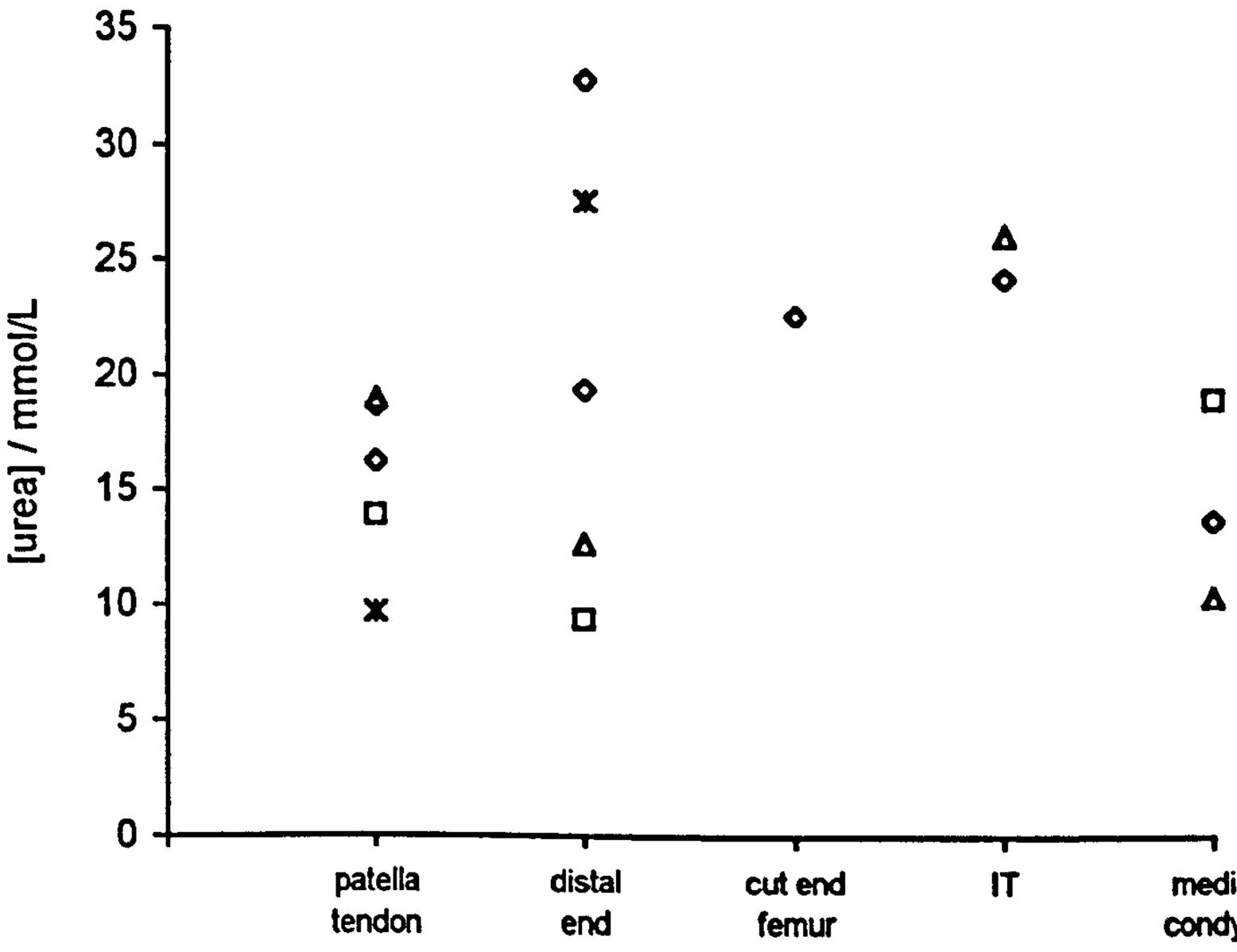

Figure 8-6 Urea concentration of sweat collected from various sites within the lower limb amputee prosthetic socket. Symbols represent individual subjects.

Subject 9 presented for investigation twice and gave consistent sweat metabolite concentrations at the ischial tuberosity. For example, the two sessions yielded a variability of 5.46%, 14.07% and 11.30% for sweat lactate, urea and chloride respectively. However, the other sites yielded too little sweat volume for subsequent metabolite analysis and therefore inter site comparison.

Subject 10 provided sufficient sweat at the distal end and the medial condyle, both areas of the socket which are loaded, producing average pressures in excess of 260 mmHg. In addition, the medial condyle had previously been a site of tissue breakdown, and exhibited the highest interface pressure. Lactate levels at the areas of highest pressure i.e. the medial condyle were greater than those at the patella tendon i.e. 31.62 mmol/L compared to 25.77 mmol/L. By contrast, the urea and chloride concentrations were greater at the patella tendon.

8.7 Sweat Analysis in the Socket of the Athlete Amputee Population

8.7.1 Subject Selection & Data

Subjects for this investigation were selected as a result of a survey carried out by Dr Mark Brooke, Department of Sports Medicine, Royal London Hospital, Whitechapel, investigating the effect of exercise on stump volume. Subjects were either participants in the Paralympics or armed forces personnel undergoing rehabilitation at Headley Hall, Leatherhead, Surrey. In both cases, the subjects had a high level of fitness and regularly undertook physical exercise. All subjects gave informed consent.

Subject age, level of amputation, reason for amputation and time since amputation are shown in Table 8-6.

Table 8-6 Subject data for amputee athletes.

No.	Age	Sex	Level	Reason	Time Since	Type of Socket
1	31	M	A/K	Neoplasm	5 years	Plastic shell
2	26	M	T/K	Trauma / RTA	11 years	Silicon liner
3	20	M	A/K	Trauma / RTA	12 months	ICEROSS
4	25	M	B/K	Trauma / RTA	12 months	ICEROSS
5	21	M	B/K	Trauma / mine	16 months	Plastic shell
6	24	M	B/K	Trauma / mine	9 months	ICEROSS

8.7.2 Protocol

The protocol for this investigation was approved by the relevant ethical committee. Prior to each investigation a visual assessment of the residual stump was made in order to identify bony prominences and areas of high weight bearing. Sweat pads were attached to both high load bearing areas and low load bearing or control areas (sometimes outside the socket). In addition, a control pad was placed on the forehead of subjects 3 to 6 as a potential indicator of general sweating, which might be assumed to be exacerbated within the closed environment of the socket.

The subject donned the prosthesis and mounted the automatic treadmill. The subjects were asked to run on the treadmill at a comfortable pace, for at least 10 minutes. Throughout the exercise period the subjects were asked to define the perceived intensity of the activity using the Borg Scale detailed in Table 8-7. At the end of the exercise period the subjects heart rate was recorded using a pulse meter. The subject doffed the prosthesis and the sweat pads were removed, placed in the pre-weighed bottles, and stored in the frozen state until biochemical analysis was carried out following the procedure described in Section 4.3.4.

Table 8-7 Table describing the Borg Scale used for defining level of exertion during exercise.

Scale	Description
6	
7	very, very light
8	
9	very light
10	
11	fairly light
12	
13	somewhat hard
14	
15	hard
16	
17	very hard
18	
19	very, very hard

8.7.3 RESULTS

The complete results of exercise protocols, heart rate, amount of sweat collected and, where appropriate, metabolite concentrations are shown in Table 8-8.

Table 8-8 Summary of sweat analysis at stump socket interface of athletic amputees running on a treadmill.
* indicates which samples were analysed for sweat metabolites

SUBJECT 1 *WALKING SPEED 5.1 KM/H DURATION 10 MINS. BORG RATE 13*

	Site	Sweat amount mg	Heart Rate	Lactate mmol/L	Urea mmol/L	Chloride mmol/L
1	Anterior mid thigh	113.9*		37.53	16.44	14.64
	Lateral mid thigh	146.7*	-	43.44	19.47	15.21
	IT	100.7*		80.94	31.05	25.71

SUBJECT 2 *WALKING SPEED 4.9 KM/H DURATION 12 MINS. BORG RATE 12-13*

2	distal end	73.9*		35.16	18.51	100.8
	lateral mid thigh	14.0	-			
	anterior upper thigh	136.0*		36.9	10.08	52.65

SUBJECT 3 *WALKING SPEED 4.8 KM/H DURATION 12 MINS. BORG RATE 9-11*

3	distal end	11.4				
	anterior mid thigh	25.8	139 bpm			
	posterior mid thigh	7.5				
	forehead	212.5*		18.75	22.47	29.58

SUBJECT 4 *WALKING SPEED 6.4 KM/H DURATION 12 MINS. BORG RATE 15*

4	distal end	8.3				
	patella tendon	5.7	163 bpm			
	anterior mid thigh	12.8				
	forehead	226.3*		12.48	18.24	67.02

SUBJECT 5 *WALKING SPEED 7.5 KM/H DURATION 12 MINS. BORG RATE 11-13*

5	distal end	24.1				
	patella tendon	35.5	91 bpm			
	anterior mid thigh	140.4*		32.72	26.19	62.07
	forehead	233.3*		16.77	15.09	72.3

SUBJECT 6 *WALKING SPEED 5.6 KM/H DURATION 12 MINS. BORG RATE 9-13*

6	distal end	11.4				
	patella tendon	3.8				
	below PT	3.4	122 bpm			
	anterior mid thigh	30.7				
	forehead	212.8*		37.14	21.12	26.31

There were clear differences in the results obtained for the six subjects. In three subjects the sweat collected at the sites of the stump socket interface was sufficient for subsequent analysis. In the other subjects the exercise protocol was sufficient to produce significant sweat on the unloaded forehead, as evidenced by the saturated sweat pads but on inspection the pads within the socket were relatively dry. Consequently it is again appropriate to discuss subject results separately.

Subject 1 yielded significant levels of sweat at all three collection sites during the 10 minutes hard exercise period at a Borg Rate of 13. Individual sweat concentrations were significantly higher for all three metabolites at the ischial tuberosity compared to the pads located on the unloaded thigh. For example, the former site yielded a twofold increase in lactate concentration compared to the non-loading bearing sites within the socket. This would suggest a higher degree of ischaemia at the ischial tuberosity, an area which carries the majority of load in an above knee socket.

Subject 2, a trans knee amputee, showed similar lactate levels at the distal end compared to the control pad on the thigh. However, both urea and chloride concentrations were higher at the load bearing distal end of the residual limb.

The remaining four subjects, numbers 3 to 6, showed high sweat rates in the forehead pad, with a mean vale of 18.44 ± 0.74 mg/min. However, only one subject provided sufficient sweat within the socket for analysis. Subject 5 demonstrated a higher sweat lactate and urea levels in sweat collected at the medial thigh within the socket, than that collected at the forehead.

8.8 Discussion

8.8.1 Pressure Measurement

The use of a small single cell of a monitoring system to measure pressure repeatably is fraught with difficulties. These include precise location of a cell on an anatomical site and ensuring the cell remains in position when the prosthesis is donned. A small displacement of the pressure cell during donning, may dislodge the cell, and hence the interface pressure measurements may not reflect the area of interest. This was

especially notable where bony prominences are covered by fleshy soft tissues, such as the ischial tuberosity, where there is large relative movement between the tissue layers.

8.8.2 SWEAT YIELD

Sweat rate is known to decrease with degree of ischaemia [1162,2071] but this relationship was not consistently borne out in the results, with some subjects demonstrating the highest sweat yield at areas of tissue which experience the highest load bearing. However, in general the low sweat yields could be attributed to the occlusion of blood flow to the tissues of the residual stump during ambulation. The relationships between sweat metabolites and sweat rate in the amputee population are discussed further in Section 9.6. The low levels of sweat collected would suggest that a longer collection period is required, however, this may not be feasible in a clinical setting, especially in subjects who are not active or who are prone to discomfort during ambulation. Since the major limiting factor in the biochemical analysis of collected sweat is the sample minimum of 50 mg, a more sensitive analysis technique would enable smaller sweat samples to be analysed, this is discussed further in Section 9.2.4.

8.8.3 EFFECT OF DIFFERENT SOCKETS

There is anecdotal evidence to suggest that silicone sockets such as the ICEROSS socket produce excessive sweating within the first few months of wear. Excessive sweating in the socket is more likely to lead to maceration of the tissue which, in turn, may increase the likelihood of tissue breakdown. From the results in this investigation it was not possible to examine the significance of this effect due to insufficient samples collected which yielded adequate sweat quantities for subsequent analysis of metabolites. In addition, the filter paper sweat collection technique is not ideal for determining the effect of different socket materials on sweating at the stump/socket interface, due to the sensitivity of sweat glands to the local environment [58]. This would mean that the sweat glands which are adjacent to the filter paper sweat collection pad may not respond in the same manner as those in contact with the socket material, and it may be more pertinent to employ collection of whole socket sweat to determine the effect of socket materials.

However, the present technique may be more useful for identifying the pressure distributions within different sockets and the response of residual stump tissues to different socket designs.

8.8.4 INDICATOR OF TISSUE STATUS

As a measure of tissue status the filter paper method of sweat collection is ideally suited to the stump socket interface due to its flexibility and minimal thickness. To date, the only measurements made within the socket have been physical measurements of interface pressure and shear [127,208,224]. The present measurement of sweat metabolite concentrations as an indicator of ischaemia in tissues subjected to high loading has proved a novel innovation. Where sufficient sweat was collected, biochemical analysis suggested that in both the general and athlete amputee groups, elevated levels of lactate and urea were found at sites corresponding to high load bearing or bony prominences. Subject 1 in the athlete amputee population demonstrated a very high lactate concentration (80.9 mmol/L) at the ischial tuberosity, a high load bearing area in above knee amputees; and Subjects 1,5,6 and 7 showed elevated metabolite levels at areas such as the patella tendon and distal end (Figure 8-6). The results were not as consistent as those found in the experiments on healthy controls, though it is possible that there may be some pathological changes in the soft tissues of amputee subjects, as a result of trauma, which may alter sweat gland function. Therefore, it would be necessary to fully investigate the function of sweat glands in the residual tissues before this method can be utilised clinically. A further complication is the collection of a control sample of sweat, ideally the control sweat sample should be collected from a low weight bearing area inside the socket to ensure similar temperature and humidity conditions. However, in practice, collection of such a sample is not always possible. Despite some limitations, this method has definite potential in indicating tissue status within the residual stump tissues contained in a lower limb prosthesis.

8.9 SUMMARY

Both transcutaneous gas tensions and sweat biochemistry analysis techniques have proved fairly successfully in assessing the patient support interfaces of two clinically relevant patient groups. Although some improvements are required in terms of the sensitivity of the sweat analysis techniques in patient groups where low yield of sweat is produced, both techniques have the potential to provide simple and non-invasive indicators of soft tissue status.

9. General Discussion & Future Work

9.1 Introduction

The functional integrity of healthy soft tissues is essential to protect the internal organs of the body from potentially damaging physical and chemical stimuli. In a number of clinical situations, such as prolonged wheelchair sitting, prone bed lying and within the socket of an amputee prosthesis, mechanical stresses or pressures may lead to damage to the soft tissues particularly at the site of a bony prominence.

Tissue ischaemia induced by external pressure is characterised by a reduction in pO_2 and an increase in pCO_2. Anaerobic metabolism occurring in the absence of adequate blood supply can lead to an altered tissue biochemistry and a build up of toxic waste products. These factors can lead to severely compromised tissue viability, cell necrosis and potentially lead to the accumulation of tissue breakdown.

The primary objective of this work was to non-invasively monitor tissue status or viability using two distinct techniques, namely, transcutaneous gas tension measurement and sweat biochemical analysis. These techniques were used to determine the effect of varying levels of applied pressure and time on tissue status at clinically relevant sites in both control healthy volunteers and susceptible patient groups. Oxygen and carbon dioxide tensions give an indication of the blood supply to a localised area of tissue, whereas analysis of sweat composition can indicate some of the biochemical processes occurring within the skin and underlying tissues.

9.2 Experimental Techniques

9.2.1 Selection of Soft Tissue Sites

The problem of tissue breakdown, as a result of prolonged pressure induced ischaemia, most commonly occurs at the site of a bony prominence. Within this thesis, clinically relevant sites were chosen for investigation. This is in contrast to previous studies examining the effects of pressure ischaemia, which have been largely carried out on the forearm, an accessible site for loading [73,157,207]. In the present work,

involving healthy volunteers, the sacrum was generally used as a clinically relevant site for investigation. The sacrum has one of the highest incidences of tissue breakdown, as highlighted in Figure 2-8. It is commonly loaded during both supine lying and sacral sitting and in addition, it has the advantage in the present work as it is a body area with an associated high sweat rate [158].

In the clinical groups, measurements of tissue status were made within the residual tissues at the stump socket interface of lower limb amputees, and at the ischium, sacrum and greater trochanter of spinal cord injured patients. With respect to the stump socket interface, it is clear from the literature that at present the only measurements made within the amputee socket have been confined to those of pressure and shear. The collection of sweat and subsequent analysis would give additional information about the status of the residual limb tissues.

9.2.2 Method of Pressure Application

The literature review highlighted the different methods of producing pressure induced ischaemia, the two main methods involved tourniquet loading [115,191] and uniaxial loading using a small, shaped indenter [147,175]. The investigations in this thesis on the control group of healthy volunteers, utilised a cylindrical indenter with curved edges to minimise stress concentrations, through which pressure was applied using a bed mounted loading jig (Figure 4-10). This latter method attempted to simulate the clinical situation whereby pressure is applied to the soft tissues adjacent to the bony prominences when supported by an orthotic or prosthetic surface. By comparison, tourniquet ischaemia is more analogous to conditions associated with arterial and venous occlusive diseases. The experiment in Section 5.3 highlighted the differences in the transcutaneous gas tension response to both types of loading. Figure 5-4 shows a greater reduction in pO_2 with uniaxial loading via an indenter than that associated with an occlusive tourniquet cuff. This difference may be compared to the results of Polliack *et al.* [157] on sweat metabolite concentrations obtained from ischaemic tissues [157]: sweat lactate, urea and chloride concentrations were each elevated when uniaxial

compression was employed, whereas there was little change when the tissues were rendered ischaemic with the use of a tourniquet.

In the clinical studies tissue status was measured during normal physiological activities, such as ambulation in the amputee population and wheel chair sitting in the spinal cord injured population.

9.2.3 Transcutaneous Gas Tension Measurement

Transcutaneous gas tension measurement was originally developed to monitor arterial blood gas tension in neonates. However, as described in Section 3.3.2 a number of limitations led to criticism of its use on adults. More recently transcutaneous gas tensions, most commonly oxygen, have been used as an objective indicator of soft tissue viability, to assess relative changes under different loading regimens [24,55,66]. The technique provides continuous, non-invasive measurement of oxygen and carbon dioxide tensions within the superficial tissues. The main disadvantages of this technique is the initial cost of the monitoring system and the elevated temperatures required to measure the tissue gas levels, the latter deviating from the normal physiological situation.

Within this thesis, pO_2 and pCO_2 measurements were made at the sacrum of healthy volunteers and the ischium of spinal cord injured subjects. An electrode temperature of 44.5°C was used based on the experiment described in Section 5.2. It was not possible to measure gas tensions within the amputee sockets due to the necessary intimate association between the residual tissues and prosthetic socket, which precluded the introduction of the rigid gas tension electrode without causing discomfort and pain to the subject. However, it may be possible in future to design an electrode that is thinner and flexible, based on a disposable Clark electrode recently developed [197], which may be incorporated into the socket; this would enable measurement of gas tensions *in situ*.

9.2.4 Sweat Collection & Analysis

The sweat collection technique comprising of filter paper pad covered by an impermeable plastic sheet is simple, non-invasive and cheap. It provides a method of obtaining sweat samples from an interface without distorting the tissues and the

geometry of the surfaces. Other reported techniques for collecting sweat as described in Table 3-5 would not have been appropriate for quantitative collection of sweat at an interface. The present technique is particularly meritorious in the investigation of soft tissue status within the lower limb amputee socket, where there is a close association between the residual tissue and the socket. It is also important if this method is to be used as a clinical tool as any non-compliant transducer which may inherently induce high pressures or tissue distortion due to its shape would not be clinically acceptable.

Sweat lactate, urea and chloride concentrations have been accurately estimated using spectroscopic methods [202]. However, the sweat urate concentration, which is three orders of magnitude smaller than sweat lactate concentration was initially analysed using spectroscopic methods although they proved insufficiently accurate to carry out further analysis. Thus a new technique would need to be developed, possibly utilising high performance liquid chromatography (HPLC). This technique could also enable the analysis of further sweat metabolites which may be of interest, such as hypoxanthine, xanthine and creatinine.

In order to enable accurate analysis of sweat lactate, urea and chloride, a minimum sample weight of 50 mg was required. Temporal studies of sweat response in the unloaded state (Figures 6-2 to 6-4) suggested that a period of 20 minutes acclimatisation at a temperature of 36°C was required to ensure a satisfactory sweat rate and a constant sweat composition over a subsequent period of up to 90 minutes. Within the present work, the longest single collection period was 60 minutes. Although in a previous study sweat has been collected continuously at ambient temperatures for 9 hours [202], this would inevitably involve fatigue of the sweat glands. Indeed, this process has been reported after periods of 3 hours [187]. A number of previous studies have looked at the day to day changes in sweat output [45,207] within individuals. To eliminate inaccuracies due to inter- and intra- individual changes a control sweat collection pad was always placed adjacent to the experimental pad and results are expressed as a ratio loaded to unloaded value.

Sweat collections in the amputees and spinal cord injured subjects were made at room temperatures of 26°C and 22°C respectively during the summer months.

However, despite these conditions low sweat rates were generally observed for both groups, particularly the spinal cord injured population, although this may be a direct result of alterations in the sudomotor response due to cord injury. As a clinical tool, collection periods of longer than 60 minutes might prove impractical. Therefore it is possible that sweating would have to be induced using techniques such as iontophoresis of a sweat stimulators like pilocarpine in order to promote sufficient sweat rate over a shortened collection period. The sweat composition of thermally and chemically induced sweat has been shown to be not significantly different [73]. However, the problem with promoting sweating is that increased moisture at the patient support interface can cause tissue maceration and lead to increased chance of tissue breakdown, therefore it would not be ethical to promote sweating in susceptible patient groups.

The present sweat collection technique does not introduce any adverse conditions at the tissue interface, however, for clinical use the sensitivity of the analysis technique may need to be improved in order to analyse smaller quantities of sweat. The ideal sweat collection system would reduce sampling time, in order to attain a continuous measurement of sweat biochemistry. This would also indicate the exact time at which changes in sweat composition occurred.

9.3 Effect of Applied Pressure on Tissue Status

One of the primary aims of this thesis was to investigate the effect of prolonged pressure induced ischaemia on tissue status. Tissue status was measured using two independent, non-invasive methods, transcutaneous gas tension monitoring and sweat biochemistry analysis. Both measurement techniques were found to be sensitive to changes in tissue status induced by applied pressures and their results were complementary in assessing tissue status.

9.3.1 Transcutaneous Oxygen and Carbon Dioxide Tensions

Tissue oxygen tension, pO_2, was monitored both at the sacrum of healthy volunteers (Figure 7-2) and at the ischium of seated spinal cord injured subjects (Table 8-2). In

the former case, a parameter was derived which reflected the percentage reduction in pO_2 as a result of applied pressure. This approach which has been previously reported in other studies [7,10,147] ensured normalisation of any individual differences in unloaded pO_2 values.

Oxygen tension was shown to decrease with an increasing applied pressure, in agreement with previous researchers [11,147,191]. These findings suggest a reduction in available oxygen due to occlusion of the tissue blood supply caused by the applied pressure. An 80% reduction in pO_2 was observed at applied pressures greater than 80 mmHg as shown in Figure 7-2. In addition, pO_2 values below 5 mmHg, reflecting a reduction greater than 80%, were demonstrated at the ischium of the spinal cord injured subjects with associated interface pressures in excess of 90 mmHg (Table 8-2 and Figure 8.2).

The literature reports an inverse relationship between applied pressure and oxygen tension [147,191] concordant with the results in this study (Figures 5-2 and 7-2). The exact relationship appears to depend upon experimental technique, including method of applying pressure and body location. Previous researchers have quoted applied pressures required to reduce pO_2 levels to zero [11,147,191], however the physiological significance of zero pO_2 readings has been disputed [195]. Within the present work, no zero pO_2 values were recorded. Animal models have suggested that pathological tissue changes occur at pressures in excess of 60 mmHg [98,115,125]. However no safe minimum levels of pO_2 have been proposed to ensure tissue viability. It is clear from the results of this thesis that as a single measure of tissue viability, the use of pO_2 measurements is limited.

Tissue carbon dioxide tension, pCO_2, was simultaneously monitored using the combined gas tension electrode and this measurement could provide additional information about tissue status. A number of parameters were defined to enable description of the carbon dioxide tension response to applied load. Primarily, three distinct modes of pCO_2 were noted with respect to applied load as described in Section 5.4, namely Mode 1, 2 and 3. These represented no change in pCO_2 with load, slight increase to a new elevated level and a continuous increase with time respectively.

These three modes were discernible in both the normal healthy volunteers (Figures 5-8 and 7-9) and in the spinal cord injured subjects (Table 8-2).

Two further parameters were defined to describe the pCO_2 response to applied pressure; the area calculated beneath the loaded response curve with time, and the percentage time which carbon dioxide levels exceeded a threshold value (Figure 5.9). The latter approach has been described by Bogie *et al.* [24-25], who defined two threshold levels in subjects in the acute phase of spinal cord injury. These authors defined a lower threshold value of 36 mmHg, which was appropriate for some spinal cord injured subjects. It was proposed that these subjects exhibited depressed levels as a result of the increased clearance rate caused by an imbalance in arterial supply and venous drainage [24]. However, in the present studies involving healthy volunteers, no such depressed levels were exhibited. Therefore for these subjects, a single threshold value of 50 mmHg was selected as pCO_2 values above this represent abnormal soft tissue levels [32].

The results of this investigation highlighted a strong correlation between pO_2, pCO_2 and applied pressure. The frequency distribution of pCO_2 Modes 1, 2 and 3 with respect to median loaded pO_2 values (Figure 7-9) reveal that the majority of subjects displayed an increased pCO_2 level at low levels of pO_2 coincident with high applied pressures. In addition, Figure 7-10 shows that increased pCO_2 tensions occur for a significant period of loading time, when the pO_2 levels are reduced by at least 60% compared to their unloaded values.

An increase in tissue levels of carbon dioxide, a metabolic waste product, could indicate stasis in blood and lymph flow which may reflect an accumulation in other potentially harmful waste products whose presence would compromise tissue viability. Build up of carbon dioxide will also lead to a decrease in pH and the problems associated with acidosis. An elevated carbon dioxide tension is a vasodilator and can result in reduced vasomotor tone [32]. During periods of applied pressure ischaemic conditions may be exacerbated by further occlusion of the blood vessels whose critical closing pressure is decreased as a result of reduced tone.

It is interesting to note, that not all subjects demonstrated an associated Mode 3 pCO_2 response to low pO_2 levels. This suggested an individual capacity to prevent

accumulation of pCO_2, presumably by the removal of waste products even during periods of high applied pressures. With respect to the spinal cord injured group, 3 of the four subjects (75%) who had a history of sores demonstrated a Mode 3 pCO_2 response during wheelchair sitting, compared to 2 (40%) of the remaining patients who had no history of sores (Table 8-2). These results suggest that transcutaneous carbon dioxide tension can give additional information regarding the status of soft tissues. Thus its use in conjunction with transcutaneous oxygen tensions is recommended.

9.3.2 Sweat Biochemistry

The majority of reported effects of arterial occlusion on sweat biochemistry have been carried out at the forearm using tourniquet occlusion techniques [162,207,212-213]. One of the main aims of the present work was to investigate the effect of prolonged ischaemia on sweat biochemistry collected from clinically relevant sites of both healthy volunteers and two patient groups.

Sweat analysis was carried out on thermally stimulated samples collected from the sacral area of healthy volunteers, at both loaded and unloaded sites. Pressures between 40 and 120 mmHg were applied and the results showed a significant increase in levels of lactate, urea, urate and chloride compared to control sites (Figure 7-5 to 7-8). In addition, a significant positive linear correlation was found between applied pressure and values of loaded/unloaded ratios of sweat lactate ($p<0.01$), urea ($p<0.01$) and chloride ($p<0.05$). The increased levels of sweat lactate and urea correspond to the increases reported by researchers using tourniquet techniques [207], and uniaxial compression techniques [73,157], at single applied pressures. Sweat urate levels had only been previously measured by one other researcher [157] and their findings generally follow those of the present study.

The sweat chloride levels in the present work were also shown to increase with increasing load. Tourniquet ischaemia experiments have shown an initial fall in chloride followed by a rapid increase [207]. By contrast, Polliack *et al.* [157] measured sweat sodium levels, which are generally considered to follow sweat chloride levels, and found a decrease with applied load with respect to control levels. The main difference

between the two studies involved the time period of sweat collection, which was in excess of 2 hours [157] compared to collection in the present study which did not exceed 60 minutes. Sweat chloride is derived from a combination of passive diffusion and active reabsorption and its concentration is dependent on sweat rate [31]. Its presence is also highly dependent on dietary intake [81].

Elevated levels of sweat lactate and urea were also demonstrated in sweat collected from the residual tissues of the amputee stump associated with areas of high load bearing (Figures 8-5 and 8-6, Tables 8-5 and 8-8). A previous study on a clinically relevant group has shown elevated levels of sweat lactate and urea and reduced levels of sodium collected at the sacrum [158].

LACTATE

The presence of lactate in eccrine sweat is generally thought to be a by-product of the gland itself [187,207,212-213]. The main metabolic pathway of the eccrine sweat gland during normal metabolism is believed to be oxidative phosphorylation [184], with glycolysis playing a smaller role. However, during periods of ischaemia or reduced oxygen supply, the relative importance of the two pathways is altered with a reduction in phosphorylation and an increase in glycolysis [70]. This is evidenced by the increase in lactate content of sweat during periods of ischaemia [214]. The Embden-Meyerhoff pathway, as detailed in Figure 9-1, describes the production of energy by the breakdown of glucose to pyruvate. In the absence of oxygen, continuous production of pyruvate can lead to deficiency in oxidised nicotinamide adenine dinucleotide (NAD^+) which is required for the continued breakdown of glucose to pyruvate. This process leads to an imbalance in the relative levels of ATP, ADP, and AMP and in order to regenerate levels of NAD^+ pyruvate is converted to lactate.

The elevated levels of sweat lactate collected from loaded sites at the sacrum (Figures 6-6 to 6-8 and 7-5 to 7-8) and, to a lesser degree, the residual stump tissues of lower limb amputees (Figures 8-5 and 8-6) would suggest that the tissues at these sites had been subjected to ischaemic conditions, resulting in anaerobic respiration of the eccrine sweat gland and increased production of lactate. The degree of ischaemia can be monitored by the use of transcutaneous oxygen tension measurements, indeed

data in Figure 7-11 indicates an inverse relationship between pO_2 levels and sweat lactate concentration at the sacrum. In addition, Figure 7-13 demonstrates a strong positive correlation between sweat lactate ratio and percentage reduction in pO_2 at the loaded sacrum of healthy volunteers above a threshold level of 60%. The restoration of blood supply results in the conversion of lactate back to pyruvate, this is demonstrated in the return to basal levels of lactate after load is removed (Figures 6-6 and 6-9).

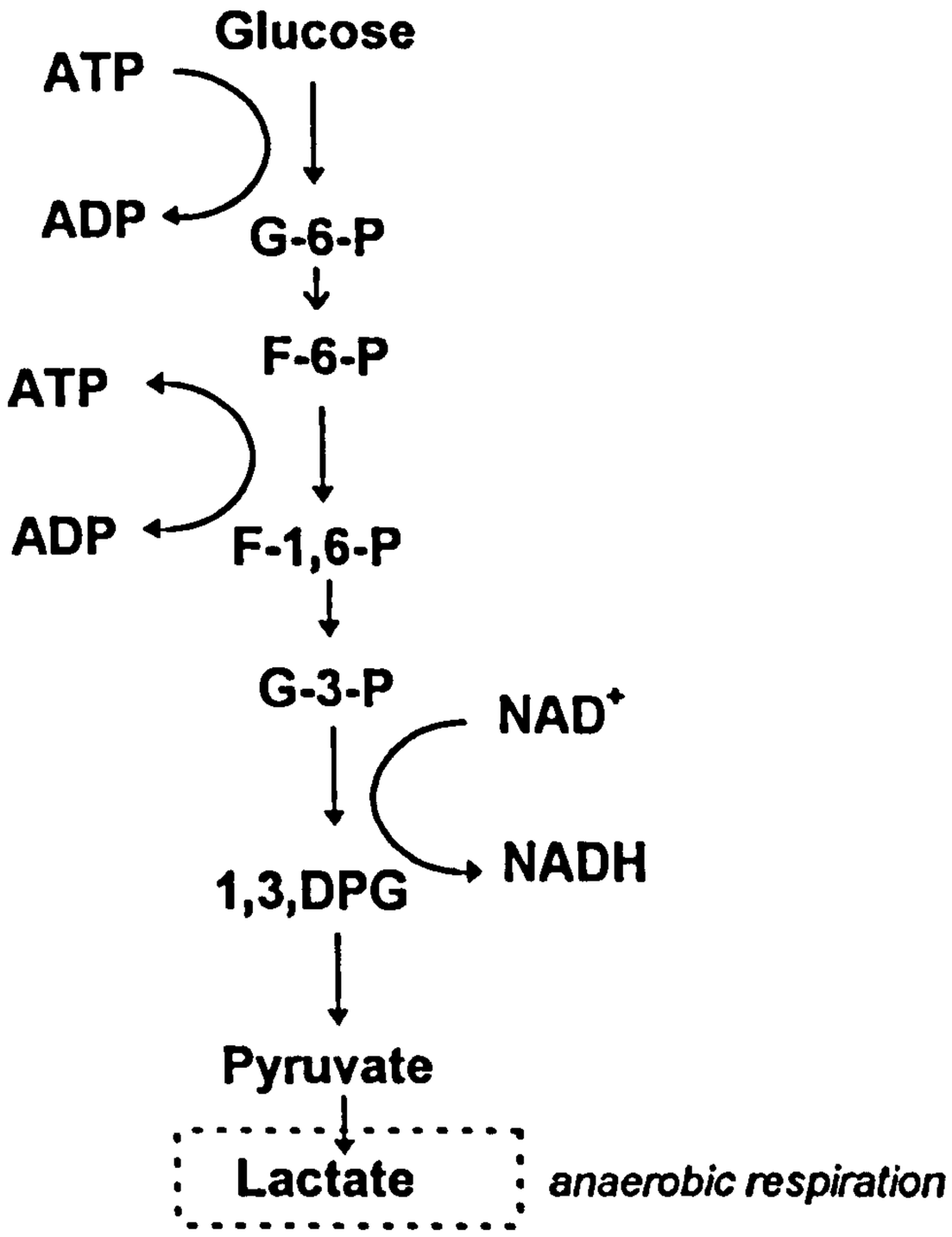

Figure 9-1 Embden-Meyerhoff glycolytic pathway.

UREA

It is not fully understood whether urea is present in the sweat purely by passive diffusion from the plasma [113], or whether it a metabolic product of the gland itself [207]. Urea is present in greater quantities in sweat than in plasma, and it has been suggested that this is because water is reabsorbed in the sweat gland in preference to urea [60]. It is the main breakdown product of protein metabolism and is hydrolysed to carbon dioxide and ammonia by the action of the catalyst urease. Urea in the urine is a sign of

protein metabolism and elevated levels can be found in spinal cord injured patients at risk from tissue breakdown [85]. Ischaemic conditions can lead to the damage of muscle tissue which would produce increases in plasma urea. Any passive diffusion of plasma urea into sweat would suggest that elevated sweat urea levels may be an indicator of muscle damage in underlying tissues. A significant increase in sweat urea was demonstrated at the sacrum for loads of 40 mmHg and greater. In addition, there was a similar relationship between transcutaneous pO_2 and sweat urea concentration as that described for sweat lactate (Figures 7-12 and 7-14). During a reperfusion period, the urea levels were restored to basal levels (Figures 6-7 and 6-9).

URATE

During prolonged periods of ischaemia the Embden-Meyerhoff cycle is regulated by the purine nucleotide cycle (PNC), shown in Figure 9-2, the end product of which is uric acid. Elevated sweat urate levels may indicate the utilisation and degradative losses of high energy phosphate metabolites and has previously been used as an indicator of cell energy depletion [75,219]. In addition, the increased flux from inosine to urate (Figure 9-2) during ischaemia, may have implications for free radical formation, which can be potentially damaging to soft tissues [133].

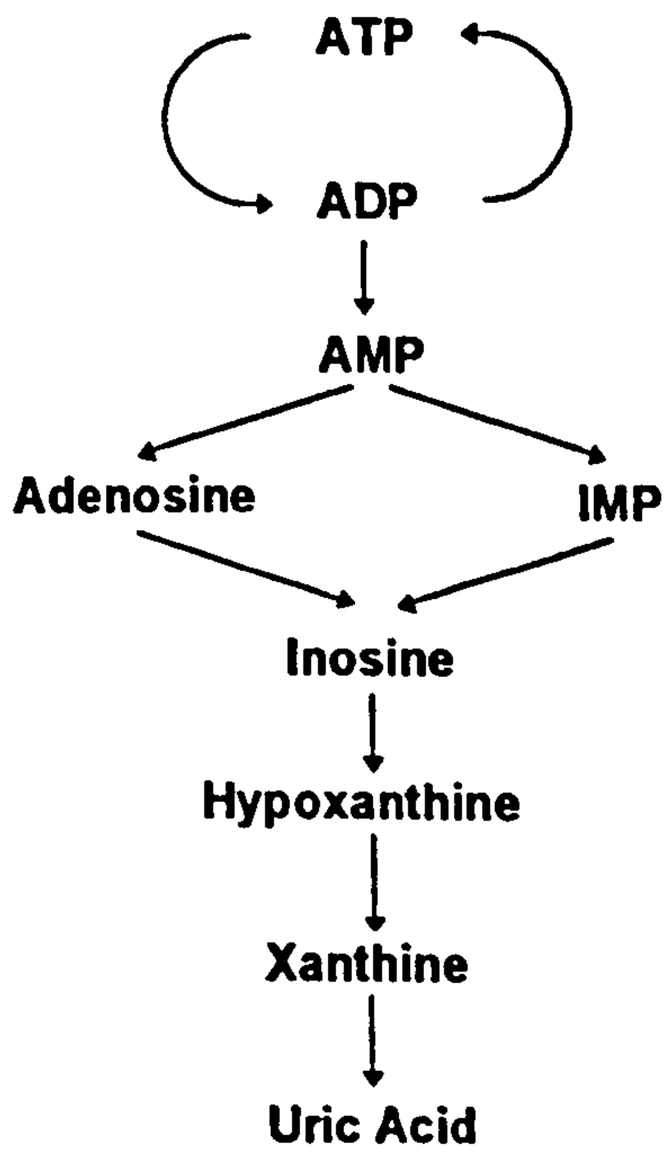

Figure 9-2 Purine nucleotide cycle with uric acid as an end product.

The results of this thesis suggest that sweat lactate, urea and urate are sensitive indicators of tissue status during periods of ischaemia, whereas sweat chloride does not appear to be as sensitive and may be strongly influenced by nutritional factors [81]. In addition, further potential markers of soft tissue status are indicated including xanthine, and hypoxanthine, and it may be possible to detect these biochemicals in sweat in future using more sensitive techniques.

9.4 Effect of Time on Soft Tissue Status

Time has been highlighted as an important factor in the development of soft tissue breakdown [50,53,170]. Within this thesis, tissue status was monitored at the sacrum of healthy subjects during two separate experiments. The first, described in Section 6.3, involved sweat samples collected over discrete 30 minute periods for a total period of up to 120 minutes; the second experiment, described in Chapter 7, consisted of sweat samples collected for single periods of 30, 45 and 60 minutes. During both experiments samples were collected from both loaded and unloaded sites. The results from the former experiment suggested that there was no significant difference between sweat metabolite concentrations collected during each consecutive period (Figures 6-6 to 6-8), providing a 20 minute thermal equilibrium period was undertaken. Furthermore, there was no significant difference between the sweat metabolite concentrations collected during 30, 45 and 60 minute periods for the same applied pressure (Figure 7-4).

The results in this thesis suggest that time is not a critical determinant in the status of loaded soft tissues, at least within the limits of the experimental procedures. It should be noted that the prolonged loading experiments in the present work were restricted to healthy volunteers and collection periods did not exceed 90 minutes to minimise discomfort. Although time may not appear to be a relevant using tissue status measurements such as sweat metabolite concentrations which have shown no temporal changes, methods such as transcutaneous carbon dioxide measurements (pCO_2) do appear to have temporal sensitivity. Tissue damage may be the result of the cumulative effect of several different factors, indeed accumulation of carbon dioxide was demonstrated in a number of situations (Figures 5-5, 7-9 and 7-10, Table 8-2).

At present hospital policy is to provide pressure relief every two hours to prevent tissue damage. However, it is suggested that this may be insufficient in some susceptible subjects where the complete recovery of blood flow is impaired following pressure ischaemia [89,107,136].

9.5 Effect of Prolonged Pressure on Reperfusion

Adequate reperfusion to a tissue area that had previously been rendered ischaemic is very important in the recovery of the tissue and the avoidance of tissue breakdown. Normally a period of increased blood flow, known as reactive hyperaemia, follows a period of ischaemia and the main aim of this increased perfusion is to repay the oxygen debt. The exact mechanism of reactive hyperaemia is not fully understood, although it may be due to a build up of vasodilator substances during the period of stasis or ischaemia [32]. An impaired reactive hyperaemic response has been demonstrated in spinal cord injured subjects using transcutaneous oxygen tensions [107] and reflectance spectroscopy [89], and in the elderly using laser Doppler flowmetry [189] and temperature techniques [137]. Furthermore a positive correlation has been shown between impaired blood flow recovery and susceptibility to formation of tissue breakdown [189].

Within this thesis, reperfusion response was measured using both transcutaneous gas tension measurements (Chapter 5) and sweat biochemistry techniques (Chapter 6). The graph in Figure 5-12 show an increased half time for recovery of pO_2 with applied pressure. It was originally intended to measure reperfusion O_2 and CO_2 gas tensions at the sacrum during the combined sweat and gas tension experiments. However, it was found to be impractical to replace the sweat pads beneath the indenter following loading without dislodging the electrode attachment to the skin surface. Sweat metabolite concentrations (lactate, urea and chloride) were measured in sweat collected at the sacrum during a 30 minute reperfusion period following 90 minutes of loading at 100 mmHg (Figure 6-6 to 6-8). Figure 6-9 shows the sweat metabolite concentration during loaded, control and reperfusion periods. It is clear, that during the reperfusion periods the sweat metabolite concentration returns to control or basal levels, or just below. However, although there was insufficient data to conduct rigorous statistical analyses, these results suggest that sweat gland metabolism returns

to normal levels during the 30 minute period of reperfusion. Sapega *et al.* [182] showed that after a period of tourniquet ischaemia, cellular recovery was initiated before tissue pO_2 values returned to normal levels. In addition, Hyman & Artigue [99] showed that the washout of accumulated lactic acid in muscle is prolonged compared to tissue pO_2 recovery. The results in this thesis and other reports [107] suggest that pO_2 values return to basal levels within approximately 5 minutes, and therefore the collection period of 30 minutes for reperfusion sweat may be longer than is necessary for the complete recovery of sweat gland metabolism. The present analysis technique required a minimum sample sweat weight of 50 mg and utilising thermal stimulation techniques a period of at least 30 minutes was required to collect this amount. In order to accurately follow the recovery of soft tissue using sweat biochemistry methods, it may be necessary to devise a collection technique that has a greater sensitivity requiring smaller sample weights or ideally a real time analysis technique.

9.6 Effect of Sweat Rate on Sweat Biochemistry

Examination of the literature highlights two important relationships with respect to sweat rate:

- Ischaemia causes a reduction in sweat rate [45,119]
- The dependence of sweat metabolite concentrations on sweat rate under normal conditions; chloride concentration is proportional to sweat rate [31] whereas lactate and urea concentrations are inversely proportional [213-214,218].

However, there is still debate as to whether the relationships between sweat rate and metabolite concentrations follow during periods of ischaemia [212] because experimental techniques have largely precluded the accurate measurement of sweat rates [70,207]. In order to investigate these relationships in the present work, the sweat metabolite concentrations obtained from three separate experiments were plotted against the inverse of sweat rate. Sweat rate was defined by Equation 9-1.

$$\textit{Sweat Rate} = \frac{\textit{Sweat Amount} - \textit{mg}}{\textit{Collection Period} - \textit{min}}. \qquad \textit{Equation 9-1}$$

Three sets of data are presented, each set involving sweat lactate and sweat urea concentrations:-

i. Figure 9-3 and 9-4 show the sweat metabolite concentrations collected at the sacrum of healthy volunteers for periods of 30, 45 and 60 minutes during phases of loading at applied pressures of 40, 80 and 120 mmHg (Chapter 7) and unloading. This combined data was collected on sweat pads of area 1.14×10^{-3} m^2.

ii. Figures 9-5 and 9-6 represent the combined results from Chapter 6, where sweat was collected at the sacrum of healthy volunteers during consecutive periods of 30 minutes, in loaded , unloaded and reperfusion phases, using sweat pads with an area of 1.25×10^{-3} m^2.

iii. Figures 9-7 and 9-8 represent the sweat metabolite concentrations from the residual stump tissues of normal and athlete lower limb amputees, and the forehead of the latter group. This data was collected on sweat pads with an area of 1.25×10^{-3} m^2.

Linear models were applied to all the relationships and the Pearson correlation coefficient was calculated. Significance levels are indicated by * ($p<0.05$ (5%)), ** ($p<0.01$ (1%)), and *** ($p<0.001$ (0.1%)).

Close examination of the three sets of graphs revealed a significant correlation between the inverse of sweat rate and sweat lactate and sweat urea concentrations from data derived from the combined technique experiments described in Chapter 7 (Figures 9-3 and 9-4). For both metabolites the slopes and intercepts of the linear models were higher for the loaded compared to the unloaded data as shown in Table 9-1, by approximately 20% and 30% for lactate and urea respectively. In addition, the intercept of the loaded lactate model is greater than that for the unloaded model by approximately 28%, whereas there appears to be no difference between the intercepts of the loaded and unloaded urea models.

Table 9-1 Gradients and intercepts of linear models describing relationship between inverse of sweat rate and sweat lactate and urea concentration.

	LACTATE		UREA	
	loaded	**unloaded**	**loaded**	**unloaded**
Gradient, m	62.29	51.14	61.19	45.77
Intercept, c	28.53	22.34	11.67	10.99

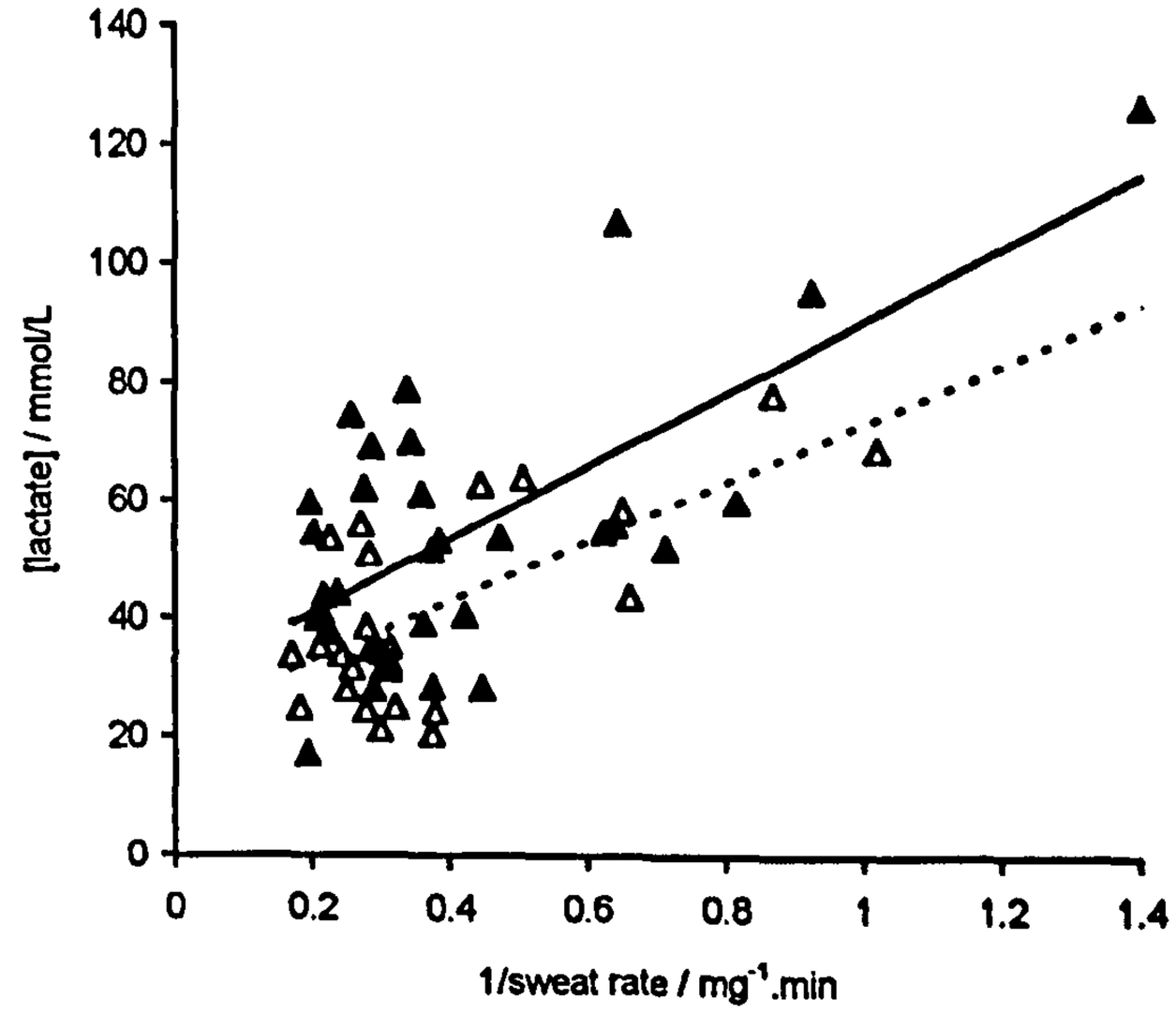

Figure 9-3 Relationship between sweat lactate concentration and inverse of sweat rate for thermally stimulated sweat collected from the sacrum of healthy volunteers.
(Δ) unloaded sweat, linear model (-------) *y=51.14x+22.34 r =0.676* **.
(▲) loaded sweat, linear model (——) *y=62.29x+28.53 r=0.667* **

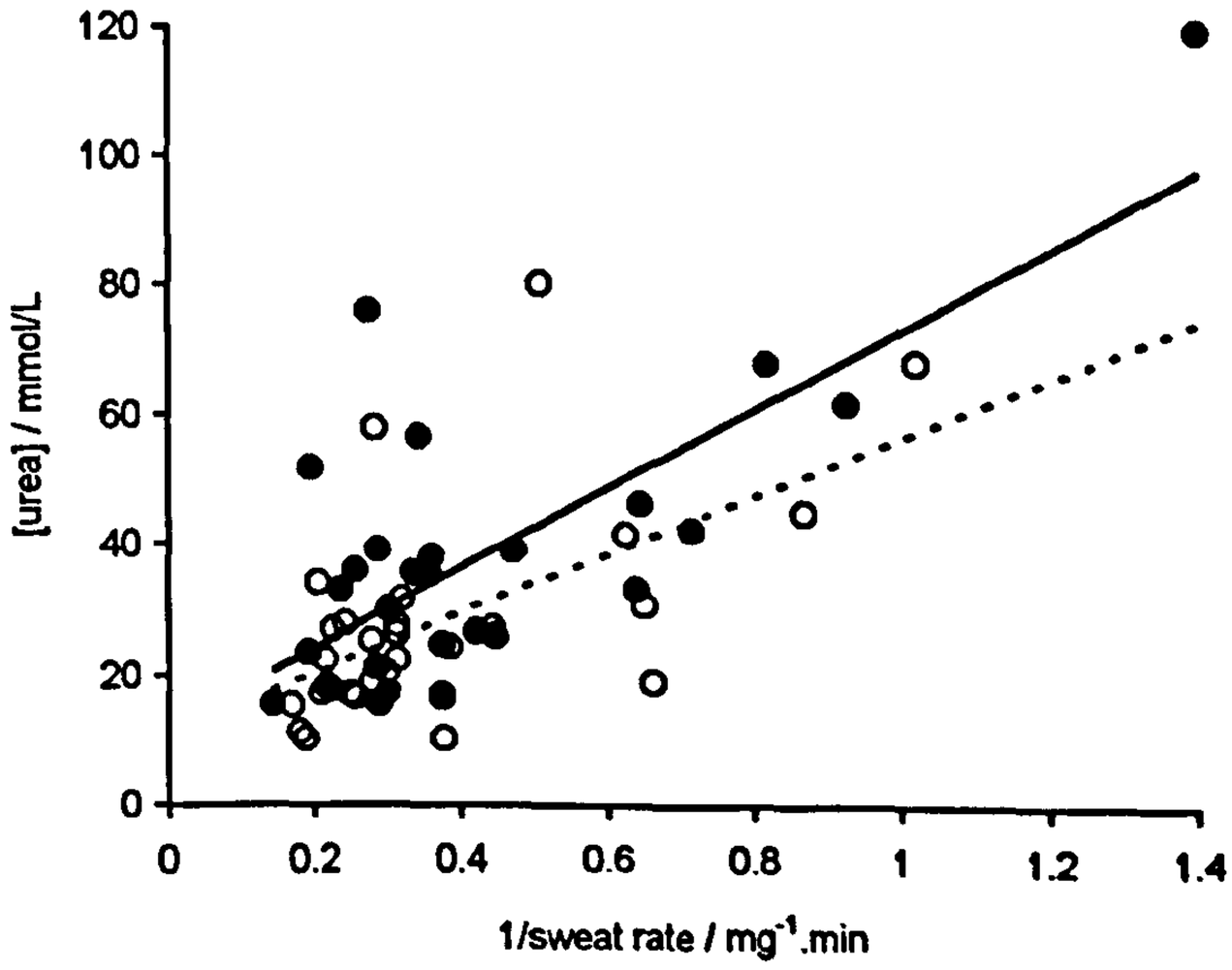

Figure 9-4 Relationship between sweat urea concentration and inverse of sweat rate for thermally stimulated sweat collected from the sacrum of healthy volunteers,
(○) unloaded, linear model (-------) *y=45.77x+10.99; r=0.575* **.
(●) loaded linear model (——) *y=61.19x+11.67; r=0.745***

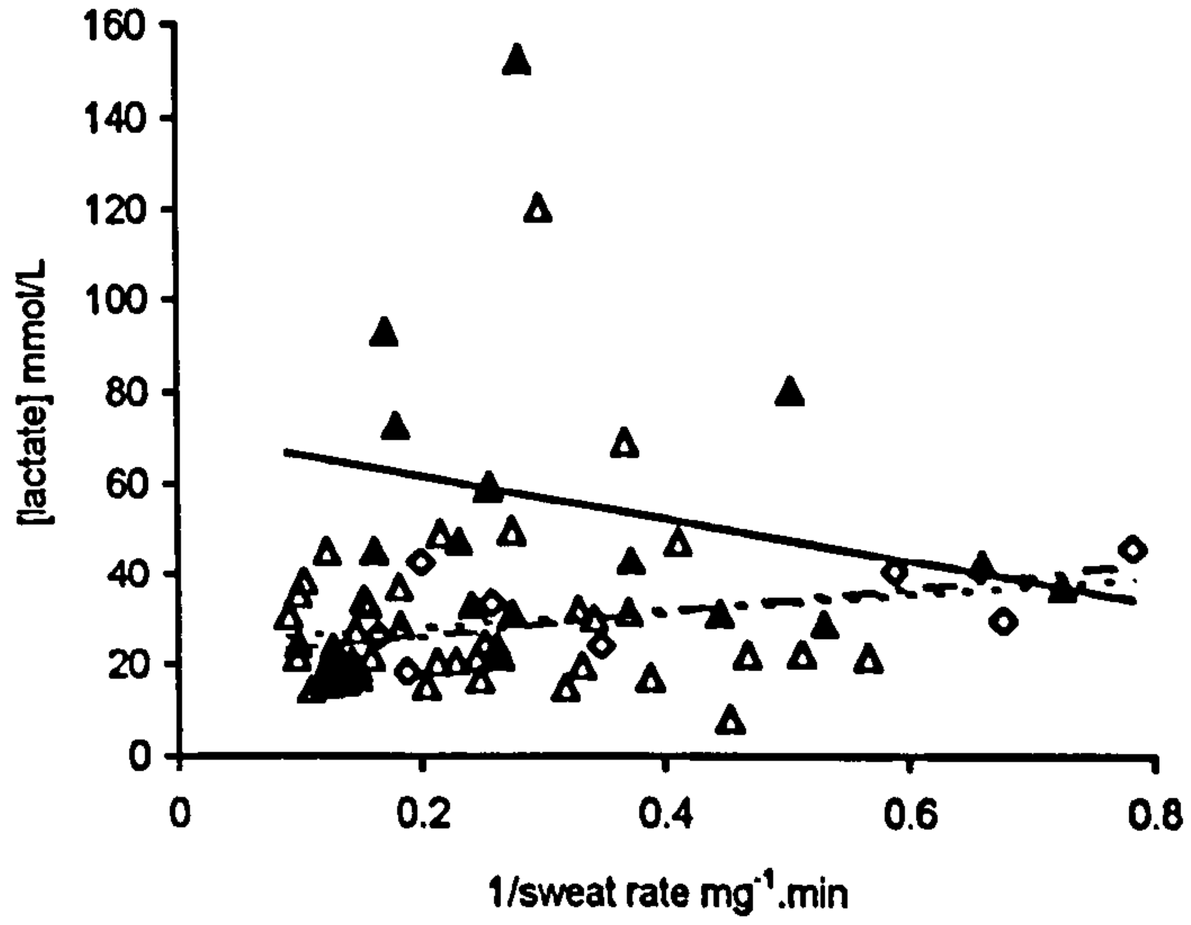

Figure 9-5 Relationship between inverse of sweat rate and sweat lactate concentration for thermally stimulated sweat collected at the sacrum of healthy volunteers using 40 mm diameter sweat pad.
(Δ) unloaded, linear model (------) *y=18.92x+24.42; r= 0.126.*
(▲) loaded, linear model (——) *y=-46.09x+70.95; r =0.242.*
(◇) reperfusion, linear model (- — -) *y=27.15x+20.81; r=0.608.*

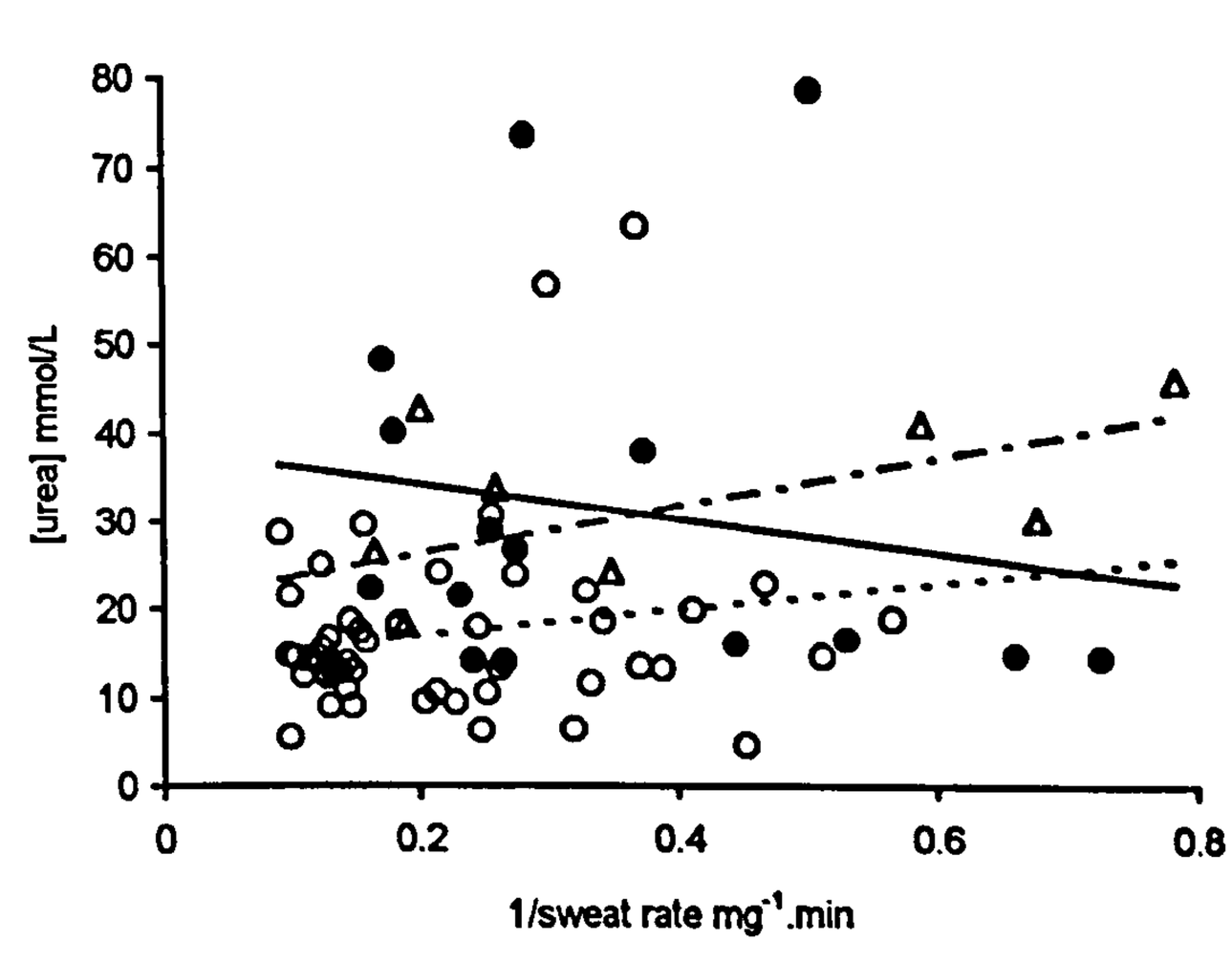

Figure 9-6 Relationship between sweat urea concentration and inverse of sweat rate for thermally stimulated sweat collected at the sacrum of healthy volunteers using a 40 mm diameter sweat pad.
(○) unloaded, linear model (------) *y=14.70x+14.08; r=0.164.*
(●) loaded, linear model (——) *y=-19.47x+38.14; r=0.167.*
(Δ) reperfusion, linear model (- — -) *y=27.15x+20.82; r=0.608.*

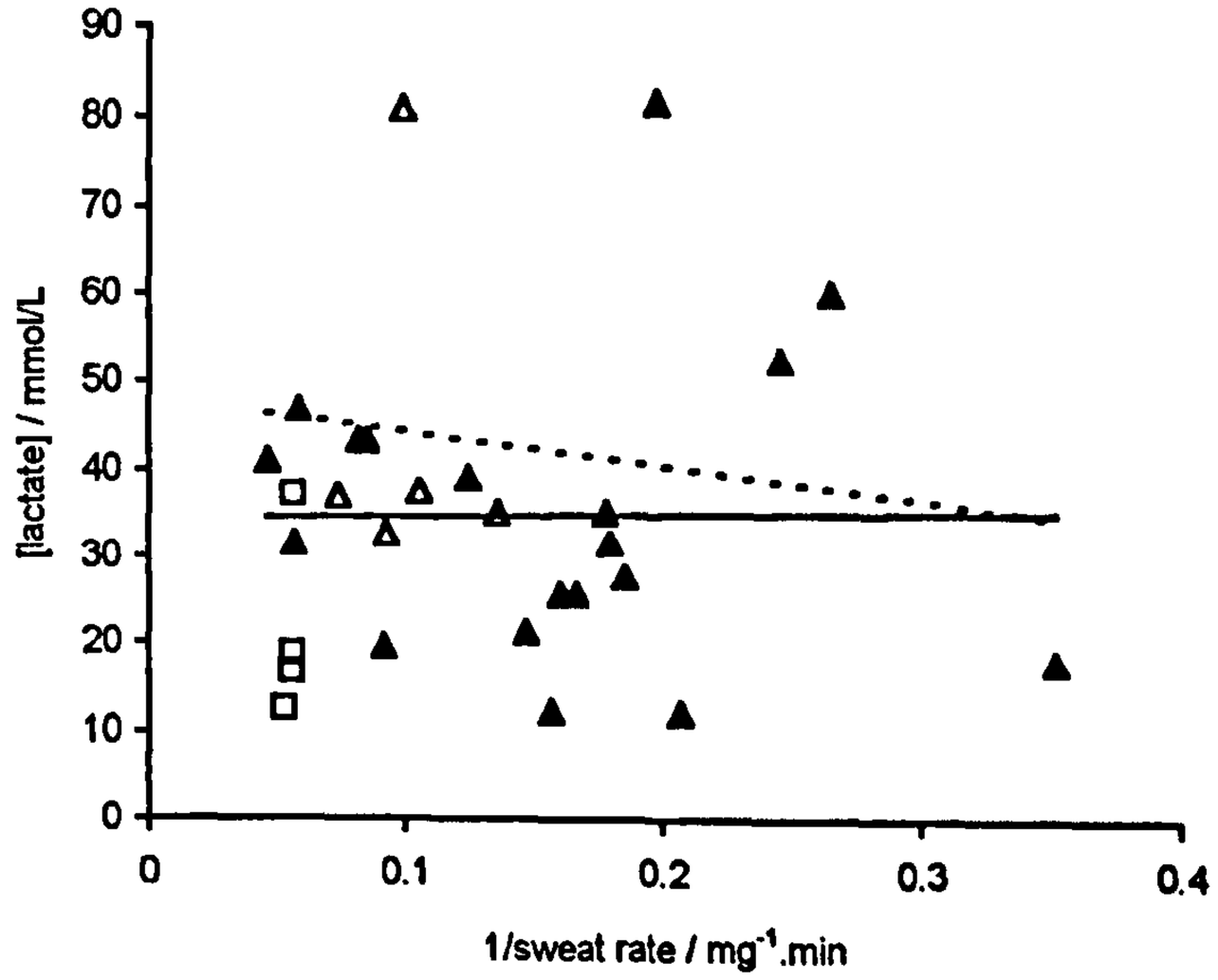

Figure 9-7 Relationship between inverse of sweat rate and lactate concentration in sweat collected in the amputee socket.
(▲) normal pop^{n}, linear model (——) *y=3.2x+34.26; r =0.014.*
(Δ) athlete pop^{n}, linear model (- — -) *y = -38.08x +48.18; r=0.044.*
(□) forehead sweat from athlete population.

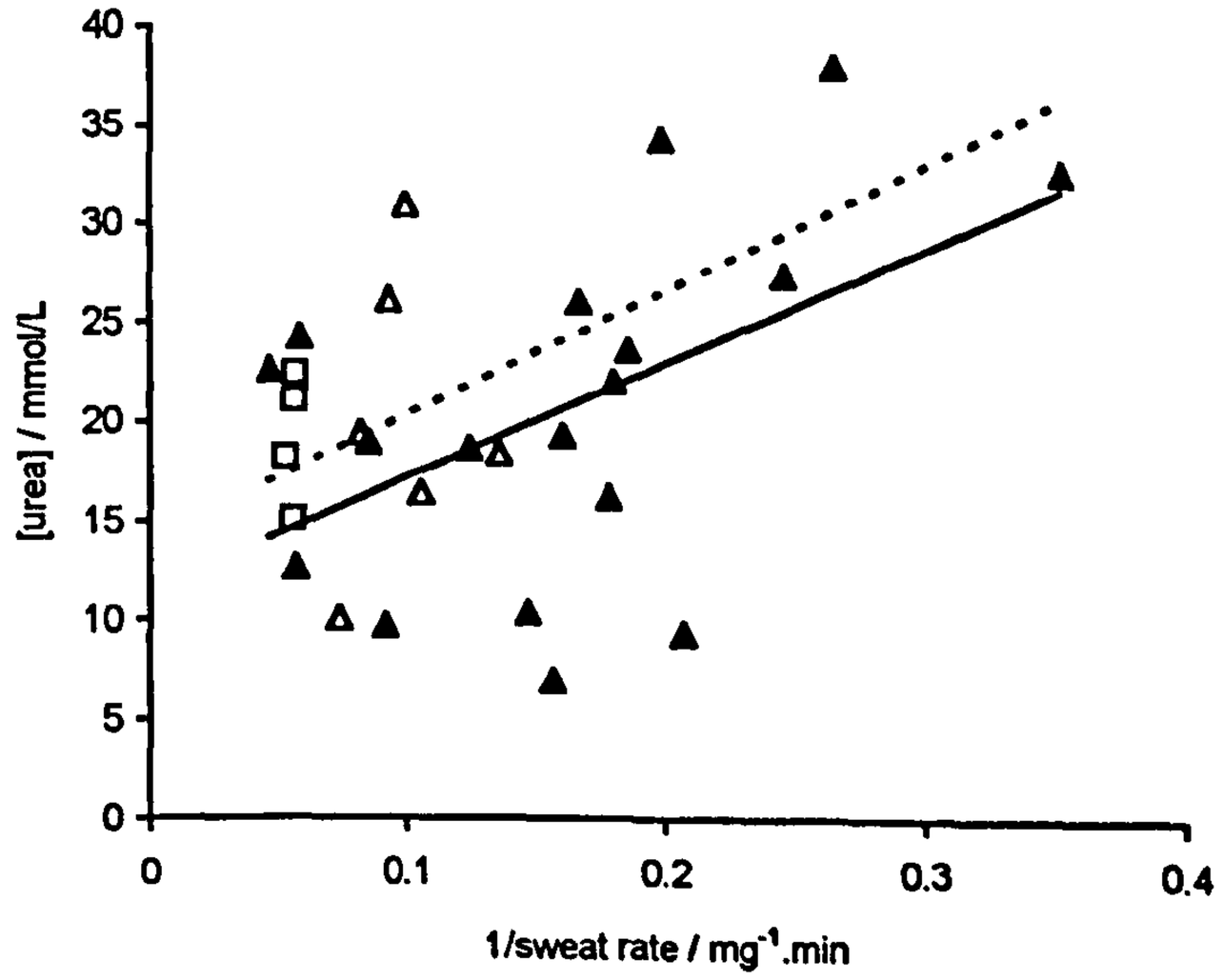

Figure 9-8 Relationship between inverse of sweat rate and urea concentration in sweat collected in the amputee socket.
(▲) normal population, linear model (——) *y=58.21x+11.43; r=0.509.*
(Δ) athlete population, linear model (- — -) *y =63.85x+14.03; r =0.187.*
(□) forehead sweat from athlete population.

This would indicate that the increase in sweat lactate and urea concentrations is higher during the ischaemic loaded period than is predicted by a decrease in sweat rate alone. In order to test this hypothesis, the sweat lactate and urea concentrations were normalised against sweat rate (metabolite concentration / sweat rate), and the significance of the difference between the normalised parameter for loaded and control sweat was tested using a Mann-Whitney U test for large samples. The loaded sweat lactate and urea showed a significant increase from control levels at the 5% level, when normalised to sweat rate, confirming that sweat metabolite concentrations are greater than can be accounted for by a reduction in sweat rate alone.

There was no significant correlation between inverse of sweat rate and sweat urea and lactate concentration in the second data set (Figures 9-5 and 9-6), representing the sweat collected in consecutive 30 minutes periods over a total of 2 hours. The sweat rate in the later collection periods may reflect some degree of sweat gland fatigue in terms of output, which may alter the relationship between metabolite concentration and sweat rate.

No significant relationship was observed for data derived from stump tissues (Figures 9-7 and 9-8). It is possible that the sweat glands present in the skin of the residual stump tissues may have undergone pathological changes due to the trauma of amputation which may result in alterations in the normal function of the sweat glands.

The data pertaining to chloride concentrations showed no significant correlations with sweat rate for any of the three experimental groups. However, the data in Figure 6-8 and Figure 7-7 exhibits an increase in chloride concentration with applied load, and an associated decrease in sweat rate. These results appear to contradict previous reported findings that sweat chloride concentration increases with increasing sweat rate during normal sweating [31], although no relationship between loaded sweat chloride concentration and sweat rate has been previously reported.

The literature states that the reduction in sweat rate during ischaemia may be due to a reduction in oxygen tension at the sweat gland, which reduces the sensitivity of the gland to its neurotransmitter [59]. This may be examined by relating percentage reduction in pO_2 levels to the ratio of loaded to unloaded sweat rates at the sacrum of healthy volunteers, as presented in Figure 9-9. No clear relationship is revealed, due

possibly to the nature of the method of collecting sweat. In addition, the transcutaneous oxygen tension measurement technique described in this thesis, which measures tissue pO_2 at the skin surface, may not accurately represent the O_2 tension at the sweat gland itself.

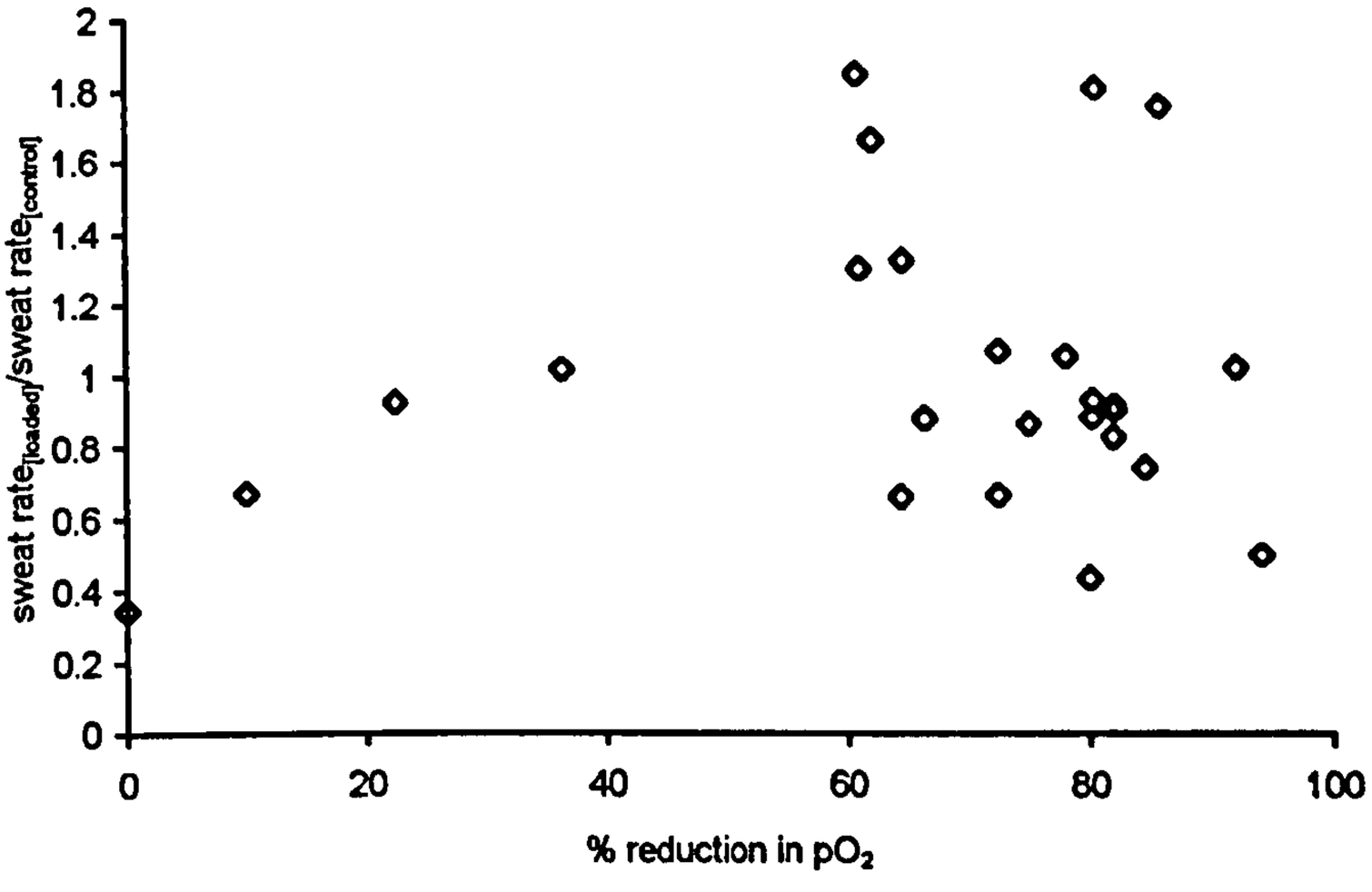

Figure 9-9 Relationship between percentage reduction in pO_2 and sweat rate ratio collected at the sacrum of healthy volunteers

The technique used in this thesis has a maximum threshold capacity of about 300 mg, as discussed in Section 4, when the collection pad is saturated. This would produce an underestimate of sweat rate at high values.

Other inaccuracies with sweat collection methods include evaporation from the sweat pad, and reabsorption of sweat into the skin. It is also worthy of note that sweat rates tend to decrease with an increase in skin wettedness [34,161], known as hidromeisosis, which may also affect the accuracy of sweat rate measurements. A possible solution to this problem would be the use of a more absorbent collection substrate and the use of a one way liner which would keep the surface of the skin dry. A wound dressing, Release ® (Johnson & Johnson, UK) which claims to have these properties was used for the collection of sweat in one of the amputee subjects (Chapter 8). However this

pilot study did not indicate any marked increase in magnitude and nature of sweat collected, although they may be more useful in long term sweat collection studies.

In conclusion, although the measurement of sweat rates may have some limitations, where a correlation was evident there are clear differences in the relationship between sweat rate and sweat lactate and urea concentrations in both the unloaded and loaded situation. The relationship between sweat rate and sweat metabolite concentration has not previously been reported in the loaded state. The results in this thesis suggest that the increase in sweat metabolite concentrations during a loaded period are not the results of a decrease in sweat rate alone, but also indicate an altered sweat gland metabolism.

9.7 Inter-relationship between Sweat Metabolite Concentrations

There is considerable evidence in this thesis to suggest that sweat metabolite levels of lactate, urea and chloride may be related. The graphs in Figures 9-10 to 9-15 show the relationship between pairs of these metabolites, namely, sweat lactate and sweat urea, and sweat lactate and sweat chloride. Again the data is derived from three separate experiments described in Chapter 7 (Figures 9-10 and 9-11), Chapter 6 (Figures 9-11 and 9-12) and Chapter 8 (Figures 9-14 and 9-15), the latter obtained from the amputee population. Linear regression models were applied to the data and the significance levels determined, as described in the previous section.

It is clear that there is a statistically significant positive correlation, at the 0.1% level between sweat lactate and sweat urea concentration for sweat collected from the sacrum of the healthy volunteers at both loaded and control sites (Figures 9-10 and 9-12). There was also a positive correlation between these two metabolites in the amputee population, although statistical significance was only achieved with the general amputee population. These results would suggest that the presence of urea and lactate in the sweat is the result of similar mechanisms; these could be the metabolic production by the sweat gland itself, passive diffusion and reabsorption or a combination of the two.

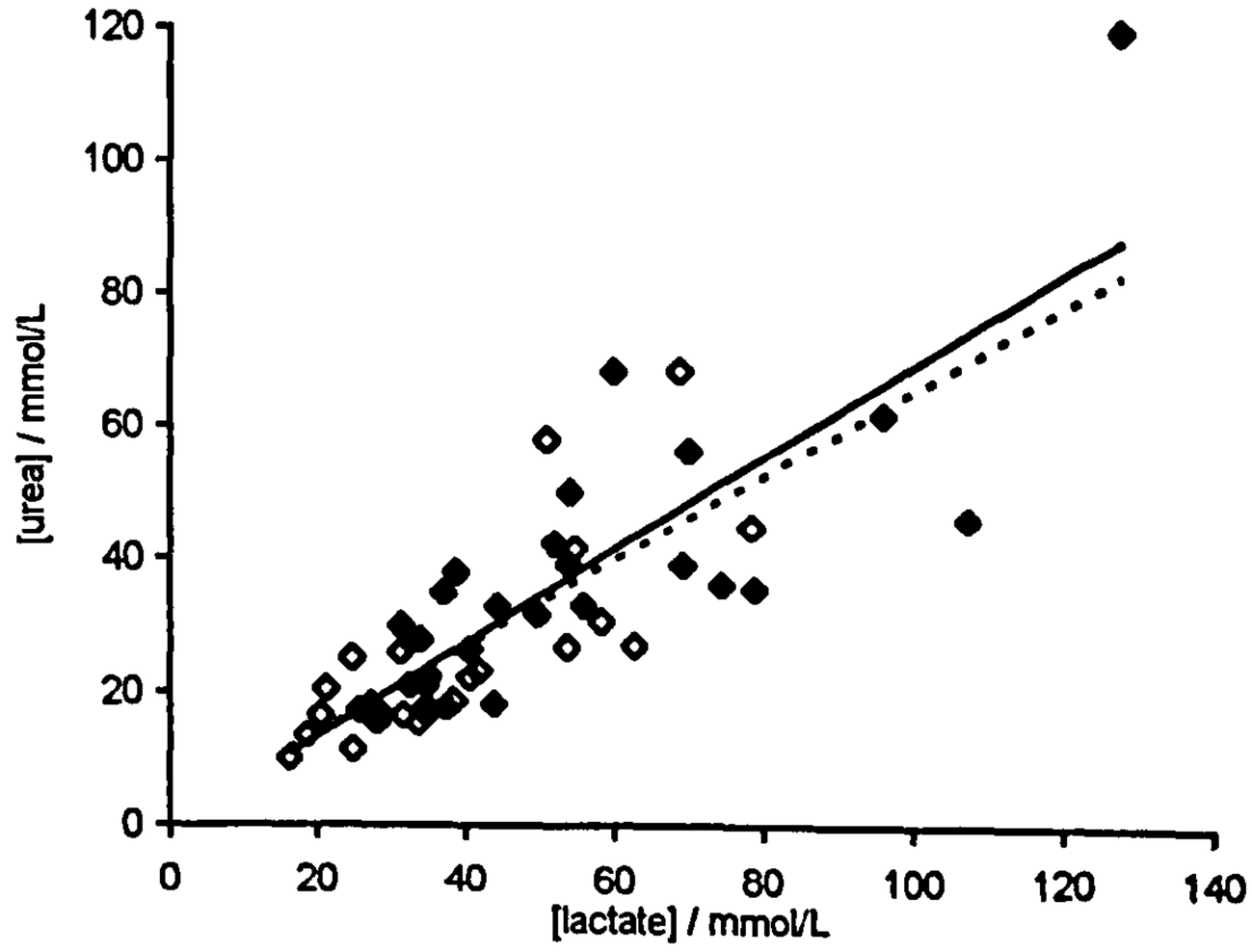

Figure 9-10 Relationship between sweat lactate concentration against sweat urea concentration collected at the sacrum of healthy volunteers.
(◇) unloaded sweat, linear model (------) *y=0.65x+0.77; r=0.766* ***
(◆) loaded sweat, linear model (———) *y=0.70x-0.81; r =0.816* ***,

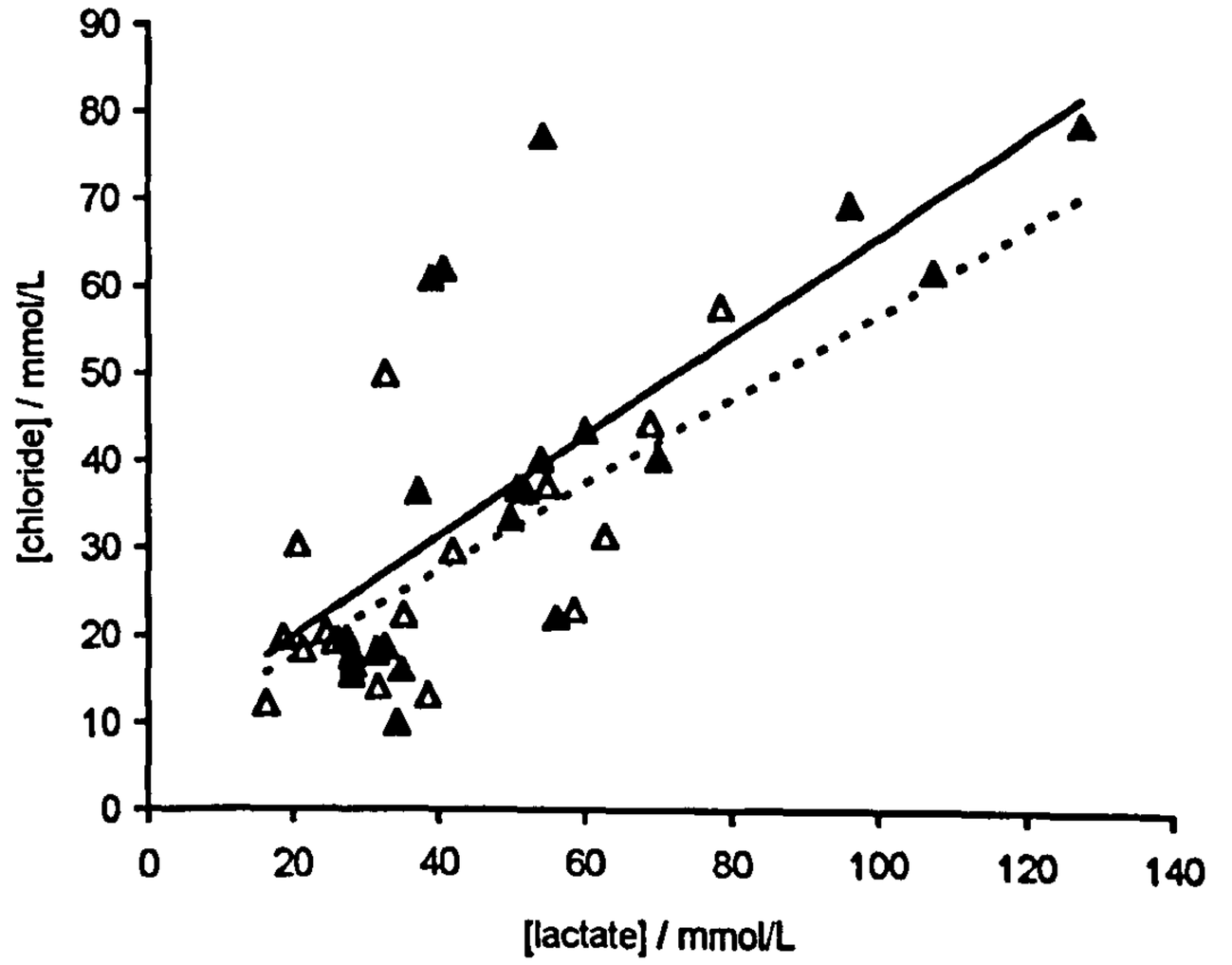

Figure 9-11 Relationship between sweat lactate concentration against sweat chloride concentration collected at the sacrum of healthy volunteers.
(Δ) unloaded sweat, linear model (------) *y=0.49x+7.52; r=0.698* ***
(▲) loaded sweat, linear model (———) *y=0.58x+8.21; r =0.718* ***

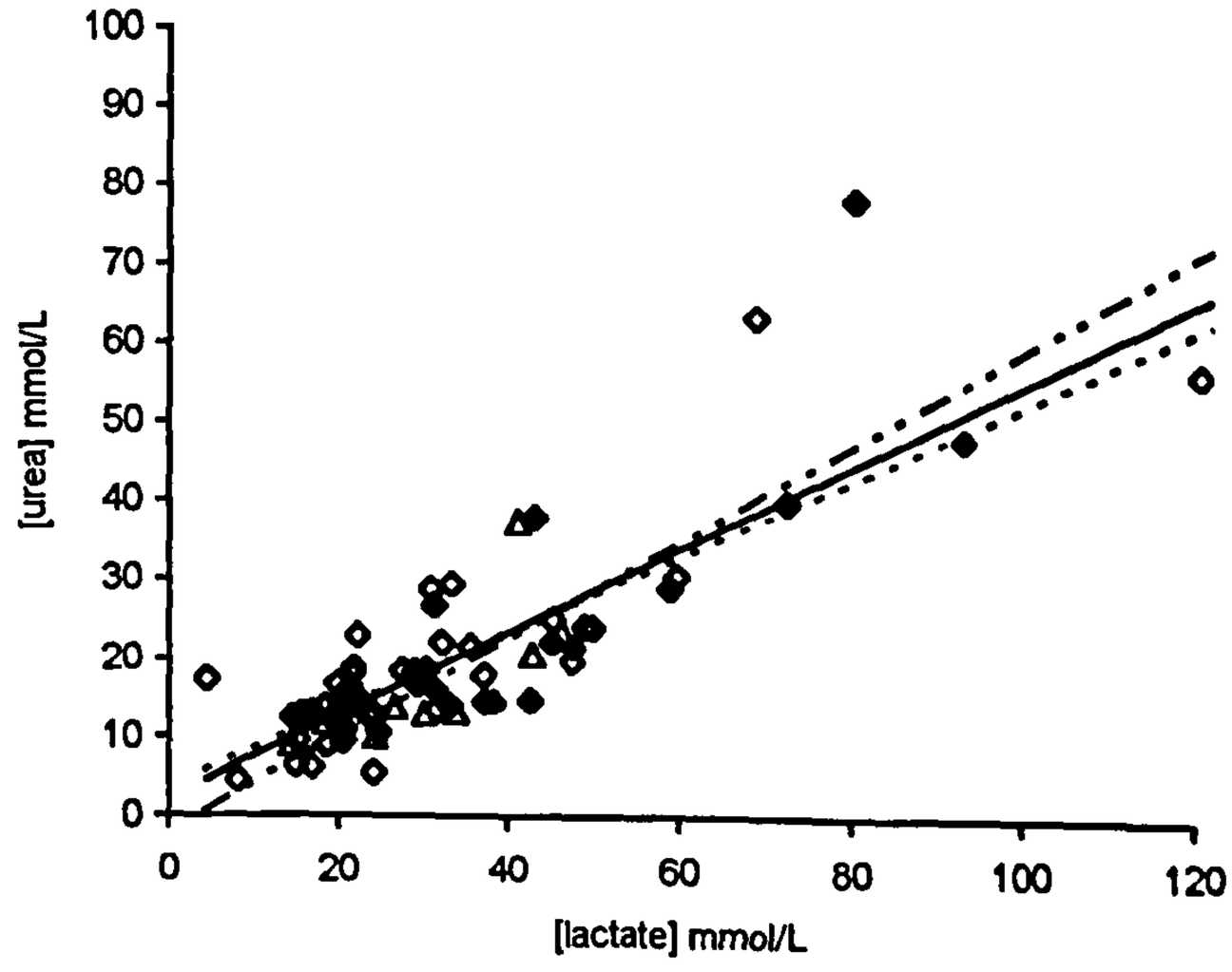

Figure 9-12 Relationship between sweat lactate and sweat urea concentration in thermally stimulated sweat collected at the sacrum of healthy volunteers.
(◇) unloaded sweat, linear model (-------) *y=0.49x+3.59; r=0.839* ***,
(◆) loaded sweat, linear model (———) *y=0.53x+2.31; r=0.849* ***,
(Δ) reperfusion sweat, linear model (-- —— --) *y=0.61x-2.10; r=0.751* **.

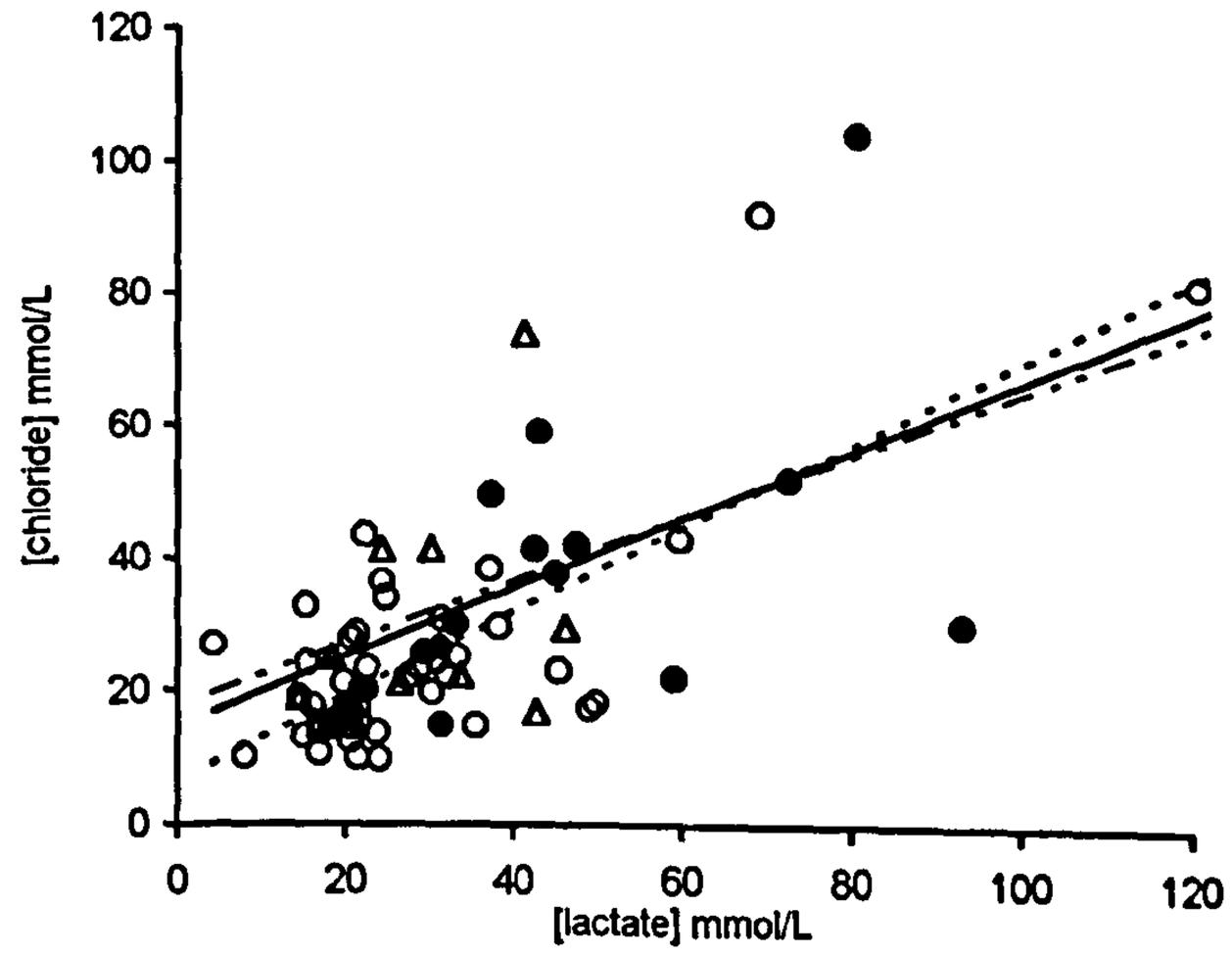

Figure 9-13 Relationship between sweat lactate and sweat chloride concentration in thermally induced sweat collected at the sacrum of healthy volunteers.
(○) unloaded sweat, linear model (-------) *y=0.64x+6.34; r=0.745* ***
(●) loaded sweat, linear model (———) *y=0.52x+14.68; r =0.684* **,
(Δ) reperfusion sweat, linear model (-- —— --) *y=0.48x+17.45; r= 0.293.*

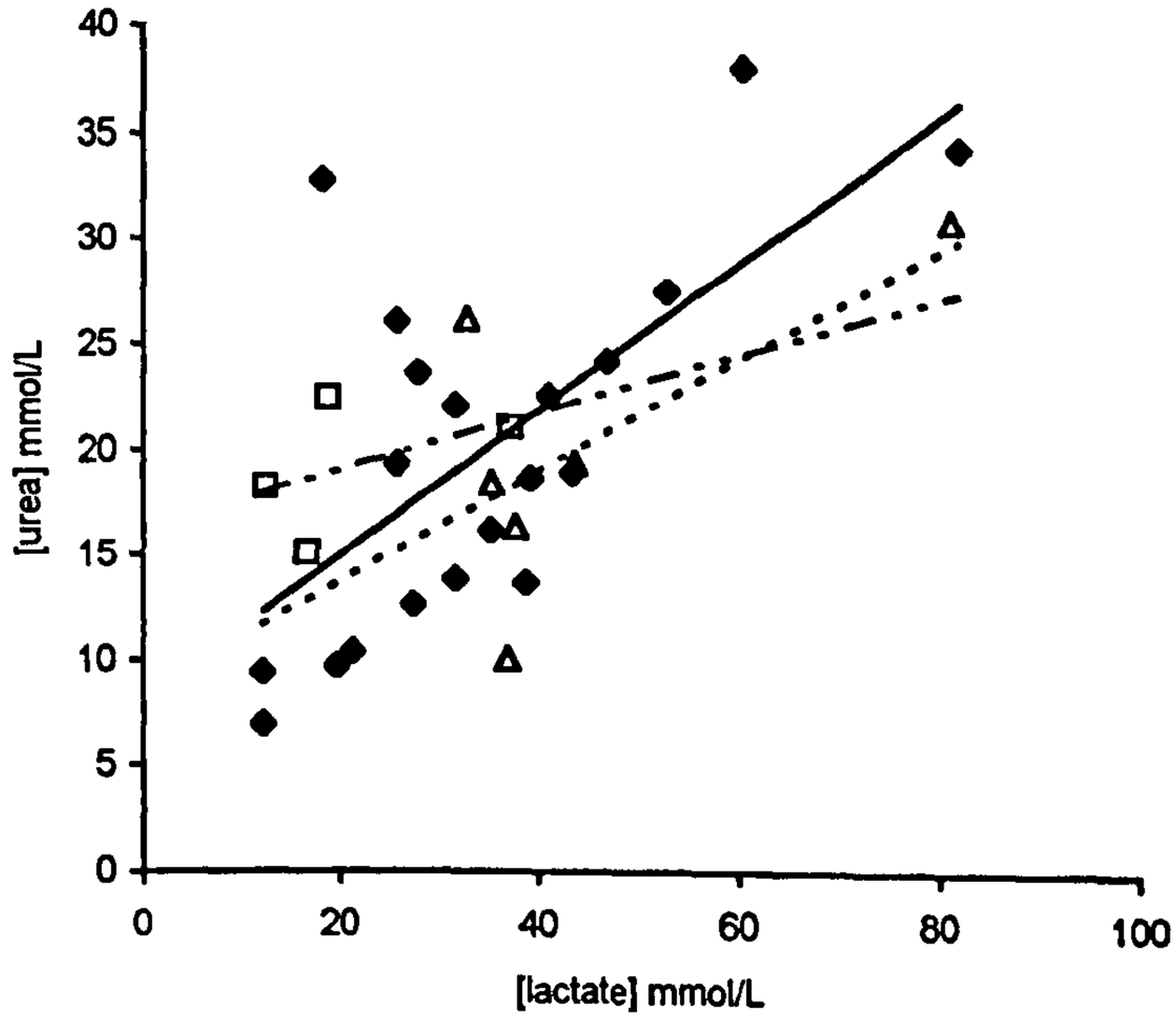

Figure 9-14 Relationship between sweat lactate and sweat urea concentration collected from sockets of lower limb amputees.
(◆) general population, linear model (———) *y=0.34x+8.04; r=0.671****,
(Δ) athlete population, linear model (-------) *y=0.26x+8.39; r=0.658*,
(□) athlete population, forehead sweat, linear model (-- —— --) *y=0.14x+16.28; r=0.461*,

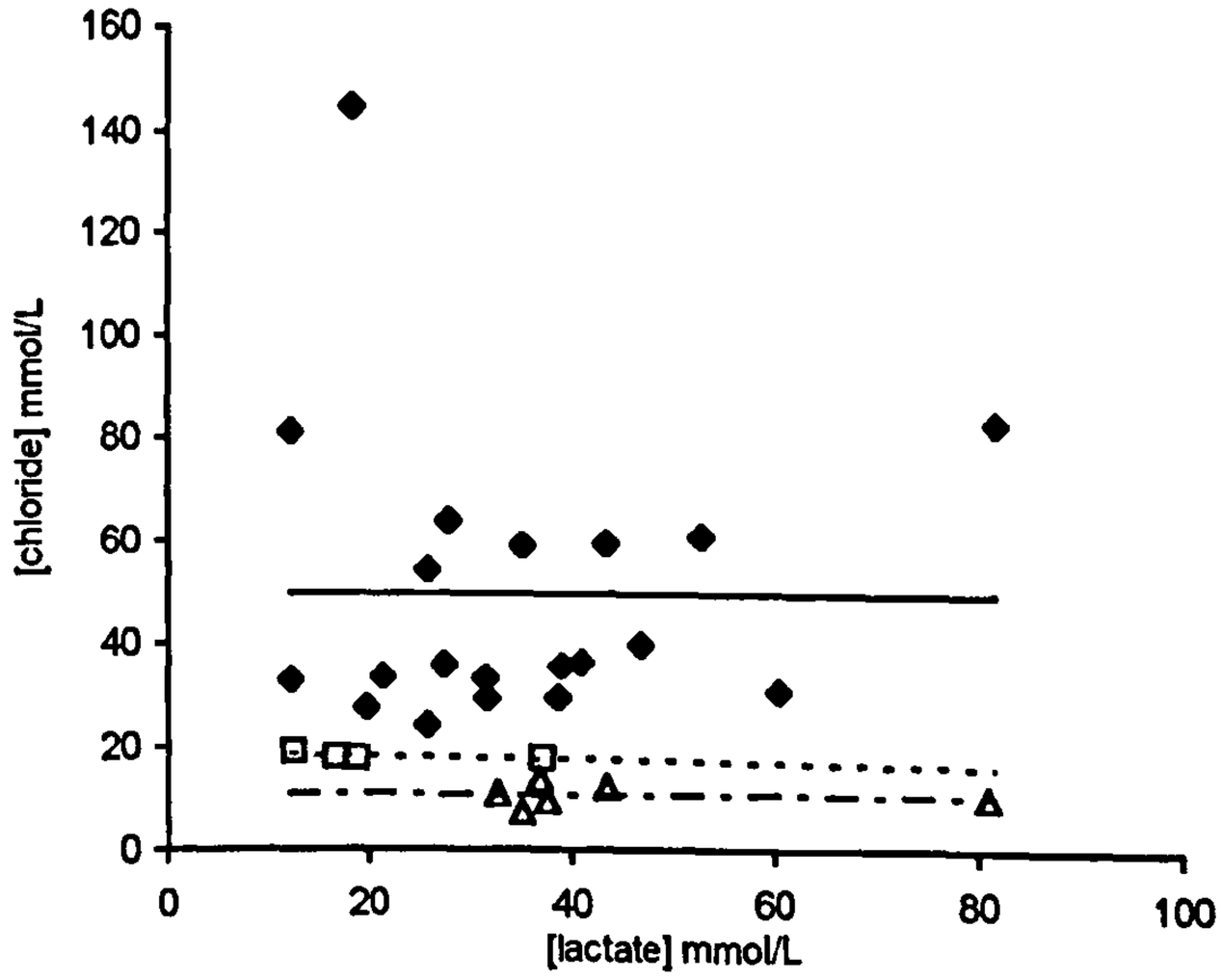

Figure 9-15 Relationship between sweat lactate and sweat chloride concentration collected from the sockets of lower limb amputees.
(◆) normal population, linear model (———) *y=0.003x+49.74; r=0.002*,
(Δ) athlete population, linear model (-------) *y=0.031x+18.71; r=0.614* ,
(□) athlete population, forehead sweat, linear model (-- —— --), *y=-0.005x+10.82; r =0.044.*

Sweat chloride was also statistically significantly correlated to sweat lactate in the healthy volunteers (Figures 9-11 and 9-13) and may reflect changes in the absorption characteristics of the sweat gland, although interestingly there was no significant correlation between sweat lactate and sweat chloride in the amputee population. Sweat chloride is known to be altered by dietary intake of sodium chloride, and again the sweat glands of the residual stump tissues may be affected by the nature of the amputation.

There are clear relationships between the sweat metabolites analysed in this thesis, which suggests that there are similarities in the mechanisms governing the concentrations of the metabolites in sweat during both unloaded and loaded periods. Previous researchers have noted similar relationships between sweat lactate and ammonium [141] and sweat lactate and urate [158], however, these relationships were only observed in the normal state. The correlation of sweat metabolites in both loaded and unloaded states, as well as in a clinically relevant patient group, has previously been unreported.

9.8 Recommendations for Future Work

9.8.1 Extension of Specific Metabolite Markers

The analysis techniques described in this thesis (Section 4.3.4) provided accurate and reproducible measurement of sweat lactate, urea and chloride concentrations. However, it may be necessary to increase the sensitivity of the analysis technique to detect further biochemicals which may be of importance as metabolic markers, but are present in much smaller quantities. The use of high performance liquid chromatography (HPLC) may expedite the development of assays for the following biochemicals in sweat which may be implicated in tissue status:

- urate
- xanthine
- hypoxanthine

- phosphocreatinine

9.8.2 ISCHAEMIA/REPERFUSION INJURY

Reperfusion is undoubtedly an important factor in the ability of tissue to recover from ischaemic onslaught. It has been shown, in the present work, that sweat biochemistry is a sensitive indicator of tissue status during loading and reperfusion (Figures 6-5 to 6-9). Sweat lactate and urea levels, which were elevated during a period of ischaemia, returned to basal levels during a subsequent period of reperfusion. It is proposed that further studies should be carried out to investigate changes in sweat biochemistry collected following varying periods of prolonged ischaemia, and the relationship with tissue status.

In addition, it would seem pertinent to use the knowledge gained from other fields such as cardiology and nephrology, to identify further biochemicals, such as nitric oxide, which may be implicated in tissue breakdown during ischaemia/reperfusion injury.

9.8.3 REAL TIME MONITORING OF SOFT TISSUE STATUS

One of the most obvious progressions from the work of this thesis would be the development of a continuous real time monitor of sweat biochemistry. This would enable direct comparison to be made between sweat metabolite concentration and other continuous methods of tissue status measurement, such as transcutaneous blood gas tension monitoring. This would also enable more accurate investigation of the reperfusion response in terms of sweat gland function.

It is proposed that a multi-sensor could be developed utilising either vibrational spectroscopy or biosensor techniques to enable monitoring of a wide variety of tissue status parameters.

VIBRATIONAL SPECTROSCOPY

As described in Section 3.5 spectroscopy has been used to measure a number of diverse but relevant parameters such as blood oxygenation [89], cerebral blood flow [68],

and composition of human epidermis [215]. The former utilised infrared spectroscopy, whilst the latter utilised Raman scattering effects.

Raman spectroscopy was used, in the present study, in a preliminary investigation into the analysis of sweat. Water has a very strong infrared spectra but a weak Raman spectra and since sweat is an aqueous solution it was considered appropriate to utilise Raman spectroscopy. Aqueous solutions of lactic acid and urea were analysed using a FT-Raman spectroscope (experimental details are described in Appendix E). The data in Figure 9-16 shows the Raman shift absorbance at wavenumbers of 840 cm^{-1} and 1008 cm^{-1} for lactic acid and urea respectively; these wavenumbers represent well established specific peaks which are strong in the relevant spectra. However, when lactic acid and urea solutions with concentrations comparable to those expected in sweat, namely 20-50 mmol/L, were analysed no discernible spectra was obtained.

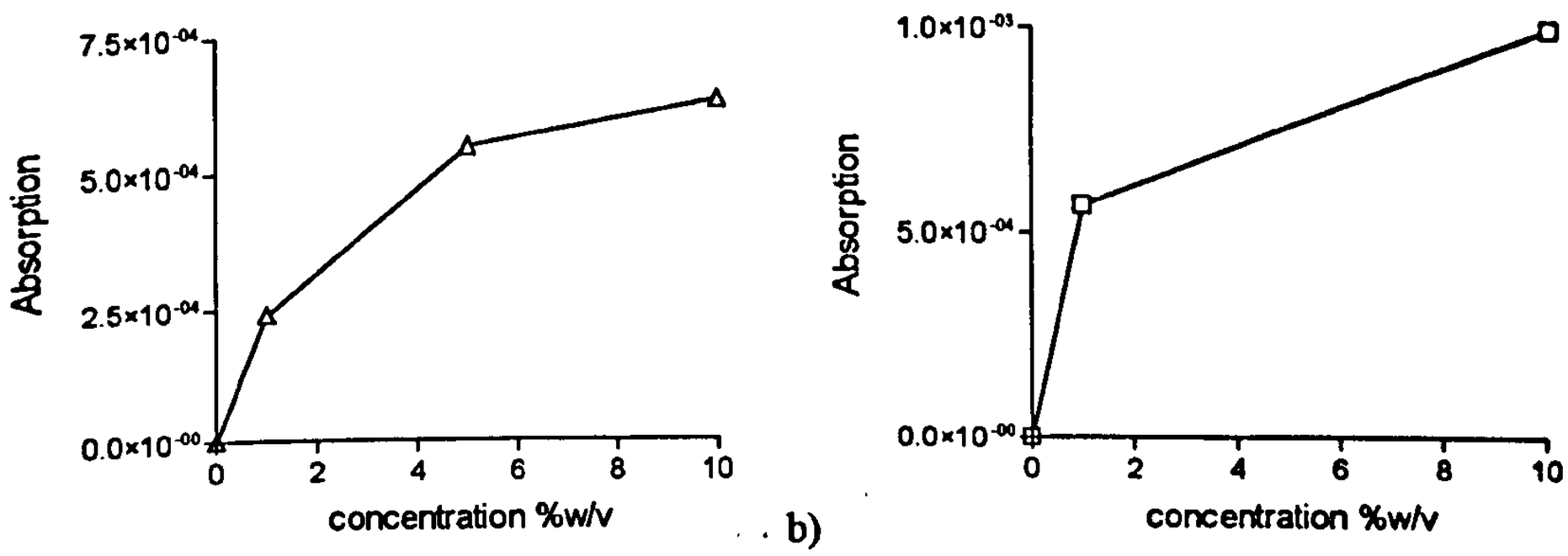

Figure 9-16 Raman spectra absorbance intensity at different sample concentrations of lactic acid and urea.
a) lactic acid peak at 840 cm^{-1}
b) urea peak at 1008 cm^{-1}

As described in Section 3.5 the Raman microscope provides a greater sensitivity in detection of compounds than sample solutions. Therefore, a freeze dried sample of thermally stimulated sweat was analysed under the Raman microscope (experimental details are described in Appendix E). The spectra obtained from the freeze dried sweat sample and a control sample of pure lactic acid are shown in Figure 9-17.

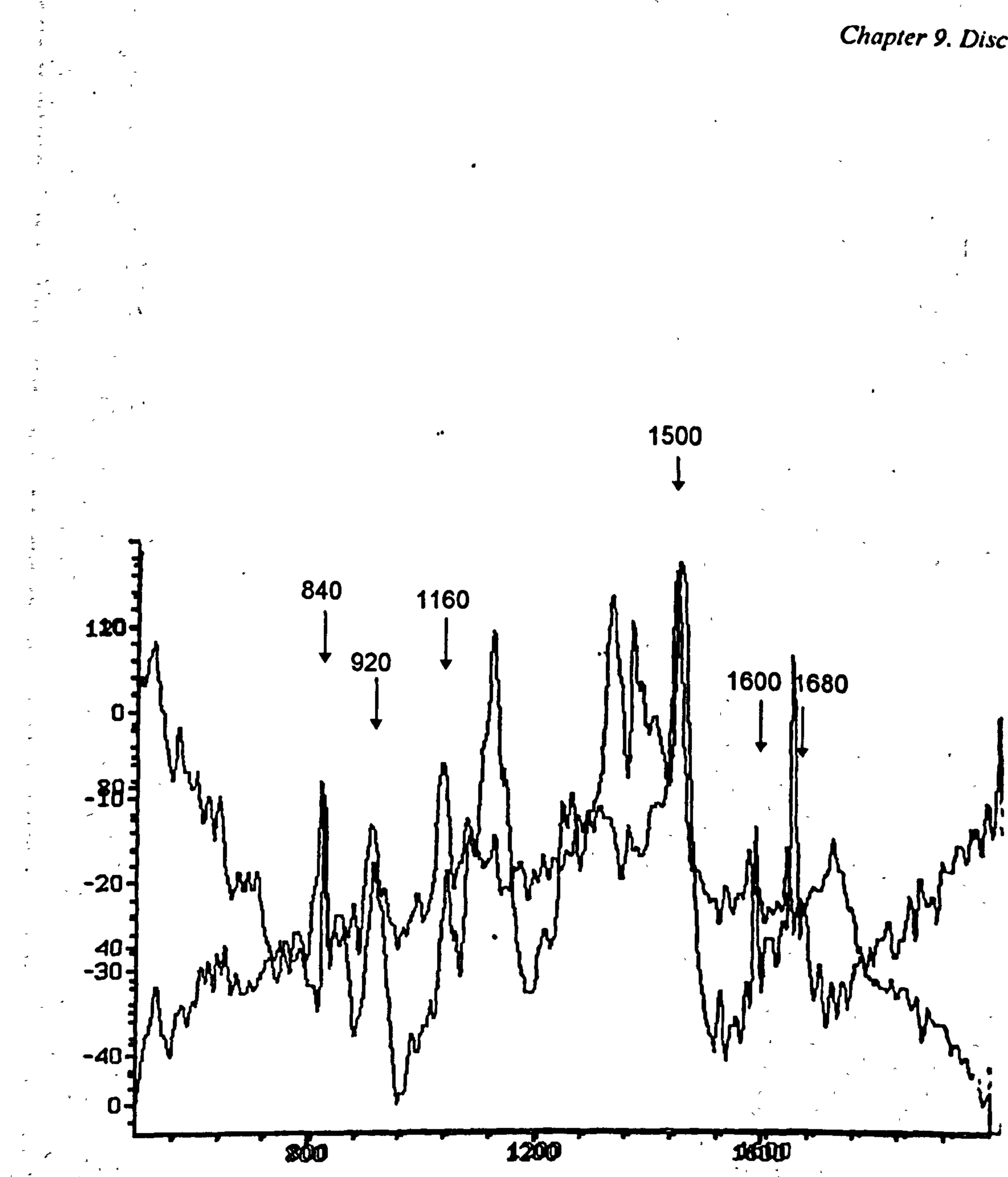

Figure 9-17 Raman microscope spectra obtained from
a) freeze dried human sweat, b) pure lactic acid.
Both samples have been background subtracted with the glass spectra.

There is a strong indication that some of the peaks in the sweat spectra coincide with those in the spectra of pure lactic acid, indicating that Raman microscope spectroscopy is capable of detecting lactate in human sweat. Previous research has shown that urate and other purine derivatives can be detected in biological samples using the Raman microscope [206]. Therefore it is possible that this technique could be developed to ultimately provide a real time analysis of sweat biochemistry, utilising fibre optic techniques.

BIOSENSORS & MICRODIALYSIS

Molecular biosensors have been used to measure levels of biochemicals, particularly glucose, *in vivo*, *in vitro* and *ex vivo*. Biosensors generally comprise of a biological mediator, either an enzyme or ion species, and an electrochemical sensor, either potentiometric or amperometric. Indeed, the combined transcutaneous oxygen and carbon dioxide electrode is a good example of a continuous *ex vivo* biosensor. This form of biosensor could be modified to incorporate a lactate sensor, to simultaneously monitor O_2, CO_2 and sweat biochemistry.

Microdialysis is a relatively new technique which has been used to continuously monitor plasma lactate *in vivo*. de Boer *et al.* [22,23] devised a system to monitor plasma lactate non-invasively, however his samples were contaminated by the high levels of lactate found in sweat.

It is proposed that this technique could be modified to provide continuous non-invasive monitoring of sweat lactate. The system would incorporate a modified electrode probe (Figure 9-18), which consists of a cellulose acetate membrane impregnated with immobilised lactate oxidase.

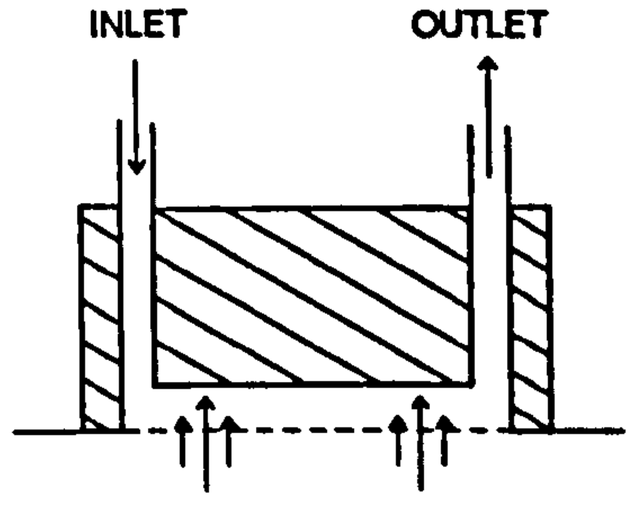

Figure 9-18 Diagram of probe for use with continuous monitoring of sweat lactate. Based on [22-23].

By using a similar experimental set up to that described by de Boer *et al.* [22,23] (Figure 9-19), lactate concentration in the dialyse can be measured by continuous flow injection analysis and fluorescence detection of NADH in the same reaction described in Section 4.3.4 to provide continuous sweat lactate monitoring *in vivo*.

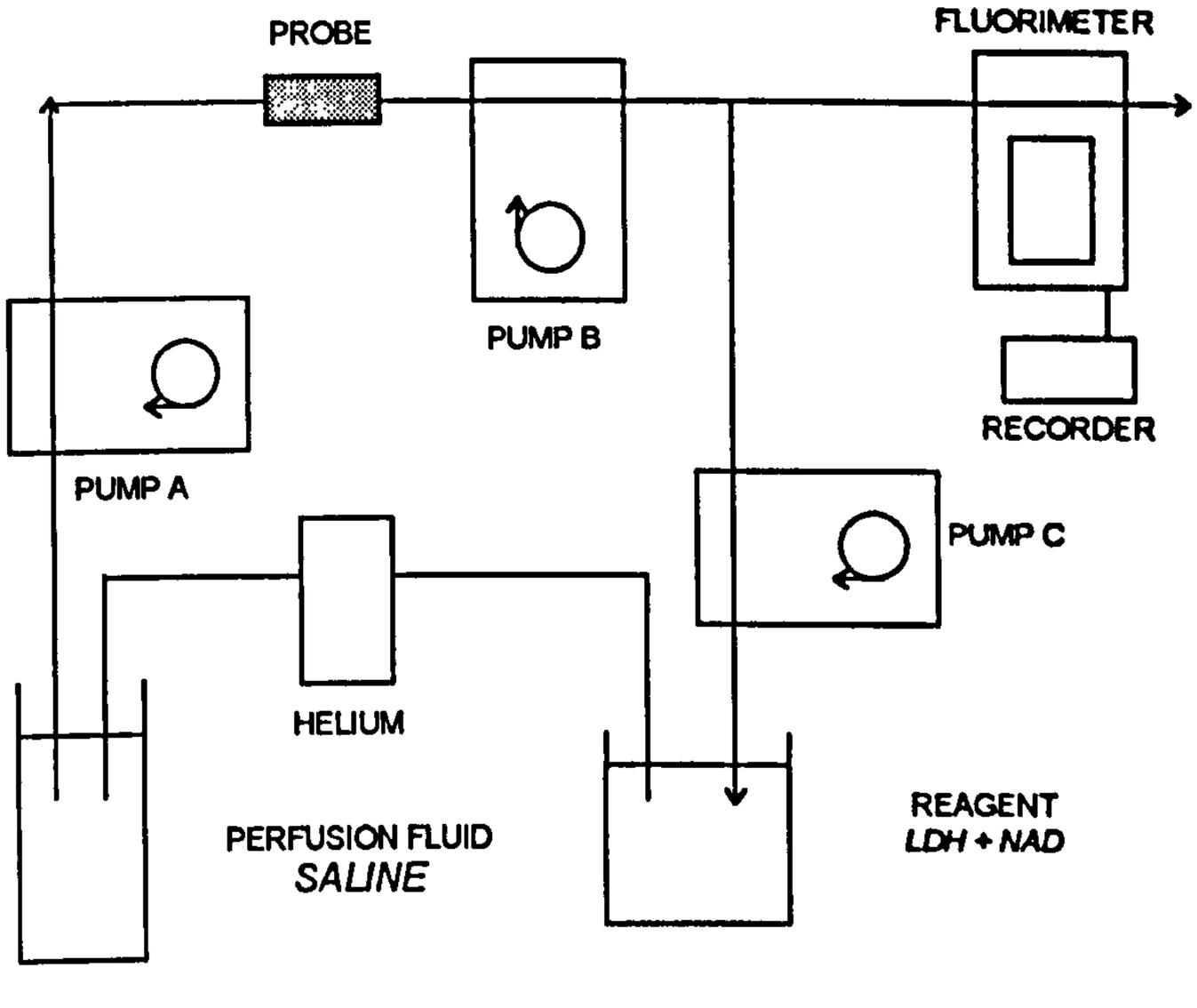

Figure 9-19 Diagram of experimental set up for continuous sweat lactate monitoring [22-23].

9.8.4 Extension of Clinical Groups

The techniques in this thesis have been reasonably successful when applied with two patient groups, namely SCI subjects and lower limb amputees. It is suggested that these studies should be extended and then widened to include other patient groups such as multiple sclerosis sufferers, who are often at risk of developing pressures sores.

9.9 General Summary & Clinical Implications

The major aim of this thesis was to combine two non-invasive techniques for determining soft tissue status and to use them to monitor the effect of prolonged loading at a clinically relevant site. This was successfully carried out by the simultaneous measurement of transcutaneous oxygen and carbon dioxide tensions and sweat biochemistry analysis at the sacrum of healthy volunteers and in clinically

relevant patient groups. In addition, the work in this thesis has yielded several novel findings with regard to sweat biochemistry which are detailed below:

- Thermally stimulated sweat metabolite concentrations remain constant for a period of up to 2 hours in both loaded and unloaded states, provided a period of 20 minutes acclimatisation is undertaken.
- Sweat lactate and urea concentration are dependent upon sweat rate, however, the relationship is also dependent upon whether sweat was collected from an unloaded or loaded site (Figures 9-3 and 9-4).
- Sweat lactate and urea concentrations are related in both loaded and unloaded sweat (Figures 9-10 to 9-13)
- Sweat lactate, urea and chloride concentrations are sensitive to the degree of applied pressure (Figures 7-5 to 7-7).
- Sweat lactate and urea concentrations are related to degree of tissue ischaemia as measured by transcutaneous pO_2 (Figures 7-13 and 7-14).
- Sweat has been successfully collected and analysed from a clinically relevant patient group (Section 8.6-8.7).
- Sweat lactate has been detected using Raman microscope techniques.

Clinicians have long heralded the use of 'thresholds' in the prevention of tissue breakdown at the patient-support interface. The most widely used of these threshold is based on the work of Landis [121] on the critical capillary closing pressure, and as a result the 32 mmHg pressure threshold is often quoted. Advances in tissue status monitoring led to the use of transcutaneous oxygen monitoring, although no minimum threshold levels of pO_2 have been declared as safe to ensure adequate tissue viability [5,9].

The work in this thesis presents the novel use of transcutaneous pO_2 and pCO_2 tensions in conjunction with sweat biochemistry measurements to monitor tissue status during prolonged loading. There is strong evidence in this thesis to suggest that a 60% reduction in pO_2 from initial values alters the biochemistry of the skin and underlying tissues. The novel combined use of transcutaneous oxygen and carbon dioxide tensions

and sweat biochemistry measurements has produced a number of interesting findings which are detailed below:-

- An inverse relationship between loaded pO_2 and sweat lactate and urea concentrations (Figure 7-11 and 7-12).
- A statistically significant correlation between loaded:unloaded sweat lactate and urea concentrations and % reduction in pO_2 above a 60% threshold (Figure 7-13 and 7-14).
- A statistically significant correlation between area under the pCO_2 curve and loaded:unloaded sweat lactate and urea concentrations (Figures 7-15 and 7-16).
- A bimodal relationship between the % time $pCO_2 > 50$ mmHg and the % reduction in pO_2, with a threshold at 60% reduction in pO_2 (Figure 7-10).

Therefore, it is proposed on the basis of these results that a pO_2 which is reduced by more than 60% of its initial value can indicate a compromised tissue status.

APPENDIX A

QBASIC PROGRAM FOR FILE CONVERSION

```
 ' Program for converting downloaded files from
'TINA Transcutaneous Gas Tension Monitor into readable test files
'skips every 4 lines of data
'
'(c) sarah gigg 1995
''
'                 ---------------------------------
'                    To exit press Alt-F+x
'                 ---------------------------------
'
10 CLS
PRINT
PRINT
PRINT
INPUT "  Enter filename of TINA file to be converted: ";n$
OPEN n$ FOR INPUT AS #1
PRINT
INPUT "  Enter name for converted file: ";m$
OPEN m$ FOR OUTPUT AS #2
PRINT #2,
PRINT #2, "Filename:"; m$
PRINT #2,
PRINT #2,
PRINT #2, "O2 / mmHg"; ","; "CO2 / mmHg"; ","; "Temp / C"; ",";
"Power / mW"; ","; "Site Timer"
PRINT #2,
count = 0
DO UNTIL EOF(1)
   LINE INPUT #1, b$
   IF ASC(b$) = 68 THEN count = count + 1
   IF count = 5 THEN
   PRINT #2, MID$(b$,5,5); ","; MID$(b$,12,5); ","; MID$(b$,19,4);
","; "MID$(b$,30,5)
   count = 0
   ELSE
   END IF
LOOP
CLOSE
CLS
PRINT
 PRINT "    ---------------------------------------
PRINT
PRINT "    ******** File conversion completed ********
PRINT
PRINT "    ---------------------------------------
PRINT
 INPUT "  Do you wish to convert another file: Y or N"; a$
IF a$="Y" THEN 10
IF a$="N" THEN END
CLS
```

PRESSURE APPLICATION DEVICE

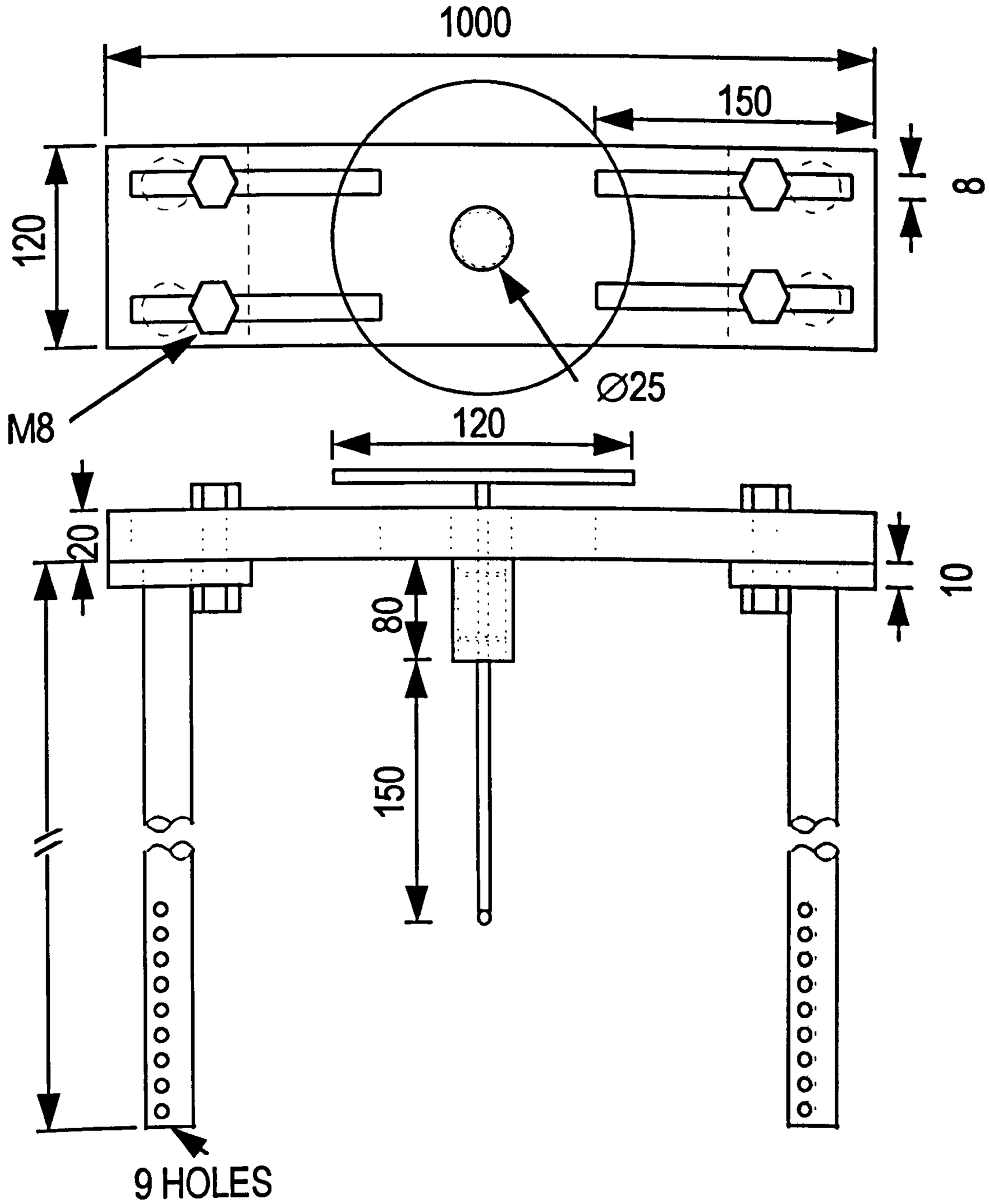

ALL DIMENSIONS IN MM

CALIBRATION OF LVDT & PRESSURE APPLICATION DEVICE

The LVDT and pressure application system described in Section 4.5 and 4.7 were calibrated to investigate linearity. Figure A-1 shows the calibration curve of the LVDT over its range of 11.5 mm, calibration was attained with the use of 0.0127 mm slip gauges.

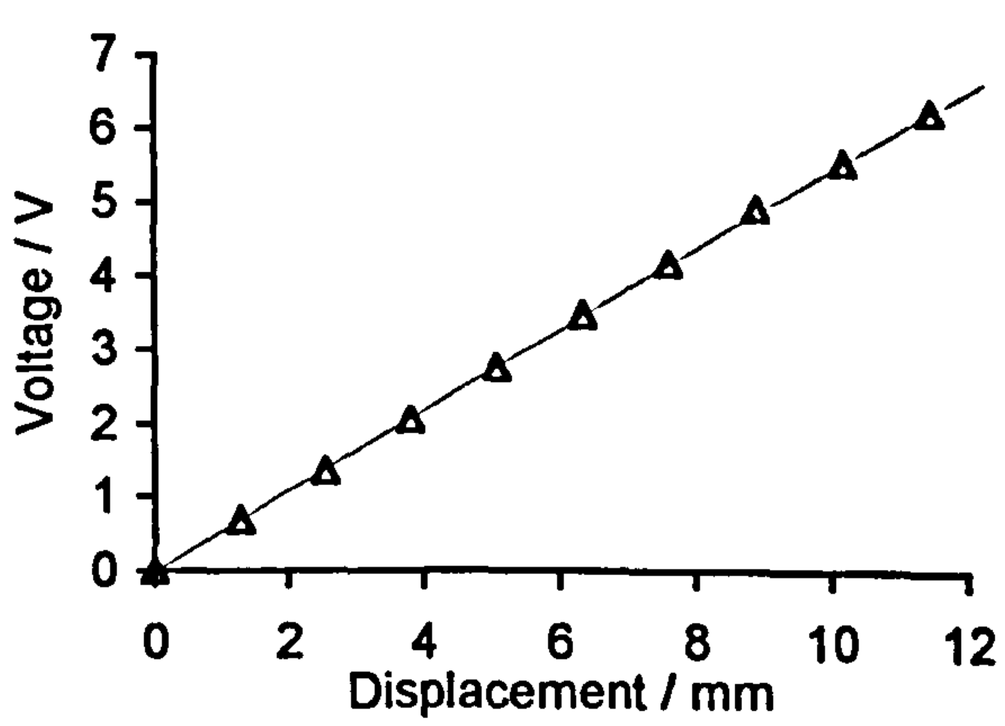

Figure A-1 Calibration curve of linear displacement voltage transducer.

The pressure application device was calibrated using standard weights and a calibrated spring. The deformation of the spring was measured with the LVDT for each applied weight. Figure A-2 shows the calibration curve for the pressure application device in response to a number of applied loads.

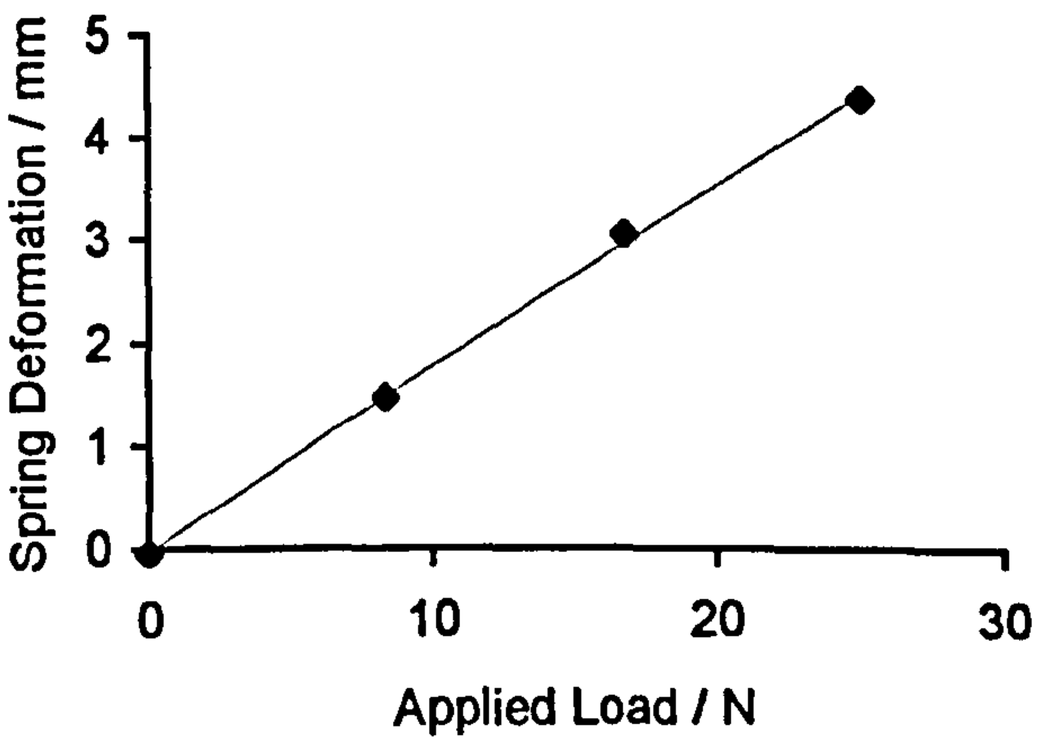

Figure A-2 Calibration of pressure application device.

APPENDIX B

TISSUE DEFORMATION MEASUREMENTS

The tissue deformation in response to various applied loads of 6 healthy volunteers (age 23-41 years) was measured, using the techniques described in Section 4.7 and shown in Figure 4-10. An incremental series of weights was applied to the sacrum via the pressure application device and the output of the LVDT was calibrated to indicate tiddue deformation. The loads were then removed and re-aplied and deformation measured again. Figure B1 shows the deformation in response to the applied loads.

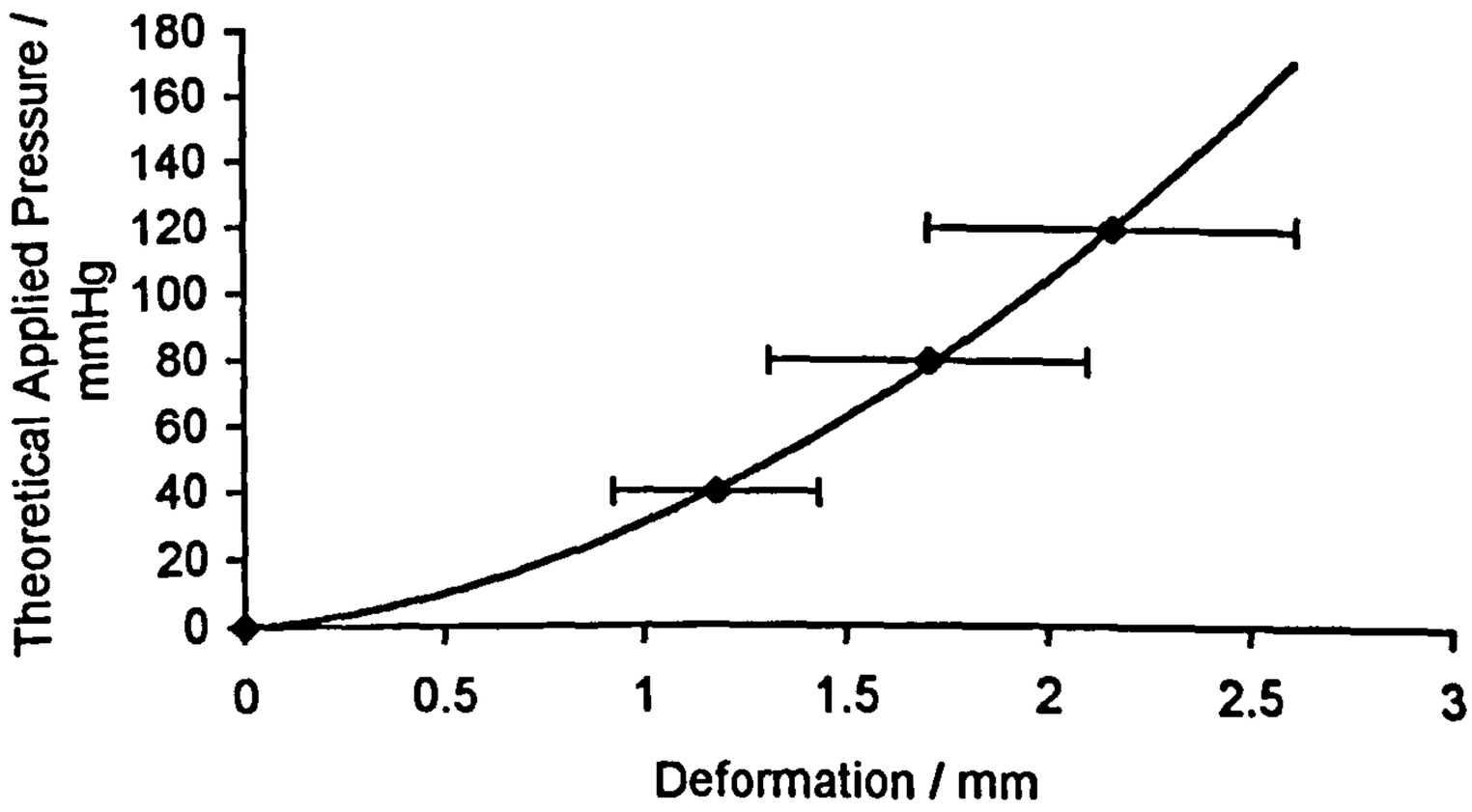

Figure B-2 Pressure deformation relationship of sacral tissue of six healthy volunteers, (♦) mean deformation. Error bars denote one standard deviation.

Subject	Pressure mmHg	Test	Site	Time min	sweat Amount / mg	Lactate mmol/L	Urea mmol/L	Chloride mmol/L	Urate µmol/L	pO_2 mmHg	% time $pCO_2 > 50$	Mode	Area
60 minutes													
1	40	loaded	sacrum	60	133.9	28.14	25.92	27.54		63	0.00	1	525.00
1	40	control	sacrum	60	199.5	21.24	20.43	18.27		70			
2	40	loaded	sacrum	60	205.8	28.05	15.54	15.33		35	85.24	1	586.88
2	40	control	sacrum	60	158	24.35	10.14	12.18		90			
3	40	loaded	sacrum	60	64.8	95.76	62.07	69.9		13	94.34	3	4515.09
3	40	control	sacrum	60	69.2	78.33	45.03	58.11		66			
4	40	loaded	sacrum	60		49.74	31.68	33.54		37	44.82	2	378.18
4	40	control	sacrum	60		41.82	23.31	29.79		78			
5	40	loaded	sacrum	60	199	34.2	17.34	10.02		62	0.00	1	306.89
5	40	control	sacrum	60	214.6	38.55	18.81	13.05		80			
6	40	loaded	sacrum	60	93.5	55.95	33.06	22.11		56	42.37	2	461.02
6	40	control	sacrum	60	92	58.44	30.6	22.95		88			
7	40	loaded	sacrum	60		27.3	18.27	19.62		77	0.00	1	0
7	40	control	sacrum	60		25.62	17.25	19.26		76			
8	40	loaded	sacrum	60	73.5	60	68.31	43.53		58	96.55	2	951.72
8	40	control	sacrum	60	212	50.88	57.9	36.9		58			
9	80	loaded	sacrum	60	159.3	28.38	16.92	16.5		19	95.08	3	6305.00
9	80	control	sacrum	60	237.3	28.02	17.16	17.97		69			
10	80	loaded	sacrum	60	210.1	34.83	21.09	16.05		10	87.71	3	3259.65
10	80	control	sacrum	60	231.4	31.68	16.59	14.07		56			
11	80	loaded	sacrum	60	174	69.96	56.49	40.41		12	94.73	3	1919.30
11	80	control	sacrum	60	96	54.78	41.52	37.35		62			
12	80	loaded	sacrum	60	141.9	40.5	26.58	62.01		14	100.00	2	1561.67
12	80	control	sacrum	60	160	20.49	16.56	30.42		71			
13	120	loaded	sacrum	60	197.8	31.38	29.97	18.33		12	93.33	2	1568.96
13	120	control	sacrum	60	215	24.57	25.17	20.34		67			

Subject	Pressure mmHg	Test	Site	Time min	sweat Amount / mg	Lactate mmol/L	Urea mmol/L	Chloride mmol/L	Urate µmol/L	pO_2 mmHg	% time $pCO_2 > 50$	Mode	Area
14	120	loaded	sacrum	60	126.8	53.91	39.06	40.32		28.5	95.16	3	10438.7
14	120	control	sacrum	60	191.2	35.1	22.41	22.35		80			
15	120	loaded	sacrum	60		32.61	20.97	18.75		27	86.44	3	3771.19
15	120	control	sacrum	60		27.78	17.52	17.4		80			
16	120	loaded	sacrum	60	83.7	51.93	42.24	36.66		15	66.10	3	4479.66
16	120	control	sacrum	60	190.5	31.38	26.2	17.91		75			
17	120	loaded	sacrum	60	165.5	38.82	38.01	61.08		15	98.31	3	5524.59
17	120	control	sacrum	60	190.5	32.55	27.63	49.95		60			
18	120	loaded	sacrum	60	42.9	127.26	120	79.35		12	100.00	3	4974.57
18	120	control	sacrum	60	58.8	68.97	68.61	44.43					
30 minute													
19	40	loaded	sacrum	30	155.3	17.25	23.4	68.43		28	63.33	1	590.00
19	40	control	sacrum	30	93.4	24.99	31.47	86.46		74			
20	40	loaded	sacrum	30	147.2	54.54	26.85	26.67		23	95.00	1-2	525.675
20	40	control	sacrum	30	111	55.8	25.14	27.27		65			
21	80	loaded	sacrum	30	46.5	107.1	46.41	62.16		16.5	87.50	1-2	1912.90
21	80	control	sacrum	30	67.4	62.76	27.06	31.35					
22	80	loaded	sacrum	30	109.1	62.1	76.14	87		34	96.29	2	1193.33
22	80	control	sacrum	30	59	63.87	80.34	85.17		87			
23	120	loaded	sacrum	30	79.9	51.57	24.63	51.87		12	96.60	3	4696.60
23	120	control	sacrum	30	45.3	43.62	18.84	55.89		85			
24	120	loaded	sacrum	30	152.9	59.7	51.84	84.72		16	87.09	3	7996.55
24	120	control	sacrum	30	144.4	40.02	34.05	48.45		73			
25	120	loaded	sacrum	30	83.5	60.9	35.43	36.48		17	96.60	3	4696.60
25	120	control	sacrum	30	77.7	53.28	24.27	29.58		62			

Subject	Pressure mmHg	Test	Site	Time min	sweat Amount / mg	Lactate mmol/L	Urea mmol/L	Chloride mmol/L	Urate µmol/L	pO_2 mmHg	% time $pCO_2 > 50$	Mode	Area
45 minute													
26	120	loaded	sacrum	45	133.4	78.9	35.6		16.9	4	95.35	3	5141.86
26	120	control	sacrum	45	264.3	33.6	15.3		12.6	68			
27	120	loaded	sacrum	45	174.8	74.6	36		10.8	22.5	53.85	1	917.94
27	120	control	sacrum	45	197.8	53.7	26.9		7.2	67			
28	80	loaded	sacrum	45	156.6	69.2	39.1		44.4	10	7.89	1	271.052
28	80	control	sacrum	45	208.9	40.7	22.3		26.4	65.0			
29	80	loaded	sacrum	45	199.8	37.5	17.8		9.6	8.5	82.06	2	1222.27
29	80	control	sacrum	45	212.7	35.3	17.2		14.4				
30	80	loaded	sacrum	45	189.5	44.3	32.9		18.0	4.0	95.23	3	5109.09
30	80	control	sacrum	45	184.1	33.9	27.9		15.6	51.0			
31	80	loaded	sacrum	45	206.1	43.8	18.3		19.8	9.0	95.23	3	6940.47
31	80	control	sacrum	45	247.2	24.7	11.3		12.6	50.0			

APPENDIX D

STOKE MANDEVILLE PATIENT CONSENT FORM

NATIONAL SPINAL INJURIES CENTRE
STOKE MANDEVILLE HOSPITAL
in conjunction with IRC BIOMEDICAL MATERIALS, UNIVERSITY OF LONDON

TITLE

Analysis of Sweat Metabolites in Sweat Collected from Loaded Sites in The Spinal Cord Injured Subject

INVESTIGATORS

Sarah L Gigg
Dan L Bader

INFORMATION FOR PATIENTS

We are trying to find out why pressure sores develop in spinal cord injured subjects who are confined to wheelchair or bed. We hope to further understand the problem and evaluate the performance of the support cushions for each person. We wish to measure the way in which the buttocks pressures, which vary on different cushions, affects the metabolism of the skin. This is done by collecting small amounts of sweat on filter paper attached to the skin with medical adhesive tape. The sweat pads are attached to the skin with medical adhesive tape. The sweat pads are attached to the skin for no more than 120 minutes, as the tests will be performed on the hospital bed and the wheelchair of each subject.

There is no obligation to take part in this study and, if you agree you can ask to have the sweat pads removed at any time during the study.

I, ...of..... agree to/for ..... to take part in this study. I understand the procedures involved which have been explained to me. I understand that I can withdraw/ ..... from the study at any time without giving reason for doing so. I realise that the study may not be direct benefit to me/ ..... I have been told that there are no risks/of the risks involved and that the confidentiality normally applied to medical records will be maintained.

Signed .....Subject/next of kin/guardian Date.....
Signed .....Investigator Date.....
Signed .....Witness Date.....

KING'S HEALTHCARE PATIENT CONSENT FORM

KING'S HEALTHCARE
RESEARCH RECORD/CONSENT FORM
UNIT NO:

SURNAME: **HOSPITAL:**

FIRST NAMES: **DEPARTMENT:**

DATE OF BIRTH: **WARD or CLINIC**

CONSENT BY PATIENT or PARENT/GUARDIAN

I, ...of.....
hereby consent i) to undergo the procedure
ii) to the submission of my child .....
to undergo the procedure
of .....

Signed .....
(Patient, Parent/Guardian)

I confirm that I have explained the nature and effect of this research procedure
i) to the patient
ii) to the child's parent/guardian
Witnesses by Nurse in Charge of Ward present * **Signed .....**
(Researcher)
Name (IN CAPITALS) ..... **Name (IN CAPITALS) .....**
Designation ..... **Designation .....**
Date .....

Date approved by Ethical Committee:

SUMMARY RECORD OF PROCEDURES
(nature of procedure, period over which carried out and number of samples)

Each volunteer will be asked to sit down to remove the prosthetic limb and two load bearing sites will be identified. Single cells of the Oxford Pressure monitor will be placed over these sites, the prosthesis will be replaced and the interface pressures recorded in the weigh bearing stance phase. The cells will then be replaced with sweat pads over the identical two sites. In addition, over a site adjacent to the socket a third sweat will be attached; The volunteer will don the prosthetic limb and start to walk in a controlled manner in the assessment area for 20-30 minutes. After the allotted time period the subject should sit down again and the sweat pads will be removed and the collected sweat will be stored in labelled tubes in the frozen state.

*** In outpatients or Departments an independent witness may sign in absence of nursing staff.**
(Top Copy) This form to be filed in [patients medical and dental record folder.
(2nd Copy) This form to be sent to GP

APPENDIX E

RAMAN ANALYSIS OF LACTATE AND UREA SOLUTIONS

A Nicolet 910 ™ FT-Raman spectroscope was used to analyse a range of solutions of chemicals found in human eccrine sweat. The FT-Raman spectroscope was set up using the following parameters shown in Table E-1.

Table E-1 Settings for the FT-Raman Spectroscope

Parameter	Value
Gain	16
Resolution	4 cm^{-1}
Laser Power	13.00 mW
Scans	500
Correction	White light
Sample	50μL in glass tube

Solutions of lactic acid, uric acid, hypoxanthine, and urea were prepared and analysed using the spectroscope. The spectra were compared with library spectra of the pure compound. Uric acid and hypoxanthine spectra obtained were too weak to detect peaks. The spectra of urea and lactic acid showed strong peaks at 840 cm^{-1} and 1008 cm^{-1} respectively. The results of these are shown in the Figure 9-16.

A Renshaw Raman microscope with light source 15802.78 cm^{-1} and exposure time 120 s was used to analyse a freeze dried sample of human eccrine sweat. The sample was lipholysed (freeze-dried) whereby the sample is cooled at low pressure so that the water component sublimes from solid to gaseous state leaving just solutes. Figure E-1 shows a micrograph obtained from the lipholysed sample. The Raman spectra of the sweat sample and a pure lactic acid sample are shown in Figure 9-17 the background spectra of glass was subtracted from each spectra.

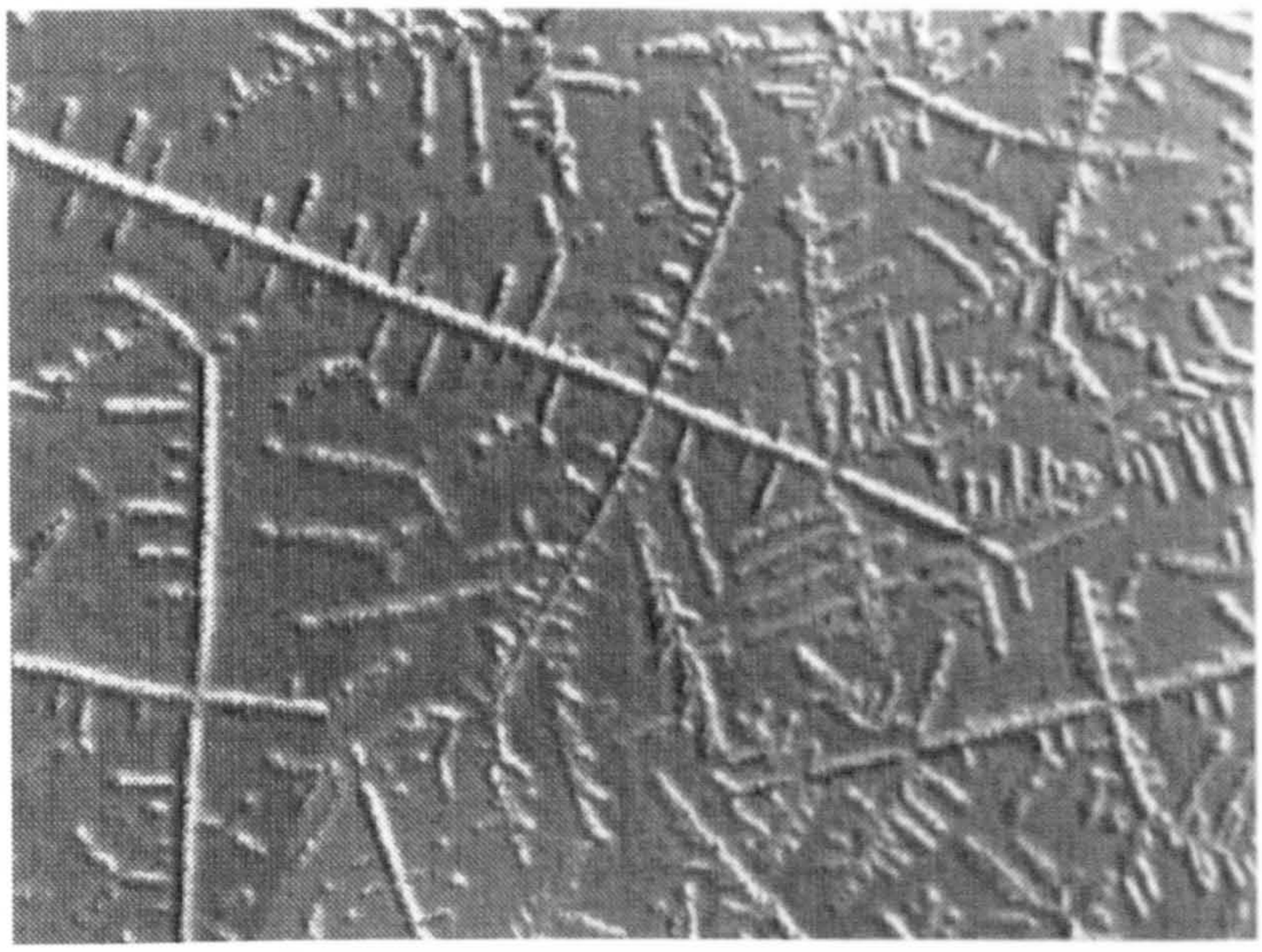

Figure E-1 Freeze dried sample of human eccrine sweat (x100).

REFERENCES

1. Abernathy J. An essay on the nature of the matter perspired and absorbed from the skin. *Surgical and Physiological Essays.* 1793;Part 2:107-165.
2. Al-Tamer Y, Hadi E. Age dependent reference intervals of glucose, urea, protein, lactate and electrolytes in thermally induced sweat. *Journal of Clinical Chemistry and Clinical Biochemistry* 1994;32:71-77.
3. Altomare DF, Regina G, Lovreglio R, Memeo V. Acetylcholine sweat test: an effective way to select patients for lumbar sympathectomy. *Lancet.* 1994;344:976-978.
4. Ayad S, Boot-Handford RP, Humphries MJ. The extracellular matrix facts book. Academic Press. London. 1994.
5. Bader D, Barnhill R, Ryan T. Effect of externally applied skin surface forces on tissue vasculature. *Archives of Physical Medicine and Rehabilitation.* 1986;67:807-811.
6. Bader D, Bowker P. Mechanical characteristics of skin and underlying tissue in vivo *Biomaterials* 1983;4:305-308.
7. Bader D, Gant C. Changes in transcutaneous oxygen tension as a result of prolonged pressure at the sacrum. *Clinical Physics and Physiological Measurement* 1988;9:33-40.
8. Bader D, Gant C. Effects of prolonged loading on tissue oxygen levels. In: Spence C, ed. Practical Aspects of Skin Blood Flow Measurements. Biological Engineering Society, London: 1985:82-85.
9. Bader D, Hawken M. Pressure distribution under the ischium of normal subjects. *Journal of Biomedical Engineering* 1986;8:353-357.
10. Bader D. The recovery characteristics of soft tissues following repeated loading. *Journal of Rehabilitation Research & Development* 1990;27(2):141-150.
11. Bar C. Dynamic pressure measurements in the evaluation of cushions. *Proceedings of the 5th International Seating Symposium.* 1989.
12. Barbanel J, Jordan M, Nicol S. Incidence of pressure sores in the Greater Glasgow Health Board Area. *The Lancet* 1977;September 10:548-550.
13. Barbanel JC, Evans JH, Finlay JB. Stress-strain-time relations for soft connective tissues. In: *Perspectives in Biomedical Engineering.* ed. Kenedi RM. Macmillan, London. 1972:165-172.
14. Bardeletti G, Sechaud F, Coulet P. A reliable l-lactate electrode with a new membrane for enzyme immobilisation for amperometric assay of lactate. *Analytica Chimica Acta* 1986;187:47-54.
15. Barratt E. A review of risk assessment methods. *Care, Science and Practice* 1984;6(2);49-52.

16. Baumberger JP, Goodfriend RB. Determination of arterial oxygen tension by calibration through intact skin. *Federation Proceedings.* 1951;10:10

17. Bennett L, Kavner D, Lee B, Trainor F. Shear vs. pressure as causative factors in blood flow occlusion. *Archives of Physical Medicine and Rehabilitation.* 1979;60:309-314.

18. Benson JW, Buja ML, Thompson RH, Gordon RS. Glucose utilisation by sweat glands during fasting in man. *Journal of Investigative Dermatology.* 1974;63(3):287-291.

19. Beran A, Tolle C, Huxtable R. Cutaneous blood flow and its relationship to transcutaneous O_2 / CO_2 measurements. *Critical Care Medicine* 1981;9(10):736-741.

20. Berenson PJ, Robertson WG. Temperature. In *Bioastronautics Data Book.* Parker JF, and West VR, eds. NASA, Washington DC. 1973:65-148.

21. Bliss M. Acute pressure area care: Sir James Paget's legacy. *The Lancet* 1992;339:221-224.

22. Boer J, Plitjer-Groendijk H, Korf J. Microdialysis probe for transcutaneous monitoring of ethanol and glucose in humans. *Journal of Applied Physiology.* 1993;75(6):2825-2830.

23. Boer J, Plitjer-Groendijk H, Visser K, Mook G, Korf J. Continuous monitoring of lactate during exercise in humans using subcutaneous and transcutaneous microdialysis. *European Journal of Applied Physiology and Occupational Physiology* 1994;69:281-286.

24. Bogie K, Nusiebeh I, Bader D. Transcutaneous gas tensions in the sacrum during the acute phase of spinal cord injury. *Journal of Engineering in Medicine* 1992;206:1-6.

25. Bogie KM, Nuseibeh I, Bader DL. Early progressive changes in tissue viability in the seated spinal cord injured subject. *Paraplegia.* 1995;33:141-147.

26. Bogie KM, Nuseibeh I, Bader DL. New concepts in the prevention of pressure sores. In Frankel HL. ed. *Handbook of Clinical Neurology: Spinal Cord Trauma.* Elsevier Science Publishers BV. 1992;16(61):347-366.

27. Boisvert P, Nakamura K, Shimai S, Brisson GR, Tanka M. A modified local sweat collector for warm and humid conditions. *European Journal of Applied Physiology & Occupational Physiology.* 1993;66:547-551.

28. Brandeis GH, Ooi WL, Hossain M, Morris JN, Lipsitz LA. A longitudinal study of risk factors associated with the formation of pressure ulcers in nursing homes. *Journal of the American Geriatrics Society.* 1994;42(4):388-393.

29. Brunski JB, Roth V, Reddy N, Cochran GVB. Finite element stress analysis of a contact problem pertaining to formation of pressure sores. *Journal of Biomechanical Engineering - Transactions of the ASME.*53-56

30. Bush C. Study of pressure on skin under ischial tuberosities and thighs during sitting. *Archives of Physical Medicine and Rehabilitation.* 1969;50:207-213.

31. Cage G, Dobson R. Sodium secretion and reabsorption in the human eccrine sweat gland. *Journal of Clinical Investigation* 1965;44(7):1270-1276.

32. Campbell EJM, Dickenson CJ, Slater JDH. Clinical Physiology. Blackwell Scientific, Oxford. 1974;111.
33. Candadai RS, Reddy N. Stress distribution in physical buttock model:- effect of simulated bone geometry. *Journal of Biomechanics*. 1992;25(2):1403-1411.
34. Candas V, Libert JP, Vogt JJ. Human skin wettedness and evaporative efficiency of sweating. *Journal of Applied Physiology*. 1979;46(3):522-528.
35. Cattell M. The physiological effects of pressure. *Biological Reviews* 1936;11:441-474.
36. Charcot JM. Lectures on diseases of the nervous system. Translated by Sigerson G. New Sydenham Society. London. 1872.
37. Cheatle T, Potter L, Cope M, Delpy D, Coleridge-Smith P, Scurr J. Near-infrared spectroscopy in peripheral vascular disease. *British Journal of Surgery* 1991;78(4):405-408.
38. Chevion M. The role of free radicals and transition metals in biological aberration: the relevance to ageing of the skin. *Bioengineering and the Skin* 1988;4:39-52.
39. Chow W, Odell E. Deformations and stresses in soft body tissues of a sitting person. *Journal of Biomechanical Engineering* 1978;100(5):79-87.
40. Christalli C, Neuman MR, Ursino M. Studies on soft tissue pressure distribution in the arm, during non-invasive blood pressure measurement. *16th Annual IEEE Conference on Engineering in Medicine & Biology*. 1994
41. Clark M, Rowland L, Wood H, Crow R. The measurement of soft tissue thickness over the sacrum of elderly hospital patients using B mode ultrasound. *Journal of Biomedical Engineering* 19889;11:200-202.
42. Clark M, Rowland L. Comparison of contact pressures measured at the sacrum of young and elderly subjects. *Journal of Biomedical Engineering* 1989;11(5):197-199.
43. Claus-Walker J, Campos RJ, Carter RE, Chapman M. Electrolytes in urinary calculi and urine of patients with spinal cord injuries. *Archives of Physical Medicine and Rehabilitation*. 1973;54:109-114.
44. Claus-Walker J, Differante N, Halstead LS, Tavella D. Connective tissue turnover in paraplegia. *American Journal of Physical Medicine*. 1982;61(3):130-140.
45. Collins K, Sargent F, Weiner J. The effect of arterial occlusion on sweat gland responses in the human forearm. *Journal of Physiology* 1959;148:615-624.
46. Crow RA, Clark M. Current management for the prevention of pressure sores. In: *Pressure Sores - Clinical Practice and Scientific Approach*. Macmillan, London. 1990;
47. Dabnichki P, Crocombe A, Hughes S. Deformation and stress analysis of supported buttock contact. *Journal of Engineering in Medicine* 1994;208:9-17.
48. Daly CH, Odland GF. Age related changes in the mechanical properties of human skin. *Journal of Investigative Dermatology*. 1979;73:84-87.

49. Daly C. Biomechanical properties of the dermis. *Journal of Investigative Dermatology* 1982;79:17s-20s.

50. Daniel R, Priest D, Wheatley D. Etiologic factors in pressure sores: An experimental model. *Archives of Physical Medicine and Rehabilitation.* 1981;62:492-498.

51. Daniel R, Wheatley D, Priest D. Pressure sores and paraplegia. An experimental model. *Annals of Plastic Surgery* 1985;15(1):41-49.

52. Dhamelincourt P. Developments and applications of the MOLE laser Raman microprobe. *Microbeam Analysis.* 1979;155-164.

53. Dinsdale S. Decubitus ulcers: the role of pressure and friction in causation. *Archives of Physical Medicine and Rehabilitation.* 1974;55:147-152.

54. Dover H, Pickard W, Swain I, Grundy D. The effectiveness of a pressure clinic in preventing pressure sores. *Paraplegia.* 1992;30:267-272.

55. Dowd G, Linge K, Bentley G. Measurement of transcutaneous oxygen pressure in normal and ischaemia skin. *Journal of Bone and Joint Surgery.* 1983;65B(1):79-83.

56. Dowd G, Linge K, Bentley G. Transcutaneous pO_2 measurement in skin ischaemia. *The Lancet* 1982;January 2:48.

57. Eickhoff J, Jacobsen E. Is transcutaneous oxygen tension independent of variations in blood flow and in arterial pressure. *Biotelemetry & Patient Monitoring* 1982;9:175-184.

58. Elizondo R. Local control of eccrine sweat gland function. *Federation Proceedings* 1973;32(5):1583-1587.

59. Elizondo RS, Banerjee M, Bullard RW. Effect of local heating and arterial occlusion on sweat electrolyte content. *Journal of Applied Physiology.* 1972;32(1):1-6.

60. Emrich HM, Stoll E, Friolet B, Colombo JP, Richterrich R, Rossi E. Sweat composition in relation to rate of sweating in patients with cystic fibrosis of the pancreas. *Pediatric Research.* 1968;2(6):464-478.

61. Evans N, Naylor P. Steady states of oxygen tension in human dermis. *Respiration Physiology.* 1966;2:54-60.

62. Evans N, Naylor P. The dynamics of changes in dermal oxygen tension. *Respiration Physiology* 1966;2:61-72.

63. Evans N, Naylor P. The oxygen tension gradient across human epidermis. *Respiration Physiology* 1967;3:38-42.

64. Ewald U. Evaluation of transcutaneous oxygen method used at 37°C for the measurement of reactive hyperaemia in the skin. *Clinical Physiology* 1984;4:413-423.

65. Exton-Smith AN, Sherwin R. The prevention of pressure sores: the significance of spontaneous bodily movements. *Lancet.* 1961;ii:1124-1126.

66. Fairs S, Ham R, Conway B, Roberts V. Limb perfusion in the lower limb amputee-a comparative study using laser Doppler flowmeter and a transcutaneous oxygen electrode. *Prosthetics and Orthotics International* 1987;**11**:80-84.

67. Fardinia M, Palleshi G, Lubrano G, Guilbrault G. Amperometric biosensor for determination of lactate in sweat. *Analytica Chimica Acta* 1993;**278**:35-40.

68. Faris F, Rolfe P, Thorniley M. Non-invasive optical monitoring of cerebral blood oxygenation in the foetus and new-born: preliminary investigation. *Journal of Biomedical Engineering* 1992;**14**(7):303-306.

69. Feather J, Hajizadazeh-Saffar M, Leslie G, Dawson J. A portable scanning reflectance spectrophotometer using visible wavelengths for the rapid measurement of skin pigments. *Physics in Medicine and Biology* 1989;**34**(7):807-820.

70. Fellmann N, Fabry R, Coudert J. Calf sweat lactate in peripheral arterial occlusive disease. *American Journal of Physiology* 1989;**257**:H395-H398.

71. Fellmann N, Grizard G, Coudert J. Human frontal sweat rate and lactate concentration during heat exposure and exercise. *Journal of Applied Physiology.* 1983;**54**(2):355-360.

72. Ferguson-Pell M, Hagisawa S, Masiello R. A skin indentation system using pneumatic bellows. *Journal of Rehabilitation Research & Development* 1994;**31**(1):15-19.

73. Ferguson-Pell M, Hagisawa S. Biochemical changes in sweat. *Journal of Rehabilitation Research & Development* 1988;**25**(3):57-62.

74. Foster K, Ellis F, Dore C, Exton-Smith A, Weiner J. Sweat responses in the aged. *Age and Ageing* 1976;**5**:91-101.

75. Fox I, Palella T, Kelley W. Hyperuricemia: a marker for cell energy crisis. *The New England Journal of Medicine* 1987;July:111-112.

76. Frey MJ. A quantitative colorimetric method for the determination of serum chloride using the Technician RA 1000 system. *Clinical Chemistry.* 1983;**29**:1255.

77. Fukomoto T, Tanaka T, Fujioka H, Yoshihara S, Ochi T, Kuriowa A. Differences in composition of sweat induced by thermal exposure and running exercise. *Clinical Cardiology* 1988;**11**:707-709.

78. Gaebelein G, Labbe A, Gachon A, Coudert J. Sweat lactate in cystic fibrosis and in normal children. *European Journal of Applied Physiology and Occupational Physiology* 1985;**54**:511-516.

79. Garber S, Campion L, Krouskop T. Trochanteric pressure in spinal cord injury. *Archives of Physical Medicine and Rehabilitation.* 1982;**63**:549-552.

80. Gendreau R. Fourier transform infrared spectroscopy as a biomedical tool. *Trends in Analytical Chemistry* 1986;**5**(3):68-71.

81. Gordon R, Cage G. Mechanisms of water and electrolyte secretion by the eccrine sweat gland. *The Lancet* 1966;June 4:1246-1250.

82. Gray's Anatomy: the anatomical basis of medicine and surgery. 38th edition. Eds Williams PL. Churchill Livingstone, New York. 1995.

83. Grieve AP. Soft tissue mechanical properties and the design of pressure distributing seat cushions. PhD Thesis, 1989. Queen's University Belfast.

84. Gutmann I, Whalefield AW. L(+)lactate determination with lactate dehydrogenase and NAD. In: Bergmeyer HV, ed *Methods of Enzymatic Analysis*. 2nd edition. Weinheim Verlag Chemie. 1974:1464-1468.

85. Guttmann L. Spinal cord injury - comprehensive management and research. ed. Guttmann L. Blackwell Scientific Publications, Oxford. 1973.

86. Guyton A, Taylor A, Brace R. A synthesis of interstitial fluid regulation and lymph formation. *Federation Proceedings* 1976;35:1881-1885.

87. Guyton AC. Interstitial fluid pressure and dynamics of lymph formation. *Federation Proceedings*. 1976;35:1861-1862.

88. Hackler RH. A 25 year prospective mortality study in the spinal cord injured patient: Comparison with long-term living paraplegia. *Journal of Urology*. 1977;117:486-488.

89. Hagisawa S, Ferguson-Pell M, Cardi M, Miller D. Assessment of skin blood content and oxygenation in spinal cord injured patients during reactive hyperaemia. *Journal of Rehabilitation Research & Development* 1994;31(1):1-14.

90. Hagisawa S, Ferguson-Pell M, Palmieri V, Cochran G. Pressure sores: A biochemical test for early detection of tissue damage. *Archives of Physical Medicine and Rehabilitation*. 1988;69:668-671.

91. Hampson N, Piantadosi C. Near infrared monitoring of human skeletal muscle during oxygenation and during forearm ischaemia. *Journal of Applied Physiology*. 1988;64(6):2449-2457.

92. Hannon D, Quinton P. Ultramicro assay of lactate by fluorescence microscopy. *Analytical Chemistry* 1984;56:2350-2351.

93. Hargens AR, Akeson WH. Stress effects on tissue nutrition and viability. In *Tissue Nutrition and Viability*. eds Hargens AR. Springer Verlag. New York.1993: 1-23.

94. Hickman K, Lindan O, Reswick J, Scanlan R. Deformation and flow in compressed skin tissues. *Proceedings of the Symposium on Fluid Mechanics*. ASME, 1966.

95. Higo M, Kamata S. Inelastic electron tunnelling spectroscopic study of biological compounds in human sweat adsorbed on alumina. *Analytical Chemistry* 1994;66:818-823.

96. Hoaglund FT, Jergeson HE, Wilson LCP, Lamoreux L, Robers R. Evaluation of problems and needs of veteran lower limb amputees in the San Francisco Bay area during the period 1977 to 1980. *Journal of Rehabilitation Research & Development.* 1983;20(1):57-71.

97. Hunter J. Lectures on the principles of surgery: functions of nutrition and absorption. In Palmer J. ed. *Works of John Hunter.* Vol 1. Longman. London. 1835:247-258.

98. Husain T. An experimental study of some pressure effects on tissues with reference to the bed sore problem. *Journal of Pathology and Bacteriology.* 1953;LXVI:347-358.

99. Hyman WA, Artigue RS. Oxygen and lactic acid transport in skeletal muscle: effect of reactive hyperaemia. *Annals of Biomedical Engineering.* 1977;5:260-266.

100. Jacob RA, Otradovec CL, Russell RM, Munro HN, Hartz SC, McGandy RB, Marrow FD, Sadowski JA. Vitamin C status and nutrient interactions in a healthy elderly population. *American Journal of Clinical Nutrition.* 1988;48(6):1436-1442.

101. Jensen TT, Junker Y. Pressure sores common after hip operation. *Acta Orthopaedica Scandinavia.* 1987;58:209-211.

102. Jobsis FF, Keizer JH, LaManna JC, Rosenthal M. Reflectance spectrophotometry of cytochrome aa3 *in vivo*. *Journal of Applied Physiology.* 1977;43:858-872.

103. Johnson AT. Thermal Responses. in *Biomechanics and Exercise Physiology.* 1991. John Wiley & Sons, Canada.

104. Johnson KL. Contact Mechanics. Cambridge University Press, Cambridge. 1989.

105. Jordan MM, Nicol SM, Melrose AL. Report on the incidence of pressure sores in the patient community of the Borders Health Board Area on the 13th October 1976. Bioengineering Unit, University of Strathclyde and Borders Health Board. 1977.

106. Jordan MM, Clark MO. Report on the incidence of pressures sores in the patient community of the Greater Glasgow Health Board Area on 21st January 1976. Bioengineering Unit, University of Strathclyde and Greater Glasgow Health Board. 1977.

107. Kabagambe M, Swain I, Shakespeare P. An investigation of the effects of local pressure on the microcirculation of the skin (reactive hyperaemia) in spinal cord injured patients. *Journal of Tissue Viability* 1994;4(4):110-123.

108. Kadaba M, Ferguson-Pell M. Palmieri V, Cochran G. Ultrasound mapping of the buttock-cushion interface. *Archives of Physical Medicine & Rehabilitation.* 1984;65:467-469.

109. Kegel B. Sports and recreation for those with lower limb amputation or impairment. *Journal of Rehabilitation Research & Development Clinical Supplement.* 1985;1:1-125.

110. Kett RL, Levine SP. A dynamic model of time deflection in a seated individual. *Proceedings of the Annual Conference of Rehabilitation Engineering Society of North America.* 1987;10:524-526.

111. Kirk E, Kvorning S. Quantitative measurements of the elastic properties of the skin and subcutaneous tissues in young and old individuals. *Journal of Gerontology* 1949;4(4):273-282.

112. Klieber M. The fire of life. Robert E. Krieger Publishing Company, Huntingdon, NY. 1974.

113. Komives G, Robinson S, Roberts J. Urea transfer across the sweat glands. *Journal of Applied Physiology*. 1966;21(6):1681-1684.

114. Kondoh Y, Kawase M, Ohmon S. D-lactate concentrations in blood, urine and sweat before and after exercise. *European Journal of Applied Physiology and Occupational Physiology*. 1992;65:88-93.

115. Kosiak M, Kubicek WG, Olson M, Danz JN, Kottke FJ. Evaluation of pressure as a factor in the production of ischial ulcers. *Archives of Physical Medicine and Rehabilitation*. 1959;39(10):623-629

116. Kosiak M. Etiology of decubitus ulcers. *Archives of Physical Medicine and Rehabilitation*. 1961;92:20-29.

117. Krouskop TA. A synthesis of the factors that contribute to pressure sore formation. *Medical Hypotheses*. 1983;11(2):255-267.

118. Krouskop TA, Brown J, Goode B, Winningham D. Interface pressures in above knee sockets. *Archives of Physical Medicine and Rehabilitation*. 1987;68(10):713-714.

119. Kuno Y. Human Perspiration. Charles C Thomas. Springfield, Illinois. 1956

120. Laccoureye O, Bernard D, de Lacharriere O, Bazin R, Brasnu D. Frey's syndrome analysis with biosensor. *Archives of Otolaryngology* 1993;119(9):940-944.

121. Landis EM. Micro-injection studies of capillary blood pressure in human skin. *Heart*. 1929;18:209-228.

122. Lentner C. ed. *Geigy Scientific Tables*. Ciba Geigy, Basle, Switzerland. 1981;vol 1:108-112.

123. Levy SW. Skin problems of the leg amputee. *Prosthetics and Orthotics International*. 1980;4(1):37-44.

124. Liddington M, Shakespeare P. Laser Doppler flowmetry in abnormal skin. *Journal of Tissue Viability*. 1992;2(2):52-54.

125. Lindan O. Etiology of decubitus ulcers, an experimental study. *Archives of Physical Medicine and Rehabilitation*. 1961;42:774-783.

126. Lowthian PT. A review of pressure sore pathogenesis. *Nursing Times*. 1982;78(3):117-121.

127. Mak FT, Liu GHW, Lee SY. Biomechanical assessment of below-knee residual limb tissue. *Journal of Rehabilitation Research & Development*. 1994;31(3):188-198.

128. Manley M, Wakefield E, Key A. The prevention and treatment of pressure sores in the sitting paraplegic. *The South African Medical Journal* 1977;52:771-775.

129. Manschot J, Brakkee A. The measurement and modelling of the mechanical properties of human skin in vivo - II. The model. *Journal of Biomechanics* 1986;19(7):517-521.

130. Manschot J, Brakkee A. The measurement and modelling of the mechanical properties of human skin in vivo -I. The measurement. *Journal of Biomechanics* 1986;19(7):511-515.

131. Mansour J, Davis B, Srour M, Therberge R. A method for obtaining repeatable measurements of the tensile properties of skin at low strains. *Journal of Biomechanics* 1993;26(2):211-216.

132. Matsen FA, Wyss CR, King RV, Barnes D, Simmons CW. Factors affecting the tolerance of muscle circulation and function for increased tissue pressure. *Clinical Orthopaedics.* 1981;155:224-230.

133. McCord J. Oxygen-derived free radicals in post-ischaemic tissue injury. *The New England Journal of Medicine.* 1985;312(3):159-163.

134. McGregor J, Hoogbergen M. Audit of pressure sores treated in a regional plastic surgery unit (1971-1990). *Journal of the Royal College of Surgery, Edinburgh* 1991;36(12):399-401.

135. McKendrick T. Sweat sodium levels in normal subjects, in fibrocystic patients and their relatives, and in chronic bronchitic patients. *Lancet.* 1962;(i):183-186.

136. Meijer J, Germs P, Schneider H, Ribbe M. Susceptibility to decubitus ulcer formation. *Archives of Physical Medicine and Rehabilitation.* 1994;75:318-323.

137. Meijer J, Schut G, Ribbe M. Method for the measurement of susceptibility to decubitus ulcer formation. *Medical & Biological Engineering & Computing* 1989;(September):502-507.

138. Michel CC, Gilcott H. Microvascular mechanisms in stasis and ischaemia. In: Bader DL, ed. *Pressure Sores - Clinical Practice and Scientific Approach.* Macmillan Press, London. 1990:153-163.

139. Michael S. The design of seating for wheelchair users. PhD Thesis. University of London. 1994.

140. Miller GE, Seale JL. The recovery of terminal lymph flow following occlusion. *Journal of Biomechanical Engineering.* 1987;109:48-54.

141. Mitsubayashi K, Suzuki M, Tamiya E, Karube I. Analysis of metabolism sweat as a measure of physical condition. *Analytica Chimica Acta.* 1994;289(1):27-34.

142. Morimoto T. The eccrine and apocrine glands and their function. In Jarret A. ed *The Physiology and Pathophysiology of the Skin.* Academic Press. 1978;1634-1666.

143. Munro HN. Nutrition and Ageing. *British Medical Bulletin.* 1981;37(1):83-88.

144. Nadel E, Bullard R, Stolwijk J. Importance of skin temperature in the regulation of sweating. *Journal of Applied Physiology* 1971;31(1):80-87.

145. Narang IC, Mathur BP, Singh P, Jape VS. Functional capabilities of lower limb amputees. *Prosthetics and Orthotics International.* 1984;8(1):43-51.

146. Newman P, Davis N. Thermography as a predictor of sacral pressure sores. *Age and Ageing* 1981;10:14-18.

147. Newson T, Pearcy M, Rolfe P. Skin surface pO_2 measurement and the effect of externally applied pressure. *Archives of Physical Medicine and Rehabilitation.* 1981;62(8):390-392.

148. Newson T, Rolfe P. Skin surface pO_2 and blood flow measurement over the ischial tuberosity. *Archives of Physical Medicine and Rehabilitation.* 1982;63:553-556.

149. Nola GT, Vistnes LM. Differential response of skin and muscle in the experimental production of pressure sores. *Plastic and Reconstructive Surgery.* 1980;66(5):728-733.

150. North JF. Impact characteristics of human skin and subcutaneous tissue. PhD Thesis, University of Strathclyde. 1973.

151. Ogawa T, Sugenoya J. Pulsatile sweating and sympathetic sudomotor activity. *Japanese Journal of Physiology.* 1993;43(3):275-289.

152. Omokhodion F, Howard JM. Trace elements in the sweat of acclimatised persons. *Clinica Chimica Acta.* 1994;231:23-28.

153. Paget J. The address in surgery read at the thirteenth annual meeting of the British Medical Association. *British Medical Journal.* 1862;ii:155-162.

154. Pereira J, Mansour J, Davis B. Dynamic measurement of the viscoelastic properties of skin. *Journal of Biomechanics* 1991;24(2):365-372.

155. Petersen NC, Bittmann S. The epidemiology of pressure sores. *Scandinavian Journal of Plastic & Reconstructive Surgery.* 1971;5:62-66.

156. Pettibone CA, Scott NR. Relationship of temperatures in the cervical blood vessels to brain temperatures in chickens. ASAE paper 74-5031, American Society of Agricultural Engineers, St Joseph, Michigan. 1974.

157. Polliack A, Taylor R, Bader D. Analysis of sweat during soft tissue breakdown following pressure ischaemia. *Journal of Rehabilitation Research & Development* 1993;30(2):250-259.

158. Polliack AA. DPhil Thesis. 1995. University of Oxford.

159. Potts R, Chrisman D, Buras E. The dynamic mechanical properties of human skin in vivo. *Journal of Biomechanics* 1983;16(6):365-372.

160. Pressure Sores. A key quality indicator. Department of Health. 1993.

161. Randall WC, Peiss CN. The relationship between skin hydration and suppression of sweating. *Journal of Investigative Dermatology.* 1957;28:435-442.

162. Randall WC. Reflex sweating response and the influence of arterial occlusion upon sweat gland activity. *Federation Proceedings.* 1947;6:183-184.

163. Reddy NP, Cochran GV, Krouskop TA. Interstitial fluid flow as a factor in decubitus ulcer formation. Jounral of Biomechanics. 1981;14(12):879-881.

164. Reddy N, Palmieri V, Cochran G. Subcutaneous interstitial fluid pressure during external loading. *American Journal of Physiology* 1981;240:R327-R329.

165. Reddy N, Patel H, Cochran G. Model experiments to study the stress distribution in a seated buttock. *Journal of Biomechanics* 1982;15(7):493-504.

166. Redhead RG. Total surface bearing self-suspending above knee sockets. *Prosthetics & Orthotics International*. 1979;3(3):126-136.

167. Reger S, Chung K. Comparative evaluation of pressure transducers for seating. *RESNA 8th Annual Conference Proceedings*. Memphis, Tennessee, 1985:347-349.

168. Reger SI, Chung KC, Paling M. Weightbearing tissue contour and deformation by Magnetic Resonance Imaging. *Proceedings of the 9th Annual RESNA Conference*. Minneapolis. 1986:387-389.

169. Reichel SM. Shearing force as a factor in decubitus ulcer formation. *Journal of the American Medical Association*. 1958;166:762-763.

170. Reswick WB, Rogers JE. Experience at the Rancho Los Amigos Hospital with devices and techniques to prevent pressure sores. In: *Bedsore Biomechanics*. eds. Kenedi RM, Cowden JM, Scales JT. Macmillan Press, London. 1976

171. Rithalia S. Development in transcutaneous blood gas monitoring: a review. *Journal of Biomedical Engineering* 1991;15(4'5):143-153.

172. Ruth B. Measuring the steady state value and the dynamics of the skin blood flow using the non-contact laser speckle method. *Medical Engineering & Physics*. 1994;16:105-111.

173. Ryan TJ. Biochemical consequences of mechanical forces generated by distension and distortion. *Journal of the American Academy of Dermatology*. 1989;21(1):115-130.

174. Ryan TJ. Cellular responses to tissue distortion. In Bader DL. ed. *Pressure Sores: Clinical Practice and Scientific Approach*. Macmillan, London. 1990;141-150.

175. Sacks A, O'Neill H, Perkash I. Skin blood flow changes and tissue deformation produced by cylindrical indenters. *Journal of Rehabilitation Research & Development* 1985;22(3):1-6.

176. Sacks A. Theoretical prediction of time-at-pressure curve for avoiding pressure sores. *Journal of Rehabilitation Research & Development*. 1989;26(3):27-34

177. Samman G, Ohtsuyama M, Sato F, Sato K. Volume activated K+ and Cl- pathways of dissociated eccrine clear cells. *American Journal of Physiology*. 1993;265:R990-R1000.

178. Sanders JA, Daly CH. Normal and shear stress on a residual limb in a prosthetic socket during ambulation: comparison of finite element results with experimental measurements. *Journal of Rehabilitation Research & Development*. 1993;30(2):191-204.

179. Sanders J, Daly C, Burgess E. Interface shear stresses during ambulation with a below-knee prosthetic limb. *Journal of Rehabilitation Research & Development* 1992;29(4):1-8.

180. Sanderson R, Foley P, McIvor G, Kirkaldy-Willis W. Histological response of skeletal muscle to ischaemia. *Clinical Orthopaedics and Related Research*. 1975;113:27-35.

181. Sangeorzan B, Harrington R, Wyss C, Czerniecki J, Matsen F. Circulatory and mechanical response of skin to loading. *Journal of Orthopaedic Research* 1989;7:425-431.

182. Sapega AA, Heppenstall RB, Chance B, Park YS, Sokolow D. Optimising tourniquet application and release times in extremity surgery. *Journal of Bone & Joint Surgery.* 1985;67A:303-314.

183. Sato K, Dobson RL. Effect of intracutaneous d-aldosterone and hydrocortisone on human eccrine sweat gland function. *Journal of Investigative Dermatology.* 1970;54:450-459.

184. Sato K, Dobson RL. Glucose metabolism of the isolated eccrine sweat gland II. *Journal of Clinical Investigation.* 1973;52:2166-2174.

185. Sato K, Kang WH, Saga K, Sato KT. Biology of sweat glands and their disorders. I Normal sweat gland function. *Journal of the American Academy of Dermatology.* 1989;20(4):537-562.

186. Sato K, Sato F. Methods for studying eccrine sweat gland function *in vivo* and *in vitro*. Methods in Enzymology. 1990;192:583-599.

187. Sato K. The physiology, pharmacology and biochemistry of the eccrine sweat gland. *Reviews in Physiology.* 1977;79:52-124.

188. Schock R, Brunski J, Cochran G. In vivo experiments on pressure sore biomechanics, stresses and strains in indented tissues. *ASME Advances in Bioengineering* 1982:88-91.

189. Schubert V, Fagrell B. Evaluation of the dynamic cutaneous post-ischaemic hyperaemia and thermal response in elderly subjects in an area at risk for pressure sores. *Clinical Physiology* 1991;11:169-182.

190. Schubert V, Fagrell B. Local skin pressure and its effect on skin microcirculation as evaluated by Laser-Doppler fluxmetry. *Clinical Physiology* 1989;9:535-545.

191. Seiler W, Stahelin H. Skin oxygen tension as a function of imposed skin pressure: implication for decubitus ulcer formation. *Journal of the American Geriatrics Society* 1979;XXVII(7):289-301.

192. Sheppard H, Cleak DK, Ward DJ, O'Connor BT. A review of early mortality and morbidity in elderly patients following Charnley total hip replacement. *Archives of Orthopaedic Traumatic Surgery.* 1980;97:243-248.

193. Silver IA, Bergman I. Microelectrodes in medicine. *Philosophical Transactions of the Royal Society of London.* 1987;316(1176):161-167.

194. Spence V, McCollom P, Walker W. Comparative studies of cutaneous haemodynamics in regions of normal and reduced perfusion.

195. Spence VA, McCollum PT, McGregor IW, Shewin SJ, Walker WF. The effect of the transcutaneous electrode on the variability of dermal oxygen tension changes. *Clinical Physics and Physiological Measurement.* 1985;6:139-25.

196. Spence VA, Walker WF. Tissue oxygen tension in normal and ischaemic human tissue. *Cardiovascular Research.* 1984;18:140-144.

197. Suzuki H. Disposable Clark electrode using recycled materials and its application. *Sensors and Actuators B.*1994;21:17-22.

198. Swain I, Nash R, Robertson J. Assessment of support surfaces: Comparison of Nimbus and Pegasus Mattresses. *Journal of Tissue Viability* 1992;2(2):43-45.

199. Swain I, Shakespeare P, Dunsford C, Robertson J. Assessment of support surfaces : Comparison of Pegasus Biwave and Nimbus mattresses. *Journal of Tissue Viability* 1992;2(3):87-88.

200. Swain I, Stacey P, Dunsford C, Robertson J. Assessment of support surfaces: Comparison of the BASE and Quattro mattresses and comparison of BASE and standard 3 inch foam cushion. *Journal of Tissue Viability.* 1992;2(4):123-125.

201. Swain ID, Grant LJ. Methods of measuring skin blood flow. *Physics in Medicine and Biology.* 1989;34(2):151-175.

202. Taylor R, Polliack A, Bader D. The analysis of metabolites in human sweat: analytical methods and potential application to investigation of pressure ischaemia in soft tissues. *Annals of Clinical Biochemistry* 1994;31(1):18-24.

203. Tiffany TO, Janson JM, Burtis CA, Overton JB, Scott CD. Enzymatic kinetic rate and endpoint analyses of substrate by use of a GeMSAEC fast analyser. *Clinical Chemistry.* 1972;18:829-837.

204. Timoshenko S, Goodier JN. Theory of Elasticity. Mc-Graw Hill, New York. 1951;368-371.

205. Todd B, Thacker J. Three-dimensional computer model of the human buttocks. *Journal of Rehabilitation Research & Development.* 1994;31(2):111-119.

206. Truchet M, Martoja M, Martoja R, Ballon-DuFrancais C. Applications de la MOLE à l'identification de composes puriques et de sels mineraux sur coupes histologia. *L'Actualite Chimi.* 1980:15-20.

207. Van Heyningen R, Weiner J. The effect of arterial occlusion on sweat composition. *Journal of Physiology* 1952;116:404-413.

208. Vannah W, Childress D. Modelling the mechanics of narrowly contained soft tissues: The effects of Poisson's ratio. *Journal of Rehabilitation Research & Development.* 1993;30(2):205-209.

209. Verde T, Shepard RJ, Carey P, Moore R. Sweat composition in exercise and in heat. *Journal of Applied Physiology.* 1982;53(6):1540-1545.

210. Versluysen M. Pressure sores in elderly patients: The epidemiology related to hip operations. *The Journal of Bone and Joint Surgery* 1985;67B(1):10-13.

211. Watford M, Freid S. Adipose tissue can now be directly studied in vivo. *Trends in Biochemical Science* 1991;16:201-202.

212. Weiner J, van Heyningen R. Lactic acid and sweat gland function. *Nature.* 1949:164(4165):351-352.

213. Weiner J, van Heyningen R. Observations on the lactate content of sweat. *Journal of Applied Physiology.* 1952;4:734-745.

214. Wijn PFF, Brakkee AJM, Stienen GJM, Vendrick AJH. Mechanical properties of the human skin *in vivo* for small deformations; a comparison of uniaxial strain and torsion measurements. In *Bedsore Biomechanics*. eds Kenedi RM, Cowden JM & Scales JT. Macmillan, London, 1976; 103-108.

215. Williams A, Edwards H, Barry B. Fourier Transform Raman spectroscopy: a novel application for examining human stratum corneum. *International Journal of Pharmaceuticals*. 1992;**81**:R11-R14.

216. Williams A. A study of factors contributing to skin breakdown. *Nursing Research*. 1972;**21**:238-243.

217. Witkowski J, Parish L. Histopathology of the decubitus ulcer. *Journal of the American Academy of Dermatology* 1982;**6**(6):1014-1021.

218. Wolfe S, Cage G, Epstein, Tice L, Miller H, Gordon R. Metabolic studies of isolated human eccrine sweat glands. *The Journal of Clinical Investigation* 1970;**49**:1880-1883.

219. Woolliscroft JO, Colfer H, Fox IH. Hyperuricemia in acute illness: a poor prognostic sign. *American Journal of Medicine*. 1982;**72**:58-62.

220. Yang W-J. Human micro and macro heat transfer - in vivo and clinical applications. In Perspectives in Biomechanics. Reul H, Ghista, DN, Rau G. eds Harwood, Chur, Switzerland. 1980:227-311.

221. Yates FE, Marsh DJ, Maran JW. The adrenal cortex. In Mountcastle VB. ed. *Medical Physiology*. 14th Edition. CV Mosby Company, Missouri. 1980:1558-1601.

222. Zeigert J, Lewis J. In vivo mechanical properties of soft tissues covering bony prominences. *Journal of Biomechanical Engineering* 1978;**100**:194-201.

223. Zhang M, Roberts VC. The effect of shear forces externally applied to skin surface on underlying tissues. *Journal of Biomedical Engineering* 1993; **15**(6):451-456.

PRESENTATIONS

Importance of pressure and time in determining soft tissue status.

DL Bader, **SL Gigg** & AA Polliack.

2nd World Congress on Biomechanics.

Amsterdam, Holland. 1994.

Establishing predictive indicators of soft tissue status.

SL Gigg, DL Bader.

17th Annual Conference of IEEE Engineering in Medicine and Biology.

Montreal, Canada. 1995.

Predicting the status of soft tissues subjected to prolonged loading.

SL Gigg, RP Taylor, AA Polliack, DL Bader.

10th Conference of the European Society of Biomechanics.

Leuven, Belgium. 1996